SARACEN: A New Approach to Combining Gas Electron Diffraction and *Ab Initio* Data

Carole A. Morrison

A thesis presented for the degree of
Doctor of Philosophy
in the Faculty of Science at the
University of Edinburgh, 1997

To Mum, Dad and to Bill

for their love and support

Declaration

This thesis has not been submitted, in whole or in part, for any degree at this or any other university. The work is original and my own, carried out under the direction of Prof. D.W.H. Rankin; where this is not so credit has been duly given.

Acknowledgements

I would first like to thank my supervisor, Prof. D.W.H. Rankin, for his help and encouragement over the past three years, and for the many opportunities he has given me.

Thanks are due to Drs. Paul Brain and Bruce Smart for their advice and experience in electron diffraction and *ab initio* calculations. In particular I would like to thank Bruce for his help and encouragement to 'write everything up as I went along'. The construction of this thesis was not nearly so painful as a result! Thanks are also due to Dr. Heather Robertson for obtaining the electron diffraction data and Dr. Simon Parsons for the X-ray crystallographic work. I would also like to thank Edinburgh University for funding my research.

Finally, thanks to everyone at Edinburgh University, in particular fellow in-mates in Room 110, for making the last three years a very enjoyable time.

List of Abreviations

r =   bond distance.

$<$ =   bond angle.

u =   amplitude of vibration.

r_e =   equilibrium distance between the positions of atomic nuclei corresponding to the minimum of the potential well.

r_a =   effective internuclear distance in the expression of the molecular contribution to electron scattering intensities.

r_α^0 =   distance between average nuclear positions in the ground vibrational state.

s =   electron diffraction angular parameter, given by
$4\pi(\sin\theta/2)/\lambda$, where

         θ = electron diffraction scattering angle

         λ = wavelength of electron beam.

D =   dipolar coupling constant.

B =   rotation constant.

K   =   Kelvin.

pm   =   pico (10^{-12}) metre.

Å   =   Angstrom (10^{-10} m).

Z =   atomic number.

Abstract

The problems associated with refining a molecular structure using gas-phase electron diffraction (GED) data alone are well known. In particular, similar interatomic distances may be strongly correlated, and the positions of light atoms (particularly hydrogen) are poorly determined due to their low electron scattering ability. These problems make it necessary to fix some geometric parameters at assumed values. This is undesirable for two reasons, which are closely related. First, because this parameter is tacitly assumed to be correct, its effect on other refining parameters cannot be gauged; second, fixing parameters can result in unrealistically low estimated standard deviations for correlated parameters.

It has been found that the inadequacies of GED data can, to some extent, be overcome by combining the data with those obtained by other structural techniques, particularly rotational spectroscopy and/or liquid crystal NMR (LCNMR) spectroscopy. This is the ideal approach, as the resulting structure is based entirely on experiment. However, sufficient experimental data are often not available.

Work undertaken for this thesis concerned the development of a new technique to complete GED structural refinements using data obtained from *ab initio* molecular orbital calculations. The new method (called SARACEN - Structure Analysis Restrained by *Ab initio* Calculations for Electron diffractioN) is fully described in this thesis and illustrated with examples from two different classes of compounds. The first series of compounds are small chlorinated aromatic ring systems which serve as model compounds for larger biological systems. The second series is an extensive array of compounds based on the *arachno* boron hydride, tetraborane(10), with general formulas $H_2MB_3H_8$ and $(CH_3)_2MB_3H_8$, where 'M' represents a Group 13 element B, Al, Ga and In. Wherever possible gas-phase structures obtained are compared to solid-phase structures (either already known or derived as a part of this work).

Contents

Chapter 1

Introduction

1.1 General Introduction

Molecular structure is the very essence of chemistry, with the size and shape of a molecule dictating its chemical and physical properties. It therefore follows that investigations into molecular structure and, indeed, new methods by which to obtain increasingly accurate results lie at the very heart of chemical research.

Ideally, any accurate structural investigation should take place in the gas phase, rather than the crystalline state, as molecules will be free from external constraints and packing forces which can distort the structure or even change it completely. Small, simple molecules are most suited for this type of work and it is hoped that knowledge of these simple structures will lead to an understanding of larger, more complicated systems. For the most part, this is achieved by studying a range of closely related compounds, rather than isolated cases, so that definite structural trends can be identified.

Work undertaken for this thesis includes studies of several different classes of compounds, including small chlorinated aromatic systems which serve as model compounds for larger biological systems, and an extensive series of derivatives based on the *arachno* boron hydride, tetraborane(10). These electron deficient molecules are not yet fully understood and so structural studies have valuable contributions to make in increasing our understanding of structure and bonding in these types of molecules.

Structural investigations undertaken for this thesis have involved the use of three major experimental techniques for determining molecular structure in the fluid phase. Electron diffraction has been the technique primarily used, and wherever possible the results obtained from rotational spectroscopy and liquid crystal NMR spectroscopy have been included to provide a more complete structural determination. In addition *ab initio* molecular orbital calculations have been applied throughout, to help both in the investigation of molecular geometry and in the understanding of molecular vibrational motion.

The remainder of this chapter is devoted to providing background information for all the experimental and theoretical techniques used in this work. It will be shown that each technique has its merits and its limitations and as such it is rare that any one method (except for theory) can produce a complete structure. However, the data the techniques provide are complementary and it is therefore possible to obtain complete structural determinations by combining data from several different sources.

1.2 Gas-Phase Electron Diffraction (GED)[1]

1.2.1 Background

Electron diffraction is one of the major techniques for determining accurate molecular structures in the gas phase. Historically, the technique developed as a natural extension to the famous "Young's Slit Experiment", which established the wave nature of light. In essence the experiment demonstrated that light can be diffracted by a pair of slits, producing an interference pattern of alternating high and low intensity bands on a nearby screen. The distance between the points of maximum intensity depends on the wavelength of the light and the separation between the slits. A clear, measurable pattern will be obtained if the wavelength of the light source used is comparable to the distance separating the slits.

In the electron diffraction experiment, a beam of electrons of known wavelength in the Angstrom (10^{-10}m) range replaces the light source, and the pairs of atoms in the molecule under study replace the diffraction slits. As bond distances are typically of the order 1-2 Å, a clear interference pattern is obtained. Since molecules in a gas are free to adopt any orientation in space, the resulting interference pattern appears as a series of concentric circles, rather than a one dimensional array of light and dark bands. From the positions and intensities of these circles, accurate structural information can be extracted.

1.2.2 Instrumentation

A schematic diagram illustrating the basic layout of the electron diffraction experiment set-up is shown in Figure 1.1. Electrons are generated from a heated filament and accelerated towards an anode. An accelerating voltage of the order of 50 kV is required in order to generate a beam of electrons with an associated wavelength in the Angstrom range. The voltage supply must be as stable as possible as the diffraction patterns produced must be interpreted on the basis of a single electron wavelength. Once the beam passes the anode it is collimated and focused through a series of apertures and magnetic lenses in order to generate a narrow electron beam. This is important as the intersection with the sample must occur in as small a volume as possible.

The sample is introduced into the evacuated diffraction chamber through a fine nozzle and intersects the electron beam at right angles. Once diffracted the sample is collected in a cold trap. The molecular sample beam must be comparable in diameter with the electron beam in order to reduce the intersection volume.

After passing through the sample, the diffracted beam continues through the diffraction chamber towards the detector, typically a photographic plate, which records the scattered electron pattern. Most of the scattering intensity will be located in the centre of the plate, decreasing sharply as the scattering angle increases (roughly inversely as the fourth power of the angle), but as the photographic medium is only sensitive over a limited range of intensity it is necessary to attenuate the beam using a rotating sector. The sector is placed immediately in front of the photographic plate and is designed to reduce the effective exposure time towards the centre of the plate. To trap the portion of the beam which remains undiffracted a beam stop, consisting of an aluminium cylinder, is positioned at the centre of the sector. This will, of course, prevent data being recorded for very small scattering angles, but is necessary to prevent back reflection of the electron beam.

It is common practice to record the interference pattern with two (or more) nozzle-to-plate distances. This allows the scattering data to be recorded more accurately over a wider scattering angle range (see Figure 1.1). The electron diffraction image obtained over the longer distance can typically be recorded on a photographic plate in less than twenty seconds; the shorter distance in less than eighty seconds.

Electron Gun

Diffraction Chamber

Gas Sample →

Cold Trap

→ Pump

Photographic Plates
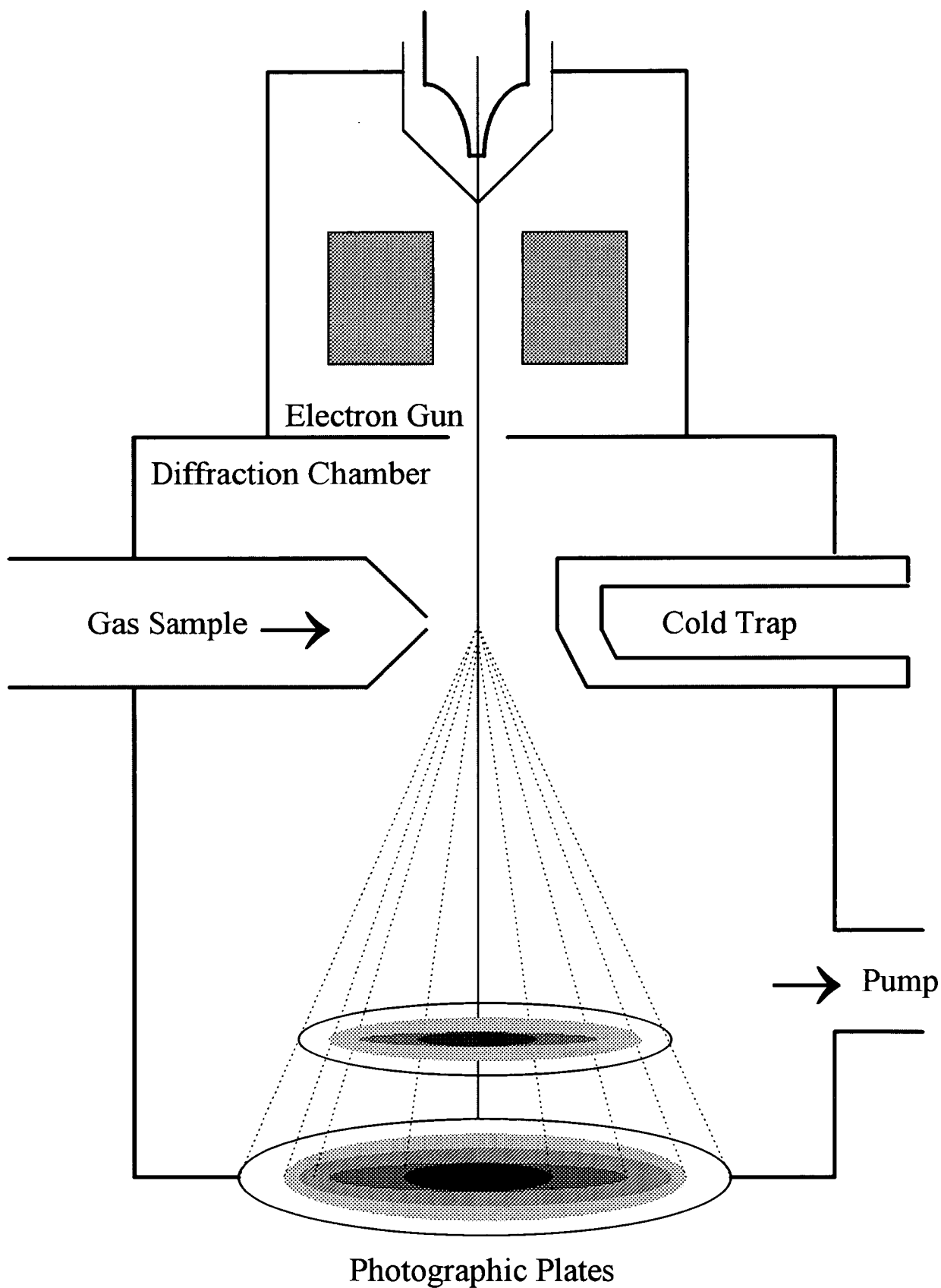
Figure 1.1 Illustration of a typical lay-out of an electron diffraction instrument for studying the molecular structures of gases

1.2.3 Data Analysis

Once the photographic plates have been recorded and developed it is necessary to convert the patterns to numerical data for use in the structural analysis. This is achieved by scanning the plates using a Joyce Loebl Microdensitometer.[2] The raw digitised optical data then have to undergo two important steps before they can be used in a structural refinement. Firstly, the optical data must be converted into the total electron scattering intensity (I_{total}). This process takes into account several factors, including correcting for the flatness of the photographic plate, the non-linearity of the photographic emulsion (the so-called blackness correction) and the presence of the rotating sector. At any given point on the diffraction pattern the total scattering intensity can be expressed as:

$$I_{total} = I_{incoherent} + I_{inelastic} + I_{atomic} + I_{molecular} \qquad [1.1]$$

The second step that needs to be performed before structural analysis can commence involves separating the molecular scattering intensity from the incoherent, inelastic and atomic scattering intensities. The molecular scattering term involves electrons that are diffracted by pairs of nuclei, and therefore contains the structural information. Incoherent and inelastic scattering intensities (arising due to double collision scattering and electrons undergoing momentum changes during collisions, respectively) can be treated as background and removed by subtracting polynomial or cubic spline functions. The atomic scattering term arises due to single atoms diffracting the electrons. Since in this case there is only one source of diffracted electrons (and not two, as in the normal case where a pair of atoms diffract the electron beam), an interference pattern will not be formed. This atomic scattering effect is well documented, and therefore this intensity term can be readily separated using tabulated scattering factors.

1.2.4 Structural Refinement

Solving the molecular scattering intensity data ($I_{molecular}$) to deduce the molecular structure requires the construction of a mathematical model of the molecule. The model takes into account the symmetry (overall and local) of the molecule and describes the location of each atom in terms of the minimum number of bond distances and angles required to define the system completely. These bond distances and angles are referred to as geometric parameters.

It is worth noting that the structure derived by electron diffraction is not static. Although each electron is diffracted by a molecule in less than 10^{-18} seconds, and therefore does effectively observe a frozen instantaneous structure, the experiment involves accumulating data from many electrons with each seeing a molecule at a different stage of its vibrational motion. The parameters obtained by electron diffraction are therefore vibrationally averaged, and it is necessary to include the effects of vibrational motion in the model. This is achieved by including an additional set of parameters, called vibrational amplitudes, which describe the oscillating vibrational behaviour of each pair of atoms in the molecule.

Once the model defining the system has been written the molecular scattering intensity curve can be simulated and compared to the experimental data. Unfortunately the data contained within this curve are not readily interpreted [see Figure 1.2(a)]. However, performing a sine Fourier transformation of this curve yields the highly useful radial distribution curve [see Figure 1.2(b)]. The advantage of this second curve is that it is easy to interpret visually as it is effectively a one-dimensional array of every bond distance in the molecule laid out in terms of increasing distance, r. The y-axis is usually plotted as $P(r)/r$, where $P(r)$ is the probability of finding a pair of nuclei at separation r. Thus, the radial distribution curve shows clear peaks corresponding to all bonding and non-bonding distances in the molecule. Each peak has an approximately Gaussian shape and is centred on an internuclear distance within the molecule; the peak half-widths depend on the amplitudes of vibration of the

appropriate atom pairs. The relative areas of the peaks in the curve are given by the expression,

$$\text{Area} \propto \frac{n_{ij}\, Z_i\, Z_j}{r_{ij}} \qquad [1.2]$$

where n_{ij} = multiplicity of distance r_{ij}

(i.e. the number of times the distance occurs in the molecule).

Z_i, Z_j = atomic numbers of atoms I and j respectively.

Once the molecular scattering curve (and hence radial distribution curve) has been simulated from the model, parameters are then refined by a least-squares analysis until a satisfactory fit with the experimental data is reached. There are several factors which, taken together, indicate when a satisfactory fit has been obtained: ideally all geometric parameters (and as many amplitudes of vibration as possible) should refine to reasonable values with realistic standard deviations, and the so-called R_G factor, a direct measure of the fit between the experimental and simulated data sets, should typically rest somewhere below 10% for most compounds. The final indication rests with the molecular scattering and radial distribution curves themselves. In addition to these standard curves it is also possible to generate plots which represent the difference between the experimental and theoretical data sets. These difference plots are labelled 'Δ' on Figures 1.2(a) and 1.2(b), and clearly for a satisfactory refinement should be as flat as possible.
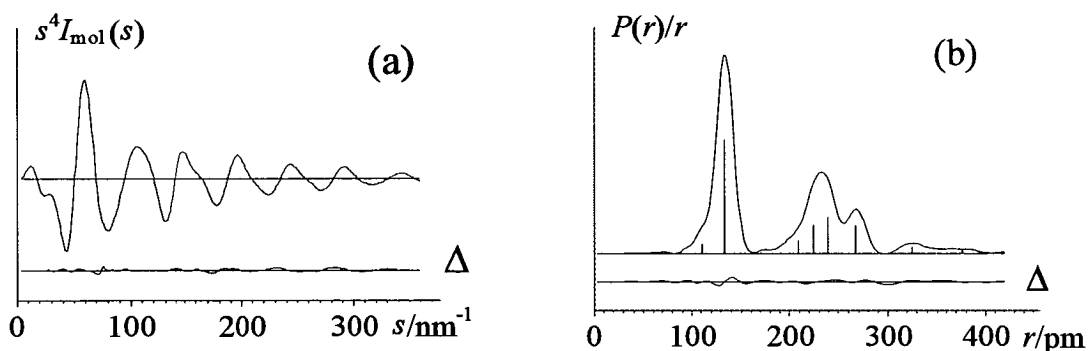
Figure 1.2 (a) A typical molecular scattering curve, Fourier transformation of this curve yields the radial distribution curve (b)

1.2.5 Limitations

Electron diffraction provides a direct measurement of all interatomic distances, and is therefore an ideal method for determining the molecular structures of gases. But there are, of course, limits to the usefulness of electron diffraction. The general requirement for most GED instruments is that the compound to be studied should have a vapour pressure of about 1 Torr or more at a temperature at which it is stable.

The volatility requirement reduces the range of compounds suitable for electron diffraction study, but even if the data can be collected, it may not be possible to determine a structure fully by this method. The problems associated with electron diffraction data are well documented,[3,4] but in particular two significant problems have been identified. Firstly, in common with X-ray diffraction, relatively little information can be retrieved relating to the position of hydrogen atoms since they have poor electron (and X-ray) scattering ability. Secondly, distances which are similar in magnitude will lie close together on the radial distribution curve and may not be readily separated. Such distances are said to be correlated, and in general the average of the two distances can be determined by the diffraction data, but not the individual values.

The two problems indicated above make it necessary to fix the values of some parameters in the GED model. It will be demonstrated in the following two chapters that fixing parameters at an assumed value is unsatisfactory, resulting in an incomplete structural refinement in which uncertainties of refining parameters may be underestimated.

1.3 Rotational Spectroscopy[5]

1.3.1 Background

Like electron diffraction, rotational spectroscopy is also a major technique for determining molecular structures in the gaseous state. The technique is based on the principle that microwave radiation causes changes in the rotational energy levels of molecules. Structures obtained from rotational spectroscopy are often determined very precisely, since the instrumental resolution in the microwave region of the electromagnetic spectrum is extremely high.

The energy change involved in a transition between two different rotational states for a linear molecule (assuming the rigid rotor approximation) is given by,

$$E_f = BJ(J+1) \qquad [1.3]$$

where E_f =   energy of rotation

           J =   rotational quantum number

           B =   rotation constant

In essence the technique relies on the determination of the rotation constant, B, as it is this value that contains the structural information, since

$$B = \frac{\hbar}{4\pi I} \qquad [1.4]$$

where $\hbar$ =   Dirac's constant

           I =   moment of inertia, which in turn can be written

$$I = \Sigma_i m_i r_i^2 \qquad [1.5]$$

where m_i =   mass of atom i

         r_i =   perpendicular distance between atom i and the rotational axis

Therefore, if the moment of inertia can be determined from the rotation constant (which in turn is determined from the energy separation between rotational levels) and the accurate masses are known, structural information (r) can be obtained.

In addition to obtaining rotation constants from microwave spectroscopy, it is also possible to derive rotation constants directly from rotational Raman Spectroscopy, and indirectly from high resolution infra-red and Raman spectroscopies, where the rotational fine structure can be measured on the vibrational transitions.

1.3.2 Limitations

The major limitation to rotational spectroscopy as a structural technique is the amount of information that can be obtained for any one species. Although a molecule is free to rotate about an infinite number of axes through its centre of gravity, and thereby generate an infinite number of moments of inertia, in practice it is only possible to determine experimentally a maximum number of three, because all other rotations are linear combinations of these three. These values are referred to as the principal moments of inertia, and correspond to rotations about axes which are perpendicular to one other. It therefore follows that a maximum of only three rotation constants can be recorded for any one isotopic species, which in turn would enable only three geometric parameters to be determined. High symmetry in some compounds can lead to two or even all three rotations being the same, thereby reducing further the amount of structural information that can be obtained.

In principle, more rotation constants can be obtained by preparing isotopically substituted species of the parent compound. However, these compounds are often too expensive or time-consuming to prepare, or in the case of atoms such as fluorine and phosphorus impossible since alternative isotopes are not available. Even then the approach is based on the assumption that the effects of isotopic substitution on the structure of the molecule are negligible or can be calculated. For the most part the assumption represents a good approximation; however, bond lengths may vary

appreciably when lighter atoms such as hydrogen are involved. For accurate structural work allowances must be made for this effect by incorporating an extra parameter into the mathematical model describing the structure to account for this change in bond distance.

It is also worth noting that the positions of atoms which have the least effect on the moment of inertia will be the least well defined. From Equation 1.5, this is true for atoms which lie relatively close to one of the principal axes of rotation and for light atoms.

Finally, the range of compounds suitable for study by microwave rotational spectroscopy is limited to those that possess a permanent dipole. Although it is possible to investigate compounds without this property by rotational Raman spectroscopy or vibrational-rotational spectroscopy these techniques are extremely specialised and their use is not widespread.

1.4 Liquid Crystal NMR Spectroscopy[6]

1.4.1 Background

In conventional nuclear magnetic resonance (NMR) spectroscopy, spectra are recorded using isotropic solvents. Solute molecules are free to take up any orientation in the solvent and rotate rapidly with respect to the NMR timescale. The resulting spectra depend upon two factors: chemical shifts (ω) and indirect (or J) coupling constants, which arise due to the interaction of two nuclei primarily through chemical bonds.

There exists, however, another method for recording NMR spectra, which is of particular interest to the structural chemist. Liquid crystal solvents are generally composed of long aromatic chains which, under normal conditions, have a tendency to align over a short range. Provided the solvent molecules are magnetic, placing the

sample in a modest magnetic field (such as that experienced in a conventional NMR spectrometer) will cause all the local directors to align with one another, thus making the bulk sample anisotropic with one overall director. If the compound to be studied is dissolved in this type of solvent and the solution placed in a magnetic field, the solute molecules will be forced into planes between the aligned liquid crystal solvent molecules. Although the solvent molecules are still free to rotate rapidly, there is no longer an equal probability for all orientations; the molecules are said to be partially orientated. The resultant NMR spectra recorded for such a system will include not just the chemical shift (ω) and indirect coupling (J) but also direct coupling (D), arising due to interactions between two nuclei directly through space. This coupling can be described mathematically by the following equation,

$$D = -\frac{\mu_o \hbar \gamma_i \gamma_j}{8\pi^2} \cdot \frac{S_{ij}}{r_{ij}^3} \qquad [1.6]$$

Where μ_o = permittivity of a vacuum

$\hbar$ = Dirac's constant

γ_i, γ_j = magnetogyric ratios of atoms i and j

S_{ij} = orientation of atom pair ij in liquid crystal with respect to magnetic field of NMR spectrometer

(*i.e.* local orientation parameter)

r_{ij} = internuclear distance between atoms i and j

(*i.e.* structural information)

Direct coupling constants therefore depend solely upon two variables: the distance between the two coupling nuclei (r_{ij}) and the average orientation of the vector joining these nuclei with respect to the magnetic field of the spectrometer (S_{ij}). In normal isotropic solvents direct coupling is not observed since the free rapid rotation averages the couplings to zero, but in liquid crystal solvents the partial orientation of solute molecules enables these couplings to be measured.

The theory behind using LCNMR spectroscopy to obtain structural information therefore relies on determining the orientations of the coupling nuclear pairs in the liquid crystal solvent (S_{ij}) and evaluating all possible D couplings. These two factors will then allow bond distances (r_{ij}) to be obtained.

However, from Equation 1.6 it can be seen that for every direct coupling constant measured, there are two unknown variables (r_{ij} and S_{ij}), which means that neither structural nor orientational information can be determined explicitly. This problem can be circumvented, however, by describing the average orientation of the whole molecule by way of an orientation tensor (S), rather than explicitly describing the average orientation of each coupling nuclear pair, such that

$$S = \begin{bmatrix} S_{xx} & S_{xy} & S_{yz} \\ S_{yx} & S_{yy} & S_{yz} \\ S_{zx} & S_{zy} & S_{zz} \end{bmatrix} \quad [1.7]$$

Therefore, once the elements of the orientation tensor (S_{xx} *etc.*, the so-called orientation parameters) have been determined, any further dipolar couplings will yield structural information. The situation improves further when the symmetry of the molecule under investigation is taken into account, since as the symmetry increases certain orientation parameters become zero. For example, the molecule 1,3,5-triazine (reported in the following chapter) having D_{3h} symmetry requires only one orientation parameter (S_{zz}) to be defined in order to determine the orientation tensor (S).

1.4.2 Limitations

As with the previous two structural methods, LCNMR spectroscopy has several limitations which confine the usefulness of this method to certain categories of molecules. Firstly, if structural data obtained by this fluid phase technique are to be compatible with gas-phase data then, ideally, compounds to be studied should have a small, rigid framework since such systems are unlikely to undergo significant

molecular distortion in the solution phase compared to the gas. The choice of liquid crystal solvent is also of primary importance since if a large solute/solvent interaction occurs, significant structural deformation is likely. These factors are clearly of fundamental importance if the structural information obtained is to be consistent with a pure gas-phase structural determination.

One further practical consideration must be addressed in identifying suitable candidates for study by LCNMR spectroscopy. In general dipolar couplings can only be observed between nuclei with spin quantum number ½. In practice hydrogen nuclei tend to be of primary interest, and to a lesser degree carbon and nitrogen, due to the high natural abundance and large magnetogyric ratio of the ^{1}H isotope, compared to other nuclei. These factors result in very precise structural information for hydrogen atoms, but limited information for other nuclei. It should be noted that this method is therefore directly complementary to the two principal gas-phase techniques previously mentioned, which can locate heavy atoms with high precision, but light atoms relatively poorly, if at all.

Finally, it is important to realise that there are restrictions to the amount of structural information that can be determined from dipolar coupling values. For an experiment to yield any structural information (r) it follows that the number of measurable dipolar coupling constants (D) must exceed the number of independent orientation parameters required (S), since the evaluation of each orientation parameter requires one dipolar coupling constant. Furthermore, it follows from Equation 1.6 that absolute internuclear distances can never be obtained from dipolar couplings. The overall scale of a molecule cannot be separated from the magnitude of the orientation parameters. Ratios of distances (and hence angles) can be determined but if a complete, scaled structure is required then a scaling factor must be obtained by some other technique.

1.5 *Ab Initio* Molecular Orbital Calculations[7]

1.5.1 Background

The evolution of modern quantum theory and the developement of fast computers has made it possible to determine the electronic structures and properties of molecules mathematically. This has important consequences for the structural chemist, as it is now possible to calculate properties of molecules free from the effects of vibrational and rotational motion and other limitations experienced by experiment.

Ab initio molecular orbital theory, as the name suggests, is an attempt to understand atomic and molecular structure from first principles. Atoms and molecules are treated as collections of positive nuclei and negative electrons moving under the influence of Coulombic potentials, with no prior knowledge of the chemical behaviour of the species used. In 1926 Erwin Schrödinger developed an equation which describes molecular wavefunctions,

$$E\Psi = H\Psi \qquad\qquad [1.8]$$

where E = total molecular energy

                Ψ = total molecular wavefunction

                       (describing the positions of nuclei and electrons)

                H = Hamiltonian operator

                       (containing the electronic and nuclear potential and kinetic energy terms)

In practice it has only proved possible to obtain an exact solution to the Schrödinger equation for one-electron systems. It is therefore necessary to simplify both the Hamiltonian operator (H) and the molecular wavefunction (Ψ) so that an approximation to the solution can be obtained for larger systems.

The Born-Oppenheimer approximation can be used to simplify the calculation of the Hamiltonian. As nuclei are several orders of magnitude heavier than electrons they move considerably slower and to a good approximation can be regarded as stationary in the field of moving electrons. In effect the approximation partitions the Hamiltonian into nuclear and electronic energy components. Moreover, the kinetic energy of the nuclei is reduced to zero and the nuclear potential term can be replaced by a constant which is dependent only upon the fixed positions of the nuclei. This constant can be separated from the remaining Hamiltonian to leave only the electronic component to be considered further.

At the most basic level of theory, the Hartree-Fock (HF) or Self-Consistent Field (SCF) method, the Hamiltonian operator is then solved in terms of one electron only, and each electron in the system moves in a uniform electronic field generated by the other electrons present. This type of system provides an excellent starting geometry of the molecule under investigation and accounts for about 99% of the total energy of the molecule. However, the component of the energy which is missing relates to the omission of instantaneous electron-electron interactions. In reality electrons do not move in a uniform field, but are repelled by each other by electrostatic forces if they come too close together. The energy missing from the basic HF calculation is termed the electron correlation energy and it is non-zero when there is more than one electron in the system. A correlated wavefunction is therefore crucial for an accurate description for most types of chemical bonds.

Fortunately there exist many different techniques for extending the HF method to incorporate electron correlation effects, and most are based on a common theory. In short, the Hamiltonian operator is still solved in terms of one electron only but instead of allowing the second electron to occupy the same region of space as the first electron, it is positioned in a different orbit. That way the two electrons can still move independently of one another, in accordance with HF, but are prevented from coming too close together as they exist in different orbits. This is the underlying principle for

higher levels of theory, such as the Møller-Plesset (MP) perturbation series, configuration interaction (CI) and coupled cluster (CC) theories.

The molecular wavefunction (Ψ) is required to describe the motion of electrons around the fixed nuclei. The wavefunction is composed of a linear combination of gaussian-type functions and should ideally cover all space. Realistically, however, describing infinite space would require an infinite number of functions and so is intractable in practice. Instead, electron motion is restricted to certain regions described by a truncated series of gaussian functions, which is termed a *basis set*. Each atom in the molecule will require its own basis set, many examples of which exist in the literature. In practice, basis sets adopted for calculations range in size from single-ξ in which one function only is used to describe each occupied atomic orbital to very large basis sets at triple-ξ (or even quadruple-ξ) where each occupied atomic orbital is described by three (or four) functions. In general, the larger the basis set, the better the description of electron motion. A typical basis set used throughout this work is a double-ξ basis set 6-31G*, where six contracted functions describe the core *s* region of the atom, a further three and one contracted functions describe the valence *s* and *p* region, and one additional function (denoted by the *), allows for the possiblity of non-uniform displacement of charge away from the atom centres of heavy (*i.e.* non-hydrogen) atoms, the so-called polarisation function.

Solving the Schrödinger equation involves determining the total molecular energy (E) for the initial trial structure. Once this entity (and the molecular wavefunction) has been calculated all other molecular properties can be obtained. For example, calculating the first derivative of the energy with respect to each nuclear coordinate will allow the location of stationary points on the potential energy surface of the species to be determined, after a number of cycles of refinement. Each stationary point corresponds to a point of zero force on the surface, *i.e.* an optimised geometry. Calculating the second derivatives of the energy with respect to the nuclear coordinates at a stationary point will determine its nature as either a potential well (where a small displacement along any of the nuclear coordinates will increase the

total energy of the system) or a saddle point (where a small displacement in one or more directions will lower the total energy). The identification of a potential well on the energy surface therefore represents a kinetically stable, real structure, whereas a saddle point represents a kinetically unstable structure, such as a transition state. Calculating the second derivative of the energy also yields quadratic force constants, which can then be used to calculate normal modes of vibration. This type of calculation therefore not only determines whether a geometry optimisation represents a real structure, but also enables vibrational information to be obtained.

In principle the quality of the approximations made to the Hamiltionian operator and molecular wavefunction can be tested by undertaking a graded series of calculations in which the basis set and level of theory are systematically improved. As the quality of calculation improves parameters will be seen to converge to give a single geometry, which can be considered to be the true solution to the Schrödinger equation. In practice, it may not be possible to do calculations of sufficient sophistication to achieve convergence, and a compromise calculation may have to suffice.

1.5.2 Limitations

The last decade has seen major improvements in the field of computational chemistry, with rapid developments in both computer technology and software allowing much more sophisticated calculations to be performed than were previously possible. However, the major limiting factor for *ab initio* quantum chemistry still remains a problem of available computational power, with the number of atoms, structural parameters and symmetry all limiting factors in the type of calculations that can be performed. Even at the basic SCF level of theory calculations scale to the fourth power of the number of basis functions used to describe the system. Electron correlation methods, essential to obtaining accurate bond length predictions for most molecules, are more expensive to run with, for example, the second order Møller-Plesset (MP2) perturbation calculation used extensively throughout this work scaling to the fifth power of the number of basis functions in the system. Many of the

correlated methods, such as CCSD, QCISD or CCSD(T), also used in this work involve an iterative solution of a set of coupled equations which adds additional computational steps and tend to scale to the sixth, or in the case of CCSD(T) to the seventh, power of the number of basis functions. Currently the size of calculations we can perform on the DEC Alpha APX 1000 workstation at Edinburgh is limited to systems of about 400 basis functions at the SCF level, about 200 basis functions at MP2 and about half that number at higher levels, such as MP3 or QCISD. Computational chemists are therefore still restricted in the size of compounds and type of calculations they can perform.

1.6 Obtaining a complete structural refinement

Electron diffraction, rotational spectroscopy, liquid crystal NMR spectroscopy and *ab initio* molecular orbital theory are the principal techniques for determining molecular structure in the fluid phases. It has been demonstrated that each technique has its limitations and (except for theory) it is rare that any one method alone can give a complete structural determination for any but the simplest of compounds.

Electron diffraction data, taken in isolation, will often not give a complete structural refinement due to correlation effects between similar interatomic distances, and since in general hydrogen atoms cannot be located accurately. Microwave spectroscopy by itself is also often unable to define a structure completely due to the limited number of rotation constants that can be obtained for any one species. It is possible, however, to combine the two techniques, as suggested by Kuchitsu[8] to increase the amount of information available and therefore determine an improved structure. Moreover, further information can be obtained from LCNMR spectroscopic data, as suggested by Rankin,[9] providing information mostly concerning the positions of hydrogen atoms, the type of information generally missing from the GED and microwave spectroscopic data. This method of obtaining fluid-phase molecular structures is termed 'Combined Analysis' or 'STRADIVARIUS' (STRucture Analysis using DIffraction and VARIoUS other data) and represents the ideal approach, since all

data are experimental. The Combined Analysis technique is the focus of Chapter 2, where a more detailed account of this method is offered, illustrated by the determination of the molecular structure of 1,3,5-triazine.

However, it is often the case that this ideal cannot be obtained, simply due to a lack of sufficient additional non-electron diffraction data. An alternative methodology has therefore been developed, utilising *ab initio* molecular orbital calculations as the source of additional data required to complete the structural refinement. The development of this new approach, termed the SARACEN method (Structure Analysis Restrained by *Ab initio* Calculations for Electron DiffractioN),[10] has been a major part of the work undertaken for this thesis. A full, in-depth discussion of this new method is given in Chapter 3, illustrated by the determination of the structure of 2,5-dichloropyrimidine. Further examples of this new approach are presented in Chapter 4, where the structural determinations of 4,6-dichloropyrimidine, 2,6-dichloropyrazine and 3,6-dichloropyridazine in both the gaseous and crystalline states by diffraction methods and by *ab initio* calculations are described. Extensive structural work using the SARACEN method has also been carried out on a range of boron compounds, based on and including the parent compound tetraborane(10), with new gas and crystal-phase structures presented for this important *arachno* borane in Chapter 5. In Chapters 6 and 7 the gas-phase structures of the tetraborane(10) derivatives, $H_2MB_3H_8$ and $(CH_3)_2MB_3H_8$, where M represents one cage wing atom replaced by another Group 13 element, B, Al, Ga or In, are determined by *ab initio* calculations and, where possible, electron diffraction.

1.7 References

1.   I. Hargittai, *Stereochemical Applications of Gas-Phase Electron Diffraction*, Part A, eds. I. Hargittai & M. Hargittai, VCH, New York, 1988, Chapter 1.

2.   S. Cradock, J. Koprowski and D.W.H. Rankin, *J. Mol. Struct.*, 1981, **77**, 113.

3.   K. Kuchitsu, *Molecular Structures and Vibrations*, ed. S.J. Cyvin, Elsevier, Amsterdam, 1972, Chapter 10.

4.   L.S. Bartell, *Stereochemical Applications of Gas-Phase Electron Diffraction*, Part A, Chapter 2, eds. I. Hargittai & M. Hargittai, VCH, New York, 1988, **55**.

5.   E.A.V. Ebsworth, D.W.H. Rankin, S. Cradock, *Structural Methods in Inorganic Chemistry*, Chapter 4, Blackwell Scientific Publications, 1987.

6.   J.W. Emsley & J.C. Lindon, *NMR Spectroscopy using Liquid Crystal Solvents*, Pergamon Press, Oxford, 1975, 1.

7.   W.J. Hehre, L. Radom, P.v.R. Schleyer, J.A. Pople, *Ab Initio Molecular Orbital Theory*, John Wiley and Sons, Inc., 1986.

8.   K. Kuchitsu, T. Fukuyama and T.Morino, *J. Mol. Struct.*, 1967-1968, **1**, 463.

9.   S. Cradock, P.B. Liescheski, D.W.H. Rankin and H.E. Robertson, *J. Am. Chem. Soc.*, 1988, **110**, 2758.

10.   A.J. Blake, P.T. Brain, H. McNab, J. Miller, C.A. Morrison, S. Parsons, D.W.H. Rankin, H.E. Robertson, and B.A. Smart, *J. Phys. Chem.*, 1996, **100**, 12280; P.T. Brain, C.A. Morrison, S. Parsons and D.W.H. Rankin, *J. Chem. Soc., Dalton Trans.*, 1996, 4589.

Chapter 2

The Combined Analysis Method

2.1 Introduction

In the fluid phases, electron diffraction, rotational spectroscopy and liquid crystal NMR (LCNMR) spectroscopy are the major techniques for determining molecular structure. Like any experimental method, however, each has its limitations[1] (see Chapter 1) and so it is rare that any one method alone can give a complete structural determination for any but the simplest of compounds. It is therefore common practice to combine data from the three techniques to arrive at a final solution - the best structure based on all available experimental information.[2-4]

When combining data obtained by different experimental methods, and particularly for molecules in different phases, it is essential that the physical meaning of geometrical parameters is consistent, and that the structure in condensed phases is unaffected by neighbouring molecules. 1,3,5-triazine is a key molecule in this respect in that it is possible to determine its structure independently in gas, solution and solid phases, and by *ab initio* calculations. As it has only three structural parameters (rC-N, rC-H and <CNC), it is possible to refine the complete structure using only gas-phase data, and all but an overall scale factor using dipolar couplings derived from LCNMR spectra.[5] The validity of combining the data from the two techniques can thus be easily assessed.

In addition to the experimental structure determination, a series of *ab initio* molecular orbital calculations was carried out to determine the molecular geometry of 1,3,5-triazine, both for comparison with experimental methods and also to obtain a scaled harmonic force field (using the ASYM40 program[6]), which in turn was also compared with an experimental force field derived from infra-red spectroscopy.[7] The two force fields were found to be in excellent agreement, and both were used to obtain vibrational amplitudes adopted in GED structure analyses. Similarly, the vibrational corrections required to convert the rotation constants and dipolar couplings to an appropriate structural type to be included as additional structural information in the GED refinement were also obtained from the two force fields. Since the experimental force field is considered to be the more reliable of the two, the

final combined analysis refinement reported for 1,3,5-triazine was obtained using the experimentally determined vibrational correction values.

The study consists of two major parts, the first comprising single-method structural analyses, the second combined studies. In Section 2.3.1 three single-method structural studies based on *ab initio,* LCNMR spectroscopic data and GED data are presented. Section 2.3.2 presents two combined studies, in which the GED data are progressively supplemented with information obtained from infra red and LCNMR spectroscopy. The advantages of combining data in this manner are fully discussed. Finally, Section 2.4 offers a comparison of the gas-phase structure with some previous solid-phase structural results.[8]

2.2 Experimental

2.2.1 *Ab Initio* Calculations

Theoretical Methods: All calculations were carried out on a DEC Alpha APX 1000 workstation using the Gaussian suite of programs.[9-10]

Geometry Optimisations: A graded series of calculations was performed, from which the effects of improvement in basis set treatment and level of theory could be gauged. Geometry optimisations were performed using standard gradient techniques at the SCF level of theory using the 3-21G*,[11-13] 6-31G* [14-16] and 6-311G** [17-18] basis sets. The two larger basis sets were used for optimisations at the MP2(FC) level of theory. In order to investigate the effects of higher order correlation treatments, calculations using the 6-31G* basis set at the MP3(FC) and MP4SDQ(FC) levels of theory were also carried out.

Frequency Calculations: Vibrational frequency calculations were performed at the 3-21G*/SCF, 6-31G*/SCF and 6-31G*/MP2 levels to verify that 1,3,5-triazine has overall D_{3h} symmetry. The force constants obtained in the highest level calculation

were used in the construction of an harmonic force field using the ASYM40 program.[6] The force field was then successfully scaled against a set of experimental vibrational frequencies,[7] giving scale constants of 0.938, 0.956 and 0.919 for bond stretches, angle bends and torsions, respectively. The symmetry coordinates used to describe the various vibrational modes of the molecule in the construction of the force field are given in Table 2.1.

Table 2.1. Internal coordinates and symmetry coordinates for 1,3,5-triazine

(a) Internal coordinates

bond stretch		angle bend		out-of-plane bend	
R_1	N(1)-C(6)	α_1	C(6)-N(1)-C(2)	τ_1	C(6)-H(9)-N(5)-N(1)
R_2	C(6)-N(5)	α_2	N(5)-C(6)-N(1)	τ_2	C(4)-H(8)-N(3)-N(5)
R_3	N(5)-C(4)	α_3	C(4)-N(5)-C(6)	τ_3	C(2)-H(7)-N(1)-N(3)
R_4	C(4)-N(3)	α_4	N(3)-C(4)-N(5)	τ_4	C(6)-N(3)-C(4)-C(2)
R_5	N(3)-C(2)	α_5	C(2)-N(3)-C(4)	τ_5	C(4)-N(1)-C(2)-C(6)
R_6	C(2)-N(1)	α_6	N(1)-C(2)-N(3)	τ_6	C(2)-N(5)-C(6)-C(4)
R_7	C(6)-H(9)	α_7	H(9)-C(6)-N(1)		
R_8	C(4)-H(8)	α_8	H(9)-C(6)-N(1)		
R_9	C(2)-H(7)	α_9	H(8)-C(4)-N(5)		
		α_{10}	H(8)-C(4)-N(3)		
		α_{11}	H(7)-C(2)-N(3)		
		α_{12}	H(7)-C(2)-N(1)		

(b) Symmetry coordinates

species	symmetry coordinate	description
a_1'	$S_1 = R_7 + R_8 + R_9$	C-H symmetric stretch
	$S_2 = R_1 + R_2 + R_3 + R_4 + R_5 + R_6$	ring symmetric stretch
	$S_3 = \alpha_1 - \alpha_2 + \alpha_3 - \alpha_4 + \alpha_5 - \alpha_6$	ring bend
a_2'	$S_4 = R_1 - R_2 + R_3 - R_4 + R_5 - R_6$	ring asymmetric stretch
	$S_5 = \alpha_7 - \alpha_8 + \alpha_9 - \alpha_{10} + \alpha_{11} - \alpha_{12}$	H wag
a_2''	$S_6 = \tau_1 + \tau_2 + \tau_3$	H symmetric out-of-plane bend
	$S_7 = \tau_4 + \tau_5 + \tau_6$	N symmetric out-of-plane bend
e'	$S_8 = -R_7 + 2R_8 - R_9$	C-H asymetric stretch
	$S_9 = 2\alpha_1 - \alpha_3 - \alpha_5$	ring bend
	$S_{10} = 2\alpha_1 - \alpha_2 - \alpha_3 + 2\alpha_4 - \alpha_5 - \alpha_6$	ring bend
	$S_{11} = \alpha_7 - \alpha_8 - \alpha_{11} + \alpha_{12}$	H wag
	$S_{12} = -R_1 + 2R_2 - R_3 - R_4 + 2R_5 - R_6$	ring stretch
e''	$S_{13} = 2\tau_1 - \tau_2 - \tau_3$	H asymetric out-of-plane bend
	$S_{14} = 2\tau_4 - \tau_5 - \tau_6$	N asymetric out-of-plane bend

As mentioned previously, this scaled theoretical force field was found to be in excellent agreement with an experimental force field derived from infra-red spectroscopy[7] with, for example, vibrational amplitudes derived from the two force fields in agreement to within 0.5%. Similarly the vibrational corrections (given in Table 2.4) (required to convert the rotation constants and dipolar couplings to an appropriate structural type to be included as additional structural information in the GED refinement) were found to agree to within 10% on average. Since the experimental force field is considered to be the more reliable of the two force fields, the final combined analysis refinement reported for 1,3,5-triazine was performed using the experimentally determined vibrational correction values.

2.2.2 Gas-phase Electron Diffraction

Sample preparation: A sample of 1,3,5-triazine (97% pure) was purchased from the Aldrich Chemical Company and used without further purification.

Experiment: Electron scattering intensities were recorded on Kodak Electron Image photographic plates using the Edinburgh apparatus.[19] The sample was maintained at a temperature of 364 K and the nozzle at 387 K. The four plates (two from the long camera distance and two from the short distance) were traced digitally using a computer-controlled Joyce-Loebl MDM6 microdensitometer at the EPSRC Daresbury laboratory.[20] Standard programs were used for the data reduction[21] with the scattering factors of Ross *et al.*[22] The weighting points used in setting up the off-diagonal weight matrix, *s* range, scale factors, correlation parameters and electron wavelengths are given in Table 2.2.

GED Model: Assuming overall D_{3h} symmetry, just three parameters are needed to define the structure of the molecule: the C-N bond distance (p_1), the CNC ring angle (p_2) and the C-H bond distance (p_3). The molecular framework is shown in Figure 2.1.

Table 2.2. GED data analysis parameters

camera distance (mm)	weighting functions (nm^{-1})					correlation parameter	scale factor, k^a	electron wavelength[b] (pm)
	Δs	s_{min}	s_1	s_2	s_{max}			
95.46	4	68	80	304	356	0.3965	0.843(20)	5.680
260.06	2	20	40	130	150	0.2432	0.788(6)	5.680

[a] Figures in parentheses are the estimated standard deviations

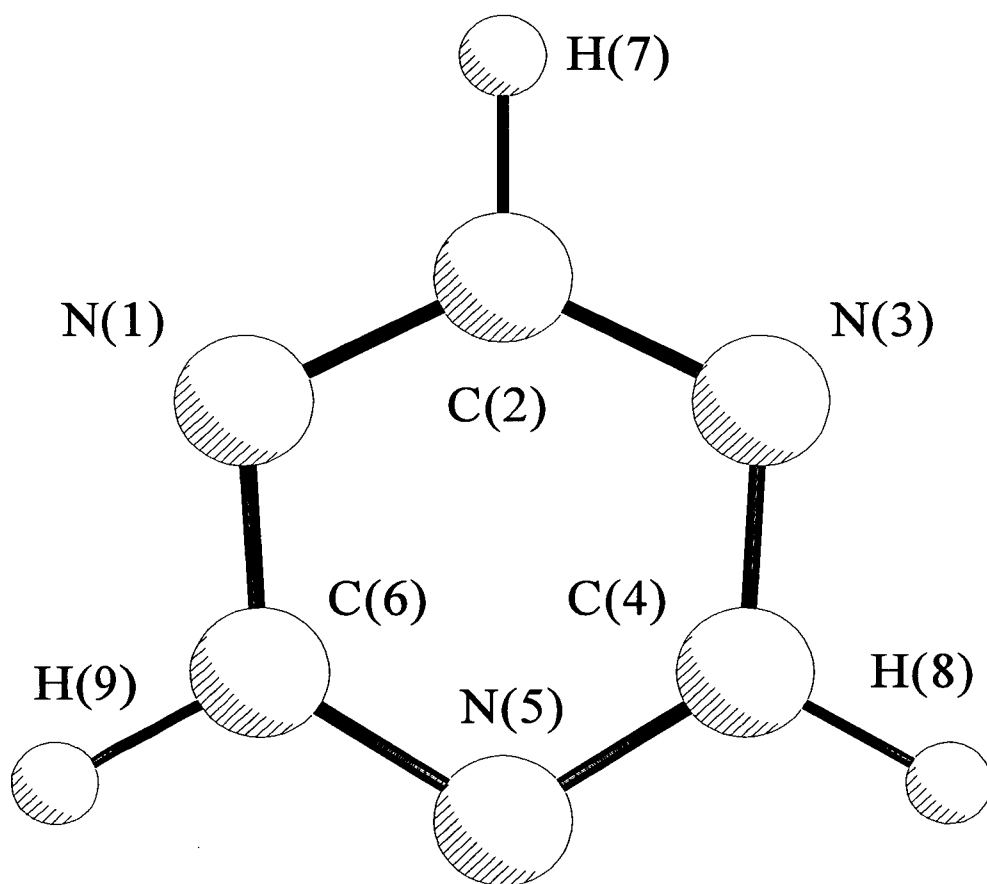[b] Determined by reference to the scattering patterns of benzene vapour

Figure 2.1 Molecular framework of 1,3,5-triazine

2.3 Results and Discussion

2.3.1 Single-Method Structural Analyses

2.3.1.1 *Ab Initio* Calculations

Geometry optimisations for 1,3,5-triazine were performed at seven levels in order to gauge the effects of improving the theoretical treatment upon the molecular geometry (see Table 2.3), and to compare the theoretical structures with those determined experimentally.

In general geometrical parameter values were largely unaffected by improvements in basis set and level of theory. The C-N bond distance proved to be insensitive to improvements in the basis set beyond 6-31G*; for example, at the SCF and MP2 levels increasing the size of the basis set to 6-311G** resulted in changes of just 0.1 and 0.2 pm, respectively. As expected, the inclusion of electron correlation was needed for an accurate description of C-N bonds,[23] with the bond distance increasing by around 2 pm when the effects of electron correlation were introduced at the MP2 level. To demonstrate that molecular parameters had converged with respect to improving both the quality of the basis set and the level of correlation, further geometry optimisations were undertaken at the MP3 and MP4SDQ levels using the 6-31G* basis set. These improvements did not result in a significant change in the C-N bond distance.

Excluding the results from the lowest level calculation, the range of predicted CNC bond angles was only 0.5°. Improving the basis set from 6-31G* to 6-311G** at both the SCF and MP2 levels resulted in no appreciable change and, similarly, the introduction of electron correlation at the MP2 level resulted in only a slight narrowing of the CNC angle, while higher levels of theory resulted in no further significant change.

31

Variations in the C-H distance were similar to those observed for the C-N distance; improvements in the basis sets beyond 6-31G* led to minor changes in the value of this parameter, while calculations at the MP2 level resulted in a slight lengthening of bonds. Further improvements in the correlation treatment to MP3 and MP4 resulted in changes in bond length of just 0.1 pm.

It has been demonstrated that all parameters for 1,3,5-triazine have successfully converged with respect to improvements in both the s,p basis and the level of electron correlation. Therefore further improvements in the size of basis set or treatment of electron correlation are unlikely to result in any appreciable change in parameter values.

Table 2.3. *Ab Initio* molecular geometries and energies (Hartrees) of 1,3,5-triazine (r_e /pm, </°)

parameter	3-21G*/SCF	6-31G*/SCF	6-311G**/SCF	6-31G*/MP2	6-31G*/MP3	6-31G*/MP4	6-311G**/MP2
bond lengths							
rC-N	133.01	131.80	131.68	134.07	133.55	133.85	133.87
rC-H	106.66	107.49	107.54	108.79	108.66	108.90	108.68
angle							
<CNC	116.45	114.39	114.39	114.00	114.05	113.89	113.90
energy	-277.101107	-278.695843	-278.756676	-279.538735	-279.547896	-279.558626	-279.653479

2.3.1.2 Liquid Crystal NMR Data Alone

A structural refinement based only on the five dipolar coupling constants of Marchal *et al.*[5] (values shown in Table 2.4) was performed to compare the solution-phase structure of $C_3N_3H_3$ with that found in the gas phase by GED, as documented below. The vibrational corrections required to convert the dipolar couplings from D_o to D_α (equivalent to the r_α^o GED structural type) were obtained from the experimental harmonic force field. Note that the vibrational corrections derived from the calculated force field are also given in Table 2.4 for comparison.

As 1,3,5-triazine has a three-fold axis, only one co-efficient $(S_{xx}=S_{yy}=-\frac{1}{2}S_{zz})$ is necessary to characterise the orientation of the molecule in the liquid crystal solvent. In analyses of LCNMR data, orientation parameters have unknown values. It is therefore normal practice to fix one or more geometrical parameters at assumed values, and to vary orientation parameters and remaining structural parameters to achieve an acceptable fit of calculated and observed coupling constants. In the present case, the orientation parameter was obtained in the combined analysis of GED and LCNMR data described below. This value was used as an additional observation in the LCNMR-only analysis, with its refined esd used as the uncertainty which defines the weight given to the extra observation.[4] The orientation parameter and all three structural parameters could then be refined simultaneously, giving esds which take into account the uncertainty in the orientation parameter. In effect, the scaling information has been derived from the GED data.

The structure derived from LCNMR data alone is presented in column one of Table 2.5. With the C-N distance refining to a value of 133.4(7) pm and the CNC angle to 114.2(11)°, the ring parameters for 1,3,5-triazine are not as well defined as in the GED refinement documented below. This result was expected since LCNMR spectroscopic measurements are limited to studying nuclei with spin quantum number ½. For the 1,3,5-triazine sample studied by Marchal *et al.*[5] dipolar couplings were observed between the nuclei ^1H, ^{15}N and ^{13}C without isotopic enrichment. Since

natural abundances for the two ring atom isotopes are only 0.4% and 1.1%, respectively, and the magnetogyric ratios for ^{15}N and ^{13}C are small compared to ^{1}H (only one tenth and one quarter of that of ^{1}H respectively), the accuracy of the ring atom positions is expected to be somewhat limited. In contrast, the natural abundance of the ^{1}H isotope is 100%. The structural information contained within the LCNMR dipolar couplings will therefore describe the positions of the hydrogen atoms more accurately than the ring atoms. This was indeed found to be the case; the C-H distance refined to a value of 108.9 pm, with an esd of just 0.2 pm.

The structure derived from the LCNMR data is insignificantly different from that calculated *ab initio*, with values for the two ring parameters in agreement to within one standard deviation and the C-H distance to within two standard deviations. This difference can be attributed to vibrational averaging effects in the experimental r_α^0 value, as opposed to the computed r_e distance.

The LCNMR data are thus complementary to the GED data, which provide information preferentially about the heavier ring atoms. Combining the two sets of data will therefore lead to a more accurate structure. This LCNMR-only analysis demonstrates that any distortion of the structure in solution is insignificantly small, and that the combination of different types of data is valid in this case.

Table 2.4. Rotation constants (B) and liquid crystal NMR spectroscopic dipolar couplings (D) for 1,3,5-triazine

constant	observed[a] (B_o/MHz or D_o/Hz)	harmonic correction[b] (MHz or Hz) Experimental force field	harmonic correction[c] (MHz or Hz) Theoretical force field	corrected (B_z/MHz or D_α/Hz)	calculated[d]	uncertainty[e]
rotation constants						
$B(H)$	6441.338(3)	-2.96	*-3.15*	6438.428	6438.769	0.3
$B(D)$	5809.083(25)	-1.93	*-2.19*	5807.153	5807.153	0.2
$B(^{13}C)$	6241.5938(18)	-2.87	*-3.04*	6238.7238	6238.708	0.3
$B(^{15}N)$	6218.032(4)	-2.85	*-3.03*	6215.182	6215.209	0.3
$B(^{13}C, {}^{15}N)$	6031.7019(27)	-2.75	*-2.92*	6028.9519	6028.599	0.3
dipolar couplings						
$D(1,7)$	80.0(6)	1.5	*1.6*	81.5	81.4	0.6
$D(2,7)$	-1300.0(6)	-91.2	*-79.3*	-1391.2	-1389.8	9.0
$D(4,7)$	-53.5(6)	-0.4	*-0.3*	-53.9	-53.3	0.6
$D(5,7)$	16.6(20)	0.1	*0.0*	16.7	13.6	2.0
$D(7,8)$	-100.3(6)	-0.8	*-0.7*	-101.1	-101.6	0.6

[a] From Ref. 5 and 7.

[b] Vibrational correction values used in final refinement.

[c] Vibrational corrections obtained from the scaled 6-31G*/MP2 *ab initio* force field, presented for comparison.

[d] From the final combined analysis refinement.

[e] Used to weight data in structure refinement; derived from experimental error plus a 10% uncertainty in the experimental harmonic correction to allow for anharmonic effects.

Table 2.5. Molecular structure ($r_a{}^o$) of 1,3,5-triazine (r/pm, $</°$)

parameter		results[a]			
		LCNMR data alone	GED data alone	GED + rotation constants	GED + rotation constants + LCNMR
structural					
p_1	rC-N	133.4(7)	133.94(10)	133.68(1)	133.68(1)
p_2	rC-H	108.92(20)	110.3(6)	108.94(19)	108.91(18)
p_3	<CNC	114.2(11)	113.9(2)	113.79(8)	113.82(9)
p_4	rC-H − rC-D	-	-	0.21(9)	0.20(8)
orientational					
p_5	S$_{zz}$	-0.1189(4)	-	-	-0.1189(5)
dependent					
	<NCN	125.8(11)	126.1(2)	126.21(8)	126.18(9)

[a] Figures in parentheses are estimated standard deviations

2.3.1.3 GED Data Alone

The purpose of this study of the molecular structure of 1,3,5-triazine in the gas phase was to demonstrate the benefits of including non-GED information in the structural analysis. For this reason three refinements have been undertaken using GED data. The first, using GED data alone, is described here. The results of the second and third refinements, incorporating first rotation constants and then dipolar couplings, are given in the following section.

The results from the GED data-only refinement are shown in column 2 of Table 2.5. The R_G factor of 6.0% indicates that the data are of good quality. The C-N distance refined to a value of 133.94(10) pm and the CNC angle to 113.9(2)°. The standard deviations recorded are extremely small, which is expected, since the ring can be fully described in terms of any two of the four independent ring distances. It is clear from the radial distribution curve obtained in the final refinement (see Figure 2.3) that

correlation effects between the individual distances are low. Thus, with all four ring distances well defined, the two parameters defining the ring should also be very well defined. The values obtained for the two parameters were also found to agree with those calculated *ab initio* at the 6-311G**/MP2 level to within one standard deviation. In contrast the C-H distance is less well defined, because hydrogen atoms contribute relatively little to the total scattering.

In addition to the three geometric parameters refining, four of the nine amplitudes of vibration were also refined successfully at this stage. These correspond to the four most prominent features on the radial distribution curve, namely u_1[N(1)-C(2)], u_3[N(1)...N(3)], u_5[C(2)...C(4)] and u_6[N(1)...C(4)]. The five remaining amplitudes of vibration which could not be refined all involved hydrogen atoms. These vibrational amplitudes were therefore fixed at values obtained from the experimental harmonic force field.

2.3.2 Combined Structural Analyses

2.3.2.1 GED Data + Rotation Constants

Five rotation constants of Pfeffer *et al.*,[7] measured from pure rotational FTIR spectra in the gas phase, were available for five different isotopomers of 1,3,5-triazine, namely the parent species, $^2H_3C_3N_3$, $H_3{}^{13}C_3N_3$, $H_3C_3{}^{15}N_3$ and $H_3{}^{13}C_3{}^{15}N_3$. The vibrational corrections necessary to convert the rotation constants from B_o to B_z structural type (which is equivalent to the $r_\alpha{}^o$ structural type derived from the GED refinement) were obtained from the experimental harmonic force field,[7] and compared to corrections obtained from the scaled *ab initio* 6-31G*/MP2 force field. The two sets of vibrational corrections were in general found to agree to within 10%. The experimental rotation constants, along with both sets of vibrational corrections and calculated rotation constants (based on the final structure reported in the next section), are given in Table 2.4. Note that the uncertainties used to weight the data

combine the experimental standard deviations with a conservative estimate of 10% error in the vibrational corrections to allow for anharmonic effects.

It is important to allow for the change in the C-H distance on deuteriation, so with the introduction of the rotation constants for the two isotopic species a fourth parameter, the difference between rC-H and rC-D, was incorporated into the model defining the structure. This parameter was assigned a predicate observation[24] of 0.2(1) pm to aid refinemen, with the value and uncertainty adopted from spectroscopic measurements.[25] Without the predicate obeservation in place this parameter refined to 0.25(22) pm, indicating the information contained within the rotation constants is concordant with values observed by spectroscopy. Calculated rotation constants were found to be in excellent agreement with the vibrationally corrected experimental values (see Table 2.4).

The results from this combined refinement are given in column three of Table 2.5. The addition of the five rotation constants was found to have a small effect on the overall geometry. The precision of all three geometric parameters was greatly improved, with the C-N distance determined to within 0.01 pm, rC-H to within 0.2 pm and <CNC to within 0.08°. Both rC-N and rC-H were found to shorten slightly with the inclusion of the extra data. In addition four extra amplitudes of vibration could now be refined, namely u_2[C(2)-H(7)], u_4[N(1)…H(7)], u_7[C(2)…H(8)] and u_9[N(1)…H(8)], giving a total of eight. The one vibrational parameter left unable to refine, amplitude u_8[H(7)…H(8)], corresponds to a feature whose intensity is just 0.4% of that of the most intense peak in the radial distribution curve and is therefore of very small weighting in the overall structural determination. The R_G factor rose slightly to 6.6%.

2.3.2.2 GED + Rotation Constants + Dipolar Couplings

To obtain the best possible structure in light of all available experimental information, the five dipolar couplings of Marchal *et al.* [5] were also included in the refinement.

The five new pieces of structure-related information resulted in only minor improvements in the quality of the final structure, the main effect being a slight improvement in the precision of four refining amplitudes of vibration u_2[C(2)-H(7)], u_4[N(1)...H(7)], u_7[C(2)...H(8)] and u_9[N(1)...H(8)]. This result was expected since the dipolar coupling constants mostly contain information relating to the hydrogen atom positions. The orientation parameter S_{zz} (p_5) was also now able to refine freely without the aid of the predicate observation. The experimental dipolar coupling values, vibrational corrections (both experimental and theoretical) and the calculated values based on the final structure obtained are reported in Table 2.4. The quoted uncertainties are a combination of experimental standard deviations with estimated 10% errors in the vibrational corrections to allow for anharmonic effects. From Table 2.4 it can be seen that all calculated dipolar couplings are in good agreement with the vibrationally corrected values; the poorest agreement is for D(5,7), which differs by just over one estimated standard deviation.

The results from this final combined analysis refinement are given in column 4 of Table 2.5; the final R_G factor was 6.7%. With all geometric parameters and all significant amplitudes of vibration refining the final standard deviations returned in the combined analysis refinement were found to be extremely small. The C-N distance refined to a final value of 133.68 pm, with a standard deviation of just 0.01 pm, the ring angle to 113.82(8)° and the C-H distance to 108.91(18) pm. Such high precision for the ring structure was obtained due to the high symmetry of the 1,3,5-triazine molecule, resulting in more peaks in the radial distribution curve than geometric parameters, and to the complementary nature of GED, rotational and LCNMR spectrocopic data, resulting in a better definition of the atom positions. The combined analysis thus yields a structure of unusual precision, particularly for a molecule with as many as nine atoms.

The experimental structure of free molecules in the gas/solution phases should be directly comparable to that calculated *ab initio*. In the case of 1,3,5-triazine the

agreement between the *ab initio* and the combined analysis structure is excellent. *Ab initio* calculations give the static equilibrium structure (r_e) for one discrete molecule, which should closely resemble the vibrationally averaged experimentally determined structure of the undistorted molecule, although there will be small systematic differences between the r_α° and r_e distances. For 1,3,5-triazine *ab initio* predicts a C-N bond distance of 133.87 pm and a CNC ring angle of 113.90°, compared to the experimental values of 133.68(1) pm and 113.82(9)°. Finally, the C-H bond distance was also found to be in close agreement by the two methods: 108.68 pm *ab initio*, 108.9(2) pm by experiment.

The full list of bond distances, along with the final vibrational amplitude values, is given in Table 2.6 and the covariance matrix in Table 2.7. The combined molecular scattering and difference curves, for the long and short camera distance plates, are given in Figure 2.2 and the final radial distribution and difference curves in Figure 2.3.

Table 2.6. Interatomic distances (r_a/pm) and amplitudes of vibration (u/pm) for the combined GED/rotation constants/LCNMR study of 1,3,5-triazine

i	atom pairs	distance	amplitude
1	N(1)-C(2)	133.7(1)	5.1(2)
2	C(2)-H(7)	110.2(2)	5.3(11)
3	N(1)...N(3)	238.4(1)	6.2(4)
4	N(1)...H(7)	207.3(1)	12.4(12)
5	C(2)...C(4)	224.0(1)	6.1(5)
6	N(1)...C(4)	266.9(1)	6.5(4)
7	C(2)...H(8)	323.0(2)	13.1(16)
8	H(7)...H(8)	413.0(3)	12.6[a] fixed
9	N(1)...H(8)	375.9(2)	12.0(29)

[a]Amplitude unable to refine is fixed at value derived from the experimental force field.

Table 2.7. Least-squares correlation matrix (x100) for the combined GED/rotation constants/LCNMR study of 1,3,5-triazine[a]

p_2	p_3	p_4	p_5	u_1	u_2	u_3	u_4	u_5	u_6	u_7	u_9	k_1	k_2	
-93	-15	-93	62	4	-4	-4	-3	-12	0	-1	3	17	5	p_1
	-17	**93**	**-62**	-4	3	-3	5	2	0	2	-2	-16	-3	p_2
		6	-1	-2	0	26	-6	29	-2	-1	0	-2	-3	p_3
			-60	-4	3	2	3	9	0	1	-2	-17	-4	p_4
				2	-2	0	-2	-5	0	-1	1	11	2	p_5
					3	17	9	17	16	-1	4	**49**	**69**	u_1
						-1	-2	0	-2	1	0	-10	-9	u_2
							52	**64**	14	2	-2	23	23	u_3
								42	-4	5	0	10	13	u_4
									5	1	-2	22	21	u_5
										-16	3	10	24	u_6
											-12	1	-2	u_7
												3	6	u_9
													40	k_1

[a] The most significant values are shown in **bold**. k is a scale factor
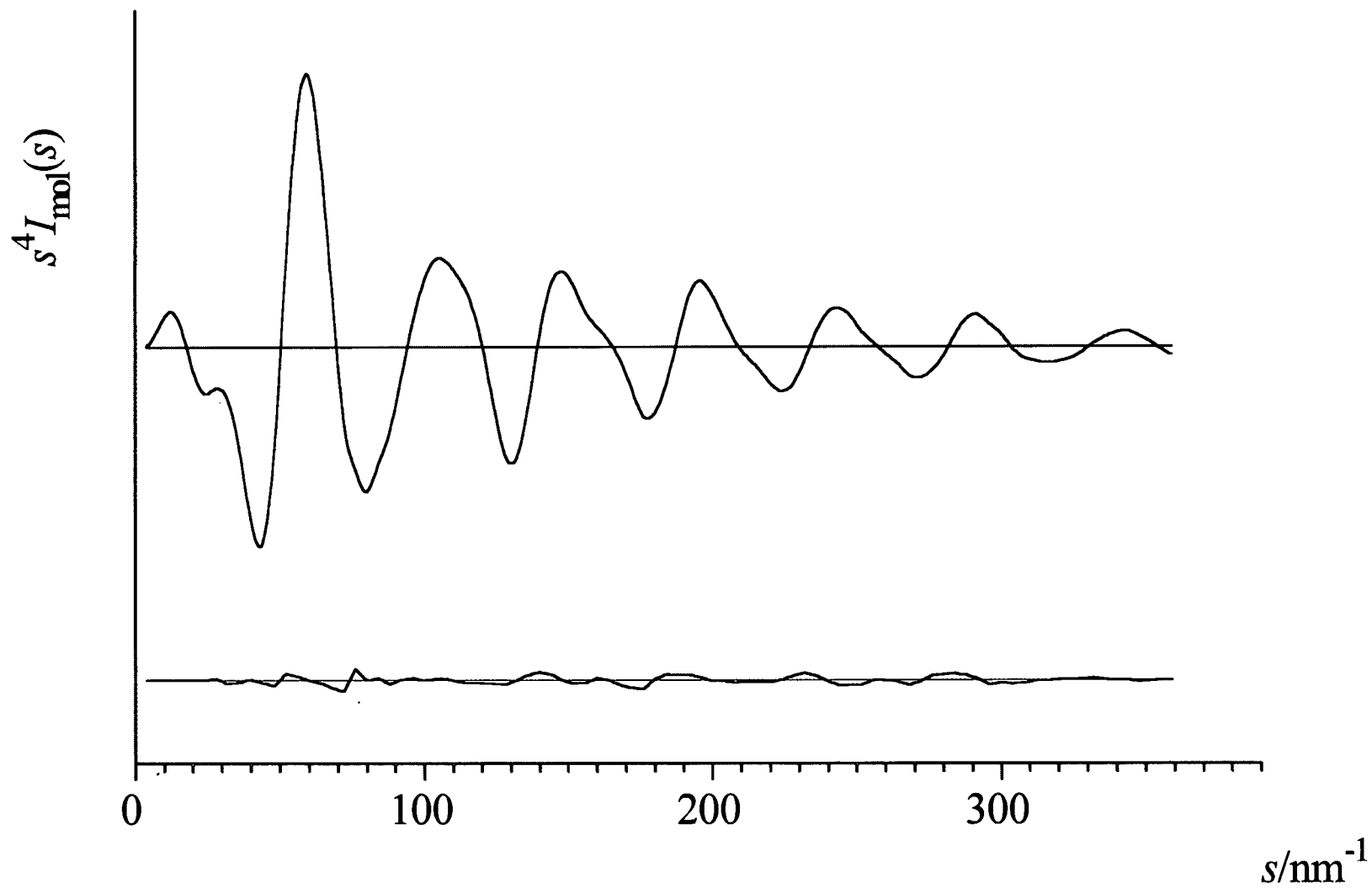
42

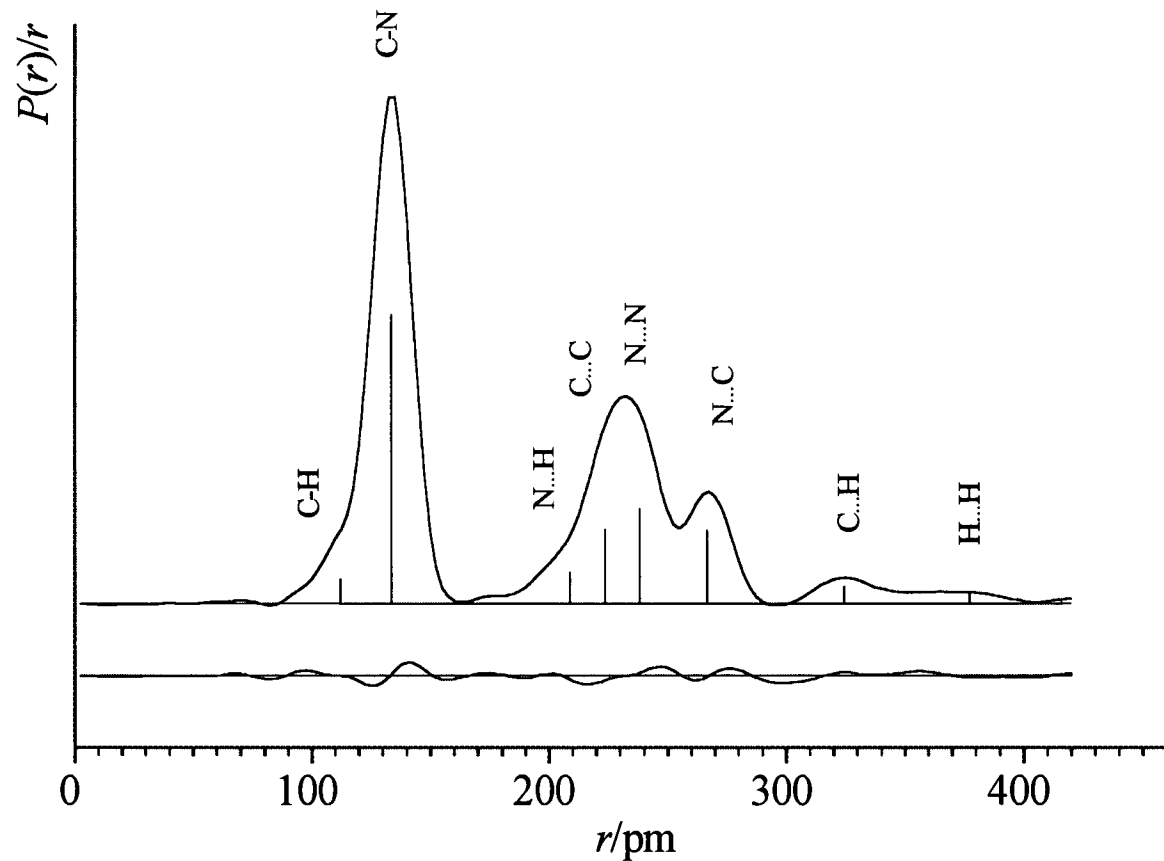Figure 2.2 Observed and final weighted difference molecular scattering curves for 1,3,5-triazine

43

Figure 2.3 Observed and final difference radial-distribution curves for 1,3,5-triazine.

Before Fourier inversion the data were multiplied by $s.\exp(-0.00002s^2)/(Z_C\text{-}f_C)(Z_N\text{-}f_N)$.

2.4 Comparison of Gas and Solid Phase Structures

Three independent crystal structure determinations of 1,3,5-triazine at 297-299 K have previously been reported by Coppins[8] using X-ray (both copper and molybdenum radiation sources) and neutron diffraction studies. The crystal possesses the space group $R\ \bar{3}c$. The crystal parameters, reported in Table 2.8, were not found to deviate from D_{3h} molecular symmetry. Individual C-N bond distances varied from 131.5 pm to 131.7 pm, about 2 pm shorter than that found in the gas phase, and the CNC ring angle from 113.4° by X-ray diffraction to 114.8° by neutron diffraction, compared to the gas phase angle of 113.82(9)°. The apparent ring contraction in the solid phase can be readily attributed to two factors. Firstly, there exists a difference in bond length definition between gas-phase electron diffraction and X-ray diffraction, with the former method measuring inter-nuclear distance and the latter the difference between centres of electron density. Secondly, vibrational averaging effects will be different for the two phases, as the two experiments were performed at different temperatures. Since neutron diffraction, like GED, measures inter-nuclear distances, correcting this structure for librational effects should result in a structure that is directly comparable to that observed in the gas-phase, provided there are no strong intermolecular interations in the solid phase giving rise to molecular distortion.

Table 2.8 Structural Parameters obtained for 1,3,5-triazine in the solid phase[8]

| | X-ray Crystallography | | Neutron Diffraction | | |
	Cu	Mo	uncorrected	librational correction[a]	corrected
rC-N	131.5	131.7	131.7	1.9	133.6
rC-H	-	-	104.5	1.4	105.9
<CNC	113.4	113.4	114.8	-0.1	114.7

[a] Ref. 26

The structure obtained by neutron diffraction after correcting for librational effects is given in Table 2.8 and also in Table 2.9, for comparison with structures obtained in the fluid phases and by *ab initio* calculations. From this it can be see that the C-N distance lengthens by about 2 pm to 133.6 pm, compared to the gas-phase structure of 133.68(1) pm, whilst the <CNC ring angle remains largely unaffected by the correction process. In effect, the ring contraction effect observed in the solid phase has been removed by the librational correction, with both the carbon and nitrogen atoms moving out from the centre of the ring by about 2 pm. The difference in internal ring angle of about 1° between the gas and the solid phases may be due to molecular packing effects.

Table 2.9 Comparison of the structural parameters for 1,3,5-triazine (r/pm, $</°$) in the three phases and calculated *ab initio*

		combined analysis (gas/solution phase)	LCNMR (solution phase)	neutron diffraction[a] (solid phase) 25°C	*ab initio* (6-311G**/MP2)
p_1	rC-N	133.68(1)	133.4(7)	133.6	133.87
p_2	rC-H	108.9(2)	108.9(2)	105.9	108.68
p_3	<CNC	113.82(9)	114.2(11)	114.7	113.90

[a] Corrected for librational effects, ref. 26.

2.5 Conclusion

The molecular structure of 1,3,5-triazine has been determined independently by *ab initio* calculations, gas-phase electron diffraction and liquid crystal NMR spectroscopy. All three methods yield structures which agree with one other to within one standard deviation. Thus the inclusion of solution phase data derived from LCNMR spectroscopy into the combined structural analysis is validated.

Combined analysis refinements were also undertaken with the GED data progressively supplemented with five rotation constants and five LCNMR dipolar couplings, resulting in a structure of greatly improved precision. It has been demonstrated that

the ring structure has been extremely well defined by the GED data due to low correlation effects between the four independent ring distances, but the C-H distance was less well defined by this method as a result of the poor electron scattering by hydrogen. In contrast, the structure derived from the LCNMR spectroscopic data defines the C-H distance precisely, with the ring less well defined. Agreement between experiment and theory is excellent.

2.6 References

1.   P. B. Liescheski and D.W.H. Rankin, *J. Mol. Struct.,* 1988, **178**, 227.

2.   B.T. Abdo, I.L. Alberts, C.J. Attfield, R.E. Banks, A.J. Blake, P.T. Brain, A. P. Cox, C. R. Pulham, D.W.H. Rankin, H.E. Robertson, V. Murtagh, A. Heppeler and C. A. Morrison, *J. Am. Chem. Soc.,* 1996, **118**, 209.

3.   L. Hedberg and K. Hedberg, *J. Phys. Chem.,* 1993, **97**, 10349.

4.   S. Cradock, P.B. Liescheski, D.W.H. Rankin and H.E. Robertson, *J. Am. Chem. Soc.,* 1988, **110**, 2758.

5.   J. P. Marchal and D. Canet, *J. Chem. Phys.,* 1977, **66**, 2566.

6.   ASYM40 version 3.0, update of program ASYM20. L. Hedberg and I.M. Mills, *J. Mol. Spectrosc.,* 1993, **160**, 117.

7.   M. Pfeffer, W. Bodemüller, R. Ruber, B. Macht, A. Ruoff and V. Typke, University of Ulm. Personal communication.

8.   P. Coppins, *Science* 1967, **158**, 1577.

9.   Gaussian 92, Revision F.4, M.J. Frish, G.W. Trucks, M. Head-Gordon, P.M.W. Gill, M.W. Wong, J.B. Foresman, B.G. Johnson, H.B. Schlegel, M.A. Robb, E.S. Replogle, R. Gomperts, J.L. Andres, K. Raghavachari, J.S. Binkley, C. Gonzalez, R.L. Martin, D.J. Fox, D.J. Defrees, J. Baker, J.J.P. Stewart, and J.A. Pople. Gaussian, Inc., Pittsburgh, PA. 1992.

10.   Gaussian 94, Revision C.2, M.J. Frisch, G.W. Trucks, H.B. Schlegel, P.M.W. Gill, B.G. Johnson, M.A. Robb, J.R. Cheeseman, T. Keith, G.A. Petersson, J.A. Montgomery, K. Raghavachari, M.A. Al-Laham, V.G. Zakrzewski, J.V. Ortiz, J.B. Foresman, J. Cioslowski, B.B. Stefanov, A. Nanayakkara, M. Challacombe, C.Y. Peng, P.Y. Ayala, W. Chen, M.W. Wong, J.L. Andres,

E.S. Replogle, R. Gomperts, R.L. Martin, D.J. Fox, J.S. Binkley, D.J. Defrees, J. Baker, J.P. Stewart, M. Head-Gordon, C. Gonzalez, and J.A. Pople. Gaussian, Inc., Pittsburgh, PA. **1995**.

11. J.S. Binkley, J.A. Pople and W.J. Hehre, *J. Am. Chem. Soc.,* 1980, **102**, 939.

12. M.S. Gordon, J.S. Binkley, J.A. Pople, W.J. Pietro and W.J. Hehre, *J. Am. Chem. Soc.,* 1982, **104**, 2797.

13. W.J. Pietro, M.M. Francl, W.J. Hehre, D.J. Defrees, J.A. Pople and J.S. Binkley, *J. Am. Chem. Soc.,* 1982, **104**, 5039.

14. W.J. Hehre, R. Ditchfield and J.A. Pople, *J. Chem. Phys.,* 1972, **56**, 2257.

15. P.C. Hariharan and J.A. Pople, *Theor. Chim. Acta* 1973, **28**, 213.

16. M.S. Gordon *Chem. Phys. Lett.,* 1980, **76**, 163.

17. A.D. McLean and G.S. Chandler, *J. Chem. Phys.,* 1980, **72**, 5639.

18. R. Krishnan, J.S. Binkley, R. Seeger and J.A. Pople, *J. Chem. Phys.,* 1980, **72**, 650.

19. C.M. Huntley, G.S. Laurenson and D.W.H. Rankin, *J. Chem. Soc., Dalton Trans.,* 1980, 954.

20. S. Cradock, J. Koprowski and D.W.H. Rankin, *J. Mol. Struct.,* 1981, **77**, 113.

21. A.S.F. Boyd, G.S. Laurenson and D.W.H. Rankin, *J. Mol. Struct.,* 1981, **71**, 217.

22. A.W. Ross, M. Fink and R. Hilderbrandt, *International Tables for Crystallography.* Ed. A.J.C. Wilson, Kluwer Academic Publishers: Dordrecht, The Netherlands, Boston, MA, and London, 1992, Vol. C, p 245.

23. W.J. Hehre, L. Radom, P.v.R. Scheyer and J. A. Pople, *Ab Initio Molecular Orbital Theory*, John Wiley and Sons, Inc. New York, 1986.

24. *Molecular Structure by Diffraction Methods,* Specialist Periodical Reports, The Chemical Society. 1975, p72.

25. *Molecular Structure by Diffraction Methods,* Specialist Periodical Reports, The Chemical Society. 1972, p191.

26. Dr. S. Parsons, University of Edinburgh. Personal communication.

Chapter 3

The SARACEN Method

3.1 Introduction

The problems associated with refining a molecular structure using gas-phase electron diffraction (GED) data alone are well known.[1] In particular, similar interatomic distances may be strongly correlated, and the positions of light atoms (particularly hydrogen) are poorly determined due to their low electron scattering ability. These problems often make it necessary to fix some parameters at assumed values. This is undesirable for two reasons, which are closely related. First, because this fixed parameter is tacitly assumed to be absolutely correct, its effect on other refining parameters cannot be gauged; secondly, fixing parameters can result in unrealistically low estimated standard deviations for correlated parameters.

It has been found that the inadequacies of GED data can, to some extent, be overcome by combining the data with those obtained by other structural techniques, particularly rotational spectroscopy and/or liquid crystal NMR (LCNMR) spectroscopy. Structures of many small compounds have been determined successfully using this combined approach. Examples include an array of chlorobenzenes[2-5] heteroaromatics,[1, 6-8] silyl compounds,[9, 10] perfluorocyclobutene[11] and N-chloroazetidine.[12]

Bartell also demonstrated[13] that estimates of geometrical parameters (so-called *predicate observations*) with their uncertainties, could be used in the same way as extra experimental observations to supplement GED data. Schäfer first supplemented GED data with *ab initio* data in a procedure described as *molecular orbital constrained electron diffraction* (MOCED),[14] whereby parameters (usually differences between related bond lengths or angles) which could not be refined are fixed at values calculated *ab initio*.

A new approach utilizing data obtained from *ab initio* calculations has now been proposed to allow the refinement of all geometric parameters, and it is the natural extension of these two methodologies. In essence this method, called the SARACEN (Structure Analysis Restrained by *Ab Initio* Calculations for Electron diffractioN)

method, hinges on two points: the use of calculated parameters as flexible restraints, instead of rigid constraints; and choosing to refine all geometrical parameters as a matter of principle.

For example, if two bond distances are correlated, the difference between the *ab initio* predictions for these distances can be added to the GED refinement as an extra observation. It is necessary to provide an estimate of the uncertainty associated with this new information. There is, of course, no standard deviation associated with a parameter calculated *ab initio,* so the estimated uncertainty must be subjective to some extent. It can be obtained by performing a series of *ab initio* calculations and observing the size of any changes as the quality of the calculations is improved, or it can be based on experience of the known accuracy of calculations at that level. In practice these restraints are introduced to the electron diffraction analysis by means of an extra subroutine defining appropriate parts of the structure, written at the end of the mathematical model which describes the structure. Extra observations concerning these parameters (whether from spectroscopic experiments, *ab initio* calculations or, for example, chemical intuition based on studying a series of closely related structures) can then be entered in the refinement in the usual way.

If the refined value for a parameter and its standard deviation turn out to be exactly the same as those entered as supplementary data it is clear that the experimental data contain no information regarding that parameter. In this case it is particularly important to take great care to ensure that the value of the additional datum and its uncertainty represent the most realistic estimates that can be made. If, however, the refined value is different, or its standard deviation is lower than the uncertainty of the extra observation, then information about this parameter is contained within the experimental data set. But even in the less favourable case, it is possible to refine all geometric parameters, and the resulting structure is the best obtainable in the light of all relevant information, experimental and theoretical, and all parameters have realistic standard deviations. Moreover, estimated standard deviations of other refining parameters may change. They may decrease as a consequence of the addition of extra

'observations', or they may increase, if they are correlated with parameters which are added to the refinement.

In this chapter the molecular structure of 2,5-dichloropyrimidine is used to illustrate this new procedure. The *ab initio* calculations performed are described in Section 3.3.1 and in addition a detailed discussion of the assignment of uncertainties to *ab initio* parameters is presented in Section 3.3.2. The limited structural refinement obtained using only the GED data is presented in Section 3.3.3, and the complete structural analysis based on a combination of GED data and *ab initio* restraints in Section 3.3.4. Finally the molecular structures obtained by the different techniques are compared in Section 3.4.

3.2 Experimental

3.2.1 *Ab Initio* Calculations

Theoretical Methods: Ab initio molecular orbital calculations were performed to predict geometrical parameters and to obtain a theoretical harmonic force field (using the ASYM40 program[15]) from which estimates of vibrational amplitudes could be obtained. All calculations were carried out on a DEC Alpha APX 1000 workstation using the Gaussian suite of programs.[16, 17]

Geometry Optimisations: A graded series of calculations was performed using standard gradient techniques at the SCF level of theory using the 3-21G,[18-20] 6-31G* [21-23] and 6-311G** [24, 25] basis sets. Subsequently the two larger basis sets were used for optimisations at the MP2(FC) level of theory. An additional calculation was undertaken at the 6-31+G*[21-23]/MP2 level to gauge the effects of diffuse functions on molecular parameters.

Frequency Calculations: Vibrational frequency calculations were performed at the 3-21G*/SCF and 6-31G*/SCF levels to verify that 2,5-dichloropyrimidine has C_{2v}

symmetry. The force field used in ASYM40 was constructed from the Cartesian force constants obtained from the 6-31G*/SCF calculation. Since no fully assigned vibrational spectrum was available for this molecule, an attempt was made to scale the force field using scaling factors 0.938 for bond stretches, 0.956 for angle bonds and 0.919 for torsions.[†] Scaling the force field was found to have little effect in the vibrational amplitude values.

3.2.2 Gas-Phase Electron Diffraction (GED)

Sample Preparation:[29] 2,5-Dichloropyrimidine was synthesised from 2-hydroxypyrimidine hydrochloride by treatment with aqueous chlorine solution.[30] Reaction of the product with phosphoryl chloride in the presence of N,N-dimethylaniline[31] gave the desired product in 40% yield. The sample was then purified by sublimation.

GED data: Electron diffraction data were captured on Kodak Electron Image photographic plates using the Edinburgh apparatus.[32] The sample was maintained at a temperature of 404 K whilst the nozzle was held at 460 K. The four plates (two from the long camera distance and two from the short distance) were traced digitally using a computer-controlled Joyce-Loebl MDM6 microdensitometer at the EPSRC Daresbury laboratory.[33] Standard programs were used for data reduction[33, 34] with the scattering factors of Ross *et al.*[35] The weighting points used in setting up the off-diagonal weight matrix, s range, scale factors, correlation parameters and electron wavelengths are given in Table 3.1.

[†] Scale constants were obtained from the successful scaling of the force field for 1,3,5-triazine against a set of experimental I.R. frequencies, as described in Chapter 2.

Table 3.1 GED Data Analysis Parameters

Camera distance (mm)	Weighting functions (nm^{-1})					Correlation parameter	Scale factor, k [a]	Electron wavelength[b] (pm)
	Δs	s_{min}	s_1	s_2	s_{max}			
95.44	4	80	100	304	356	0.1613	0.860(27)	5.707
255.56	2	20	40	140	164	0.4762	0.905(17)	5.710

[a] Figures in parentheses are the estimated standard deviations

[b] Determined by reference to the scattering patterns of benzene vapour

GED model: 2,5-Dichloropyrimidine was assumed to be planar with C_{2v} symmetry. Nine independent geometrical parameters were used to define the structure. With reference to the molecular frame shown in Figure 3.1, they are the average r(C-C)/r(C-N) ring distance (p_1), the difference between r(C-C) and the average r(C-N) distance (p_2), the difference between the two r(C-N) ring distances (p_3), the sum of and difference between the two r(C-Cl) distances (p_4 and p_5), r(C-H) (p_6), angle NCN (p_7), angle CNC (p_8) and angle NCH (p_9).
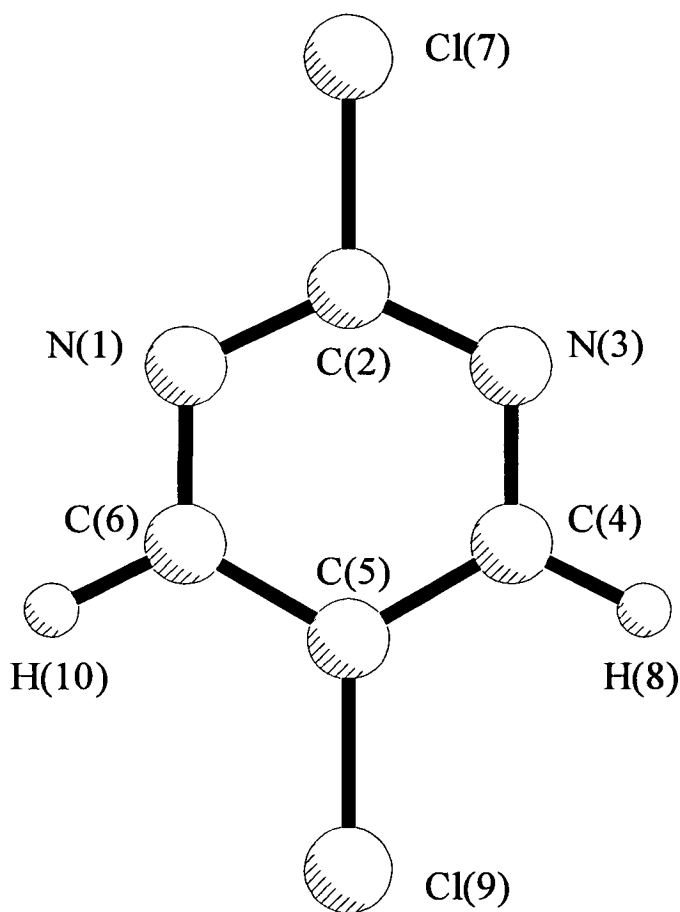

Figure 3.1 Molecular framework of 2,5-dichloropyrimidine

3.3 Results and Discussion

3.3.1 *Ab Initio* Calculations

Geometry optimisations were performed at six levels in order to gauge the effects of improving theoretical treatment upon the molecular geometry. The results are presented in Table 3.2. Calculated bond distances proved to be rather insensitive to the details of the basis set; improving the basis set from 3-21G* to 6-31G* at the SCF level of theory led to changes in bond distances which never exceeded 1 pm, while further improvements (to 6-311G*) led to smaller changes. As is characteristic of bonds which contain significant multiple-bond character, the inclusion of the effects of electron correlation at the MP2 level of theory led to a lengthening of ring bonds.[26] Bond angles were invariably found to be insensitive to the adopted theoretical treatment. If the results from the smallest of the basis sets (3-21G*) are excluded, calculated bond angles always fell within 1° of each other.

Table 3.2 *Ab Initio* molecular geometries and energies (Hartrees) of 2,5-dichloropyrimidine (r_e/pm, $</°$)

Parameter	Basis Set / Level of Theory					
	3-21G*/SCF	6-31G*/SCF	6-311G**/SCF	6-31G*/MP2	6-31+G*/MP2	6-311G**/MP2
Bond lengths						
rN(1)C(2)	132.0	131.0	130.8	133.6	133.8	133.4
rN(1)C(6)	133.0	131.9	131.7	134.1	134.2	133.8
rC(5)C(6)	138.0	138.1	137.9	139.4	139.5	139.5
rC(2)Cl(7)	172.0	172.6	172.9	172.9	172.6	172.8
rC(5)Cl(9)	172.8	172.8	173.0	172.4	172.4	172.1
rC(6)H(10)	106.8	107.4	107.5	108.8	108.8	108.7
Angles						
<NCN	124.8	127.3	127.4	127.8	127.6	127.9
<CNC	118.0	116.4	116.4	115.8	115.8	115.7
<NCC	120.9	121.6	121.5	121.6	121.7	121.7
<CCC	117.5	116.7	116.8	117.5	117.4	117.3
<NCH	117.6	117.1	117.2	117.0	116.8	117.2
Energy	-1174.839342	-1180.486148	-1180.587368	-1181.568795	-1181.585321	-1181.734489

3.3.2 Construction of Restraints; The SARACEN Method

The apparent convergence of molecular parameters with respect to improvements in the theoretical treatment suggest that restraints which are needed to allow refinement of all structural parameters for 2,5-dichloropyrimidine should be reliable. The values of restraints were always chosen to be those calculated at the 6-311G**/MP2 level and uncertainties estimated by considering the variations in calculated parameters as the level of theory was improved, with heavier weighting being placed on the higher level calculations. At these high levels of theory it is unlikely that there are significant systematic errors for a molecule of this kind, but it is wise to be conservative in estimating the uncertainties to avoid over-weighting the theoretical restraints. The values of the restraints used in the GED refinement are presented in Table 3.3.

The difference between the two C-N bond distances, parameter 3, was given a value of 0.4 pm and an uncertainty of 0.5 pm; the uncertainty was chosen so that it encompassed all estimates using the two largest basis sets. Parameter 5, describing the difference between the two C-Cl bond lengths, was given the value -0.7 pm and an uncertainty of 0.5 pm, which was derived from the MP2 level calculations only. Parameter 6 (the C-H distance) required a different type of restraint. Restraints for parameters 3 and 5 have involved differences between r_e bonds (r_e signifying the equilibrium bond length as calculated by *ab initio*). This value was used directly in the GED r_α refinement (which represents a vibrationally averaged structure), because the differences between two bonds are largely independent of the structure type (*i.e.* r_e or r_α). However, if the absolute value of a bond distance computed *ab initio* is used in the GED refinement without vibrational correction, a larger uncertainty should be used to allow for any discrepancies due to the difference in structural type. Parameter 6 was therefore chosen to be 108.7 pm with an uncertainty of 1.5 pm. Parameter 9 (the NCH angle) was taken to have a value of 117.2° with an uncertainty of 0.5°. This uncertainty is somewhat larger than is needed to encompass the values obtained using the 6-31G* and 6-311G** basis sets, but it is chosen to allow for small differences in this parameter due to vibrational averaging in the GED refinement.

Table 3.3 Derivation of Geometric Parameter Restraints (r/pm, $</°$)

Parameter	3-21G*/ SCF	6-31G*/ SCF	6-311G**/ SCF	6-31G*/ MP2	6-31+G*/ MP2	6-311G**/ MP2	Value used
rN(1)C(6) - rN(1)C(2)	1.0	0.8	0.9	0.4	0.5	0.4	0.4(5)
rC(5)Cl(9) - rC(2)Cl(7)	0.1	0.2	0.1	-0.6	-0.2	-0.7	-0.7(5)
rCH	106.8	107.4	107.5	108.8	108.8	108.7	108.7(15)
<NCH	117.6	117.1	117.2	117.0	116.8	117.2	117.2(5)

It can be seen that in the case of 2,5-dichloropyrimidine, the calculated ring bond differences change little even though the absolute values of these bond lengths are altered by the inclusion of the effects of electron correlation. This result is not surprising since the electronic environments found in the C-C and C-N bonds are not dissimilar; both have a bond order of approximately 1.5. Consequently, it is expected that changes in bond lengths due to either an incomplete basis set or the neglect of electron correlation will be very similar for both bonds. Although there is a significant change in the absolute value of the bond lengths the difference remains largely unchanged; for example estimates of the difference between the two C-N ring bonds fall across a range of only 0.6 pm, while the absolute values of the two bond lengths vary by at least 2.5 pm. In general, when electronically similar bonds are correlated in the GED refinement reliable estimates of the difference in bond lengths should be obtained, even at modest levels of theory.

Assigning values for the difference between two bond lengths and the associated uncertainty becomes much more problematic when electronically dissimilar bonds are considered. Under these circumstances, the limitations of the theoretical treatment may have different effects on the two bonds concerned, and hence the difference between the bond distances may change substantially with improvements in the theoretical method. In particular, electron correlation is known to be important for describing multiple bonds or bonds between atoms which contain lone pairs. Thus, although a predicted C-N bond distance is expected to be essentially unaffected by electron correlation, a C=C double bond or an N-O or N-F bond is almost certain to become longer when the effects of electron correlation are included.[23]

Unfortunately, there is a necessary degree of subjectivity in choosing both restraint parameter values and their uncertainties. For this reason a series of guidelines based upon different computational resources for estimating bond differences and uncertainties has been suggested:

1. Restraints should preferably be applied to differences between electronically similar bond distances or angles, rather than to absolute values of structural parameters.

2. Ideally a graded series of calculations in which both the size of the basis set and the level of theory are varied should be performed. A series of calculations of this type should allow the effects of improving both basis set and level of theory to be gauged with confidence and hence allow reliable estimates of structural parameters and their uncertainties to be obtained.

3. When ambitious calculations of the type described in 2 are beyond available resources, one must rely on experience of calculations at various levels to assess their reliability. Calculations using basis sets of double-ζ plus polarisation quality (for example 6-31G*, or the double-ζ basis sets of Dunning[27]) at the MP2 level of theory should allow satisfactory estimates of differences in most instances, even when comparing bonds which are electronically dissimilar. However, particular care should be taken if the molecule contains O-F, O-O or N-F bonds since it is well established that bonds between electronegative elements are particularly sensitive to the level of correlation.[26]

4. In cases where calculations are restricted to the SCF level of theory, differences will in general be reliable if bonds are electronically similar, although care is urged when distances between two electron-rich atoms or two highly electronegative atoms are involved. Extreme caution should be taken when the lengths of electronically dissimilar bonds are correlated in the GED refinement. In cases such as these it may be that more reliable estimates of bond length differences can be obtained by estimating the effects of electron correlation from reported bonds of the same type in other systems. Clearly the value of both the restraint and its uncertainty need to be chosen carefully in this case.

5. Uncertainties in restraints of this type should always be set too high rather than too low. This method is intended to allow the maximum information to be extracted from experimental data. Over-tight restraints will always guarantee that the results agree with the theory, regardless of the experimental evidence: this pitfall must be avoided at all costs.

6. When restraints have to be applied to angles (or angle differences), caution is again urged in the size of uncertainty adopted, since an over-tight restraint can result in a geometric parameter value with an unrealistically small standard deviation. In work presented in this thesis angle restraint uncertainties of the order 1° have typically been adopted.

It is worth mentioning at this stage that the use of restraints need not be confined to the independent parameters used to define the structure. It could equally well be applied to a specific bond distance, for example the C-C distance in 2,5-dichloropyrimidine, which is not defined as a independent parameter in the model. In principle restraints can also be applied to vibrational amplitudes; however, calculated force constants obtained *ab initio* are subject to systematic errors which must be reduced by application of empirical or refined scale factors.[28] For this reason care must be taken. Two methods are available:

1. A restraint is applied directly to a specific vibrational amplitude. In such a case it is recommended that an uncertainty of at least 10% be adopted.

2. Preferably, a restraint is applied to the ratio of the amplitudes of vibration for two atom pairs which are electronically similar and whose interatomic distances lie very close together. Since *ab initio* force fields are more accurate at determining ratios of vibrational amplitudes, rather than their absolute values, the use of a lower uncertainty (of the order of 5%) is recommended for such cases. For example, in the case of 2,5-dichloropyrimidine, this method would be suitable for restraining ratios of vibrational amplitudes for C-C and C-N bonds, but less suitable for pairing C-Cl with C-C, C-N or C-H bonds, because of the strongly differing electronic environments, which may be more or less affected by the use of a finite basis set and an incomplete description of electron correlation.

In 2,5-dichloropyrimidine several restraints were applied to vibrational amplitude ratios and values. With reference to Table 3.4 (and Table 3.7 on page 70, where a full bond listing is given) bond distances were grouped together in the following way:

1. Restraints were placed on the three amplitudes of vibration for the ring bonded distances. All three amplitudes were allowed to refine freely but the ratios of u_2 [N(1)-C(2)] and u_3[C(5)-C(6)] to u_1[N(1)-C(6)] were restrained.

2. The two C-Cl bond distance amplitudes refined, with the ratio u_5 to u_4 restrained.

3. The two-bond ring distances were grouped, so that the ratios u_7/u_8 and u_{12}/u_8 were restrained. The remaining two-bond ring distance, C(2)...C(6), was treated separately since it was shorter than the rest of the group by more than 10 pm. This amplitude u_{11}, was therefore restrained directly. All four amplitudes refined.

4. The two-bond N(C)...Cl distances refined freely, with the ratio u_{13}/u_9 restrained.

5. The two three-bond ring distances refined with the ratio u_{17}/u_{15} restrained. In this case it was found that u_{15} also had to be directly restrained to give a meaningful refinement.

6. The three-bond N(C)...Cl distances refined, with u_{19}/u_{16} restrained.

7. Finally, the two four-bond C...Cl distances refined, with u_{26}/u_{23} restrained.

Table 3.4 Derivation of Vibrational Amplitude Restraints

Amplitude Ratio	Value[a]	Uncertainty[b]
u_2[N(1)-C(2)]/u_1[N(1)-C(6)]	1.015	0.051
u_3[C(5)-C(6)]/u_1	1.047	0.052
u_4[C(2)-Cl(7)]/u_5[C(5)-Cl(9)]	0.992	0.050
u_7[N(1)...N(3)]/u_8[N(1)...C(5)]	0.957	0.048
u_{12}[C(4)...C(6)]/u_8	1.001	0.050
u_{11}[C(2)...C(6)]	4.991	0.499
u_{13}[C(4)...Cl(9)]/u_9[N(1)...Cl(7)]	1.081	0.054
u_{17}[C(2)...C(5)]/u_{15}[N(1)...C(4)]	0.960	0.048
u_{15}[N(1)...C(4)]	5.665	0.566
u_{19}[C(4)...Cl(7)]/u_{16}[N(1)...Cl(9)]	0.976	0.049
u_{26}[C(5)...Cl(7)]/u_{23}[C(2)...Cl(9)]	1.001	0.050

[a] Values taken from 6-31G*/SCF scaled force field.

[b] Uncertainties are 5% of the amplitude ratio value; 10% of absolute value applied directly to one atom pair.

It will be shown in Section 3.3.3.2 that with the introduction of these eleven vibrational amplitude restraints the amplitude of each distance giving rise to a feature larger than 10% of the most intense component peak of the radial distribution curve could refine independently, giving values in good agreement with the *ab initio* force field.

3.3.3 Gas-Phase Electron Diffraction (GED)

3.3.3.1 GED Data Alone

The r_α^0 structural parameters determined from the GED data alone are given in the first data column of Table 3.5. As expected the three distinct ring bond distances $r[N(1)-C(2)]$, $r[N(1)-C(6)]$ and $r[C(5)-C(6)]$ could not all be refined because they were strongly correlated, and so parameter 3 was fixed at the calculated 6-311G**/MP2 *ab initio* value. The difference between the two C-Cl bond lengths could also not be determined: parameter 5 was therefore fixed at the *ab initio* value from the same calculation. Finally, the data set contained little information regarding the positions of the two hydrogen atoms, so parameters 6 and 9 were also fixed at the 6-311G**/MP2 *ab initio* values.

Table 3.5 Structure (r_α^0) of 2,5-dichloropyrimidine (r/pm, $</^\circ$). Estimated standard deviations, obtained in the least-squares refinement, are given in parentheses.

Parameter		Results	
		GED data alone	GED + restraints
Independent			
p_1	$[r\text{N}(1)\text{C}(2) + r\text{N}(1)\text{C}(6) + r\text{C}(5)\text{C}(6)]/3$	134.8(2)	135.0(2)
p_2	$r\text{C}(5)\text{C}(6) - [r\text{N}(1)\text{C}(2) + r\text{N}(1)\text{C}(6)]/2$	5.4(15)	6.4(15)
p_3	$r\text{N}(1)\text{C}(6) - r\text{N}(1)\text{C}(2)$	0.4 (fixed)	0.6(4)
p_4	$[r\text{C}(5)\text{Cl}(9) + r\text{C}(2)\text{Cl}(7)]/2$	172.5(2)	172.5(2)
p_5	$r\text{C}(5)\text{Cl}(9) - r\text{C}(2)\text{Cl}(7)$	-0.7 (fixed)	-0.6(5)
p_6	$r\text{CH}$	108.7 (fixed)	109.9(12)
p_7	$<\text{NCN}$	127.4(4)	127.9(4)
p_8	$<\text{CNC}$	116.1(7)	116.3(7)
p_9	$<\text{NCH}$	117.2 (fixed)	117.2(5)
Dependent			
	$<\text{NCC}$	121.3(9)	120.6(8)
	$<\text{CCC}$	117.9(7)	118.3(6)
	$r\text{CC}$	138.5(12)	139.3(11)
	$r\text{N}(1)\text{C}(6)$	133.3(3)	133.2(4)
	$r\text{N}(1)\text{C}(2)$	132.8(3)	132.5(5)
	$r\text{C}(5)\text{Cl}(9)$	172.1(2)	172.2(3)
	$r\text{C}(2)\text{Cl}(7)$	172.8(2)	172.8(3)

The average ring bond distance (parameter 1) was found to be 134.8(2) pm and as the small uncertainty suggests, this value is determined to a high degree of accuracy. However, it is the individual bond distances, rather than the average, which are of most interest. To obtain all three of the distances in the ring separately it is necessary to include parameters 2 and 3 in the refinement. Parameter 2, describing the difference between the C-C and average C-N bond distances, refined to 5.4(15)pm; the difference between the two C-N bond lengths (defined by parameter 3) was kept fixed at 0.4 pm at this stage. The three ring distances were thus found to be 138.5(12) pm, 133.3(3) and 132.8(3) pm for the C-C and two C-N bonds respectively. The average C-Cl bond distance (parameter 4) refined satisfactorily to 172.5(2) pm, but the difference between the two bonds (parameter 5) had to be fixed at -0.7 pm. With this parameter fixed the quoted uncertainty for each of the individual bond distances must be identical to that of the average distance. The individual values and uncertainties for the two bonds were therefore 172.1(2) pm and 172.8(2) pm. Clearly, uncertainties of 0.2 pm are too small since there is insufficient information to allow the refinement of the two parameters which define them.

There is no straightforward way to obtain reliable uncertainties using this method and so inevitably those which are reported are too small. Electron diffraction alone cannot lead to a set of structural parameters which are both reliable and have realistic uncertainties. It will be shown in the next section that the introduction of restraints enables more realistic errors to be obtained, and hence more reliable structures to be derived.

3.3.3.2 Restrained GED results

The introduction of the four independent parameter restraints presented in Table 3.3 allowed all nine independent geometric parameters to refine. In addition the eleven vibrational amplitude restraints described in Table 3.4 permitted amplitudes to refine for all eighteen distances responsible for features greater than 10% of the most intense component peak in the radial distribution curve. The final structural parameters

obtained are given in column 2 of Table 3.5 along with the results based on the GED data alone for direct comparison. In general, the introduction of restraints and refinement of additional parameters led in this case to only modest changes (up to just over one standard deviation) in the values of the independent parameters which had already been refined. For example, the average ring bond distance changed by just 0.2 pm to 135.0(2) pm, whilst parameter 2 changed by 1 pm to 6.4(15) pm. The two parameters defining ring angles (parameters 7 and 8) changed by no more than 0.5° to 127.9(4)° and 116.3(7)° respectively. In all four cases standard deviations remained unchanged.

Several specific points are worth noting about the consequences of introducing restraints:

1. Parameter 3, describing the difference between the two C-N bond distances refined to 0.6(4) pm , which is different from the *ab initio* restraint of 0.4(5) pm, but lies well within the uncertainty limit. This demonstrates that the restraint was indeed flexible. Some information about this parameter must have been present in the GED data, but it was not sufficient to allow this parameter to refine unassisted. The introduction of the restraint permitted this information to be retrieved. With all three parameters describing the ring distances now refining, standard deviations for individual distances were expected to increase. This was found to be the case for the two C-N bonds, with final values 133.2(4) pm and 132.5(5) pm. However, the standard deviation for the C-C bond distance fell by 0.1 pm as this parameter refined to 139.3(11) pm.

2. Similarly, parameter 5 refined to -0.6(5) pm as compared to its restraint of -0.7(5) pm. With this parameter now refining the absolute values of the two C-Cl bond distances changed by no more than 0.1 pm and standard deviations rose from 0.2 pm to 0.3 pm.

3. Parameter 6, the C-H distance, refined to 109.9(12) pm. This differs from the value used as a restraint [108.7(15) pm] but lies within its uncertainty limit. As in the cases given above this indicates that some information about this parameter was contained within the experimental data set. However, if this parameter is not

restrained in the suggested way the bond distance refines to 120(3) pm, which is obviously an unreliable value.

4. Parameter 9, the NCH angle, refined to $117.2(5)°$, in exact agreement with its *ab initio* restraint. Clearly the GED data contained no information about this parameter. Special care is needed in choosing such a restraint since the GED refinement will always echo the *ab initio* result, but nevertheless this situation is still an improvement on the earlier method (*i.e.* using fixed constraints) since the uncertainty suggested by the restraint generates the same realistic uncertainty (*i.e.* standard deviation) in the GED refinement, rather than an artificial uncertainty of zero. Moreover, the effects of uncertainty in this parameter are now included in standard deviations for other parameters with which it may be correlated, and so these standard deviations are more reliable.

5. The eleven vibrational amplitude restraints enabled the amplitudes for the eighteen most significant interatomic distances to refine. Refined amplitudes gave values well within the uncertainties of the applied restraints in all but one case, with u_{13}/u_9 just falling outwith the 5% uncertainty range.

The final least-squares correlation matrix, presented in Table 3.6, highlights another important feature relating to the use of restraints. In addition to giving realistic uncertainties, the introduction of restraints results in greatly reduced correlations between parameters in the GED refinement. With the restraints in place only thirty-six incidences of correlation between refining parameters higher than 50% were found, with a total of twenty-nine parameters refining. In contrast, when a refinement was performed with the same parameters and amplitudes refining, but with the restraints removed, the number of such incidences rose to fifty-one. This is, of course, expected, since each restraint will enable a previously unrefinable parameter (or amplitude) to refine, or in other words, to become less dependent on other parameters. Since high correlation between parameters is often the cause of a parameter failing to refine properly, use of restraints can be a useful technique to relieve high correlation effects found in some GED mathematical models.

Table 3.6 Least-squares correlation matrix for 2,5-dichloropyrimidine.

All elements are scaled by a factor of 100, and only off-diagonal elements with absolute values >50% are included.

	Parameter		Amplitude											
	p_2	p_8	u_1	u_2	u_3	u_5	u_8	u_9	u_{12}	u_{13}	u_{17}	u_{19}	u_{26}	$k_2{}^a$
p_1	74	65	-60	-63	-53			-68		-64				
p_2		81	-87	-85	-84			-81		-77				
p_8			-73	-72	-70			-53						
u_1				93	94			75		73				
u_2					89			74		72				
u_3								72		70				
u_4						78								56
u_5														56
u_7							83		69					
u_8									84					
u_9										92				
u_{15}											86			
u_{16}												78		
u_{23}													82	

^{a} k is a scale factor

69

The complete list of interatomic distances (r_a structure) and amplitudes of vibration determined in this final refinement is given in Table 3.7. In addition, the combined molecular scattering intensities and final differences are shown in Figure 3.2 and the radial distribution and final difference curves can be found in Figure 3.3.

Table 3.7 Interatomic distances (r_a) and amplitudes of vibration for 2,5-dichloropyrimidine[a] (r/pm, $</°$).

i	Atom Pair	Distance	Amplitude[b]
1	N(1)-C(6)	133.4(4)	4.2(6)
2	N(1)-C(2)	132.6(4)	4.4(6)
3	C(5)-C(6)	139.4(11)	4.3(6)
4	C(2)-Cl(7)	173.3(3)	4.5(3)
5	C(5)-Cl(9)	172.7(3)	4.4(3)
6	C(6)-H(10)	110.9(12)	7.7 fixed
7	N(1)...N(3)	238.1(9)	6.1(5)
8	N(1)...C(5)	236.8(6)	6.4(5)
9	N(1)...Cl(7)	260.1(5)	8.0(8)
10	N(1)...H(10)	208.4(11)	9.3 fixed
11	C(2)...C(6)	225.8(6)	4.9(5)
12	C(4)...C(6)	239.1(22)	6.4(6)
13	C(4)...Cl(9)	271.5(10)	9.1(10)
14	C(5)...H(10)	219.1(22)	9.4 fixed
15	N(1)...C(4)	273.2(7)	6.2(5)
16	N(1)...Cl(9)	395.2(6)	10.1(6)
17	C(2)...C(5)	262.8(6)	5.9(6)
18	C(2)...H(8)	325.2(12)	9.0 fixed
19	C(4)...Cl(7)	383.3(6)	10.1(7)
20	C(4)...H(10)	341(3)	9.0 fixed
21	Cl(9)...H(10)	292(2)	13.2 fixed
22	N(1)...H(8)	383.3(15)	8.9 fixed
23	C(2)...Cl(9)	434.9(6)	10.2(8)
24	Cl(7)...H(8)	468.0(12)	10.3 fixed
25	H(8)...H(10)	435(4)	12.1 fixed
26	C(5)...Cl(7)	435.5(6)	10.2(8)
27	Cl(7)...Cl(9)	607.5(5)	11.6(7)

[a] Estimated standard deviations, obtained in the least-squares refinement, are given in parentheses.

[b] Amplitudes which could not be refined are fixed at values derived from the scaled 6-31G*/SCF force field.
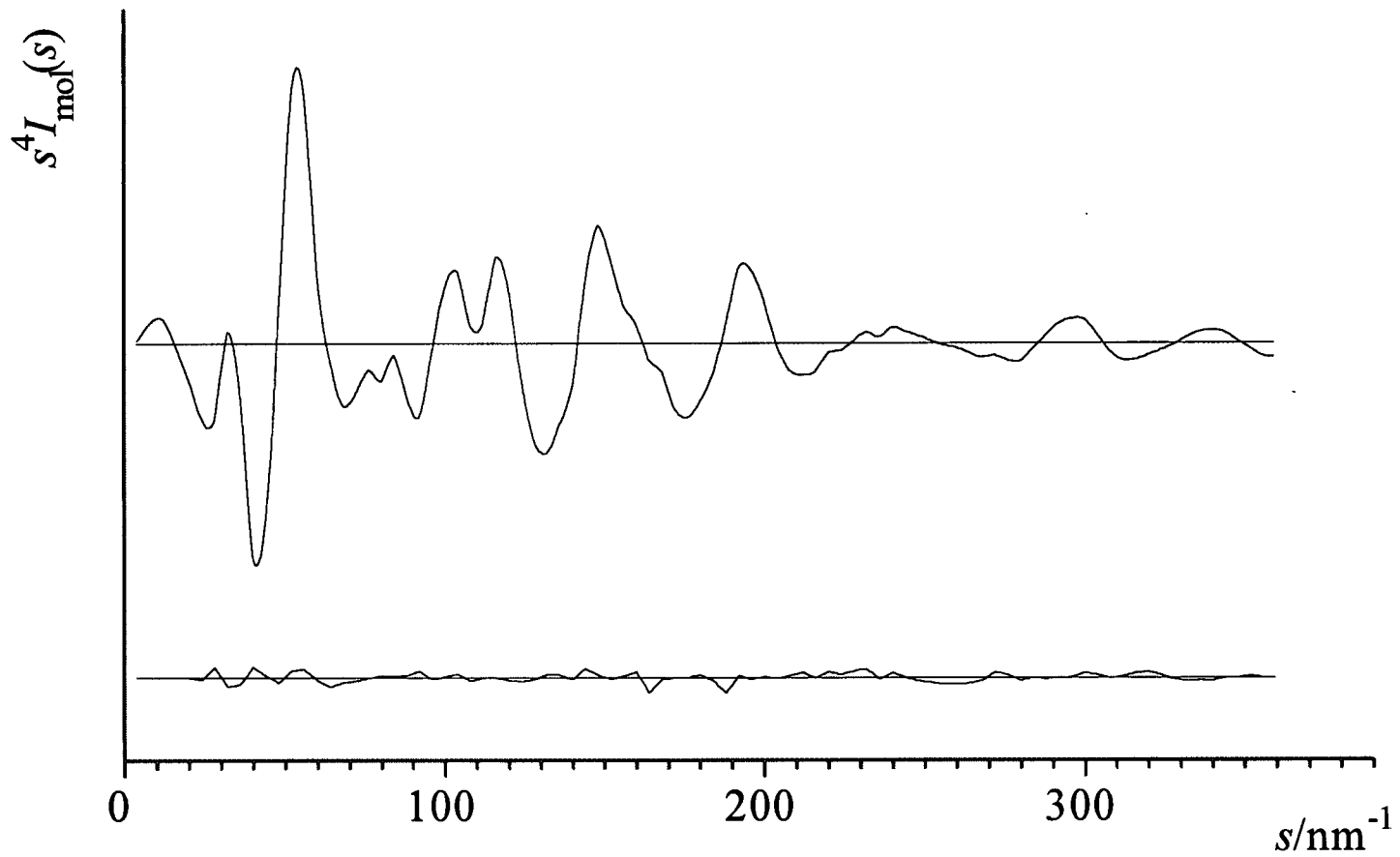
Figure 3.2 Observed and final difference combined molecular scattering curves for 2,5-dichloropyrimidine
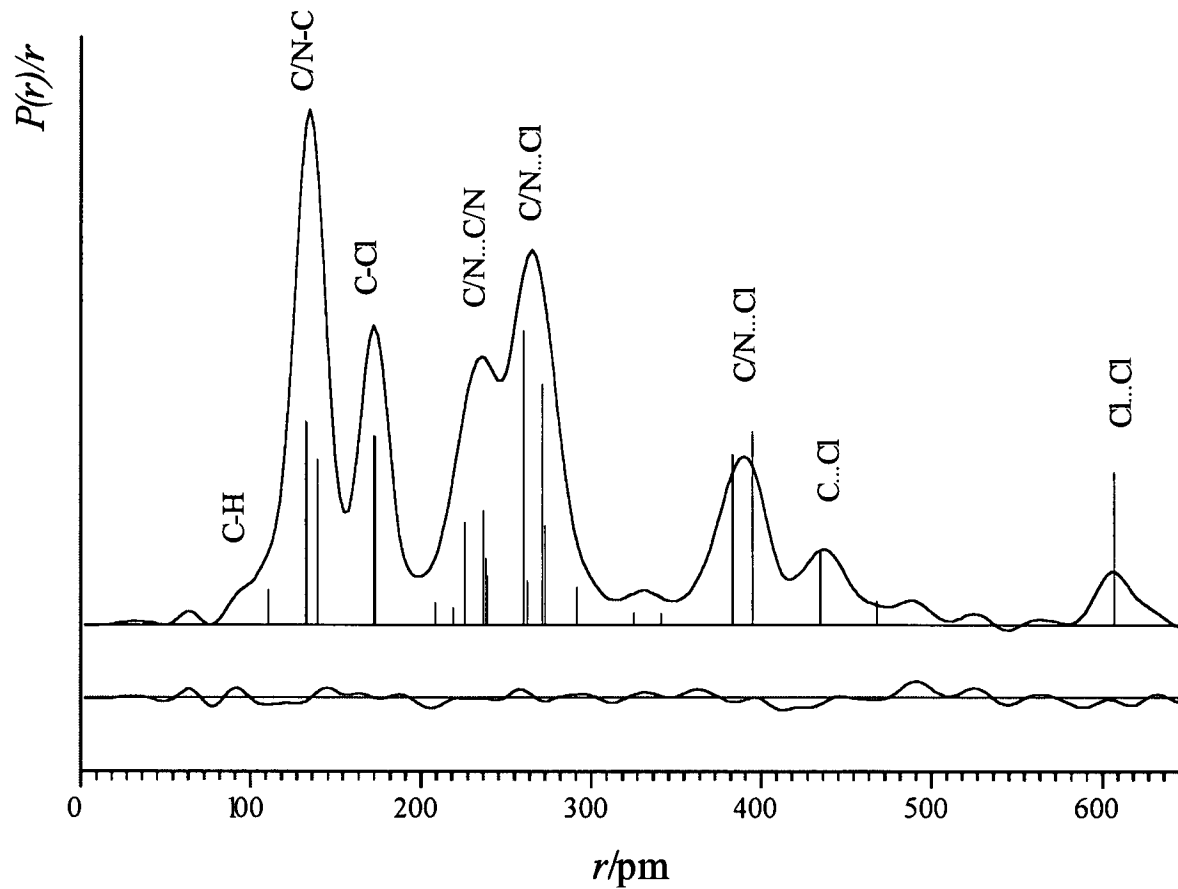
Figure 3.3 Observed and final difference radial distribution curves for 2,5-dichloropyrimidine. Before Fourier inversion the data were multiplied by $s.\exp(-0.00002s^2)/(Z_{Cl}\text{-}f_{Cl})(Z_N\text{-}f_N)$.

3.4 Comparison of GED and *Ab Initio* Structures

The final results for the molecular structure of 2,5-dichloropyrimidine found by gas-phase electron diffraction with flexible restraints and by *ab initio* calculations are summarised in Table 3.8.

Ab initio calculations give a discrete molecular structure, which should therefore complement the results obtained from the GED experiment. Some differences would be expected, however, since *ab initio* calculations give the equilibrium structure, and are not subject to the vibrational averaging effects which influence the dynamic GED structure. However, these differences are small and *ab initio* and GED parameters were found to be in excellent agreement, with all fitting within one or two standard deviations. The only substantial difference concerned the C-H bond length, found to be 109.9(12) pm by GED compared to 108.7 pm by *ab initio*. This parameter is poorly determined by the GED experiment, but can be refined satisfactorily when subject to a flexible restraint.

Table 3.8 Comparison of the molecular structure of 2,5-dichloropyrimidine from GED and *ab initio* calculations. (r/pm, $</°$)

	GED + restraints[a]	6-311G**/MP2
Bond lengths		
rN(1)C(2)	132.5(5)	133.4
rN(1)C(6)	133.2(4)	133.8
rC(5)C(6)	139.3(11)	139.5
rC(2)Cl(7)	172.8(3)	172.8
rC(5)Cl(9)	172.2(3)	172.1
rC(6)H(10)	109.9(12)	108.7
Angles		
<NCN	127.9(4)	127.9
<CNC	116.3(7)	115.7
<NCC	120.6(8)	121.7
<CCC	118.3(6)	117.3
<NCH	117.2(5)	117.2

[a] GED results refer to r_α^0 structure; see Table 3.7 (page 70) for r_a distances.

3.5 Conclusion

In this chapter a method (SARACEN) of obtaining improved geometric parameters by combining GED data with restraints based on a graded series of *ab initio* calculations has been described. It has been shown that it yields more reasonable estimates of uncertainties (and hence more realistic structures) as previously fixed parameters can now refine, the restraints having relieved the effects of parameter correlation in the GED model of the structure and provided information about parameters which have little influence on the GED scattering. Parameters which correspond directly to restraints have been shown to behave in two ways; they may refine to give a sensible value different from the restraint but within the error limit, indicating that some information is present in the GED data, or they may refine to give the same value and error as the restraint, indicating that little or no information was provided by the experimental data. Even in this case it has been demonstrated that the technique is valuable since parameters affected now have realistic standard deviations and the refined structures obtained in this way represent the sum of all available knowledge, experimental and theoretical, and are thus as reliable as possible at present.

3.6 References

1.   S. Cradock, P.B. Liescheski, D.W.H. Rankin, H.E. Robertson, *J. Am. Chem. Soc.* 1988, **110**, 2758.

2.   S. Cradock, J.M. Muir, D.W.H. Rankin, *J. Mol. Struct.* 1990, **220**, 205.

3.   D.G. Anderson, S. Cradock, P.B. Liescheski, D.W.H. Rankin, *J. Mol. Struct.* 1990, **216**, 181.

4.   P.B. Liescheski, D.W.H. Rankin, H.E. Robertson, *Acta Chem. Scand., Ser. A.* 1988, **42**, 338.   ·

5.   S. Cradock, P.B. Liescheski, D.W.H. Rankin, *J. Mag. Reson.* 1991, **91**, 316.

6.   S. Cradock, C. Purves, D.W.H. Rankin, *J. Mol. Struct.* 1990, **220**, 193.

7.   P.B. Liescheski, D.W.H. Rankin, *J. Mol. Struct.* 1989, **196**, 1.

8. P.B. Liescheski, D.W.H. Rankin, *J. Mol. Struct.* 1988, **178**, 227.

9. P.D. Blair, A.J. Blake, R.W. Cockman, S. Cradock, E.A.V. Ebsworth, D.W.H. Rankin, *J. Mol. Struct.* 1989, **193**, 279.

10. C.A. Brookman, S. Cradock, D.W.H. Rankin, H.E. Robertson, P. Vefghi, *J. Mol. Struct.* 1990, **216**, 191.

11. L. Hedberg, K. Hedberg, *J. Phys. Chem.* 1993, **97**, 10349.

12. H. Fujiwara, T. Egawa, H. Takeuchi, S. Konaka, *J. Mol. Struct.* 1993, **301**, 113.

13. *Molecular Structure by Diffraction Methods,* Specialist Periodical Reports, The Chemical Society. 1975, p.72.

14. V.J. Klimkowski, J.D. Ewbank, C.v. Alsenoy, J.N. Scarsdale, L. Schäfer, *J. Am. Chem. Soc.* 1982, **104**, 1476.

15. ASYM40 version 3.0, update of ASYM20 program. L. Hedberg, I.M. Mills, *J. Mol. Spectrosc.* 1993, **160**, 117.

16. Gaussian 92, Revision F.4, M.J. Frish, G.W. Trucks, M. Head-Gordon, P.M.W. Gill, M.W. Wong, J.B. Foresman, B.G. Johnson, H.B. Schlegel, M.A. Robb, E.S. Replogle, R. Gomperts, J.L. Andres, K. Raghavachari, J.S. Binkley, C. Gonzalez, R.L. Martin, D.J. Fox, D.J. Defrees, J. Baker, J.J.P. Stewart, J.A. Pople, Gaussian, Inc., Pittsburgh PA. 1992.

17. Gaussian 94, Revision C.2, M.J. Frisch, G.W. Trucks, H.B. Schlegel, P.M.W. Gill, B.G. Johnson, M.A. Robb, J.R. Cheeseman, T. Keith, G.A. Petersson, J.A. Montgomery, K. Raghavachari, M.A. Al-Laham, V.G. Zakrzewski, J.V. Ortiz, J.B. Foresman, J. Cioslowski, B.B. Stefanov, A. Nanayakkara, M. Challacombe, C.Y. Peng, P.Y. Ayala, W. Chen, M.W. Wong, J.L. Andres, E.S. Replogle R. Gomperts, R.L. Martin, D.J. Fox, J.S. Binkley, D.J. Defrees, J. Baker, J.P. Stewart, M. Head-Gordon, C. Gonzalez, J.A. Pople, Gaussian, Inc., Pittsburgh PA. 1995.

18. J.S. Binkley, J.A. Pople, W.J. Hehre, *J. Am. Chem. Soc.* 1980, **102**, 939.

19. M.S. Gordon, J.S. Binkley, J.A. Pople, W.J. Pietro, W.J. Hehre, *J. Am. Chem. Soc.* 1982, **104**, 2797.

20. W.J. Pietro, M.M. Francl, W.J. Hehre, D.J. Defrees, J.A. Pople. J.S. Binkley, *J. Am. Chem. Soc.* 1982, **104**, 5039.

21. W.J. Hehre, R. Ditchfield, J.A. Pople, *J. Chem. Phys.* 1972, **56**, 2257.

22. P.C. Hariharan, J.A. Pople, *Theor. Chim. Acta* 1973, **28**, 213.

23. M.S. Gordon, *Chem. Phys. Lett.* 1980, **76**, 163.

24. A.D. McLean, G.S. Chandler, *J. Chem. Phys.* 1980, **72**, 5639.

25. R. Krishnan, J.S. Binkley, R. Seeger, J.A. Pople, *J. Chem. Phys.* **1980**, 72, 650.

26. W.J. Hehre, L. Radom, P.v.R. Schleyer, J.A. Pople, *Ab Initio Molecular Orbital Theory*, publishers John Wiley and Sons, Inc., 1986.

27. T.H. Dunning, P.J. Hay, *Modern Theoretical Chemistry*, publishers Plenum, New York, 1976, chapter 1, pp. 1-28.

28. L. Doms, H.J. Geise, C. Van Alsenoy, L. Van Den Enden, L. Schäfer, *J. Mol. Struct.* 1985, **129**, 299.

29. Dr. H. McNab, University of Edinburgh, Personal Communication.

30. C.D. Crosby, V.R. Berthold, *J. Org. Chem.* 1960, **25**, 1916.

31. J. Chesterfield, J.F.W. McOmie, E.R. Sayer, *J. Chem. Soc.* 1955, 3478.

32. C.M. Huntley, G.S. Laurenson, D.W.H. Rankin, *J. Chem. Soc., Dalton Trans.* 1980, 954.

33. S. Cradock, J. Koprowski, D.W.H. Rankin, *J. Mol. Struct.* 1981, **77**, 113.

34. A.S.F. Boyd, G.S. Laurenson, D.W.H. Rankin, *J. Mol. Struct.* 1981, **71**, 217.

35. A. W. Ross, M. Fink, Hilderbrandt, R. *International Tables for Crystallography.* Editor A.J.C. Wilson, Kluwer Academic Publishers: Dordrecht, The Netherlands, Boston, MA, and London, 1992, Vol. C, p 245.

Chapter 4

Gas and Solid-phase Structures of the Dichloro derivatives of Pyrimidine, Pyrazine and Pyridazine

4.1 Introduction

Pyrimidine, pyrazine and pyridazine and their derivatives are key compounds in organic chemistry. Examples of each class of compound have been found in nature, most notably pyrimidine as a component part of the four bases in DNA, while pyrazines are responsible for flavouring in foodstuffs as diverse as cooked meats, cheese, tea and coffee. Many derivatives which possess biological activity have been synthesised, with applications including antibiotics and antihypertensive agents.

The purpose of the work presented in this chapter is two-fold. Firstly, the gas-phase structures of 4,6-dichloropyrimidine, 2,6-dichloropyrazine and 3,6-dichloropyridazine were obtained using the SARACEN method[1] (presented in Chapter 3) and compared with the parent compounds pyrimidine,[2] pyrazine[2] and pyridazine.[3] A chlorine substituent acts as an electron-withdrawing group on the aromatic ring, and since electron withdrawing groups are commonly found connected to these systems the dichloro derivatives are, in effect, simple models for larger, more complex organic systems. Secondly, crystal structures for the three compounds were obtained and comparisons drawn between crystal and gas-phase structures thus enabling areas of molecular distortion in the crystal structures to be identified. For this study the crystal structure of 2,5-dichloropyrimidine was also included. Note that the gas-phase structure of 2,5-dichloropyrimidine was used to illustrate the SARACEN method fully in the previous chapter.

The experimental work carried out consists of three parts. The first comprises *ab initio* calculations performed for the three dichoro derivatives and their parent compounds. The gas-phase electron diffraction results are presented next, followed by the structures obtained in the solid phase by X-ray crystallography. Changes in ring geometry induced by the electron withdrawing subsituents are discussed and finally comparisons are drawn between the structures obtained for the two phases.

4.2 Experimental

4.2.1 *Ab Initio* Calculations

Theoretical methods: Ab Initio molecular orbital calculations were performed to predict geometrical parameters and to obtain theoretical harmonic force fields using the ASYM40 program,[4] from which estimates of vibrational amplitudes could be obtained. All calculations were carried out on a DEC Alpha APX 1000 workstation using the Gaussian suite of programs.[5,6]

Geometry optimisations: A graded series of geometry optimisation calculations was carried out for each molecule, from which the effects of increasing the quality of basis set and level of theory could be gauged. In the case of 4,6-dichloropyrimidine calculations were performed using standard gradient techniques at the SCF level of theory using the 3-21G,[7-9] 6-31G* [10-12] and 6-311G** [13-14] basis sets. The two larger basis sets were subsequently used for optimisations at the MP2(FC) level of theory, and an additional calculation was undertaken at the 6-31+G*/MP2 level to assess the effects of diffuse functions for heavy atoms on molecular parameters. This effect was found to be negligible and so neither this nor the 6-311G**/SCF calculation was performed for the remaining structures.

Frequency calculations: These were performed at the 3-21G*/SCF and 6-31G*/SCF levels for each molecule, confirming C_{2v} symmetry as a local minimum in each case. The force constants obtained in the higher calculations were subsequently used in the construction of force fields for the dichloro compounds using the ASYM40 program.[4] Since no fully assigned vibrational spectra were available for these compounds, the force fields were scaled using scaling factors of 0.938, 0.956 and 0.919 for bond stretches, angle bends and torsions respectively.[†] Scaling the force fields was found to have little effect on the vibrational amplitude values.

[†] Scale constants were obtained from the successful scaling of the force field for 1,3,5-triazine against a set of experimental I.R. frequencies.

4.2.2 Gas-Phase Electron Diffraction (GED)

Sample preparation: The sample of 4,6-dichloropyrimidine was a gift from Dr. R.V.H. Jones of Zeneca p.l.c. Both 2,6-dichloropyrazine and 3,6-dichloropyridazine were bought from Lancaster Synthesis, at 99% and 98% purity, and used in the GED analysis without further purification.

GED experiments: Electron scattering intensities were recorded on Kodak Electron Image photographic plates using the Edinburgh apparatus.[15] Six plates (three from the long camera distance and three from the short distance) were recorded for each compound and traced digitally using a computer-controlled Joyce Loebl MDM6 microdensitometer[16] at the EPSRC Daresbury Laboratory. Standard programs were used for the data reduction[17] with the scattering factors of Ross *et al.*[18] The weighting points used in setting up the off-diagonal weight matrix, s range, scale factors, correlation parameters and electron wavelengths are given in Table 4.1.

GED models:

(i) 4,6-dichloropyrimidine [Figure 4.1]: Assuming C_{2v} symmetry, nine independent geometric parameters are required to define the structure completely. They are the average ring bond distance (p_1), the difference between rC-C and mean rC-N bond distance (p_2), r[C(6)-N(1)] minus r[C(2)-N(1)] (p_3), the average C-H distance and r[C(5)-H(9)] minus r[C(2)-H(7)] (p_4 and p_5), rC-Cl (p_6), the internal ring angles <NCN (p_7) and <CNC (p_8) and, finally, the external ring angle <NCCl (p_9).

(ii) 2,6-dichloropyrazine [Figure 4.2]: Assuming C_{2v} symmetry nine geometric parameters are sufficient to determine the structure of the molecule: the average ring bond distance (p_1), the difference between rC-C and mean rC-N bond distances (p_2), r[C(2)-N(1)] minus r[C(3)-N(4)] (p_3), rC-Cl (p_4), rC-H (p_5), the two internal ring angles <C(3)N(4)C(5) (p_6) and <N(4)C(3)C(2) (p_7), and the two external ring angles <CCCl (p_8) and <CCH (p_9).

(iii) 3,6-dichoropyridazine [Figure 4.3]: Assuming C_{2v} symmetry, the structure is completely defined by ten independent geometrical parameters, namely the average ring distance (p_1), r[C(3)-C(4)] minus r[C(4)-C(5)] (p_2), rN-N minus rC-N (p_3), the difference between the average rC-C bond distance and the average [rC-N, rN-N] bond distance (p_4), rC-Cl (p_5), rC-H (p_6), <NNC (p_7), <NCC (p_8), <CCCl (p_9) and <C(5)C(4)H(8) (p_{10}).

Table 4.1 GED experimental conditions

Compound	Temperature /K		Camera distance (mm)	Weighting functions (nm^{-1})					Correlation parameter	Scale factor, k^a	Electron wavelength[b] (pm)
	Sample	Nozzle		Δs	s_{min}	s_1	s_2	s_{max}			
4,6-dichloropyrimidine	400	460	95.42	4	100	120	304	356	0.0855	0.972(24)	0.05710
			255.02	2	20	40	130	150	0.4339	0.841(4)	0.05710
2,6-dichloropyrazine	424	443	97.41	4	120	140	304	356	0.1520	0.899(29)	0.05674
			257.98	2	20	40	148	158	0.4668	0.940(12)	0.05672
3,6-dichloropyridazine	440	442	97.41	4	120	140	304	356	0.3560	0.832(44)	0.05675
			257.98	2	20	40	140	164	0.4796	0.876(16)	0.05673

[a] Figures in parentheses are the estimated standard deviations

[b] Determined by reference to the scattering patterns of benzene vapour
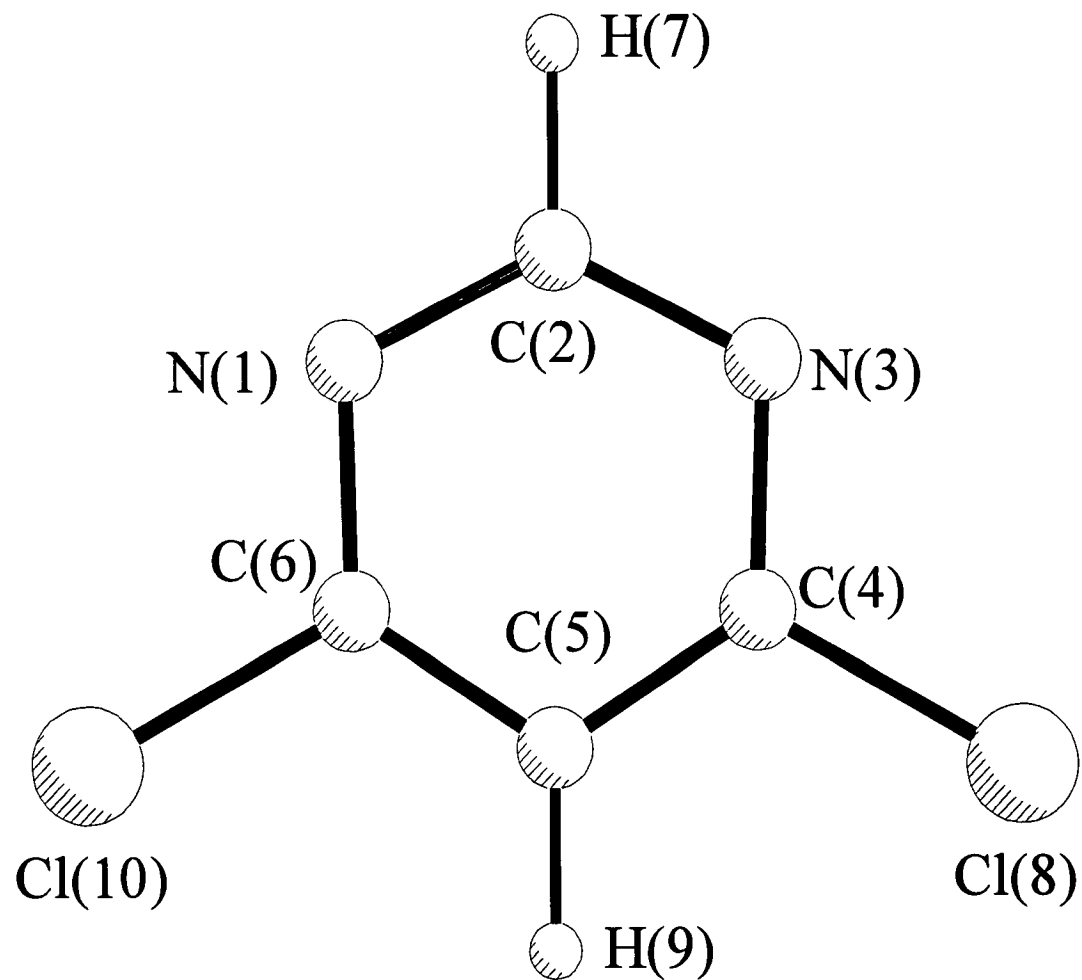
Figure 4.1 Molecular framework of 4,6-dichoropyrimidine
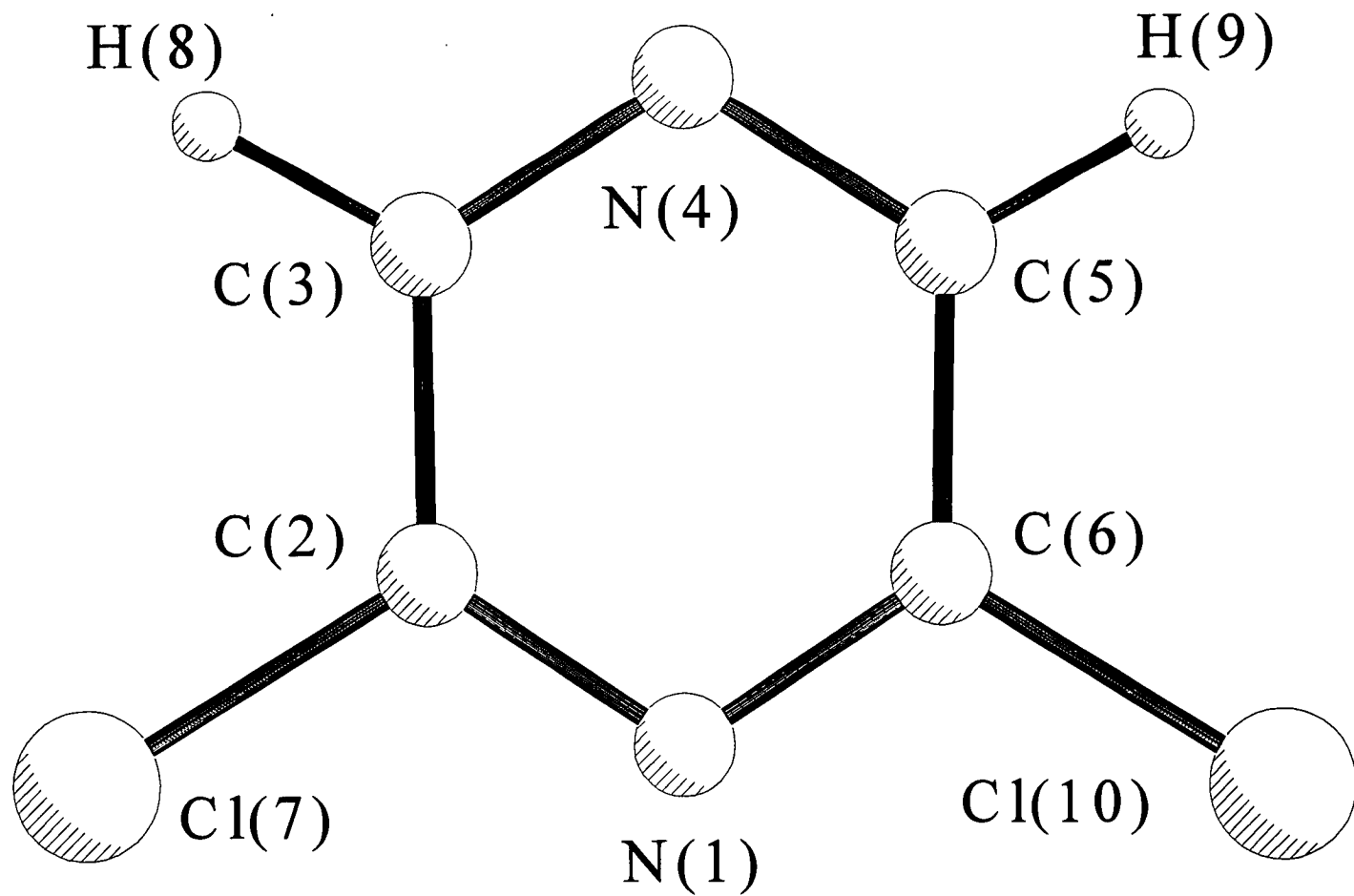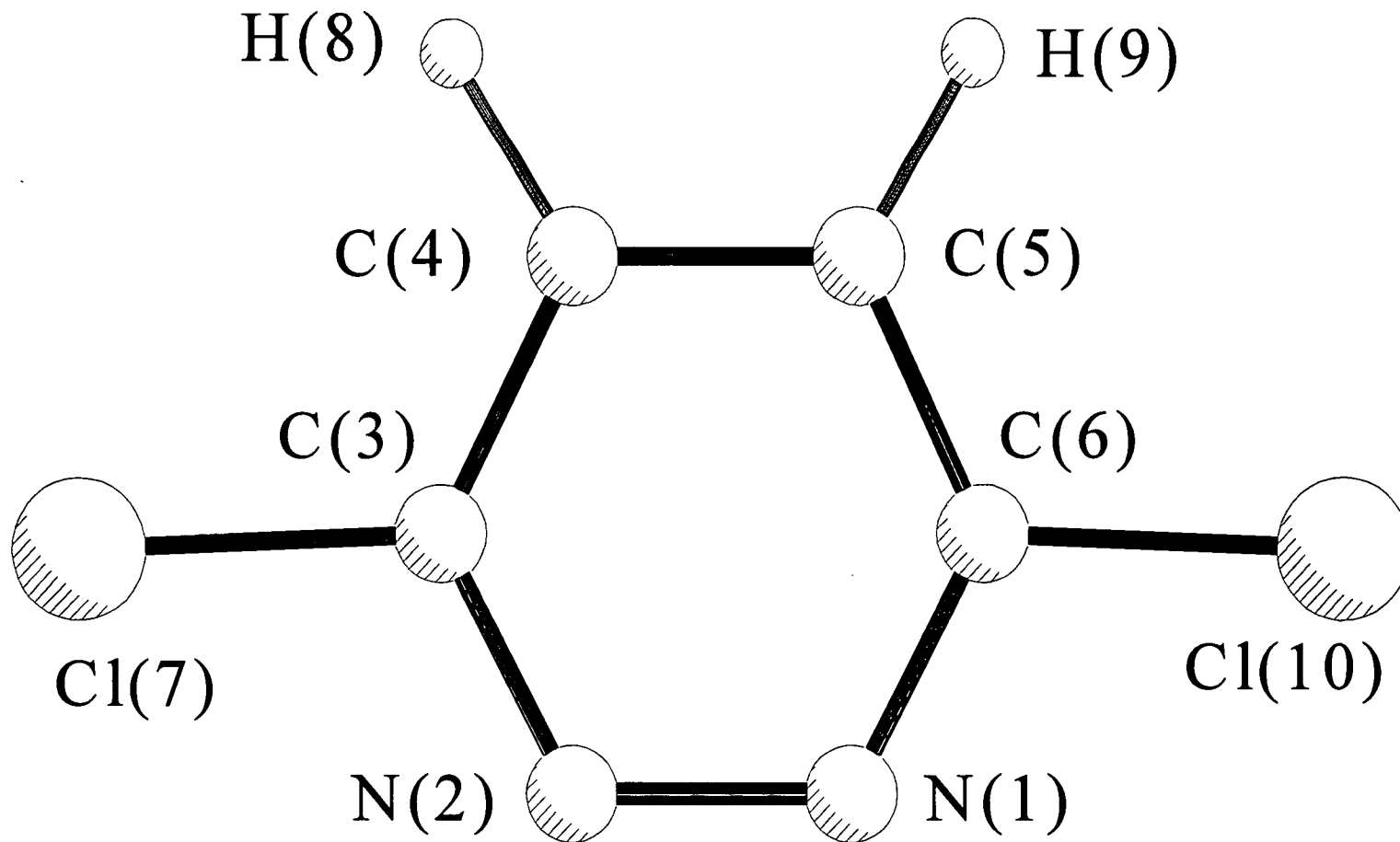
Figure 4.2 Molecular framework of 2,6-dichloropyrazine

Figure 4.3 Molecular framework of 3,6-dichoropyridazine

4.2.3 X-ray Crystallography

Crystal Data: see Table 4.2(a).

Data collection and processing: see Table 4.2(b). Stoë Stadi-4 diffractometer equipped with an Oxford Cryosystems variable-temperature device;[20] ω-θ mode, graphite monochromated Cu-Kα, Mo-Kα radiation.

Structure solution and refinement: see Table 4.2(c). Following data reduction and the application of azimuthal scans-based absorption corrections the structures were solved by automatic direct methods[21] to identify the positions of all non-H atoms. Iterative cycles of least-squares refinement and difference Fourier syntheses located the hydrogen atoms.[22] All non-H atoms were refined anisotropically and H atoms isotropically. Corrections for secondary extinction[22] refined to values given in Table 2(c). Weighting schemes adopted for the four systems were: $w^{-1} = [\sigma^2(F_o^2) + (0.082P)^2]$ where $P = \frac{1}{3}[\text{MAX}(F_o^2, 0) + 2F_o^2]$, $w^{-1} = [\sigma^2(F_o^2) + (0.1246P)^2 + 0.9949P]$, $w^{-1} = [\sigma^2(F_o^2) + (0.0590P)^2 + 0.08P]$ and $w^{-1} = [\sigma^2(F_o^2) + (0.1370P)^2 + 0.00P]$ for 2,5-dichloropyrimidine, 4,6-dichloropyrimidine, 2,6-dichloropyrazine and 3,6-dichloropyridazine respectively.

Table 4.2 X-ray crystal structures (a) crystal data

	Compound			
	2,5-dichloropyrimidine[†]	4,6-dichoropyrimidine[†]	2,6-dichloropyrazine	3,6-dichloropyridazine
(a) crystal data				
empirical formula	$C_4H_2N_2Cl_2$	$C_4H_2N_2Cl_2$	$C_4H_2N_2Cl_2$	$C_4H_2N_2Cl_2$
M	148.98	148.98	148.98	148.98
crystal description	colourless lath	colourless block	colourless block	colourless lath
crystal size /mm^3	0.66 x 0.23 x 0.08	0.66 x 0.51 x 0.19	0.56 x 0.52 x 0.19	0.51 x 0.19 x 0.08
T /K	150	150	220	220
λ /Å	0.71073	0.71073	1.54184	1.54184
crystal system	monoclinic	monoclinic	monoclinic	monoclinic
space group	$P2_1/m$	$P2_1/c$	$P2_1/c$	$P2_1/c$
unit cell determination	29 reflections	16 reflections	69 reflections	42 reflections
	$25° \leq 2\theta \leq 38°$	$30° \leq 2\theta \leq 32°$	$40° \leq 2\theta \leq 44°$	$40° \leq 2\theta \leq 44°$
	measured at $\pm\omega$	measured at $\pm\omega$	measured at $\pm\omega$	measured at $\pm\omega$
unit cell dimensions a,b,c/Å, β/°	a=6.077(3)	a=9.702(8)	a=7.277(13)	a=3.8708(13)
	b=19.771(8)	b=3.780(7)	b=10.972(3)	b=21.091(4)
	c=7.399(3)	c=31.42(4)	c=7.235(13)	c=14.262(3)
	β=101.23(6)	β=97.99(14)	β=90.21(4)	β=90.282(11)
U /Å^3	872.0(7)	1141(3)	577.7(4)	1164.3(5)
Z	6	8	4	8
D_c /gcm^{-3}	1.702	1.734	1.713	1.700
μ /mm^{-1}	0.993	1.011	9.13	9.06
$F(000)$	444	592	296	592

[†] Taken from Ref. 19.

Table 4.2 X-ray crystal structures (b) data collection and processing, (c) structure solution and refinement

	Compound			
	2,5-dichloropyrimidine[†]	4,6-dichoropyrimidine[†]	2,6-dichloropyrazine	3,6-dichloropyridazine
(b) data collection and processing				
X-ray source	Mo	Mo	Cu	Cu
Unique reflections	1586	2025	856	1718
Index ranges	$-7 \leq h \leq 7$	$-11 \leq h \leq 11$	$-8 \leq h \leq 8$	$-4 \leq h \leq 4$
	$0 \leq k \leq 23$	$0 \leq k \leq 4$	$-12 \leq k \leq 12$	$-20 \leq k \leq 23$
	$0 \leq l \leq 8$	$0 \leq l \leq 37$	$-8 \leq l \leq 8$	$-4 \leq l \leq 16$
Theta range	$3° \leq 2\theta \leq 25°$	$5° \leq 2\theta \leq 50°$	$12° \leq 2\theta \leq 120°$	$8° \leq 2\theta \leq 120°$
R_{int}	-	-	0.11	0.04
(c) structure solution and refinement				
absorption correction T_{min}/T_{max}	0.822/1.161	0.518/0.474	0.090/0.008	0.103/0.015
secondary extinction correction	0.003(3)	0.008(3)	0.0021(9)	-
R_1 $[F \geq 4\sigma(F)]$	0.0460	0.0588	0.0421	0.0646
wR_2 [all data]	0.1305	0.172	0.1163	0.1939
$S[F^2]$	1.014	1.078	1.116	1.037
no. refining parameters	128	162	82	149
$(\Delta/\sigma)_{max}$	0.20	-0.001	0.0	0.015
final ΔF synthesis no feature outwith	$+0.46 \rightarrow -0.55$ e Å^{-3}	$+0.62 \rightarrow -0.95$ e Å^{-3}	$+0.35 \rightarrow -0.32$ e Å^{-3}	$+0.49 \rightarrow -0.30$ e Å^{-3}

[†] Taken from Ref. 19.

4.3 Results and Discussion

4.3.1 *Ab Initio* Calculations

For each compound a set of calculations, with various basis sets and both including and excluding electron correlation treatment, was performed. The results showed that convergence was effectively reached in each case.

4,6-Dichloropyrimidine and pyrimidine

The results obtained from the series of calculations performed on 4,6-dichloropyrimidine and pyrimidine are given in Table 4.3; the atom numbering system is shown in Figure 4.1.

In general, geometrical parameter values for 4,6-dichloropyrimidine were largely unaffected by improvements in basis set and level of theory. All bond distances proved to be insensitive to improvements in the basis set beyond 6-31G*; for example, at both the SCF and MP2 levels increasing the size of the basis set to 6-311G** resulted in changes no greater than 0.2 pm. Similarly, the four internal ring angles and the one external ring angle, <NCCl, changed by less than 0.2° at SCF and 0.3° at MP2 for this basis set improvement. As expected for an aromatic system,[23] electron correlation was found to be important, resulting in the three ring bond distances increasing by about 2 pm. Electron correlation was also found to affect the two C-H distances, both increasing by about 1.5 pm. The C-Cl distance was affected less, lengthening by just 0.4 pm. On the inclusion of electron correlation the four internal ring angles changed by less than 1°; angle NCCl remained unchanged. The 6-31+G*/MP2 calculation, performed to assess the effects of diffuse functions on the heavy atoms C, N and Cl, gave results very little different from those obtained in the 6-31G*/MP2 calculation, indicating that these additional functions have a negligible effect. Bond distances varied, on average, by just 0.1 pm, angles by 0.1°.

Parameter values for pyrimidine were also largely unaffected by improvements in basis set and treatment of electron correlation. Improvements in basis set treatment beyond

6-31G* at MP2 level resulted in changes of less than 0.2 pm for all bond distances and less than 0.2° for all angles. Electron correlation effects were again found to be important, with the three ring distances increasing by about 2 pm, the three C-H distances by 1.3 pm and all angles changing by less than 1°.

2,6-Dichloropyrazine and pyrazine

The results obtained from the series of geometry optimisation calculations for 2,6-dichloropyrazine and pyrazine are given in Table 4.4 and the molecular framework is shown in Figure 4.2.

In general the trends in geometry observed in the 4,6-dichloropyrimidine series of calculations were also observed for 2,6-dichloropyrazine. The two molecules are electronically similar, since both aromatic rings comprise two C-N distances and one C-C distance. Note that the 6-311G**/SCF and 6-31+G*/MP2 calculations were not performed for 2,6-dichloropyrazine because further improvements in basis set treatment without the inclusion of electron correlation, and the addition of diffuse functions for the heavy atoms in the molecule, had been found to have little effect on the overall geometry of the previous structure.

Like 4,6-dichloropyrimidine, calculated bond distances proved to be rather insensitive to the details of the basis set, with improvements from 6-31G* to 6-311G** at the MP2 level of theory resulting in average changes of 0.2 pm for the three ring bond distances and the two external ring distances, rC-Cl and rC-H. Similarly, changes in the four internal ring angles and the two external ring angles, <CCCl and <CCH, were found to be small, averaging just 0.2°. The introduction of electron correlation also resulted in similar changes to those observed for 4,6-dichloropyrimidine, with the three aromatic ring bond distances increasing by about 2 pm, rC-H by about 1.5 pm, and the C-Cl distance by just 0.1 pm. Electron correlation resulted in changes in the four internal ring angles not exceeding 1°. The two external ring angles were found to

be much less affected, with <CCCl narrowing by 0.1° and <CCH remaining unchanged.

The molecular structure of pyrazine also rapidly converged with improvements in the level of calculation. Improvements in basis set treatment from 6-31G* to 6-311G** at the MP2 level gave rise to changes less than 0.2 pm in all bond lengths and less than 0.3° in all ring angles. Electron correlation again resulted in changes in bond length of the order of 2 pm and in angles by about 1°.

3,6-Dichloropyridazine and pyridazine

The results of the molecular geometry calculations for 3,6-dichloropyridazine and pyridazine are given in Table 4.5; the molecular framework is shown in Figure 4.3.

The molecular structure of 3,6-dichloropyridazine is quite distinct from those of 4,6-dichloropyrimidine and 2,6-dichloropyrazine, having four different ring bond distances (C-N, two C-C, and N-N), in contrast to just three ring bond distances in the previous two structures. In particular it is the only one of these compounds to have an N-N bond. As a result the similarities noted in the two previous series of calculations were not repeated. Strong similarities were found, however, for the two external ring bond distances, rC-Cl and rC-H.

Improvements in basis set from 6-31G* to 6-311G** at the MP2 level resulted in an increase of 0.5 pm for rN-N and a smaller change of 0.2 pm for the remaining three ring bond distances and the two external ring distances C-Cl and C-H. Values observed for the three internal ring angles and the external ring angle <CCCl changed by less than 0.2° and 0.4°, respectively. Angle CCH remained unchanged for this basis set improvement. Electron correlation effects using the 6-31G* basis set resulted in changes of about 3 pm for rN-N, 4 pm for rC-N and 2 pm for one of the rC-C distances, with the remaining rC-C distance unchanged. All ring angle changes due to

electron correlation were observed to be less than 1°. Changes recorded in the two external ring angles were 0.4° and 0.2° for <CCCl and <CCH respectively.

Finally, the geometric parameters of pyridazine also successfully converged with improvements in basis set and treatment of electron correlation. Improving the basis set beyond 6-31G* at the MP2 level gave rise to changes of the order 0.2 pm for all distances with the exception of rN-N, which shortened by 0.6 pm. All angles were also seen to converge to within 0.1°. In results closely paralleling those observed for 3,6-dichloropyridazine, electron correlation to the MP2 level was seen to increase the N-N distance by about 5 pm, rC-N by about 3 pm and one of the C-C distances by about 2 pm , with the remaining C-C distance unchanged. All angle changes due to electron correlation were observed to be less than 1°.

Table 4.3 *Ab initio* molecular geometries (r_e/pm, $</°$)and energies (Hartrees) for 4,6-dichloropyrimidine and pyrimidine

Parameter	Basis Set/Level of theory					
	3-21G*/SCF	6-31G*/SCF	6-311G**/SCF	6-31G*/MP2	6-31+G*/MP2	6-311G**/MP2
4,6-dichoropyrimidine						
r[N(1)-C(2)]	132.9	131.8	131.6	134.2	134.3	134.0
r[N(1)-C(6)]	131.8	130.9	130.7	133.2	133.4	133.0
r(C-C)	138.0	138.2	138.0	139.3	139.4	139.4
r[C(2)-H(7)]	106.5	107.3	107.4	108.7	108.6	108.6
r[C(5)-H(9)]	106.6	107.0	106.9	108.4	108.5	108.3
r(C-Cl)	172.8	172.7	172.9	173.1	172.8	172.8
<NCN	124.0	126.7	126.7	127.2	127.2	127.5
<CNC	117.8	115.9	115.9	115.2	115.3	115.1
<NCC	122.4	123.5	123.6	123.6	123.5	123.5
<CCC	115.7	114.4	114.3	115.1	115.2	115.3
<NCCl	118.0	117.2	117.3	117.2	117.1	117.5
Energy	-1174.843879	-1180.492093	-1180.593791	-1181.575465	-1181.575710	-1181.741758
pyrimidine						
r[N(1)-C(2)]	132.9	131.9		134.2		134.1
r[N(1)-C(6)]	133.2	132.1		134.4		134.2
r(C-C)	138.2	138.2		139.3		139.4
r[C(2)-H(7)]	106.7	107.5		108.8		108.7
r[C(4)-H(8)]	107.0	107.6		108.9		108.8
r[C(5)-H(9)]	106.9	107.3		108.6		108.5
<NCN	124.6	126.9		127.4		127.6
<CNC	117.7	116.2		115.6		115.5
<NCC	121.5	122.3		122.3		122.2
<CCC	116.9	116.0		116.9		116.8
<NCH	170.0	116.5		116.3		116.4
Energy	-261.206190	-262.693488		-263.509482		-263.625609

Table 4.4 *Ab initio* molecular geometries (r_e/pm, $</°$)and energies (Hartrees) for 2,6-dichloropyrazine and pyrazine

Parameter	Basis Set/Level of Theory			
	3-21G*/SCF	6-31G*/SCF	6-31G*/MP2	6-311G**/MP2
2,6-dichloropyrazine				
r(C-C)	138.1	138.6	139.9	140.1
r[C(2)-N(1)]	131.8	130.7	133.3	133.1
r[C(3)-N(4)]	132.8	131.6	134.1	134.0
r(C-Cl)	172.6	172.8	172.9	172.6
r(C-H)	106.6	107.2	108.7	108.5
<C(3)N(4)C(5)	119.4	118.2	117.0	116.6
<C(2)C(3)N(4)	119.6	120.2	120.9	121.0
<N(1)C(2)C(3)	121.3	122.4	123.0	123.1
<C(2)N(1)C(6)	118.7	116.6	115.4	115.2
<CCCl	120.2	119.8	119.7	119.4
<CCH	121.8	121.4	121.4	121.2
Energy	-1174.833506	-1180.478452	-1181.567169	-1181.733202
pyrazine				
r(C-C)	138.1	138.6	139.6	139.8
r(C-N)	133.1	131.9	134.4	134.3
r(C-H)	106.9	107.4	108.8	108.7
<CNC	118.0	116.6	115.3	115.0
<NCC	121.0	121.7	122.3	122.5
<NCH	117.7	117.4	116.6	116.7
Energy	-261.197500	-262.683005	-263.503627	-263.619887

Table 4.5 *Ab initio* molecular geometries (r_e/pm, $</°$) and energies (Hartrees) for 3,6-dichloropyridazine and pyridazine

Parameter	Basis Set/Level of Theory			
	3-21G*/SCF	6-31G*/SCF	6-31G*/MP2	6-311G**/MP2
4,6-dichloropyridazine				
r[C(3)-C(4)]	139.9	140.1	140.1	140.2
r[C(4)-C(5)]	135.8	136.0	138.2	138.4
r(C-N)	130.0	129.4	133.5	133.3
r(N-N)	136.1	131.7	134.9	134.4
r(C-Cl)	173.0	172.9	172.7	172.5
r(C-H)	106.8	107.2	108.6	108.4
<NNC	119.3	119.8	118.8	118.9
<NCC	123.6	123.8	124.5	124.6
<CCC	117.1	116.4	116.7	116.5
<CCCl	119.1	119.3	119.7	119.3
<CCH	120.3	121.0	121.2	121.2
Energy	-1174.793719	-1180.443680	-1181.535211	-1181.700630
pyridazine				
r[C(3)-C(4)]	139.5	139.4	139.7	139.9
r[C(4)-C(5)]	136.5	136.8	138.6	138.8
r(C-N)	131.6	131.0	134.4	134.3
r(N-N)	135.6	131.0	134.8	134.2
r[C(3)-H(7)]	106.9	107.4	108.7	108.6
r[C(4)-H(8)]	107.0	107.4	108.6	108.5
<NNC	119.4	120.0	119.0	119.1
<NCC	123.2	123.3	124.1	124.2
<CCC	117.4	116.7	116.9	116.8
<NCH	115.9	115.4	114.4	114.4
Energy	-261.159689	-262.650029	-263.474317	-263.590143

4.3.2 Restrained GED Results

The geometric restraints required to complete the structural refinements, given in Table 4.6, were derived from the range of *ab initio* calculations performed, in accordance with the SARACEN method.[3] In each case values for restraints are taken from the highest level calculation (*i.e.* 6-311G**/MP2) and uncertainty ranges usually estimated from a consideration of values given by the other lower level calculations, based on a working knowledge of the reliability of the calculations from a study of electronically similar systems. Restraints were also applied to ratios of vibrational amplitude values for electronically similar bond distances lying close together on the radial distribution curve. Values for amplitude restraints, described in Table 4.7, were calculated directly from the scaled *ab initio* force field and uncertainty ranges of 5% were adopted. These restraints enabled the refinement of vibrational amplitude values that would otherwise have to be rigidly tied to refining amplitudes, or remain fixed at the values obtained from the scaled harmonic force fields.

Table 4.6 *Ab initio* geometric parameter restraints (r_e/pm, <$/°$)

Compound		Parameter	Basis Set/Level of theory				
			3-21G*/ SCF	6-31G*/ SCF	6-31G*/ MP2	6-311G**/ MP2	Restraint
4,6-dichloropyrimidine	p_2	r(C-C)-av.r(C-N)	5.6	6.8	5.6	5.9	5.9(9)
	p_3	Δ r(C-N)	-1.0	-0.8	-0.9	-1.0	-1.0(2)
	p_4	av. r(C-H)	106.5	107.1	108.5	108.4	108.4(15)
	p_5	Δ r(C-H)	0.1	-0.4	-0.3	-0.3	-0.3(1)
2,6-dichloropyrazine	p_2	r(C-C)-av.r(C-N)	5.8	7.5	6.2	6.5	6.5(10)
	p_3	Δ r(C-N)	-1.1	-0.9	-0.8	-0.8	-0.8(1)
	p_5	r(C-H)	106.6	107.2	108.7	108.5	108.5(15)
	p_9	<CCH	121.7	121.4	121.4	121.2	121.2(15)
	p_6-p_7	<C(3)N(4)C(5) – <C(2)C(3)N(4)	-0.2	-2.0	-3.9	-4.4	-4.4(5)
3,6-dichloropyridazine	p_2	Δ r(C-C)	4.1	4.2	1.9	1.9	1.9(1)
	p_3	r(N-N)-r(C-N)	6.1	2.3	1.4	1.1	1.1(3)
	p_4	av. r(C-C)-av. [r(N-N), r(C-N)]	6.5	8.6	5.5	6.0	6.0(5)
	p_6	r(C-H)	106.8	107.2	108.6	108.4	108.4(15)
	p_{10}	<CCH	120.3	121.0	121.2	121.2	121.2(15)

Table 4.7 *Ab initio* vibrational amplitude restraints

Compound	Amplitude ratio	Value[a]	Uncertainty[b]
4,6-dichloropyrimidine	$u_2[C(4)-N(3)]/u_1[N(1)-C(2)]$	1.004	0.050
	$u_3[C(4)-C(5)]/u_1[N(1)-C(2)]$	1.038	0.052
	$u_{10}[N(1)...C(5)]/u_8[N(1)...N(3)]$	1.033	0.052
	$u_{12}[C(4)...C(6)]/u_{11}[C(2)...C(4)]$	1.035	0.052
	$u_{14}[Cl(8)...C(5)]/u_9[N(1)...Cl(10)]$	1.044	0.052
	$u_{16}[C(2)...C(5)]/u_{15}[N(1)...C(4)]$	0.972	0.049
	$u_{19}[C(4)...Cl(10)]/u_{17}[C(2)-Cl(8)]$	1.019	0.051
2,6-dichloropyrazine	$u_2[C(3)-N(4)]/u_1[N(1)-C(2)]$	0.998	0.050
	$u_3[C(2)-C(3)]/u_1[N(1)-C(2)]$	1.055	0.053
	$u_6[N(1)...C(3)]/u_7[C(2)...N(4)]$	1.001	0.050
	$u_{11}[N(1)...Cl(10)]/u_{13}[C(3)...Cl(7)]$	0.946	0.047
	$u_{15}[C(2)...C(5)]/u_{14}[N(1)...N(4)]$	0.944	0.047
3,6-dichloropyridazine	$u_2[N(2)-N(3)]/u_1[N(1)-N(2)]$	0.966	0.048
	$u_4[C(3)-C(4)]/u_1[N(1)-N(2)]$	1.041	0.052
	$u_6[C(4)-C(5)]/u_1[N(1)-N(2)]$	0.974	0.049
	$u_8[N(2)...C(4)]/u_7[N(1)...C(3)]$	1.022	0.051
	$u_9[C(3)...C(5)]/u_7[N(1)...C(3)]$	1.053	0.053
	$u_{10}[N(2)...Cl(7)]/u_{13}[C(4)...Cl(7)]$	0.950	0.047
	$u_{15}[C(3)...C(6)]/u_{14}[N(1)...C(4)]$	0.961	0.048
	$u_{21}[C(5)...Cl(7)]/u_{18}[N(1)...Cl(7)]$	1.014	0.051

[a] Values taken from 6-31G*/SCF scaled force fields

[b] Uncertainties are 5% of the amplitude ratio

4,6-Dichloropyrimidine

The results obtained in the structural refinement of 4,6-dichloropyrimidine are presented in Table 4.8. Of the nine geometrical parameters required to describe the structure fully, five were able to refine freely. The remaining four (p_{2-5}) were therefore assigned the *ab initio* based restraints given in Table 4.6. Similarly, only nine out of a total of twenty-seven vibrational amplitudes (u_2, u_6, u_9, u_{10}, u_{11}, u_{15}, u_{17}, u_{22} and u_{25}) were able to refine unaided. An additional seven amplitudes were successfully refined with the inclusion of the ratio amplitude restraints documented in Table 4.7, resulting in the vibrational amplitudes of the sixteen distances giving rise to the most prominent features on the radial distribution curve being able to refine. The remaining fixed amplitudes of vibration, all for atom pairs involving hydrogen, were considered to have little effect on values or standard deviations of those which were refined.

Final values obtained for the three ring distances were found to be 138.3(6) pm, 134.2(3) pm and 133.2(3) pm for rC-C, r[C(2)-N(1)] and r[C(6)-N(1)] respectively, agreeing with values calculated *ab initio* (6-311G**/MP2) to within one or two standard deviations. Similarly, a close agreement between experiment and theory was observed for the four internal ring angles, with all values in agreement to within about one experimental standard deviation or 0.5°. The chlorine atoms were readily located by the GED data, with p_6 (C-Cl distance) refining to 173.1(1) pm and p_9 (<NCCl) refining to 117.4(1)°, compared to the *ab initio* values of 172.8 pm and 117.5°. The hydrogen atoms were also successfully found with the aid of restraints, enabling r[C(2)-H(7)] and r[C(5)-H(9)] to refine to 109.4(11) pm and 109.0(11) pm, compared to their respective *ab initio* values of 108.6 pm and 108.3 pm.

The R_G factor for this refinement was 8.5%, indicating that the data are of good quality. With all nine geometric parameters and sixteen vibrational amplitudes refining, the structure is the best that can be obtained using all available data, both experimental and theoretical, and all standard deviations should be reliable estimates, free from systematic errors due to limitations of the model. The full list of bond distances and vibrational amplitudes is given in Table 4.9. The final combined

molecular scattering curve and radial distribution curve are given in Figures 4.4 and 4.5 respectively.

Table 4.8 GED results for 4,6-dichloropyrimidine (r_α° /pm,$</°$)

	Parameter	restrained GED results[a]
	Independent[b]	
p_1	av. ring distance	135.2(1)
p_2	r(C-C)-av. r(C-N)	4.6(8)
p_3	Δ r(C-N)	-1.0(2)
p_4	av. r(C-H)	109.2(11)
p_5	Δ r(C-H)	-0.3(1)
p_6	r(C-Cl)	173.1(1)
p_7	<NCN	127.8(5)
p_8	<CNC	114.6(4)
p_9	<NCCl	117.1(4)
	Dependent	
	r(C-C)	138.3(6)
	r[C(2)-N(1)]	134.2(3)
	r[C(6)-N(1)]	133.2(3)
	r[C(2)-H(7)]	109.4(11)
	r[C(5)-H(9)]	109.0(11)
	<NCC	123.8(3)
	<CCC	115.4(7)

[a] Estimated standard deviations, obtained in the least squares refinement, are given in parentheses

[b] For definition of parameters, see the text

Table 4.9 Interatomic distances (r_a/pm) and amplitudes of vibration (u/pm) for the restrained GED structure of 4,6-dichloropyrimidine [a]

i	Atom pair	Distance	Amplitude[b]
1	N(1)-C(2)	134.4(2)	5.1(3)
2	C(4)-N(3)	133.3(3)	5.2(3)
3	C(4)-C(5)	138.5(6)	5.1(3)
4	C(2)-H(7)	110.4(11)	7.4 (fixed)
5	C(5)-H(9)	110.3(11)	7.4 (fixed)
6	C(4)-Cl(8)	173.4(2)	4.9(2)
7	N(1)...H(7)	207.8(9)	9.2 (fixed)
8	N(1)...N(3)	241.4(7)	5.8(5)
9	N(1)...Cl(10)	262.1(5)	7.4(3)
10	N(1)...C(5)	239.9(6)	6.0(5)
11	C(2)...C(4)	225.1(4)	4.5(8)
12	C(4)...C(6)	234.0(6)	4.7(9)
13	C(4)...H(9)	217.8(12)	9.4 (fixed)
14	C(5)...Cl(8)	269.2(4)	7.7(4)
15	N(1)...C(4)	272.2(5)	8.7(12)
16	C(2)...C(5)	266.2(12)	8.5(12)
17	C(2)...Cl(8)	384.6(4)	9.4(5)
18	N(1)...H(9)	339.0(12)	9.0 (fixed)
19	C(4)...Cl(10)	394.5(5)	9.3(5)
20	C(4)...H(7)	323.9(11)	8.9 (fixed)
21	Cl(8)...H(9)	287.3(8)	13.3 (fixed)
22	N(1)...Cl(8)	445.2(5)	10.1(5)
23	C(2)...H(9)	375.8(16)	8.8 (fixed)
24	C(5)...H(7)	376.0(16)	8.8 (fixed)
25	Cl(8)...Cl(10)	537.4(7)	12.0(6)
26	Cl(8)...H(7)	469.4(10)	10.2 (fixed)
27	H(7)...H(9)	485.3(24)	11.1 (fixed)

[a] Estimated standard deviations, obtained in the least-squares refinement, are given in parentheses

[b] Amplitudes not refined were fixed at values calculated using the scaled 6-31G*/SCF force field
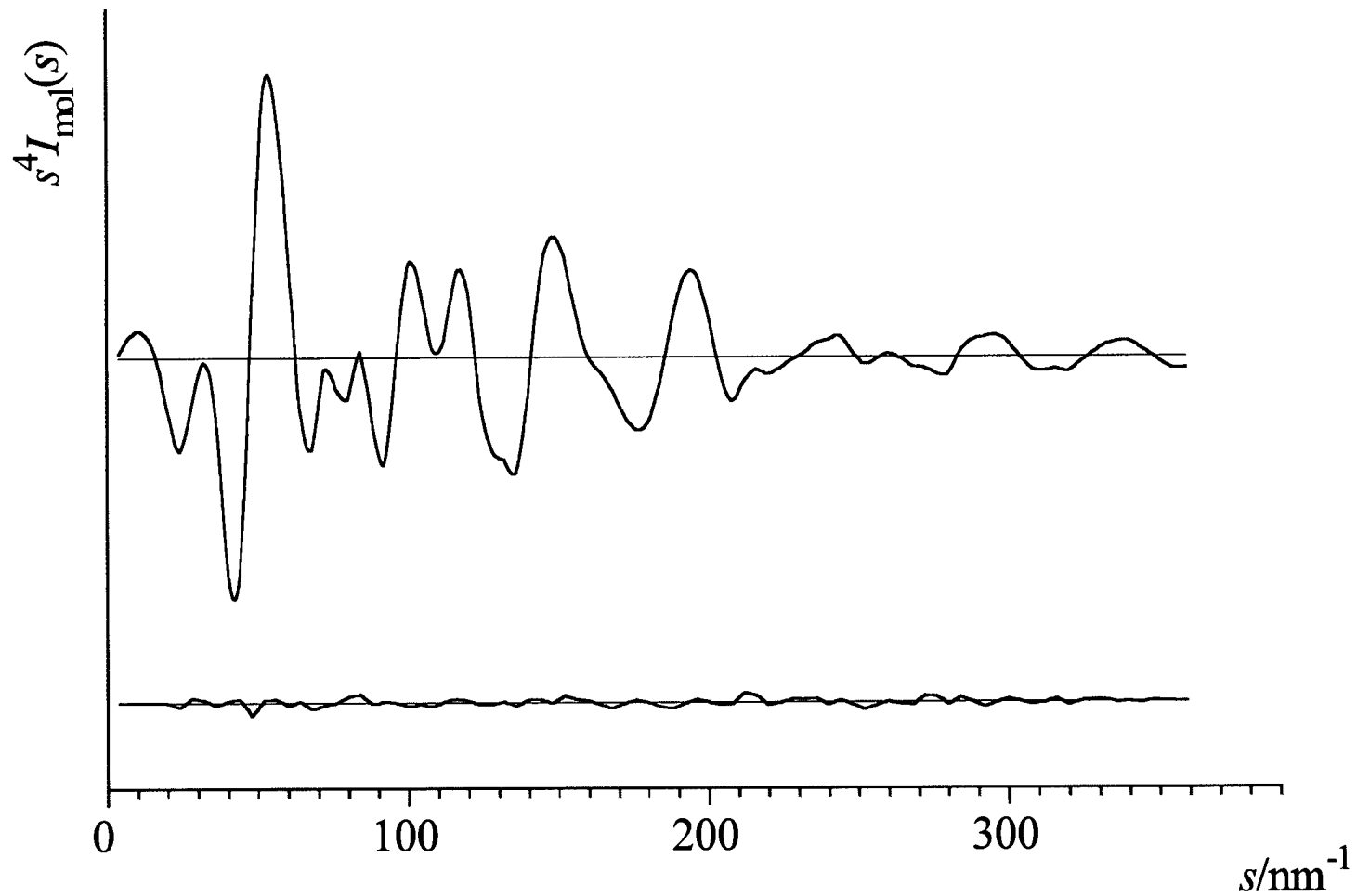
Figure 4.4 Observed and final weighted difference combined molecular scattering curves for 4,6-dichloropyrimidine
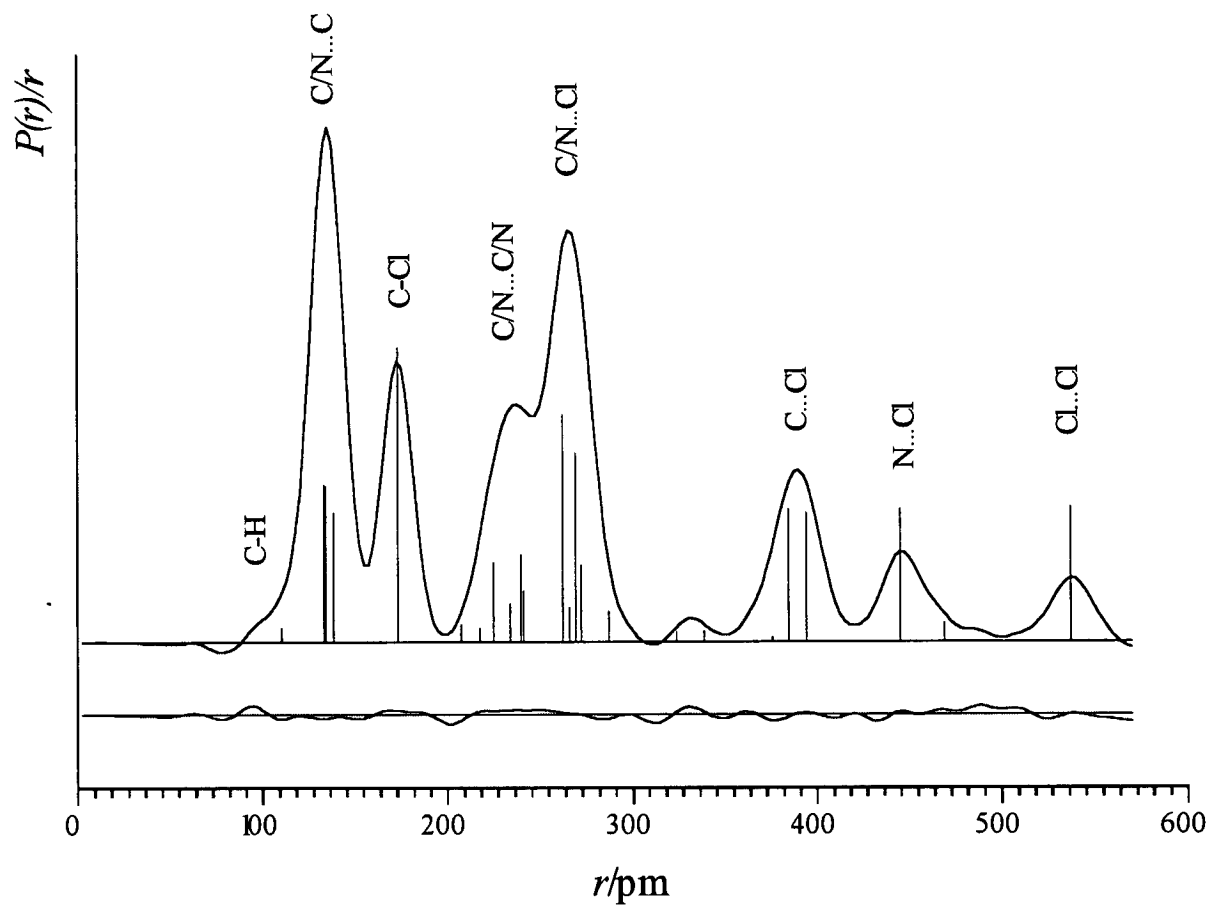
Figure 4.5 Observed and final difference radial-distribution curves for 4,6-dichloropyrimdine. Before Fourier inversion the data were multiplied by $s.\exp(-0.00002s^2)/(Z_{Cl}-f_{Cl})(Z_C-f_C)$.

2,6-Dichloropyrazine

The results obtained for the structural refinement of 2,6-dichloropyrazine are given in Table 4.10. The five geometric restraints required to allow all geometric parameters to refine to realistic values are given in Table 4.6. Of the twenty-five vibrational amplitudes, only nine successfully refined unassisted, namely u_1, u_5, u_7, u_{11}, u_{15}, u_{16}, u_{19}, u_{22}, and u_{24}. A further five vibrational amplitudes were refined with the introduction of five ratios of vibrational amplitudes, documented in Table 4.7.

The three ring distances refined to 139.1(4) pm, 134.3(2) pm and 133.4(2) pm for rC-C, r[C(3)-N(4)] and r[C(2)-N(1)] respectively, within two or three standard deviations of results obtained from the 6-311G**/MP2 calculation. The four internal ring angles also refined to values concordant with those predicted from the 6-311G**/MP2 calculation, with experiment and theory in agreement to within 1°, or three standard deviations. The chlorine atom positions were well defined, with rC-Cl (p_4) refining to 173.5(2) pm and <CCCl (p_8) to 120.0(3)°, compared to the values 172.6 pm and 119.4° calculated *ab initio*. The two parameters defining the hydrogen atom positions (p_5, rC-H and p_9, <CCH) were successfully restrained, refining to 108.2(12) pm and 122.8(13)°, compared to 108.5 pm and 121.2° from the 6-311G**/MP2 calculation.

The final R_G factor recorded for this refinement was 9.3%. Since all geometric parameters and the fourteen most significant vibrational amplitudes are refining, this structure, obtained by combining experimental and theoretical data, represents the best possible solution that can be obtained at present. The complete list of interatomic distances and amplitudes of vibration determined in this refinement are given in Table 4.11. The combined molecular scattering intensities and final differences are shown in Figure 4.6, and the final radial distribution and difference curves in Figure 4.7.

Table 4.10 GED results for 2,6-dichloropyrazine ($r_\alpha°$/pm,</°)

	Parameter	restrained GED results[a]
	Independent[b]	
p_1	av. ring distance	135.6(1)
p_2	r(C-C)-av. r(C-N)	5.2(6)
p_3	$\Delta\, r$(C-N)	-0.8(1)
p_4	r(C-Cl)	173.5(2)
p_5	r(C-H)	106.1(11)
p_6	<C(3)N(4)C(5)	117.2(2)
p_7	<C(2)C(3)N(4)	120.4(2)
p_8	<CCCl	120.0(3)
p_9	<CCH	119.3(14)
	Dependent	
	r(C-C)	139.1(4)
	r[C(3)-N(4)]	134.3(2)
	r[C(2)-N(1)]	133.4(2)
	<N(1)C(2)C(3)	123.8(3)
	<C(2)N(1)C(6)	114.4(3)
	<NCC	123.8(3)
	<CCC	115.4(7)

[a] Estimated standard deviations, obtained in the least squares refinement, are given in parentheses

[b] For definition of parameters, see the text

Table 4.11 Interatomic distances (r_a/pm) and amplitudes of vibration (u/pm) for the restrained GED structure of 2,6-dichloropyrazine [a]

i	Atom pair	Distance	Amplitude[b]
1	N(1)-C(2)	133.6(2)	5.0(3)
2	C(3)-N(4)	134.5(2)	5.0(3)
3	C(2)-C(3)	139.3(4)	5.3(4)
4	C(3)-H(8)	107.3(11)	7.4 (fixed)
5	C(2)-Cl(7)	173.8(2)	5.3(3)
6	N(1)...C(3)	240.7(4)	5.3(3)
7	C(2)...N(4)	237.4(3)	5.3 (4)
8	C(2)...C(6)	224.5(4)	5.0 (fixed)
9	C(3)...C(5)	229.6(4)	5.0 (fixed)
10	N(4)...H(8)	209.7(17)	9.3(fixed)
11	N(1)...Cl(10)	261.7(3)	8.0(5)
12	C(2)...H(8)	213.0(18)	9.4 (fixed)
13	C(3)...Cl(7)	271.3(5)	7.8(5)
14	N(1)...N(4)	281.5(4)	5.0(11)
15	C(2)...C(5)	266.3(3)	4.8(10)
16	N(4)...Cl(10)	396.3(4)	7.9(5)
17	N(1)...H(8)	335.0(14)	9.0(fixed)
18	H(8)...Cl(7)	284(2)	13.0 (fixed)
19	C(2)...Cl(10)	383.7(3)	7.2(6)
20	H(8)...C(5)	327.4(14)	9.0 (fixed)
21	H(8)...H(9)	417(3)	12.3 (fixed)
22	Cl(10)...Cl(7)	521.7(6)	11.2(6)
23	H(8)...C(6)	372.7(12)	8.8 (fixed)
24	Cl(7)...C(5)	439.5(2)	8.1(5)
25	H(8)...Cl(10)	545.8(12)	8.9(fixed)

[a] Estimated standard deviations, obtained in the least-squares refinement, are given in parentheses

[b] Amplitudes not refined were fixed at values calculated using the scaled 6-31G*/SCF force field
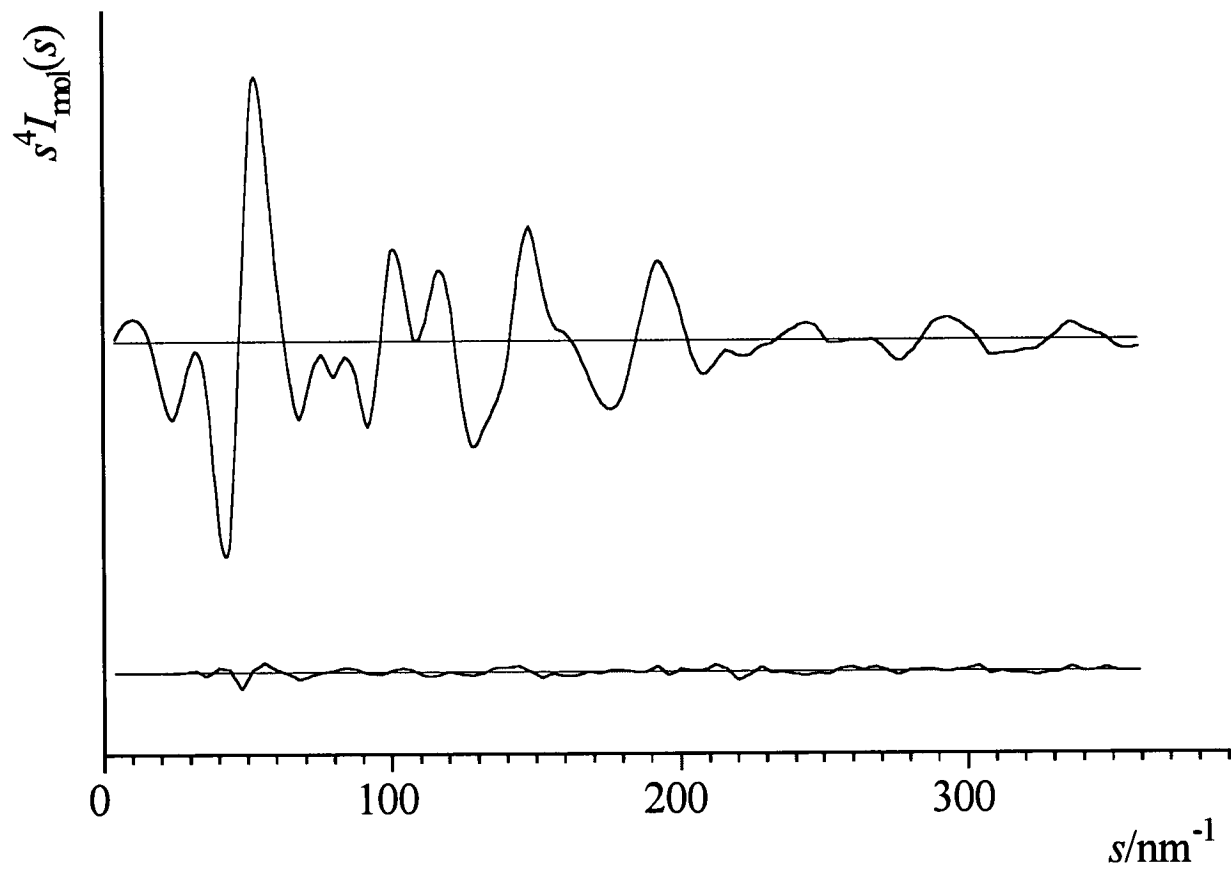
Figure 4.6 Observed and final weighted difference combined molecular scattering curves for 2,6-dichloropyrazine
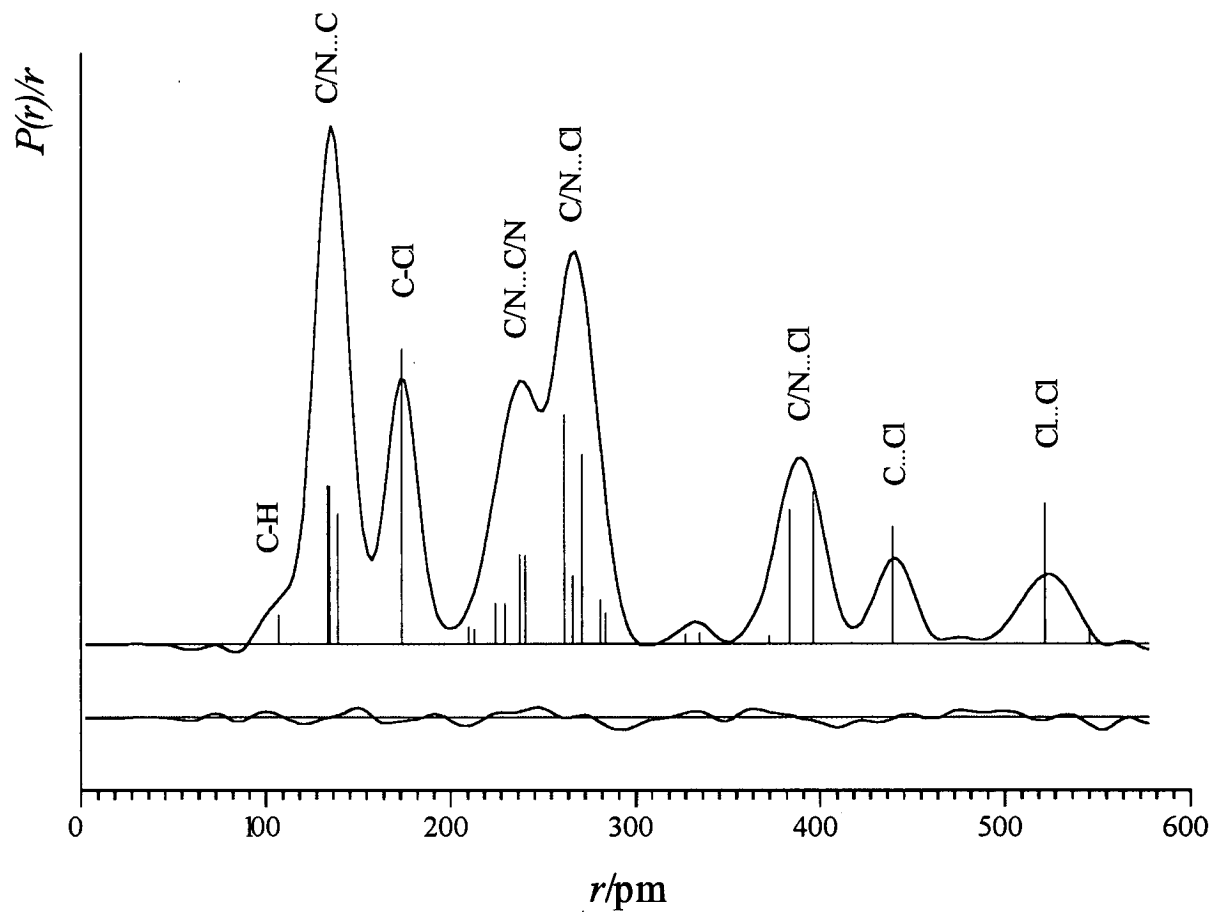
Figure 4.7 Observed and final difference radial-distribution curves for 2,6-dichloropyrazine. Before Fourier inversion the data were multiplied by $s.\exp(-0.00002s^2)/(Z_{Cl}\text{-}f_{Cl})(Z_C\text{-}f_C)$.

3,6-Dichloropyridazine

The results obtained for the structural refinement of 3,6-dichloropyridazine are given in Table 4.12. In addition to the GED data, two sets of rotation constants were available for this compound,[24] the first set corresponding to the $^{35}Cl/^{35}Cl$ isotopomer and the second to $^{35}Cl/^{37}Cl$. The structural refinement is therefore based on a combination of GED data, six rotation constants and five geometric restraints (documented in Table 4.6), resulting in a structure with all geometric parameters refining. In addition, eight amplitude ratios were restrained (see Table 4.7), enabling a total of sixteen amplitudes of vibration to refine.

To account for the change in bond distance incurred upon isotopic substitution, an extra parameter was written into the model: p_{11} is defined as $r(C\text{-}^{37}Cl)$ minus $r(C\text{-}^{35}Cl)$. Although the refined value of this parameter was found to be consistently zero, its inclusion avoided systematic under-estimation of standard deviations for other parameters with which it might be correlated. The vibrational corrections required to convert the rotation constant data from the experimental structure type B_o to B_z (equivalent to the r_α^o structural type derived from the GED data) were obtained from the scaled *ab initio* force field. Values for rotation constants, along with the vibrational corrections and calculated values based on the structure obtained, are given in Table 4.13. Note that the uncertainties, used to weight the data, are based on assumed experimental errors of 1 MHz for rotation constant A and 0.1 MHz for B and C, plus a conservative estimate of 10% error in the vibrational corrections.

The four ring distances refined to values in agreement with those obtained from the 6-311G**/MP2 calculation to within one standard deviation, with rN-N refining to 134.2(3) pm, rC-N to 133.0(3) pm and the two C-C distances to 138.1(3) pm and 140.0(3) pm. The three internal ring angles were also found to agree well with theory, with all three angles consistent with the 6-311G**/MP2 results to within 0.5°. The chlorine atoms positions were satisfactorily determined, with rC-Cl (p_5) refining to 173.1(2) pm and <CCCl (p_9) to 199.1(14)°, compared to the *ab initio* values of 172.5 pm and 119.3°. The hydrogen atoms were also successfully located with the aid of

restraints, enabling rC-H (p_6) to refine to 108.2(12) pm and <[C(5)C(4)H(8)] (p_{10}) to 122.8(13)°, compared to the *ab initio* values of 108.4 pm and 121.2°.

The final R_G factor for this refinement was 13.5%. The complete list of interatomic distances and amplitudes of vibration is given in Table 4.14. The combined molecular scattering intensities and final differences are shown in Figure 4.8 and the final radial distribution and difference curves in Figure 4.9.

Table 4.12 GED results for 3,6-dichloropyridazine ($r_\alpha°$/pm, $</°$)

	Parameter	restrained GED + rotation constants results[a]
	Independent[b]	
p_1	av. ring distance	136.4(1)
p_2	Δr(C-C)	1.9(1)
p_3	r(N-N)-r(C-N)	1.2(3)
p_4	av. r(C-C)-av.[r(N-N), r(N-C)]	6.0(5)
p_5	r(C-Cl)	173.1(2)
p_6	r(C-H)	108.2(12)
p_7	$<$NNC	118.4(2)
p_8	$<$NCC	124.7(4)
p_9	$<$CCCl	119.1(14)
p_{10}	$<$CCH	122.8(13)
p_{11}	r[(C-^{37}Cl)-(C-^{35}Cl)]	0.00(6)
	Dependent	
	r[C(5)-C(6)]	140.0(3)
	r[C(4)-C(5)]	138.1(3)
	r(C-N)	133.0(3)
	r(N-N)	134.2(3)
	$<$CCC	116.9(3)

[a] Estimated standard deviations, obtained in the least squares refinement, are given in parentheses

[b] For definition of parameters, see the text

Table 4.13 Rotation constants (B/MHz) for 3,6-dichloropyridazine as used in the gas-phase structure study

Rotation constant		Observed[a]		Calculated[c]	Difference	Uncertainty[d]
Species	Axis	B_0	B_z[b]	B_z	B_z(Obs.-Calc.)	
$^{35}Cl / {}^{35}Cl$	A	5916.6(10)	5917.2	5917.1	0.1	1.2
	B	710.02(10)	709.94	709.94	0.0	0.12
	C	634.00(10)	633.94	633.89	0.05	0.12
$^{37}Cl / {}^{35}Cl$	A	5916.1(10)	5916.7	5916.8	-0.1	1.2
	B	692.40(10)	692.33	692.35	-0.02	0.12
	C	619.90(10)	619.84	619.82	0.02	0.12

[a] from ref. 24

[b] Vibrational corrections obtained from scaled 6-31G*/SCF *ab initio* force field

[c] Calculated from the final combined analysis/SARACEN refinement

[d] Used to weight data in structural refinement, derived from experimental error plus a 10% uncertainty in the harmonic vibrational correction

Table 4.14 Interatomic distances (r_a/pm) and amplitudes of vibration (u/pm) for the restrained structure of 3,6-dichloropyridazine [a]

i	Atom pair	Distance	Amplitude[b]
1	N(1)-N(2)	134.3(3)	5.5(4)
2	N(2)-C(3)	133.1(3)	5.5(4)
3	C(3)-Cl(7)	173.6(2)	4.4(4)
4	C(3)-C(4)	140.1(3)	5.3(5)
5	C(4)-H(8)	108.5(13)	9.4 (fixed)
6	C(4)-C(5)	138.3(3)	5.2(4)
7	N(1)...C(3)	229.7(3)	4.6(6)
8	N(2)...C(4)	242.0(4)	4.7(6)
9	C(3)...C(5)	237.1(6)	4.9(6)
10	N(2)...Cl(7)	261.1(15)	7.8(12)
11	C(3)...H(8)	216.2(16)	9.0 (fixed)
12	C(5)...H(8)	218.1(18)	7.4 (fixed)
13	C(4)...Cl(7)	270.7(20)	8.3(13)
14	N(1)...C(4)	276.6(6)	6.5(13)
15	C(3)...C(6)	260.9(4)	6.3(13)
16	Cl(7)...H(8)	285(3)	10.2 (fixed)
17	H(9)...H(8)	252(5)	15.1 (fixed)
18	N(1)...Cl(7)	386.8(11)	8.4(11)
19	C(3)...H(9)	335.6(15)	9.5 (fixed)
20	N(2)...H(8)	338.3(13)	9.0 (fixed)
21	C(5)...Cl(7)	396.9(16)	7.9(11)
22	N(1)...H(8)	385.1(12)	9.1(fixed)
23	C(6)...Cl(7)	433.9(2)	8.6(7)
24	Cl(10)...H(8)	483.3(22)	13.3 (fixed)
25	Cl(7)...Cl(10)	606.6(1)	10.0(6)

[a] Estimated standard deviations, obtained in the least-squares refinement, are given in parentheses

[b] Amplitudes not refined were fixed at values calculated using the scaled 6-31G*/SCF force field
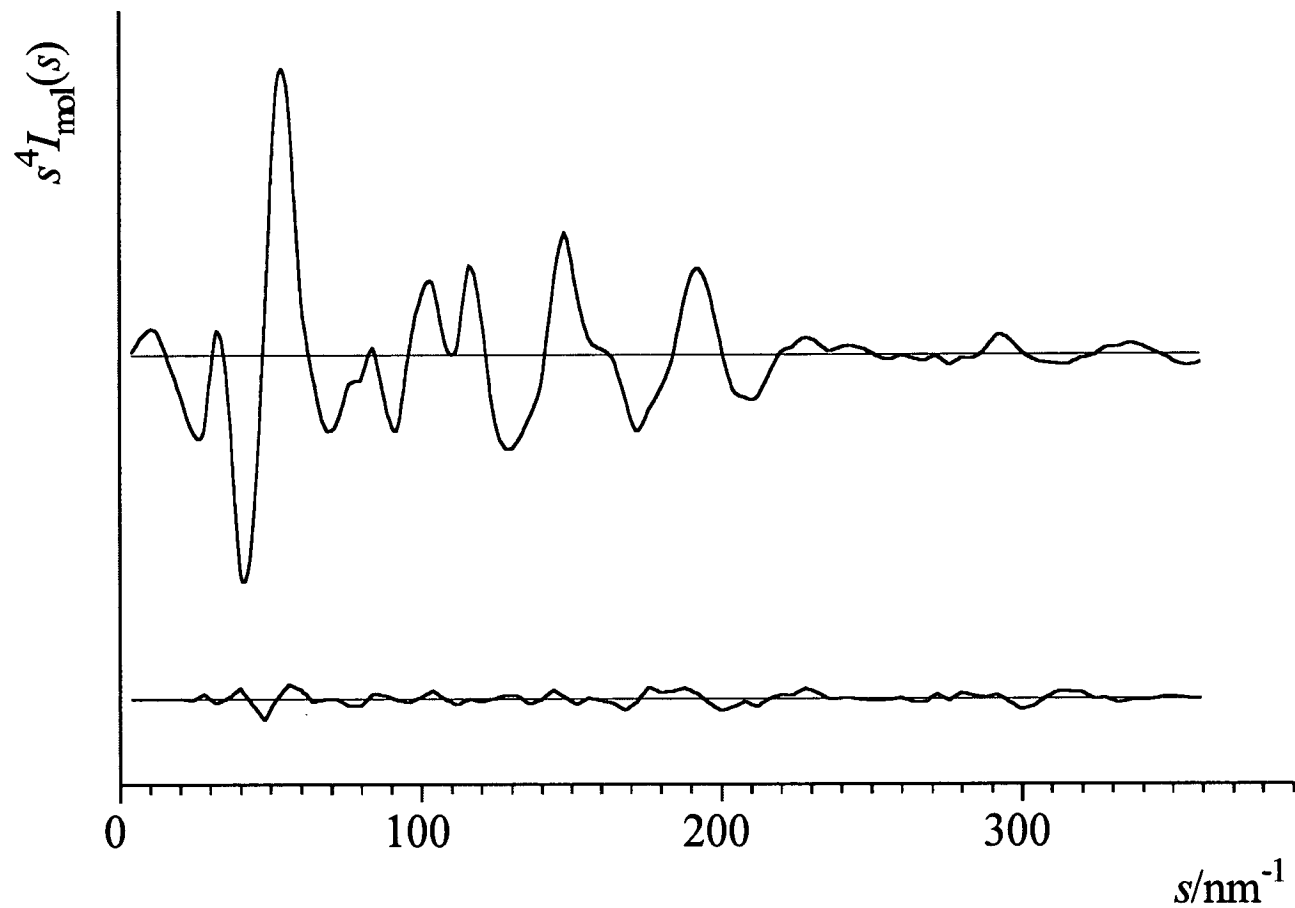
Figure 4.8 Observed and final weighted difference combined molecular scattering curves for 3,6-dichloropyridazine
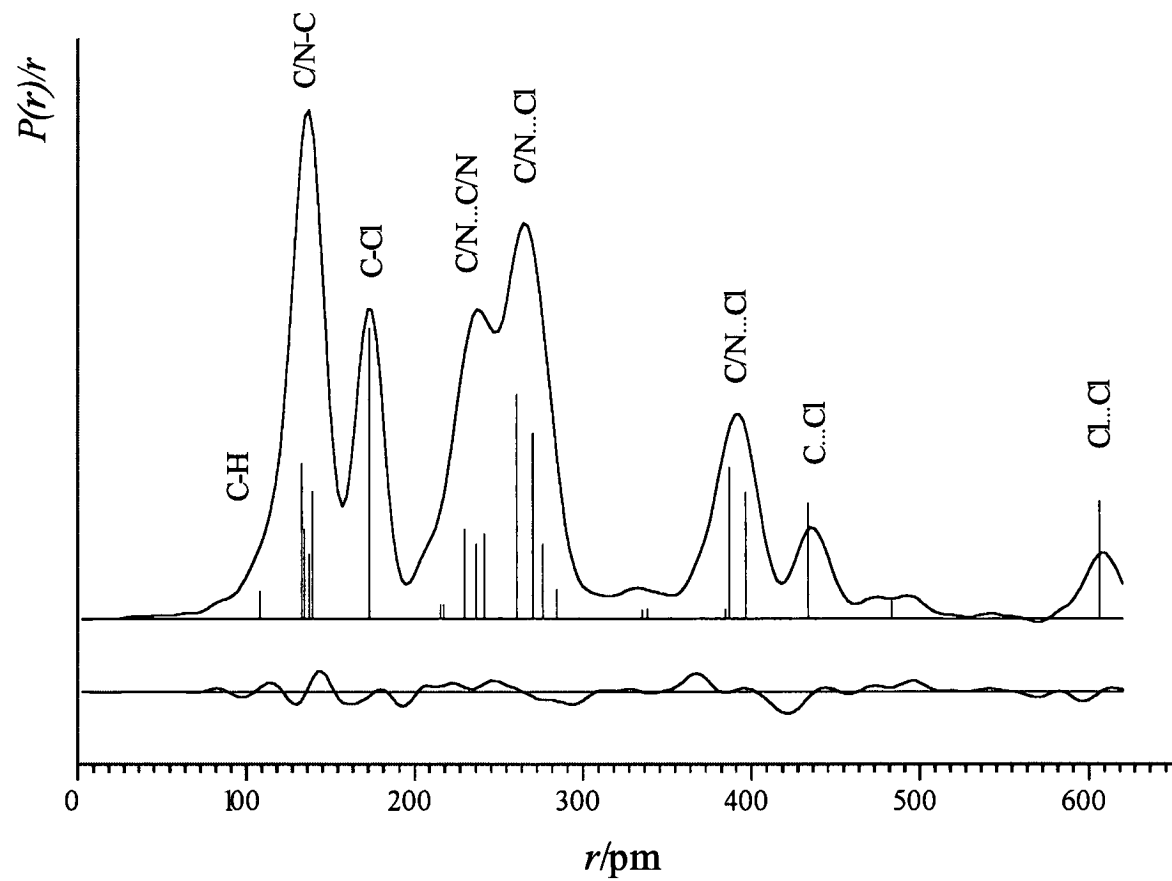
114

Figure 4.9 Observed and final difference radial-distribution curves for 3,6-dichloropyridazine. Before Fourier inversion the data were multiplied by $s.\exp(-0.00002s^2)/(Z_{Cl}-f_{Cl})(Z_C-f_C)$.

4.3.3 Crystal Structure Results

Geometric parameters recorded for the four dichloro compounds can be found in Tables 4.15 to 4.18 and crystal packing diagrams in Figures 4.10 to 4.13. For all four cases the structures of the compounds in the solid phase were found to be planar.

In the crystal strucutre of 4,6-dichloropyrimidine (see Table 4.15 and Figure 4.10), two distinct molecules were found in the asymmetric unit, linked together by C(H)...N and Cl...Cl contacts to form chains. In the case of 2,5-dichloropyrimidine (see Table 4.16 and Figure 4.11), only one and a half molecules were located in the asymmetric unit (*i.e.* one molecule lies on a mirror plane). The most significant close inter-nuclear contacts, responsible for linking the molecules together, were found between atoms C(H)...N and N...Cl. In contrast, only one molecule was found in the asymmetric unit of 2,6-dichloropyrazine (see Table 4.17 and Figure 4.12). Molecules were found to form C(H)...N bonded layers, also with close Cl...Cl contacts. Only one inter-layer contact, C...C, appears to be present, resulting in the molecules packing in a step-wise fashion. Finally, two molecules were found in the asymmetric unit of 3,6-dichloropyridazine (see Table 4.18 and Figure 4.13), linked together by three C(H)...N contacts per molecule, resulting in molecules stacking together in columns of wave-like planes.

Table 4.15 Crystal structure parameters for the molecules found in the asymmetric unit of 4,6-dichloropyrimidine (r/pm,$</°$)

	molecule 1		molecule 2	
bond lengths				
r[N(1)-C(2)]/r[N(3)-C(2)]	133.8(5)	134.2(5)	132.0(5)	134.6(5)
r[N(1)-C(6)]/r[N(3)-C(4)]	131.7(5)	131.0(5)	133.4(5)	133.3(5)
r[C(6)-C(5)]/r[C(4)-C(5)]	139.1(5)	138.4(5)	139.1(5)	137.4(5)
r[C(6)-Cl(10)]/r[C(4)-Cl(8)]	173.3(4)	174.7(4)	171.3(4)	174.1(4)
angles				
<N(1)C(2)N(3)	128.2(3)		125.9(4)	
<C(2)N(1)C(6)/<C(2)N(3)C(4)	113.5(3)	115.1(3)	115.1(3)	115.9(3)
<N(1)C(6)C(5)/<N(3)C(4)C(5)	124.7(3)	123.4(3)	125.6(3)	124.7(3)
<C(4)C(5)C(6)	114.9(3)		112.8(3)	
<N(1)C(6)Cl(10)/<N(3)C(4)Cl(8)	115.2(3)	116.6(3)	116.0(3)	117.2(3)
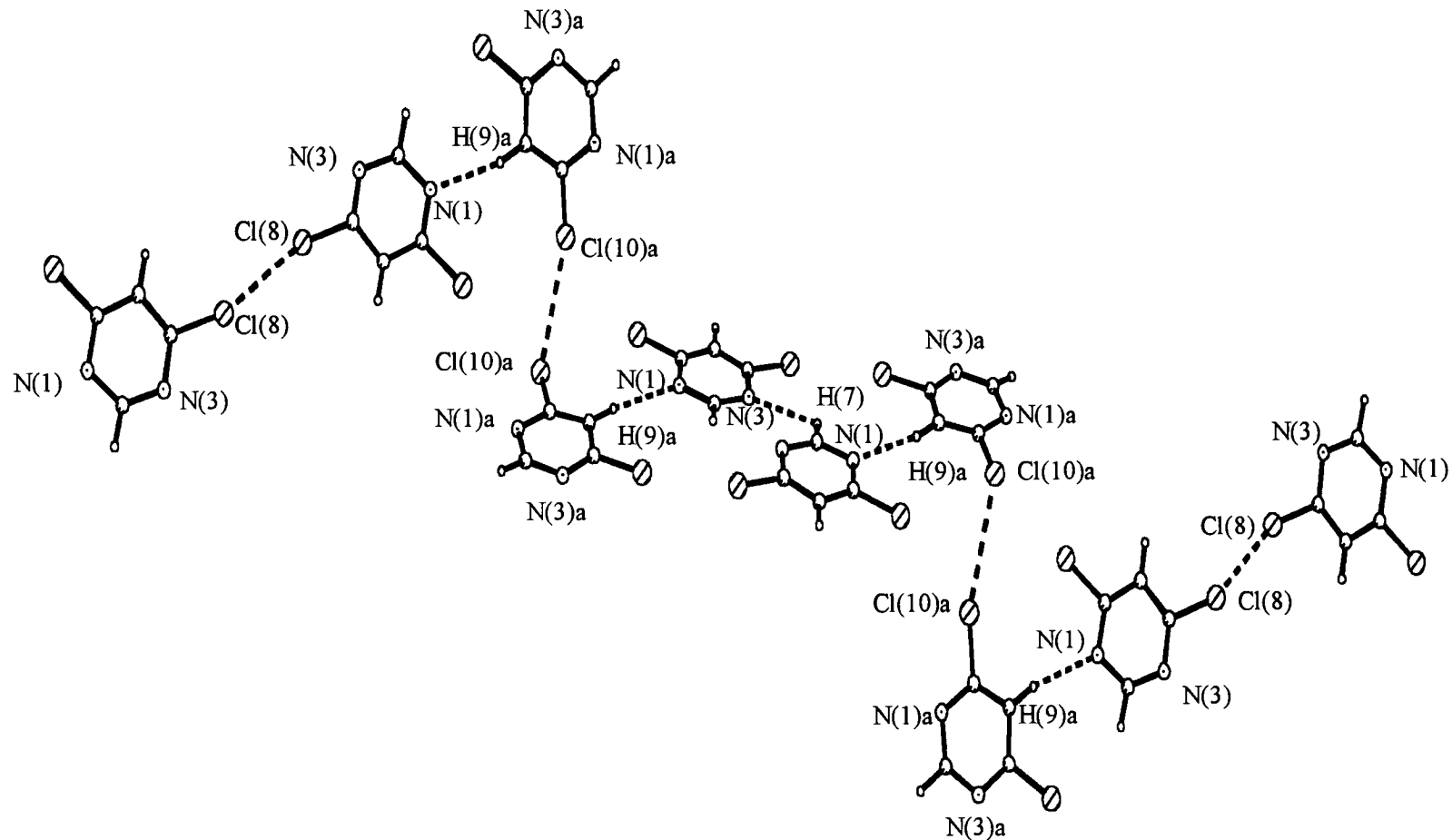
Figure 4.10 Crystal packing arrangement of 4,6-dichloropyrimidine. Molecules were found to stack in columns in alternating vertical and horizontal planes. Dotted lines indicate inter-molecular bonding giving rise to significant structural distortions from the gas-phase structure. Atoms labelled 'a' after their number are in molecule 2.

118

Table 4.16 Crystal structure parameters for the molecules found in the asymmetric unit of 2,5-dichloropyrimidine (r/pm,</°)

	molecule 1		molecule 2
bond lengths			
rN(1)-C(6)/rN(3)-C(4)	134.0(5)	133.7(5)	133.4(5)
rC(5)-C(6)/rC(4)-C(5)	137.4(6)	136.2(6)	137.3(5)
rC(2)-Cl(7)	173.5(4)		174.6(6)
rC(5)-Cl(9)	172.5(4)		173.6(6)
angles			
N(1)-C(2)-N(3)	129.2(4)		130.8(4)
C(2)-N(3)-C(4)/C(2)-N(1)-C(6)	114.5(3)	114.5(4)	114.4(4)
N(3)-C(4)-C(5)/N(1)-C(6)-C(5)	122.2(4)	121.9(4)	120.6(4)
C(4)-C(5)-C(6)	117.8(4)		119.4(6)
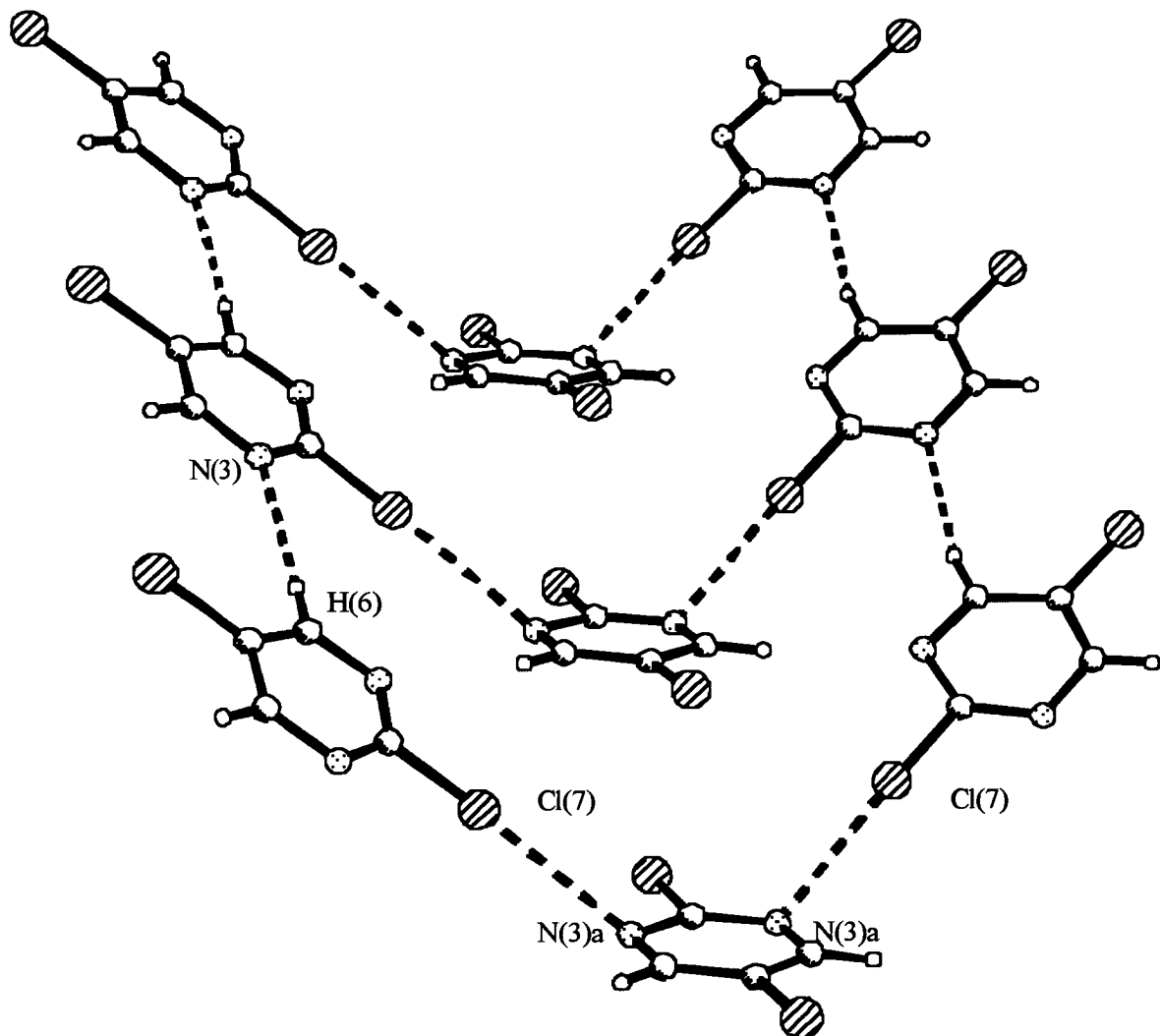
Figure 4.11 Crystal structure of 2,5-dichloropyrimidine.
Atoms labelled 'a' after their number are in molecule 2.

Table 4.17 Crystal structure parameters for the molecules found in the asymmetric unit of 2,6-dichloropyrazine (r/pm,$</°$)

	molecule 1	
bond lengths		
r[N(1)-C(2)]/r[N(1)-C(6)]	131.2(3)	131.8(3)
r[C(2)-C(3)]/r[C(6)-C(5)]	138.2(4)	137.1(4)
r[C(3)-N(4)]/r[C(5)-N(4)]	132.6(4)	132.5(3)
r[C(2)-Cl(7)]/r[C(6)-Cl(10)]	173.0(3)	173.4(3)
angles		
<C(2)N(1)C(6)	114.6(2)	
<N(1)C(2)C(3)/<N(1)C(6)C(5)	123.6(2)	123.8(2)
<C(2)C(3)N(4)/<C(6)C(5)N(4)	120.3(2)	120.6(2)
<C(3)N(4)C(5)	117.0(2)	
<N(1)C(2)Cl(7)/<N(1)C(6)Cl(10)	116.4(2)	116.5(2)
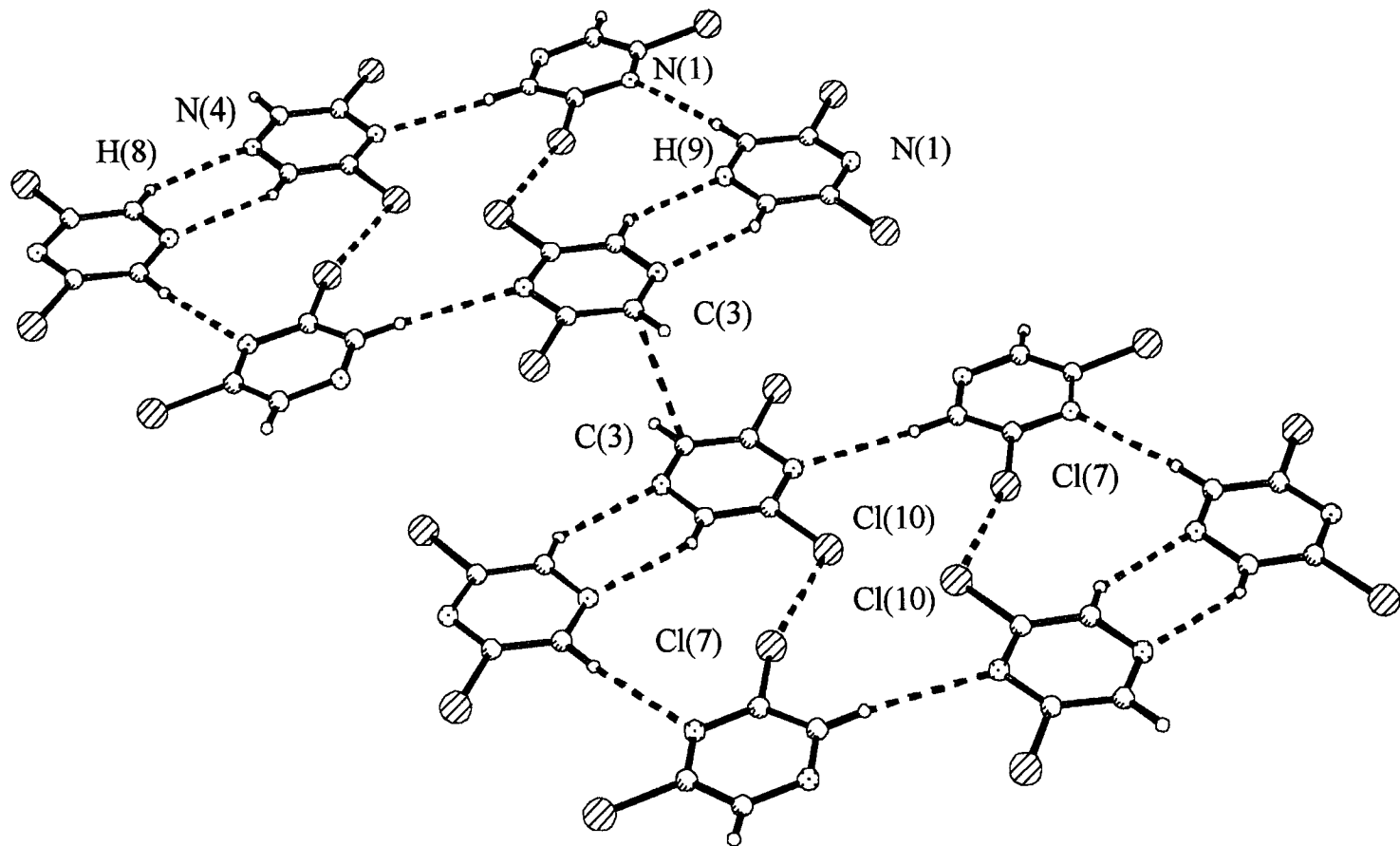
Figure 4.12 Packing arrangement of 2,6-dichloropyrazine in the crystal phase. Molecules were found to pack in planes in a step-wise fasion.

Table 4.18 Crystal structure parameters for the molecules found in the asymmetric unit of 3,6-dichloropyridazine (r/pm,</°)

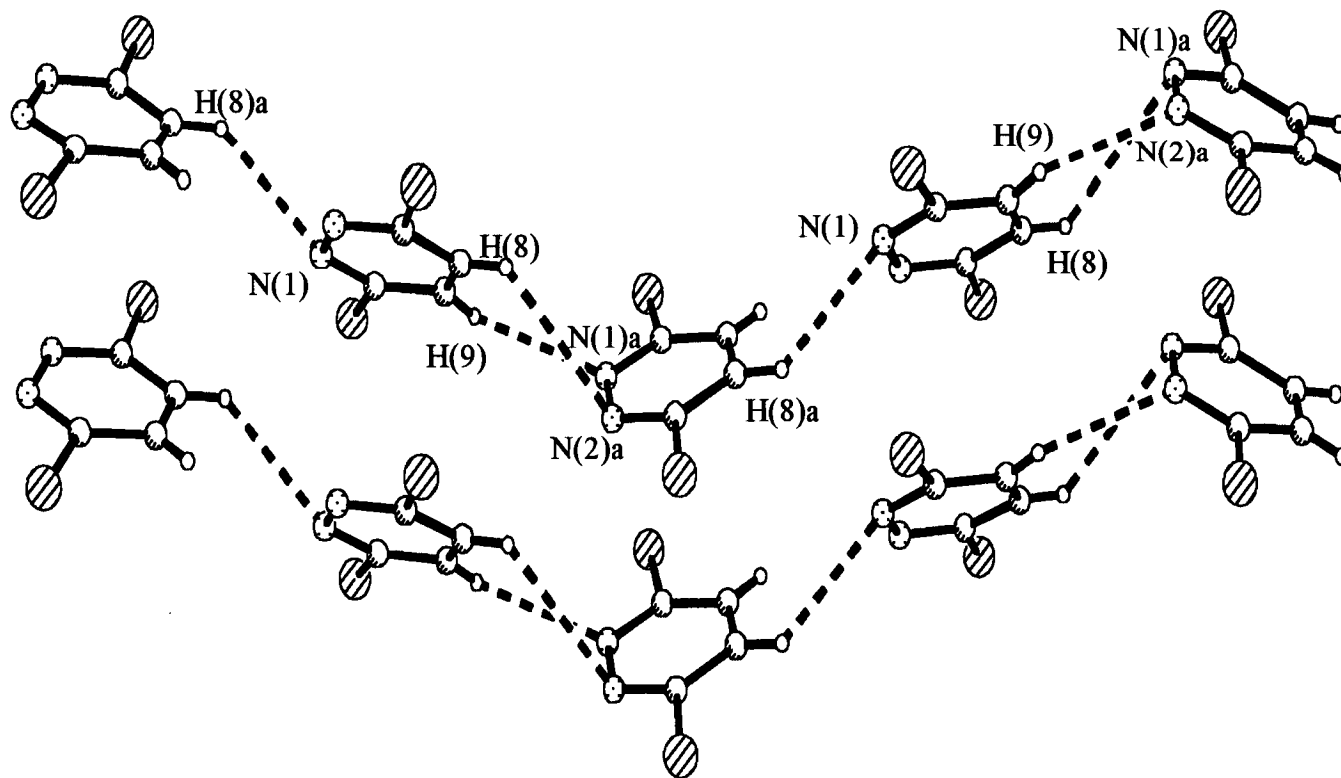|	molecule 1		molecule 2	
bond lengths				
r(N-N)	134.9(6)		135.6(7)	
r[N(2)-C(3)]/r[N(1)-C(6)]	131.5(7)	129.9(7)	131.3(7)	129.9(7)
r[C(3)-C(4)]/r[C(6)-C(5)]	137.1(8)	137.5(8)	137.9(8)	138.9(7)
r[C(4)-C(5)]	135.8(8)		133.4(8)	
r[C(3)-Cl(7)]/r[C(6)-Cl(10)]	172.6(6)	174.4(6)	173.2(6)	173.6(6)
angles				
<N(1)N(2)C(3)/<N(2)N(1)C(6)	117.8(5)	118.3(4)	118.3(5)	117.5(5)
<N(2)C(3)C(4)/<N(1)C(6)C(5)	124.9(5)	126.3(5)	124.9(6)	125.8(5)
<C(3)C(4)C(5)/<C(6)C(5)C(4)	117.5(5)	115.3(5)	117.1(5)	116.3(5)
<N(2)C(3)Cl(7)/<N(1)C(6)Cl(10)	115.2(4)	114.6(4)	114.4(4)	114.6(4)

Figure 4.13 Crystal packing diagram for 3,6-dichloropyridazine. Molecules were found to stack in columns of wave-like planes. Atoms labelled 'a' after their number are in molecule 2.

4.4 Effects of Chlorination on Ring Geometry

The gas-phase molecular structures of the dichloro derivatives of pyrimidine, pyrazine and pyridazine were compared to those of their respective parent molecules to determine the effects of electron-withdrawing substituents on the overall ring geometry. In addition to the structures of the three dichloro derivatives presented in this chapter a fourth, 2,5-dichloropyrimidine, which was presented in Chapter 3,[3] was also considered in this investigation.

The observed changes in ring geometry are presented in Table 4.19, where most structural trends identified by experiment are also clearly present in the structures calculated *ab initio*. In addition the trends observed are consistent with observations from previous studies of dichloro derivatives of benzene.[25-28] The main structural changes can be summarised as widening of the *ipso* ring angle, narrowing of the adjacent ring angles and shortening of the adjacent C-C/C-N bonds, with the C-N bonds more sensitive to change than the C-C bonds. These effects were found to be particularly pronounced for 4,6-dichloropyrimidine and 2,6-dichloropyrazine since the chlorine subsituents are *meta* with respect to each other, resulting in additive effects. The structural trends observed can be readily explained in terms of bonding hybridisation effects: since chlorine withdraws electron density from the ring an increase in p character of the *ipso* carbon sp^2 hybrid orbital will be required along the direction of the C-Cl bond. This will effectively lead to a decrease in p character of the remaining sp^2 orbitals, and hence gives rise to a widening of the *ipso* angle and shortening of the adjacent C-N/C-C bonds.

Two points regarding the C-C and C-N bonds adjacent to chlorine substituents are worth noting. Firstly, it is interesting to note that whilst from experiment the C-C bonds were found to shorten slightly or be unaffected by the chlorine atom, from *ab initio* calculations the bonds were predicted to either be unaffected or lengthen slightly. The effect is small, however, and values obtained from the two methods are indistinguishable from one another to within one or two standard deviations. Secondly, in all four cases both experiment and *ab initio* calculations indicate that

C-N distances are much more sensitive to change than C-C bonds when a chlorine atom replaces a hydrogen bonded to the carbon. Moreover, for all four molecules the two methods show that the C-N bonds shorten, in contrast to the C-C bonds which were found to be only slightly shortened or lengthened by the presence of the chlorine substituent. One possible explanation for this difference in behaviour lies with the lone pair of electrons on the nitrogen atom. The chlorine atom withdraws electron density from the carbon atom, which will therefore acquire a net positive charge. The lone pair on the neighbouring nitrogen atom will then be attracted towards the carbon atom, thereby increasing the bond order (and thus reducing the length) of the C-N bond.

Table 4.19 Effects of chlorination on ring geometries[a]

	ipso ring angle at Cl substituted carbon		ring angle at adjacent atom		rC-N; carbon Cl substituted		rC-C; one carbon Cl substituted	
								Parameter
Molecule	experiment	*ab initio*	experiment	*ab initio*	experiment	*ab initio*	experiment	*ab initio*
4,6-dichloropyrimidine	+2.6(3)	+1.3	-1.1(5) -2.4(7)	-0.4 -1.5	-1.8(8)	-1.2	-1.0(7)	0.0
2,5-dichloropyrimidine	+0.1(5) +0.5(6)	+0.3 +0.5	+0.6(8) -0.6(8)	+0.2 -0.5	-0.3(9)	-0.7	0.0(11)	+0.1
2,6-dichloropyrazine	+1.6(5)	+0.6	-1.8(3) -1.2(4)	-1.5 +0.2	-0.4(2)	-1.2	-0.6(5)	+0.3
3,6-dichloropyridazine	+0.9(4)	+0.4	-1.0(2) 0.0(3)	-0.2 -0.3	-0.8(3)	-0.9	0.0(3)	+0.3

[a] Angles in degrees, distances in pm.

4.5 Comparison of Structures in Gas and Solid Phases

It has long been recognised that the comparison of molecular structures in the gaseous and solid phases is the most direct method to investigate molecular distortions found in the crystal environment.[29] Comparing the geometry of the free molecule with that of the crystal molecule is, however, not straightforward.[30] Firstly, there is a difference in bond length definition between the two techniques, with GED measuring internuclear distances and X-ray crystallography distances between centres of electron density. Since for an aromatic ring the centres of electron density lie just inside the ring (due to π-bonding) the average ring distance will appear to be shorter in the crystal than in the gas. Secondly, structural discrepancies can also be attributed to different vibrational averaging effects in the gaseous and crystal phases, and are therefore also temperature dependent. This is illustrated by an average ring contraction of 2 pm for 2,6-dichloropyrazine and 3,6-dichloropyridazine, where data were collected at a temperature of 220 K, compared with the smaller average contraction of about 0.7 pm for 2,5-dichloropyrimidine and 4,6-dichloropyrimidine, for which data were recorded at the lower temperature of 150 K. This ring contraction effect will only cause bond distances to shorten; angles will remain unaffected. For these two reasons only significant structural distortions between the two phases of greater than three or four standard deviations have been investigated, and for any significant change in bond distance a consideration of average ring contraction for the molecule is also taken into account.

Examples of significant molecular distortions were found for all four compounds and can readily be interpreted in terms of intermolecular bonding between neighbouring molecules, with C(H)...N arising in all four compounds; Cl...Cl in two of the coupounds and both N...Cl and C...C occuring only once. In the crystal structure of 4,6-dichloropyrimidine (Figure 4.10), molecules were found to pack as chains linked by C(H)...N and Cl...Cl contacts. The most significant distortions found for the first molecule in the asymmetric unit concerned distances rN(3)C(4) and rC(4)Cl(8), distorting by -2.2(6) pm and +1.6(4) pm from the gas-phase structure which, taking

the ring contraction effect into account results in relative changes of -1.8(6) pm and +2.0(4) pm. In the second molecule the most notable differences arose for rC(6)Cl(10), <C(4)C(5)C(6) and <C(5)C(6)N(1), distorting by -1.8(4) pm (*i.e.* a relative effect of -2.2(4) pm), -2.6(8)° and +1.8(3)° respectively. From the intermolecular bonding, indicated in Figure 4.10 by dotted lines, the observed distortions can be readily explained: the angular distortions observed for molecule 2 arise due to interactions with two neighbouring molecules, via a hydrogen bond between atom H(9)a of molecule 2 and N(1) of molecule 1, and between atom Cl(10)a of molecule 2 and Cl(10)a on a neighbouring molecule 2. The lengthening of the C(4)Cl(8) bond for molecule 1 can be attributed to intermolecular contact between Cl(8) and Cl(8) of a neighbouring molecule 1.

In the crystal structure of 2,5-dichloropyrimidine (Figure 4.11), molecules were found to link together by C(H)...N and N...Cl contacts. Taking the average ring contraction effect of 1 pm into account only one substantial difference in ring geometry was found between the gas and solid-phase structures: <NCN in molecule 2 was found to be 2.9(4)° wider in the solid phase than in the free gaseous state.

In the crystal structure of 2,6-dichloropyrazine (Figure 4.12), molecules were found to form C(H)...N bonded layers, also with close Cl...Cl contacts. Only one inter-layer contact, C(3)...C(3), appears to be present. Although deviations from the gas-phase structure greater than three or four sigma were found for all four ring C-N distances, all distances were found to shorten in the crystal structure by about 2 pm, which, once the average ring contraction of 1.7 pm is taken into account, can be considered to be a negligible change. In addition, ring angle changes between the two phases average just 0.2°, which also suggests that apparent differences in structure between the two phases are due to different vibrational effects in the experimental data, and not due to crystal packing forces.

Finally, molecules in the crystal structure of 3,6-dichloropyridazine were found to stack in columns of wave-like planes, linked by three C(H)...N contacts per molecule

(see Figure 4.13). Taking the average ring contraction of -1.9 pm into account leaves only one bond distance which differs in the two phases by an amount greater than three sigma, namely r[C(4)-C(5)] in molecule 2, which is 2.8(9) pm shorter in the crystal, than in the gas phase.

4.6 References

1.	S. Cradock, P.B. Liescheski, D.W.H. Rankin and H.E. Robertson, *J. Am. Chem. Soc.*, 1988, **110**, 2758.

2.	S. Cradock, C. Purves and D.W.H. Rankin, *J. Mol. Struct.*, 1990, **220**, 193.

3.	A.J. Blake, P.T. Brain, H. McNab, J. Miller, C.A. Morrison, S. Parsons, D.W.H. Rankin, H.E. Robertson, and B.A. Smart, *J. Phys. Chem.*, 1996, **100**, 12280; P.T. Brain, C.A. Morrison, S. Parsons and D.W.H. Rankin, *J. Chem. Soc., Dalton Trans.*, 1996, 4589.

4.	ASYM40 version 3.0, update of program ASYM20. L. Hedberg and I.M. Mills, *J. Mol. Spectrosc.*, 1993, **160**, 117.

5.	Gaussian 92, Revision F.4, M.J. Frisch, G.W. Trucks, M. Head-Gordon, P.M.W. Gill, M.W. Wong, J.B. Foresman, B.G. Johnson, H.B. Schlegel, M.A. Robb, E.S. Replogle, R. Gomperts, J.L. Andres, K. Raghavachari, J.S. Binkley, C. Gonzalez, R.L. Martin, D.J. Fox, D.J. Defrees, J. Baker, J.J.P. Stewart, and J.A. Pople, Gaussian, Inc., Pittsburgh PA. 1992.

6.	Gaussian 94, Revision C.2, M.J. Frisch, G.W. Trucks, H.B. Schlegel, P.M.W. Gill, B.G. Johnson, M.A. Robb, J.R. Cheeseman, T. Keith, G.A. Petersson, J.A. Montgomery, K. Raghavachari, M.A. Al-Laham, V.G. Zakrzewski, J.V. Ortiz, J.B. Foresman, J. Cioslowski, B.B. Stefanov, A. Nanayakkara, M. Challacombe, C.Y. Peng, P.Y. Ayala, W. Chen, M.W. Wong, J.L. Andres, E.S. Replogle, R. Gomperts, R.L. Martin, D.J. Fox, J.S. Binkley, D.J. Defrees, J. Baker, J.P. Stewart, M. Head-Gordon, C. Gonzalez, and J.A. Pople. Gaussian, Inc., Pittsburgh PA. **1995**.

7.	J.S. Binkley, J.A. Pople and W.J. Hehre, *J. Am. Chem. Soc.*, 1980, **102**, 939.

8.   M.S. Gordon, J.S. Binkley, J.A. Pople, W.J. Pietro and W.J. Hehre, *J. Am. Chem. Soc.*, 1982, **104**, 2797.

9.   W.J. Pietro, M.M. Francl, W.J. Hehre, D.J. Defrees, J.A. Pople and J.S. Binkley, *J. Am. Chem. Soc.*, 1982, **104**, 5039.

10.   W.J. Hehre, R. Ditchfield and J.A. Pople, *J. Chem. Phys.*, 1973, **56**, 2257.

11.   P.C. Hariharan and J.A. Pople, *Theor. Chim. Acta* 1973, **28**, 213.

12.   M.S. Gordon, *Chem. Phys. Lett.*, 1980, **76**, 163.

13.   A.D. McLean and G.S. Chandler, *J. Chem. Phys.*, 1980, **72**, 5639.

14.   R. Krishnan, J.S. Binkley, R. Seeger and J.A. Pople, *J. Chem. Phys.*, 1980, **72**, 650.

15.   C.M. Huntley, G.S. Laurenson and D.W.H. Rankin, *J. Chem. Soc., Dalton Trans.*, 1980, 954.

16.   S. Cradock, J. Koprowski and D.W.H. Rankin, *J. Mol. Struct.*, 1981, **77**, 113.

17.   A.S.F. Boyd, G.S. Laurenson and D.W.H. Rankin, *J. Mol. Struct.*, 1981, **71**, 217.

18.   A.W. Ross, M. Fink and R. Hilderbrandt, *International Tables for Crystallography*. Editor A.J.C. Wilson, Kluwer Academic Publishers: Dordrecht, The Netherlands, Boston, MA, and London, 1992, Vol. C, p 245.

19.   Dr. H. McNab, University of Edinburgh, Personal Communication.

20.   J. Cosier, A.M. Glazer, *J. Appl. Cryst.*, 1986, **19**, 105.

21.   G.M. Sheldrick, *SHELXS-86. Acta Cryst.*, 1990, **A46**, 467.

22.   G.M. Sheldrick, *SHELXL-93*, University of Göttingen, Germany, 1993.

23.   W.J. Hehre, L. Radom, P.v.R. Schleyer and J.A. Pople, *Ab Initio Molecular Orbital Theory*, Publishers John Wiley and Sons, Inc., 1986.

24.   Prof. R. K. Bohn, University of Connecticut, personal communication.

25.   P.B. Liescheski, D.W.H. Rankin and H.E. Robertson, *Acta Chem. Scand., Ser. A.*, 1988, **42**, 338.

26.   D.G. Anderson, S. Cradock, P.B. Liescheski and D.W.H. Rankin, *J. Mol. Struct.*, 1990, **216**, 181.

27.   S. Cradock, P.B. Liescheski and D.W.H. Rankin, *J. Mag. Reson.*, 1991, **91**, 316.

28. A. Domenicano, *Stereochemical Applications of Gas-Phase Electron Diffraction.* Editors I. Hargittai and M. Hargittai, VCH Publishers, New York, 1988, 8, 281.

29. A. I. Kitaigorodskii, *Advances in Structure Research by Diffraction Methods.* Editors R. Brill and R. Mason, Pergamon Press, Oxford and Vieweg, Braunschweig, 1970, 3, 173.

30. A. Domenicano and I. Hargittai, *Acta Chimica Hungarica - Models in Chemistry,* 1993, **130(3-4)**, 347.

Chapter 5

Tetraborane(10), B_4H_{10}:
structures in the gas and solid phases

5.1 Introduction

The introduction of the SARACEN method[1,2] (documented in Chapter 3) has given rise to significant improvements in the structural analysis of electron diffraction data, since all geometric parameters and all significant amplitudes of vibration can now in principle refine, giving rise to structures which are as accurate as possible and parameters which have realistic standard deviations.

In light of these improvements data obtained for an important family of *arachno* boranes, based on the parent compound tetraborane(10), B_4H_{10}, have been re-analysed. The importance of boron hydrides in chemistry is well established and the study of these electron deficient compounds continue to contribute enormously to modern concepts of structure and bonding. The similarities of the different B-B and B-H distances in these molecules indicates that the SARACEN method is required in order to obtain the most reliable structural refinements possible.

A study of a series of structurally related compounds allows trends to become evident. Such trends are often related to changes in physical properties, reactivity *etc*. The series of compounds under investigation in this work are based on the parent compound B_4H_{10}, with the general formulas $H_2MB_3H_8$ and $(CH_3)_2MB_3H_8$, where M represents a cage wing atom substituted by the Group 13 elements boron, aluminium, gallium, and indium.

Work presented in this chapter represents the first stage of this work, with the molecular structure of B_4H_{10} re-determined in both the gaseous and crystalline phases. The crystal structure of B_4H_{10} was first determined by Lipscomb in 1953.[3] With improved methods of data collection and refinement it is now possible, in principle, to determine crystal structures with much greater precision than was possible in the 1950s. For this reason, the crystal structure of B_4H_{10} has been re-investigated.

The results of the graded series of *ab initio* calculations carried out on B_4H_{10} are presented in Section 5.3.1. The limited structural information available using only the

GED data is reported in Section 5.3.2, and results of the refinement improved by the inclusion of nine rotation constants of Simmons *et al.*[4] are presented in Section 5.3.3. The final refinement based on GED data, rotation constants and restraints derived from the *ab initio* data is then offered in Section 5.3.4. With all structural parameters refining with realistic estimated standard deviations, a new, more reliable gas-phase structure has been obtained. The new crystal structure is reported in Section 5.3.5 and compared to Lipscomb's original structure. Finally, the differences between the gas and solid phase structures are discussed, and the experimental structures are compared with that computed *ab initio* in Section 5.4.

The molecular structures of the $H_2MB_3H_8$ and $(CH_3)_2MB_3H_8$ derivatives are presented in Chapters 6 and 7, respectively.

5.2 Experimental

5.2.1 *Ab Initio* calculations

Theoretical Methods: Ab initio molecular orbital calculations were performed on a Dec Alpha APX1000 workstation using GAUSSIAN 92.[5] Optimised geometrical parameters and a theoretical harmonic vibrational force field were computed as detailed below with estimates of vibrational amplitudes being obtained using the program ASYM40.[6]

Geometry Optimisations: Some geometry calculations for tetraborane(10) had been carried out previously,[7] at the 3-21G*/SCF, 6-31G*/SCF, 6-31G*/MP2 and 6-31G**/MP2 levels. This current work has extended the range to include two larger basis sets and two higher levels of theory. These additional basis sets were 6-31+G*[8-10] (to gauge the effects of diffuse functions on the boron atoms) and a triple-ζ plus polarisation (TZP)[11] basis set with the contraction scheme [62111/411/1] for boron and [311/1] for hydrogen. The latter consisted of Dunning's TZ basis augmented with one set of *d*-polarisation functions on B (exponent 0.386) and one set of *p*-

polarisation functions on H (exponent 0.75). The two higher levels of theory employed were MP3 and CCSD(T), both used with the TZP basis set.

Frequency Calculations: The vibrational frequency calculation was performed at the 6-31G*/MP2 level, verifying that tetraborane(10) has C_{2v} symmetry. Cartesian force constants obtained from this calculation were transformed to those described by a set of symmetry coordinates using ASYM40. Since the tentative vibrational assignments derived from the infrared and Raman spectra of B_4H_{10}[12] were not found to be consistent with those from the theoretical study, it was not possible to scale the *ab initio* force constants using the experimental frequencies. Instead, as the best alternative, the force constants were scaled using scaling factors of the order of 0.9 for bond stretches, angles bends and torsions.[†] Scaling the force field was found to have only a small effect on the vibrational amplitude values; in general the scaled values increased in magnitude by the order of 10%, compared to the unscaled values.

5.2.2 Gas-Phase Electron Diffraction (GED)

GED data: The new GED refinements reported in this Chapter used the original data set.[13]

GED model: Assuming C_{2v} symmetry, twelve independent parameters are required to define the structure completely (see Table 5.1 and Figure 5.1). They were chosen to be the average B-B bond distance (p_1) , the difference between the two distinct B-B distances (p_2), the average B-H bond distance (p_3), the difference between the average bridge and terminal B(1)-H(1), B(4)-H(4)*endo/exo* distances (p_4), the difference between the outer and inner B-H bridge distances (p_5), the difference between rB(1)-H(1) and average wing B-H*endo/exo* distances (p_6), the difference between the *endo* and *exo* wing B-H distances (p_7), the angle H(2)*endo*B(2)H(2)*exo* (p_8), the angle H(1)B(1)B(3) (p_9), the butterfly angle (p_{10}), describing the angle between the two planes BBB, the angle H_b dip (p_{11}), describing the elevation of the bridging-hydrogen atoms from the BBB

[†] Varying scaling factors over the range 0.85-0.95 was found to have little effect on vibrational amplitude and correctional values.

plane, *i.e.* the angle between the planes B(1)B(2)B(3) and B(1)B(2)H(1,2), and finally a parameter describing the tilt of the BH_2 wing unit in the B(2)B(4)H(4)$_{endo}$H(4)$_{exo}$ plane (p_{12}). This parameter was defined as the angle between the bisector of the HBH angle and the BBB plane, a positive angle representing an *endo* tilt (see Figure 5.2).
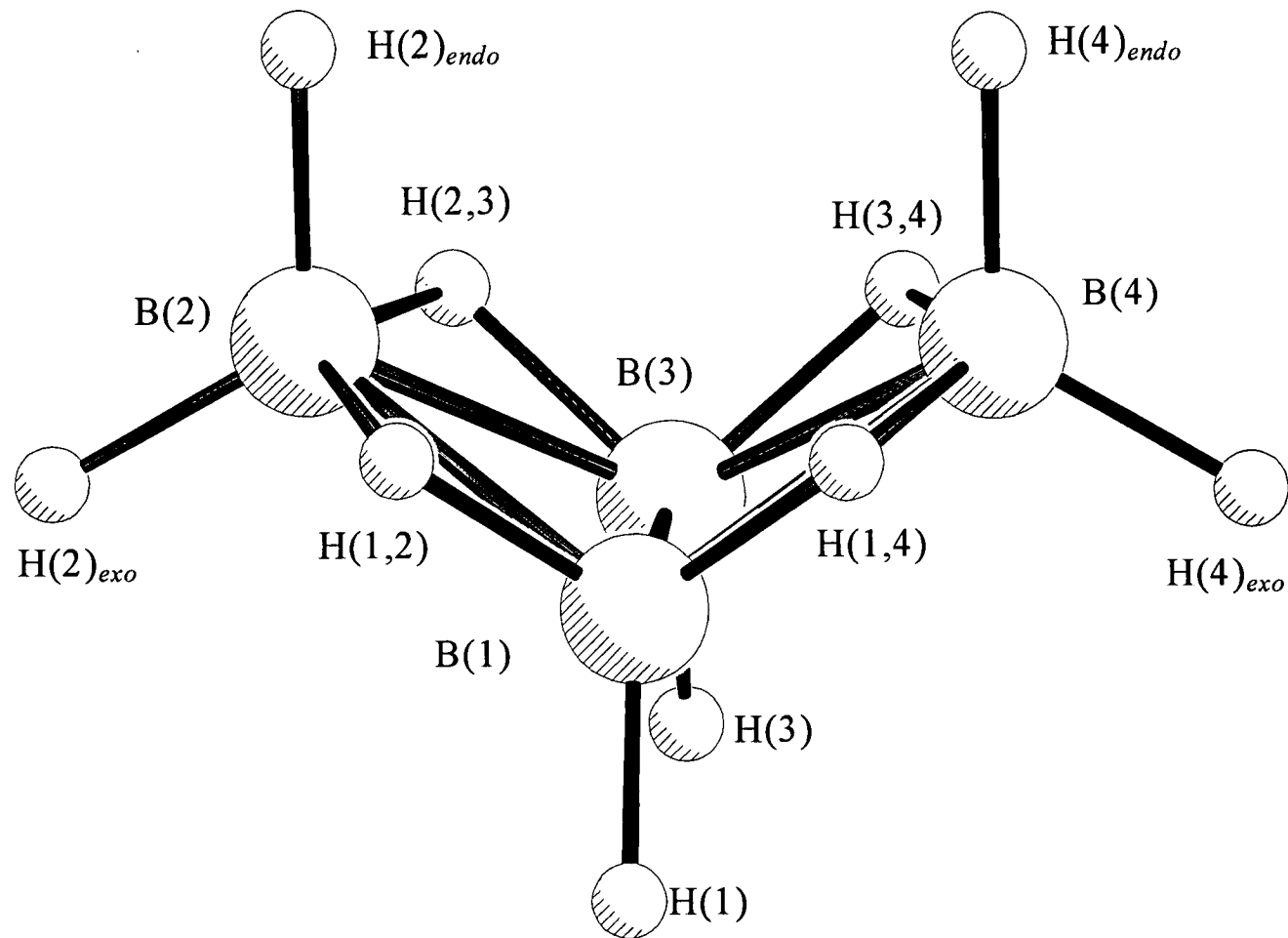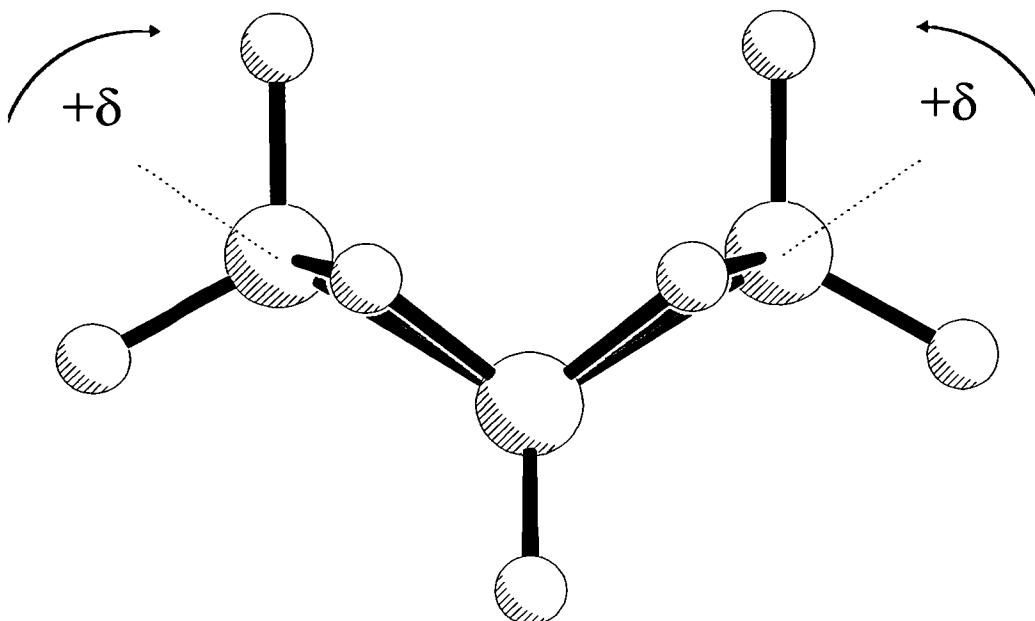
Figure 5.1 Molecular framework of B_4H_{10}

Figure 5.2 Diagram illustrating the tilt of the BH_2 unit ($p12$ in the GED model).

5.2.3 X-ray Crystallography

Crystal data:[14] B_4H_{10}, M=53.22, monoclinic $P2_1/n$, a = 5.7917(11), b = 10.145(2), c = 8.699(2) Å, β = 106.03(2)°, U = 491.3 Å³ [from 75 reflections, 30° ≤ 2θ ≤ 44°, measured at ±ω, λ = 1.54184 Å], Z = 4, D_c = 0.721 g cm⁻³, $F(000)$ = 120, T = 100 K, colourless column 0.8 x 0.15 x 0.15 mm³, μ(Cu-Kα) = 0.140 mm⁻¹.

Data collection and processing: Stoë Stadi-4 diffractometer equipped with an Oxford Cryosystems variable-temperature device;[15] ω-2θ mode on-line profile learning,[16] graphite-monochromated Cu-Kα radiation, 1268 reflections measured [-6 ≤ h ≤ 6, -5 ≤ k ≤ 11, 0 ≤ l ≤ 9, 5° ≤ 2θ ≤ 120°], 727 unique (R_{int} = 5.71%). No absorption correction was applied.

Structure analysis and refinement: For the boron-atom positions, the structure was solved by direct methods.[17] Hydrogen-atom positions were clearly visible in a ΔF

synthesis, and the structure was refined[18] against F^2 with anisotropic displacement parameters on the boron and hydrogen atoms being fully refined with isotropic displacement parameters. At convergence, R_1 [based on F and 504 data with $F > 4\sigma(F)$] was 6.66%, and $wR2$ [based on F^2 and 721 data] was 20.39% for 78 parameters. The final ΔF synthesis showed no feature outwith $+0.15 \rightarrow -0.15$ eÅ^{-3}.

5.3 Results and Discussion

5.3.1 *Ab Initio* Calculations

The results of the geometry optimisation calculations, which demonstrate the effects of improving the basis set and level of theory, are given in Table 5.1; atom numbering is as in Figure 5.1.

Table 5.1 *Ab Initio* molecular geometries (r/pm, $</°$) and energies (Hartrees) for B_4H_{10} (r/pm, $</°$)

Parameter [a]	Basis Set/Level of Theory					
	6-31G*/SCF	6-31G*/MP2(FC)	6-31+G*/ MP2(FC)	MP2(FC)/ TZP	TZP/MP3(FC)	TZP/CCSD(T)(FULL)
Bond lengths						
r[B(1)-B(3)]	174.1	171.8	171.9	173.1	173.7	173.4
r[B(1)-B(2)]	189.3	184.0	184.0	185.6	186.9	186.5
r[B(1)-H(1,2)]	124.7	125.3	125.3	125.6	125.6	125.5
r[B(2)-H(1,2)]	142.3	141.2	141.2	142.0	142.1	141.8
r[B(1)-H(1)]	118.1	118.6	118.6	118.2	118.3	118.3
r[B(2)-H(2)$_{endo}$]	118.8	119.7	119.8	119.5	119.4	119.5
r[B(2)-H(2)$_{exo}$]	118.4	119.2	119.3	119.0	119.0	119.0
Angles						
B(1)B(2)B(3)	54.8	55.7	55.7	55.6	55.4	55.4
B(2)B(1)B(3)	62.6	62.2	62.2	62.2	62.3	62.3
H(2)$_{endo}$B(2)H(2)$_{exo}$	120.2	118.7	118.6	119.6	119.7	119.6
H(1)B(1)B(3)	115.6	115.0	114.9	114.8	115.0	115.0
BH$_2$ tilt	-2.6	-2.2	-2.2	-1.7	-1.8	-1.6
Torsions						
Butterfly angle	116.9	117.4	117.4	116.6	116.3	116.0
H$_b$ dip	7.6	8.8	8.7	8.4	7.8	7.4
Energy	-104.45702	-104.84358	-104.84777	-104.95322	-105.00827	-105.10606

[a] For definitions of parameters, see the text.

Cage Structure: The B(1)-B(3) and B(1)-B(2) bond distances were found to be slightly sensitive to the quality of basis set used and to the level of theory. Improving the basis set from 6-31G* to TZP at the MP2 level led to increases in these bond lengths of about 2 pm. Diffuse functions (6-31+G* basis) were found to be less important, resulting in a 0.5 pm increase in both bond distances, relative to the 6-31G*/MP2 results. The level of theory was also found to be important; when electron correlation effects were included (*i.e.* MP2 level and above) both distances shortened, the change being most noticeable from the SCF to the MP2 level, where the distances shortened by 2.7 pm and 5.8 pm for B(1)-B(3) and B(1)-B(2), respectively. Higher levels of theory caused the bond distances to lengthen slightly, with the final, highest-level calculation at TZP/CCSD(T) predicting distances of 173.4 pm for B(1)-B(3) and 186.5 pm for B(1)-B(2).

Bridging Region: In contrast to r(B-B), the bridging B-H bond distances were found to be less sensitive to the details of the basis set and level of treatment. Improving the basis set from 6-31G* to TZP at the MP2 level resulted in the bridging distances B(1)-H(1,2) and B(2)-H(1,2) lengthening by 0.4 pm and 1 pm, respectively. Diffuse functions were again found to be less important, with both bond distances lengthening by no more than 0.2 pm relative to the 6-31G*/MP2 values. Improving the level of theory from 6-31G*/SCF to 6-31G*/MP2 resulted in an increase of 0.5 pm for r[B(1)-H(1,2)] and a decrease of 1.3 pm for r[B(2)-H(1,2)]. At higher levels, using the TZP basis set resulted in changes no greater than 0.1 pm for r[B(1)-H(1,2)] and 0.2 pm for r[B(2)-H(1,2)]. The final calculation at TZP/CCSD(T) predicted bond distances of 125.5 pm and 141.8 pm for r[B(1)-H(1,2)] and r[B(2)-H(1,2)], respectively.

Terminal Region: The terminal B-H bond distances were similarly found to be largely insensitive to both the basis set used and the level of theory. At the MP2 level, improving the basis set from 6-31G* to TZP resulted in a shortening of 0.3 pm for the r[B(1)-H(1)] distance and 0.1 pm for both B(2)-H(2) distances. Diffuse functions increased the distances by no more than 0.2 pm relative to the 6-31G*/MP2 results.

Improving the level of theory from SCF to MP2 using the 6-31G* basis set resulted in increases of 0.4 pm, 0.8 pm and 0.7 pm for the three distances. Further improvements in the level of theory using the TZP basis set gave rise to changes no greater than 0.1 pm for all three bond distances, with final values at TZP/CCSD(T) calculated to be 118.3 pm for r[B(1)-H(1)], 119.5 pm for r[B(2)-H(2)$_{endo}$] and 119.0 pm for r[B(2)-H(2)$_{exo}$].

For the series of calculations detailed in Table 5.1, it is clear that the B-H distances have effectively converged whilst further changes in B-B distances should be no more than a few tenths of a picometer.

5.3.2 GED Data Alone

The r_α° structural parameters determined from the GED data alone are given in Table 5.2. Only six of the twelve geometric parameters (*viz.* $p_{(1-5)}$ and p_{10}) could be refined at this stage, together with the vibrational amplitudes u_1[B(1)-B(3)], u_3[B(1)-H(1,2)], u_4[B(2)-H(1,2)], u_7[B(1)...B(2)], u_{20}[B(1)...H(4)$_{exo}$] and u_{27}[B(2)...B(4)]. The R_G factor for this refinement was 7.6%, indicating that the data are of good quality.

Parameters 1 and 2, the mean and difference B-B distances, both refined well, giving well determined individual distances: r[B(1)-B(2)] = 186.5(3) pm and r[B(1)-B(3)] = 174.9(9) pm. The smaller standard deviation for the former distance reflects its multiplicity of four, as compared to one for r[B(1)-B(3)]. The non-bonded B(2)...B(4) distance then defines the butterfly dihedral angle, which refined to 120.2(3)°.

The average B-H distance also refined well to 127.0(3) pm, but since all of the B-H bonded distances fall under the first peak in the radial-distribution curve (Figure 5.3), the five independent parameters defining them would be expected to be strongly correlated with one another on simultaneous refinement. Of the parameters p_{4-7}, which describe differences between various B-H distances, only two could be refined. These were p_4, describing the difference between the two bridging B-H distances, which

refined to 19.3(23) pm (indicating a very asymmetric bridge), and p_4, defining the difference between the average bridge and terminal B-H distances, which refined to 10.5(19) pm. Parameters 6 and 7, and the angles describing the H atom positions, $p_{8,9,11,12}$, could not be refined freely and were fixed at their *ab initio*, CCSD(T)/TZP level, values.

Using the GED data alone, only the geometrical parameters defining the heavy-atom cage structure, together with the average B-H bond distance, could be refined to a high degree of accuracy. It will be shown in the next two sections that the addition of non-GED data improve the definition of the structure considerably.

Table 5.2 Geometrical parameters for the GED structures ($r_\alpha°$) of B_4H_{10} (r/pm, $</°$)

	Parameter	Results [a,b]		
		GED data alone	GED + rotation constants	GED + rotation constants + restraints
	Independent [c]			
p_1	av. r(B-B)	184.2(2)	183.5(3)	184.0(2)
p_2	Δ r(B-B)	11.7(11)	13.3(7)	12.9(6)
p_3	av. r(B-H)	127.0(3)	128.0(4)	127.3(3)
p_4	av. r(B-H)$_b$ - av. r(B-H)$_t$	10.5(19)	13.7(12)	12.0(17)
p_5	Δ r(B-H)$_b$	19.3(23)	18.5(14)	18.7(16)
p_6	rB(1)-H(1) - av. r(B-H)$_{endo/exo}$	-1.0 (f)	-1.0 (f)	-1.0(3)
p_7	Δ r(B-H)$_{endo/exo}$	0.5 (f)	0.5 (f)	0.5(1)
p_8	$<$H(2)$_{exo}$B(2)H(2)$_{endo}$	119.6 (f)	119.6 (f)	119.6(13)
p_9	$<$H(1)B(1)B(3)	115.0 (f)	114.5(17)	115.0(16)
p_{10}	Butterfly angle	120.2(13)	117.0(5)	117.2(4)
p_{11}	H$_b$ dip	7.4 (f)	7.4 (f)	6.2(5)
p_{12}	BH$_2$ tilt	0.8 (f)	-0.4 (13)	1.2(12)
p_{13}	Δ r[(^{10}B-^{11}B)-(^{11}B-^{11}B)]	-	0.02(3)	0.06(2)
	Dependent			
	$<$B(1)-B(2)-B(3)	55.9(4)	55.3(2)	55.5(2)
	r[B(1)-B(3)]	174.9(9)	172.8(7)	173.7(5)
	r[B(1)-B(2)]	186.5(3)	186.1(2)	186.6(2)
	r[B(1)-H(1,2)]	121.9(19)	124.6(12)	123.0(15)
	r[B(2)-H(1,2)]	141.2(9)	143.1(8)	141.7(8)
	r[B(1)-H(1)]	120.0(8)	119.5(7)	119.8(8)
	r[B(2)-H(2)$_{endo}$]	121.6(11)	120.7(7)	121.0(8)
	r[B(2)-H(2)$_{exo}$]	121.1(11)	120.2(7)	120.5(8)

[a] Estimated standard deviations, obtained in the least squares refinement, are given in parentheses.

[b] f = fixed at the value obtained from the TZP/CCSD(T) *ab initio* calculation

[c] For definitions of parameters, see the text. Note b=bridging, t=terminal.

5.3.3 GED Data + Rotation Constants

Nine rotation constants, measured by Simmons *et al.*,[4] were introduced into the refinement. These comprised three sets; the first corresponded to a boron cage composed of ^{11}B only, the second to molecules containing one ^{10}B atom at a hinge position, and the third to molecules with one ^{10}B atom at a wing position. The original refinement[13] included the first set of rotation constants only, but since no force field for B_4H_{10} was available at that time the vibrational corrections, needed to convert these data from B_o to B_z values (which are appropriate to the r_α° structure type given in the GED refinement) could not be obtained. With the scaled force field now available, the required vibrational corrections have been obtained. The B_z rotation constants, along with the original B_o data and the calculated values based for the final new structure (given in the next section), are reported in Table 5.3. The uncertainty for each constant quoted in this Table was derived from the square-root of the sum of the squares of the standard deviation of the experimental B_o value and an assumed 10% uncertainty in the vibrational correction. It can be seen that for each rotation constant the calculated value lies well within the uncertainty limit, verifying that the structural information contained within the rotation constants was in good agreement with the GED results obtained. The R_G factor recorded for this combined analysis refinement rose slightly, to 8%.

Table 5.3 Rotation constants (B/MHz) for B_4H_{10} as used in the GED study

| Rotation Constant | | Observed [a] | | Calculated [c] | Difference | Uncertainty[d] |
Species	Axis	B_o	B_z^b	B_z	B_z (Obs. - Calc.)	
$^{11}B(1\text{-}4)$	A	11013.388(19)	11008.505	11008.154	0.351	0.52
	B	6198.643(23)	6197.392	6197.443	-0.051	0.20
	C	5592.817(21)	5586.325	5586.214	0.109	0.68
$^{10}B(1)^{11}B(2\text{-}4)$	A	11248.386(15)	11243.492	11243.842	-0.350	0.51
	B	6215.416(20)	6214.195	6214.342	-0.147	0.23
	C	5638.440(20)	5631.908	5632.323	-0.415	0.68
$^{10}B(2)^{11}B(1,3,4)$	A	11055.969(17)	11051.075	11051.062	0.013	0.52
	B	6368.152(20)	6366.946	6366.890	0.056	0.23
	C	5718.786(18)	5712.254	5711.987	0.276	0.68

[a] Taken from ref. 17.

[b] Vibrational corrections obtained from the scaled 6-31G*/MP2 *ab initio* force field.

[c] Calculated from the final combined analysis/SARACEN refinement.

[d] Used to weight data in structural refinement, derived from experimental error plus a 10% uncertainty in the harmonic vibrational correction.

With the introduction of the rotation constants for the isotopically-substituted molecules, an additional parameter had to be included in the model to account for the minute increase in the B-B bond distance that occurs when one ^{11}B atom is substituted by ^{10}B. Parameter 13 was defined as the difference $r(^{10}$B-^{11}B) - $r(^{11}$B-^{11}B). This was assumed to be constant for all substituted B-B bonds, and was allowed to refine. A value of 0.02(3) pm was returned.

The geometrical parameters obtained from this new refinement are given in Table 5.2. Small changes in the boron cage were observed, such that the average B-B distance (p_1) shortened by 0.7 pm to 183.5(3) pm and the difference between the two different B-B distances (p_2) increased by 1.6 pm to 13.3(7) pm. The butterfly angle (p_{10}) also changed, decreasing by 3.2° to 117.0(5)°. For p_2 and p_{10} the estimated standard deviations were significantly lower than for the refinement using GED data alone. The dependent B-B distances were shortened, from 174.9(9) pm to 172.8(7) pm for B(1)-B(3) and 186.5(3) pm to 186.1(2) pm for B(1)-B(2).

For the H-atom positions, two additional geometrical parameters, p_9 and p_{12}, describing angles could be refined. The angle H(1)B(1)B(3), previously held fixed at 115.0°, refined to 114.5(17)°. Parameter 12, describing the tilt of the BH$_2$ wing unit in the symmetry plane, refined to -0.4(13)°, the tiny negative value indicating that the tilt is *exo* in character. With a standard deviation of over 1°, the refined value is not significantly different from the theoretical value of -1.6°.

The main effect observed on introducing the rotation constants was that two additional parameters could be refined. Subsequently, the structure is better defined, although four geometrical parameters remain fixed. It will be demonstrated in the next section, however, that the introduction of *ab initio* based restraints allows all parameters and significant amplitudes of vibration to be refined, yielding sensible values with realistic estimated standard deviations.

5.3.4 GED Data + Rotation Constants + Restaints

The introduction of ten restraints, four for geometrical parameters and six for vibrational amplitudes (see Tables 5.4 and 5.5), allowed all geometric parameters and all significant amplitudes of vibration to refine. In the case of the four geometric parameters, values for restraints were taken from the highest level calculation, *i.e.* TZP/CCSD(T), and uncertainties chosen that reflect our experience of the reliability of such calculations for small boranes. In the refinement based on GED data alone discussed above, only seven amplitudes of vibration could be refined freely. However, with the inclusion of six restraints applied to the various ratios of amplitudes, the thirteen most significant amplitudes of vibration, associated with the bond distances giving rise to peaks greater than 10% of the most intense component peak in the radial-distribution curve, could be refined freely. The values obtained for all refining amplitudes were in good agreement with those obtained from the scaled theoretical force field.

The results obtained from the final refinement are given in Table 5.2. In general the structural parameters varied little when the restraints were introduced, with all dependent bond distances and angles agreeing with those obtained in the previous refinement within one or two standard deviations. A final R_G value of 7.8% was recorded.

Of particular interest are the four additional geometrical parameters, $p_{6-8,11}$, now refining. Parameter 6 refined to a value of -1.0(3) pm, compared to its restraint of -1.0(2) pm, and p_7 refined to 0.5(1) pm, in exact agreement with its restraint. The two angles requiring restraints, p_8 and p_{11}, refined to 119.6(13)° and 6.2(5)° respectively, compared to their restraints of 119.6(10)° and 7.4(15)°. These results demonstrate an important principle behind the SARACEN method; if a parameter refines to give a value and standard deviation in exact agreement with its restraint, then clearly no information regarding this parameter is contained within the GED data, as observed for p_7. If, however, some information is contained in the GED data contrary to the *ab initio* restraint then, since the restraint is flexible, a value and standard deviation

149

different from the restraint would be expected to be returned in the refinement. In other words, the GED result for this parameter agrees with the *ab initio* result to a certain extent, but was not forced to accept the *ab initio* prediction as law. This was noted in the case of p_{11}. Alternatively, if the information contained within the GED is in exact agreement with the restraint, the same value and a lower standard deviation would be expected (since the same information is effectively recorded twice and the overall standard deviation will be the square root of the sum of the squares of the two uncertainties).

A complete list of interatomic distances (r_a) and amplitudes of vibration (u) determined in this final refinement are given in Table 5.6. The final least-squares correlation matrix is presented in Table 5.7, the combined molecular scattering intensities and final differences are shown in Figure 5.2 and the final radial distribution and difference curves in Figure 5.3.

Table 5.4 Derivation of geometrical parameter restraints for the GED study (r/pm, $</°$)

	Parameter [a]	6-31G*/ SCF	6-31G*/ MP2	6-31+G*/ MP2	TZP/ MP2	TZP/ MP3	TZP/CCSD(T)	Value used
p_6	rB(1)-H(1)-av. r(B-H)$_{endo/exo}$	-0.5	-0.8	-0.9	-1.1	-0.9	-1.0	-1.0(2)
p_7	Δ r(B-H)$_{endo/exo}$.	0.4	0.5	0.5	0.5	0.4	0.5	0.5(1)
p_8	H(2)$_{endo}$B(2)H(2)$_{exo}$	120.2	118.7	118.6	119.6	119.7	119.6	119.6(10)
p_{11}	H$_b$ dip	7.6	8.8	8.7	8.4	7.8	7.4	7.4(15)

[a] For definitions of parameters, see the text.

Table 5.5 Derivation of vibrational amplitude restraints for the GED study

Amplitude ratio	Value [a]	Uncertainty [b]
u_2[B(1)-H(1)]/u_3[B(1)-H(1,2)]	0.906	0.045
u_5[B(2)-H(2)$_{endo}$]/u_3	0.921	0.046
u_6[B(2)-H(2)$_{exo}$]/u_3	0.912	0.046
u_{17}[B(4)...H(1)]/u_{20}[B(1)...H(4)$_{exo}$]	0.946	0.047
u_{18}[B(4)...H(1,2)]/u_{20}	1.012	0.051
u_{19}[B(1)...H(4)$_{endo}$]/u_{20}	0.982	0.049

[a] Values taken from the scaled MP2/6-31G* force field.

[b] Uncertainties are 5% of the amplitude ratios.

Table 5.6 Interatomic distances (r_a/pm) and amplitudes of vibration (u/pm) for the GED structure of B_4H_{10} [a]

i	Atom pair	Distance	Amplitude [b]
1	B(1)-B(3)	173.6(5)	6.8(8)
2	B(1)-H(1)	121.1(9)	8.5(5)
3	B(1)-H(1,2)	124.0(15)	9.4(4)
4	B(2)-H(1,2)	142.6(8)	9.7(8)
5	B(2)-H(2)$_{endo}$	122.5(9)	8.6(5)
6	B(2)-H(2)$_{exo}$	122.0(9)	8.6(5)
7	B(1)...B(2)	186.5(2)	7.7(3)
8	B(1)...H(3)	249.3(18)	13.1 tied to u_{13}
9	H(1)...H(1,2)	200.3(14)	14.1 (f)
10	H(1,2)...H(2)$_{endo}$	197.5(12)	15.8 (f)
11	H(1,2)...H(2)$_{exo}$	207.7(8)	15.8 (f)
12	H(1,2)...H(2,3)	263.8(19)	16.7 (f)
13	B(1)...H(2,3)	247.6(13)	9.6(8)
14	H(1,2)...H(1,4)	184.9(15)	15.6 (f)
15	H(2)$_{endo}$...H(2)$_{exo}$	213(3)	13.2 (f)
16	H(1)...H(3)	275(5)	20.4 (f)
17	B(4)...H(1)	277.2(8)	11.2(9)
18	B(4)...H(1,2)	268.5(9)	12.0(9)
19	B(1)...H(4)$_{endo}$	262.9(9)	11.7(9)
20	B(1)...H(4)$_{exo}$	262.5(9)	11.9(8)
21	H(3)...H(1,4)	335.3(12)	15.1 (f)
22	H(2,3)...H(1,4)	321.8(20)	15.4 (f)
23	H(4)$_{endo}$...H(1)	370.6(12)	14.0 (f)
24	H(4)$_{endo}$...H(1,2)	297.0(9)	22.9 (f)
25	H(4)$_{exo}$...H(1)	312.0(12)	21.6 (f)
26	H(4)$_{exo}$...H(1,2)	365.5(6)	14.6 (f)
27	B(2)...B(4)	281.7(5)	9.4(10)
28	B(2)...H(4)$_{endo}$	301.2(12)	20.6 (f)
29	B(2)...H(4)$_{exo}$	391.4(6)	11.6 (f)
30	H(2)$_{endo}$...H(4)$_{endo}$	269(3)	31.3 (f)
31	H(2)$_{exo}$...H(4)$_{exo}$	491.8(17)	15.1 (f)
32	H(4)$_{endo}$...H(2)$_{exo}$	421.8(14)	21.4 (f)

[a] Estimated standard deviations, obtained in the least-squares refinement, are given in parentheses.

[b] f = fixed at the value derived from the scaled 6-31G*/MP2 force field.

Table 5.7 Least-squares correlation matrix (x 100) for the GED study of B_4H_{10}. Only off-diagonal elements with absolute values >50% are shown.

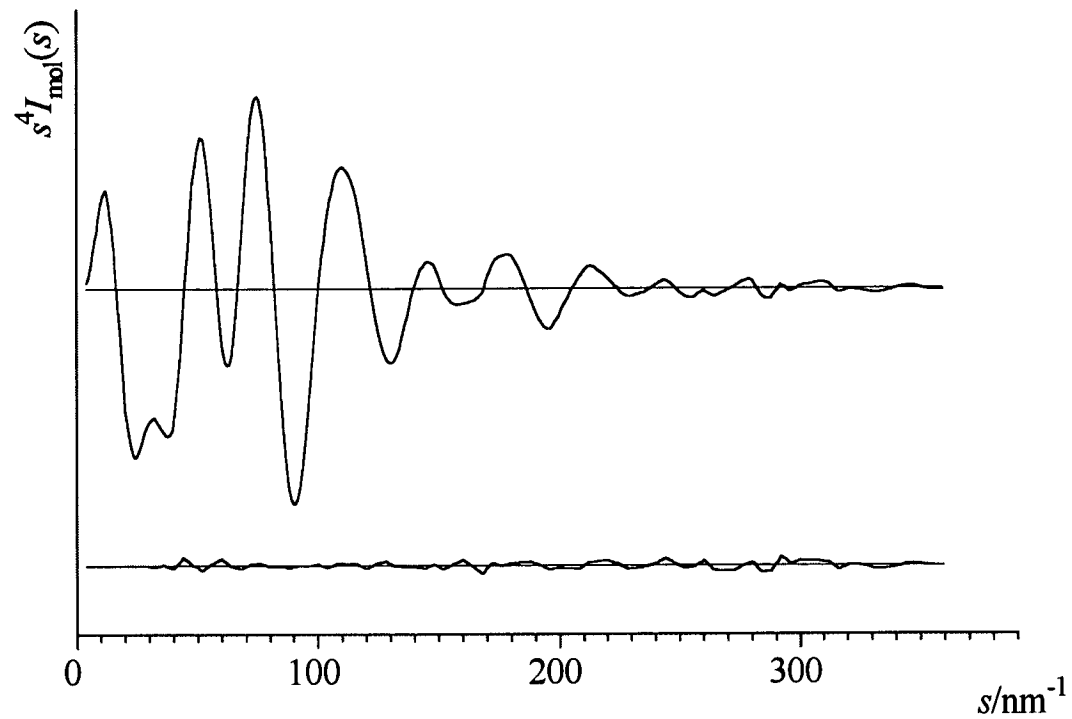|	Geometrical Parameters							Vibrational Amplitudes					Scale Factors		
	p_4	p_5	p_9	p_{10}	p_{11}	p_{12}	p_{13}	u_1	u_7	u_{13}	u_{19}	u_{20}	k_1	k_2	k_3
p_1						63	70								
p_2		-63	81	-88				-51	-63						
p_3			-72							60		51	58	53	
p_4					78						51	55			
p_5	-76			73	-58			55	57						
p_8						-55									
p_9				-82						-52	-56				
p_{10}						65	52			58					
p_{11}												55			
p_{12}							62								
u_1									81				61	57	52
u_7													76	71	66
u_{17}												66			
u_{18}												59			
u_{19}												61			
u_{20}													52		
k_1														78	71
k_2															65

Figure 5.2 Observed and final difference combined molecular scattering curves for B_4H_{10}.

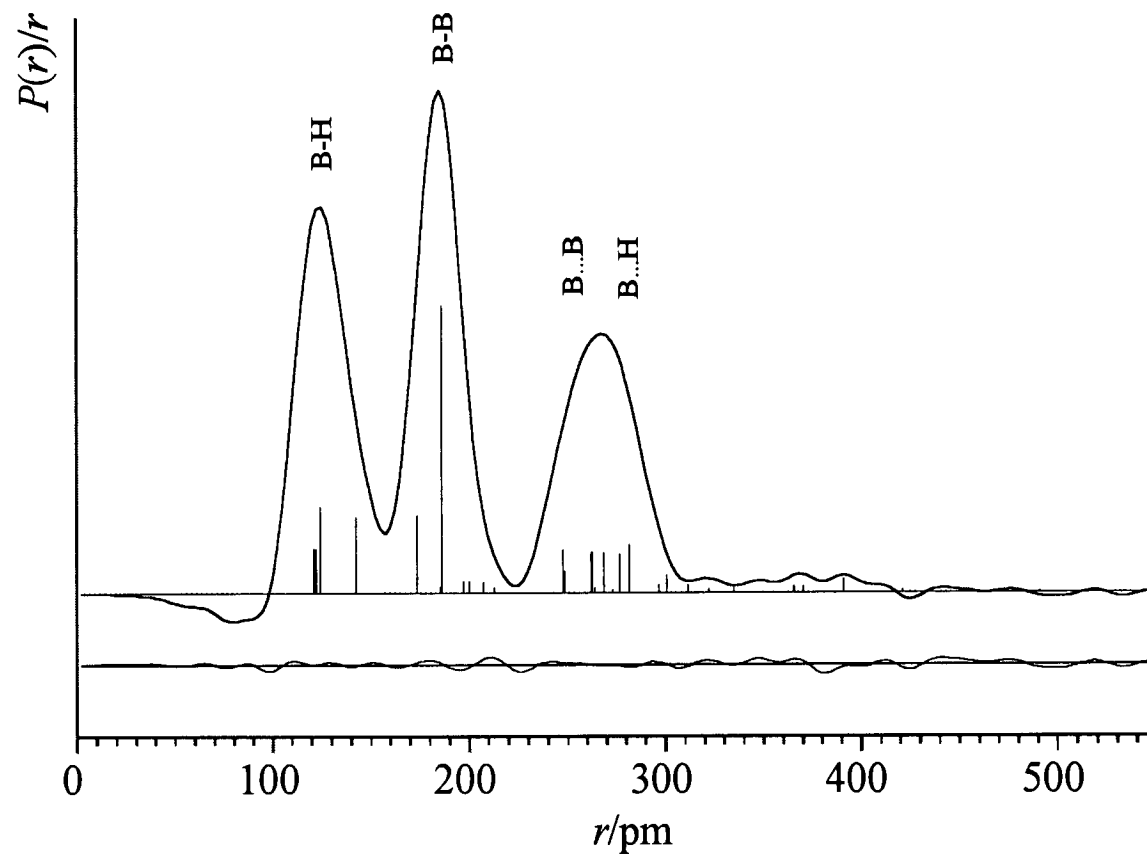Theoretical data were used in the range 0-20 nm^{-1} and 356-360 nm^{-1} for which no experimental data were available.

Figure 5.3 Observed and final difference radial-distribution curves for B_4H_{10}.

Before Fourier inversion the data were multiplied by $s.\exp(-0.00002s^2)/(Z_B-f_B)(Z_B-f_B)$.

5.3.5 Crystal Structure

Molecules of B_4H_{10} occupy general positions in the crystal structure, but are not distorted significantly from C_{2v} symmetry (see Table 5.8). There appear to be no particularly significant intermolecular interactions in the solid state; the crystal-packing arrangement is shown in Figure 5.4.

Direct comparison with Lipscomb's results is not valid since displacement parameters were refined isotropically in the earlier work.[4] Subsequently, the structure has also been refined using the original intensity data,[19] but using exactly the same scheme as reported above, *i.e.* using anisotropic displacement parameters for the boron atoms. A comparison of the resulting structural parameters revealed that although our current esd's are slightly smaller, the absolute values do not differ significantly from those refined from data recorded more than 43 years ago. Such a comparison bears witness once again to the quality of the work undertaken by Lipscomb.

Table 5.8 Structural parameters from the X-ray structure of B_4H_{10} (r/pm, $</°$)

	C_1 symmetry			
Bond Lengths				
rB(1)-B(2)/rB(2)-B(3)/rB(3)-B(4)/rB(1)-B(4)	185.2(4)	185.1(4)	185.3(4)	185.0(4)
rB(1)-B(3)	171.7(4)			
rB(1)-H(1,2)/rB(1)-H(1,4)/rB(3)-H(2,3)/rB(3)-H(3,4)	117(3)	119(2)	121(3)	110(3)
rB(2)-H(1,2)/rB(4)-H(1,4)/rB(2)-H(2,3)/rB(4)-H(3,4)	142(2)	138(3)	143(3)	135(3)
rB(1)-H(1)/rB(3)-H(3)	105(3)	107(3)		
rB(2)-H(2)$_{endo}$/rB(4)-H(4)$_{endo}$	112(3)	111(3)		
rB(2)-H(2)$_{exo}$/rB(4)-H(4)$_{exo}$	112(3)	110(3)		
Angles				
Butterfly [a]	118.2(2)			
H_b(1,2) dip/H_b(2,3) dip/H_b(1,4) dip/H_b(3,4) dip [b]	10.2(19)	6.2(25)	7.0(5)	9.9(10)
<B(3)B(1)H(1)/<B(1)B(3)H(3)	116(2)	117(2)		
<H(2)$_{endo}$B(2)H(2)$_{exo}$/<H(4)$_{endo}$B(4)H(4)$_{exo}$	121(2)	117(2)		

[a] Angle between planes B(1)B(2)B(3) and B(1)B(4)B(3).

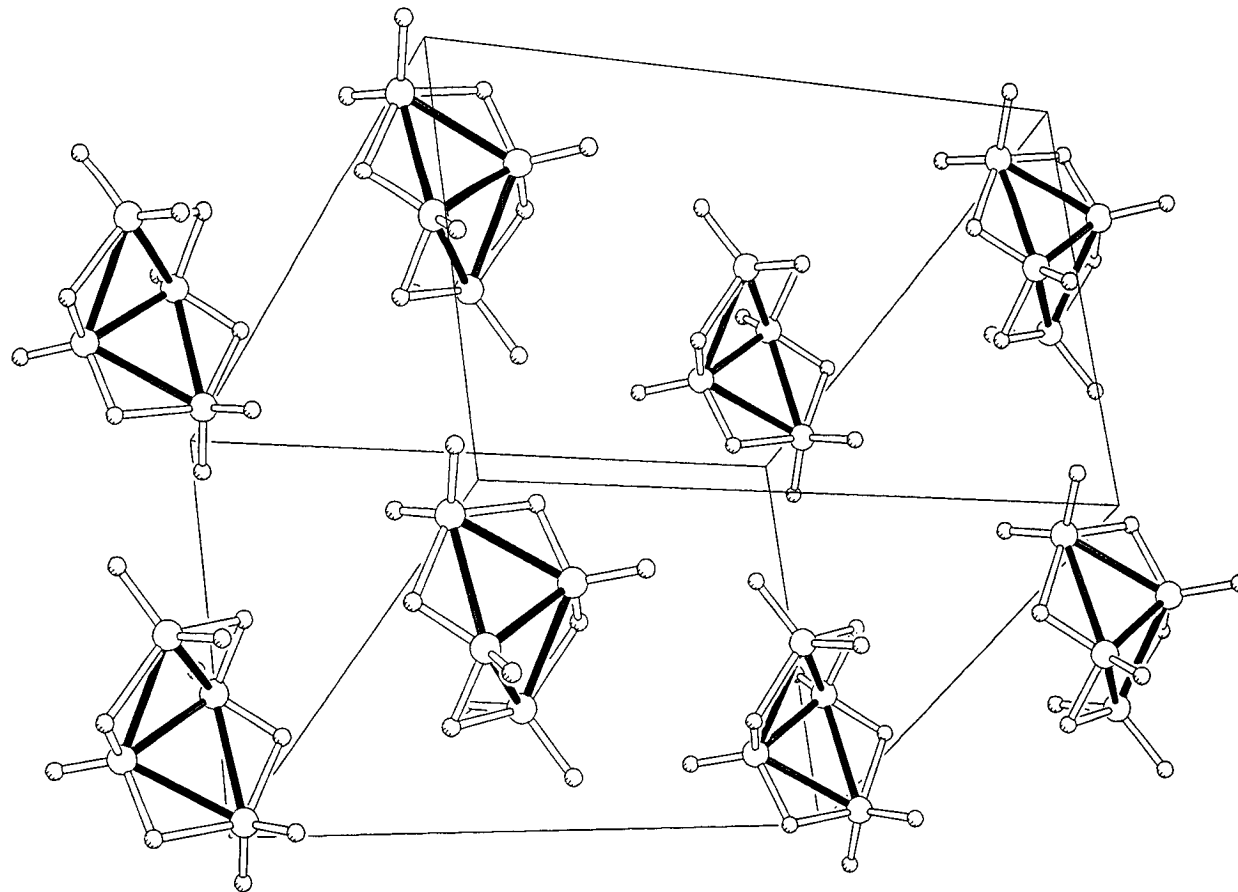[b] Angle between planes B(1)H(1,2)B(4) and B(1)B(4)B(3), *etc.*

Figure 5.4 Crystal Packing diagram of B_4H_{10}

5.4 Conclusion, Comparison of Structures

The final results for the molecular structure of B_4H_{10} determined by gas-phase electron diffraction (supplemented with rotation constants and *ab initio* based restraints), and X-ray crystallography, and predicted by *ab initio* calculations, are summarised in Table 5.9, where values of parameters related by C_{2v} symmetry have been averaged.

Gas-phase electron diffraction and *ab initio* computations both give discrete molecular structures. In other words, results should be directly comparable. Some differences are to be expected, however, since the two techniques are based on different structural definitions. *Ab initio* calculates a static equilibrium structure, which is completely free from the vibrational averaging effects experienced in the dynamic GED experiment. Since there is no large vibrational motion associated with the B_4H_{10} molecule (as judged from the vibrational spectra[12]), such differences are small and the *ab initio* and GED parameters were found to be in excellent agreement (Table 5.9). All values of GED parameters lie within one standard deviation of the *ab initio* value, with the exceptions of the butterfly angle, the H_b dip angle and the bridging distance $r[B(1)-H(1,2)]$, which agree with the *ab initio* values within three, two and two standard deviations respectively.

The absolute values recorded for parameters in the gas and solid phases differed; this would be expected since the two techniques measure different types of distances; X-ray diffraction locates the centres of electron density whereas electron diffraction measures internuclear distances. This distinction is most clearly evident in distances involving hydrogen. In general, however, the same structural trends were observed in the two phases. The average B(1)-B(2) distance, for example, was found to be *ca.* 13 pm longer than the B(1)-B(3) distance in both phases. The asymmetry of the B-H bridge was conserved, with the average inner bridge distance 24(5) pm shorter than the average outer distance in the crystal structure, a slightly but not significantly larger value than that of 18.7(16) pm measured in the GED experiment. A similar value was found for the H_b dip angle in both phases: 6.2(5)° , GED, *vs.* 8(2)°, X-ray.

The final results for tetraborane(10) thus show how state-of-the-art techniques for gas-phase structure determination, for low-temperature X-ray crystallography and for *ab initio* calculations yield data which are fully consistent with one another.

Table 5.9 Comparison of the geometrical parameters for B_4H_{10} from diffraction and theoretical methods $(r/pm, </°)$

Geometrical Parameter [a]	Method		
	GED + rotation constants + restraints $(r_\alpha°)$	TZP/CCSD(T) (r_e)	Crystal structure (average values) [b]
Bond lengths			
$rB(1)-B(2)$	186.6(2)	186.5	185.2(1)
$rB(1)-B(3)$	173.7(5)	173.4	171.7(4)
$rB(1)-H(1,2)$	123.0(15)	125.5	116(5)
$rB(2)-H(1,2)$	141.7(8)	141.8	140(4)
$rB(1)-H(1)$	119.8(8)	118.3	106(1)
$rB(2)-H(2)_{endo}$	121.0(8)	119.5	111(1)
$rB(2)-H(2)_{exo}$	120.5(8)	119.0	111(1)
Angles			
Butterfly	117.2(4)	116.0	118.2(2)
H_b dip	6.2(5)	7.4	8(2)
<HBH	119.6(13)	119.6	119(3)
<HBB	115.0(16)	115.0	116(1)
BH_2 tilt	1.2(12)	0.8	-

[a] For definitions of parameters, see the text.

[b] Figures in parentheses represent uncertainties on average structure, quoted to one sigma

5.5 References

1. A.J. Blake, P.T. Brain, H. McNab, J. Miller, C.A. Morrison, S. Parsons, D.W.H. Rankin, H.E. Robertson, and B.A. Smart, *J. Phys. Chem.*, 1996, **100**, 12280.

2. P.T. Brain, C.A. Morrison, S. Parsons and D.W.H. Rankin, *J.Chem. Soc., Dalton Trans.*, 1996, 4589.

3. (a) E.B. Moore, Jr., R. E. Dickerson, and W. N. Lipscomb, *J. Chem. Phys.*, 1957, **27**, 209. (b) C.E. Nordman and W.N. Lipscomb, *J. Chem. Phys.*, 1953, **21**, 1856.

4. N.P.C. Simmons, A.B. Burg, and R.A. Beaudet, *Inorg. Chem.*, 1981, **20**, 533.

5. Gaussian 92, Revision F.4, M.J. Frisch, G.W. Trucks, M. Head-Gordon, P.M.W. Gill, M.W. Wong, J.B. Foresman, B.G. Johnson, H.B. Schlegel, M.A. Robb, E.S. Replogle, R. Gomperts, J.L. Andres, K. Raghavachari, J.S. Binkley, C. Gonzalez, R.L. Martin, D.J. Fox, D.J. Defrees, J. Baker, J.J.P. Stewart, and J.A. Pople, Gaussian, Inc., Pittsburgh PA. 1992.

6. ASYM40 version 3.0, update of program ASYM20. L. Hedberg and I.M. Mills, *J. Mol. Spectrosc.* 1993, **160**, 117.

7. M. Bühl and P.v.R. Schleyer, *J. Am. Chem. Soc.*, 1992, **114**, 477.

8. W.J. Hehre, R. Ditchfield, and J.A. Pople, *J. Chem. Phys.*, 1972, **56**, 2257.

9. P.C. Hariharan and J.A. Pople, *Theor. Chim. Acta*, 1973, **28**, 213.

10. M.S. Gordon, *Chem. Phys. Lett.*, 1980, **76**, 163.

11. T. H. Dunning, *J. Chem. Phys.* 1970, **53**, 2823.

12. A.J. Dahl and R.C. Taylor, *Inorg. Chem.*, 1971, **10**, 2508.

13. C.J. Dain, A.J. Downs, G.S. Laurenson, and D.W.H. Rankin, *J. Chem. Soc., Dalton Trans.*, 1981, 472.

14. A single B_4H_{10} crystal was grown under the cryostream on the Edinburgh X-ray diffractometer by Dr. N. Mitzel, University of Edinburgh; data collection and structure analysis were performed by Dr. S. Parsons, University of Edinburgh.

15. J. Cosier and A.M. Glazer, *J. Appl. Cryst.*, 1986, **19**, 105.

16. W. Clegg, *Acta Cryst.*, 1981, **A37**, 22.

17. SIR92: A. Altomare, M.C. Burla, M. Camelli, G. Cascarano, C. Giacovazzo, A. Guagliardi and G. Polidoni, *J. Appl. Cryst*, in preparation.

18. SHELXTL V.5: G.M. Sheldrick, University of Göttingen, 1995.

19. Personal Communication, Dr. S. Parsons, University of Edinburgh.

Chapter 6

The Molecular Structures of $H_2MB_3H_8$,

where M=B, Al, Ga or In

6.1 Introduction

The second stage of the piece of work carried out on tetraborane(10), B_4H_{10}, involved investigating the changes in structure that occured when one wing boron atom is substituted with another Group 13 element *viz.* aluminium, gallium and indium (see Figure 6.1). By studying a number of closely related compounds in this manner (rather than a few isolated cases) definite structural patterns emerged, thereby increasing our understanding of these important types of molecules.

Each molecule in the series was investigated extensively by *ab initio* calculations. A close analysis of the calculations performed then allowed structural trends within the series to be identified. In the case of $H_2GaB_3H_8$ (and B_4H_{10} reported in the previous chapter[1]) the structure was also investigated by gas-phase electron diffraction using the SARACEN method.[1,2] A structure for this compound had already been reported,[3] but in light of the development of the SARACEN method an improved structure can now be obtained from the original data. In addition, the development of reliable *ab initio* harmonic force fields can now allow the calculation of vibrational corrections needed in the GED refinement, information which was not available at the time of the original refinement. For these reasons a new refinement is now reported.

The results of the graded series of *ab initio* calculations carried out on the four compounds are presented in Section 6.3.1, and the new gas-phase structure $H_2GaB_3H_8$ obtained from the analysis of GED data by the SARACEN method is given in Section 6.3.2. Finally, the structural trends found in the family of molecules is discussed in Section 6.4.
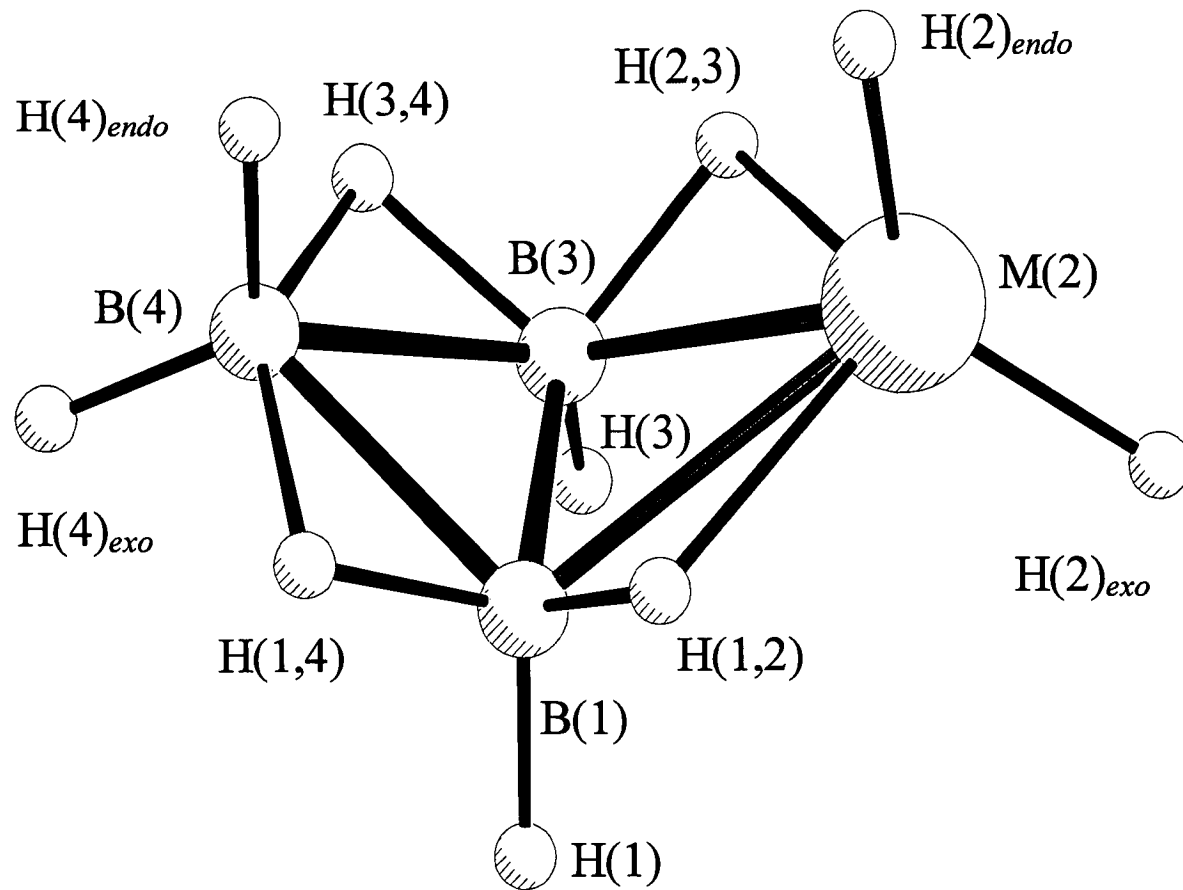
Figure 6.1 The Molecular Framework of $H_2MB_3H_8$, where M=B, Al, Ga or In

6.2 Experimental

6.2.1 *Ab Initio* Calculations

Theoretical Methods: All calculations were carried out on a DEC Alpha APX 1000 workstation using the Gaussian suite of programs.[4]

Geometry Optimisations: A graded series of calculations was performed for each of the four compounds in order to gauge the effects of basis set and electron correlation treatments on the optimised structures. Calculations were performed using standard gradient techniques at the SCF level of theory using the 6-31G*[5-7] and 6-311G**[8,9] basis sets. In the case of indium, where no standard 6-31G* or 6-311G** basis set is available, a basis set due to Huzinaga[10] was used with an additional diffuse d-polarisation function (exponent 0.10), contracted to (21s, 17p, 11+1d)/[15s, 12p, 7+1d]. This was used to describe indium thoughout the higher calculations performed. We also wished to investigate the effects of diffuse functions on heavy (*i.e.* non-hydrogen) atoms and accordingly the 6-31+G* basis set was employed in the B_4H_{10} and $H_2AlB_3H_8$ calculations.

The Gaussian frozen-core (FC) approximation divides electrons into two categories, core and valence, with only the valence electrons considered in the electron-correlation treatment. The default Gaussian FC approximation satisfactorily classified the electrons of boron and aluminium as core or valence but unsatisfactorily placed the gallium $3d^{10}$ (and indium $4d^{10}$) electrons in the core region, as a close consideration of orbital energies clearly showed that these outer core orbitals lay closer in energy to the 4s and 4p (or 5s and 5p) valence orbitals than to the remaining inner core orbitals. Calculations were therefore performed with the d orbitals of gallium and indium considered as valence rather than core functions, thereby including an additional ten electrons in the electron-correlation treatment, which was performed at MP2 level for $H_2GaB_3H_8$ and $H_2InB_3H_8$. The default FC approximation was used for the elements boron and aluminium in B_4H_{10} and $H_2AlB_3H_8$ in calculations to the levels MP2, MP3, MP4SDQ and QCISD, all with the 6-31G* basis set.

Frequency Calculations: Frequency calculations were performed at the 6-31G*/MP2 level for tetraborane(10), confirming C_{2v} as a local minimum on the potential-energy surface. For the remaining compounds, frequency calculations were performed at the 6-31G*/SCF level, confirming C_s symmetry in all three cases. For $H_2GaB_3H_8$, the force field described by Cartesian force constants at the 6-31G*/SCF level was transformed into one described by a set of symmetry coordinates using the program ASYM40.[11] As no complete assignment of the infrared and Raman spectra is available, it was not possible to scale the *ab initio* force constants using experimental frequencies. Instead, as the best alternative, the force constants were scaled empirically using scaling factors of the order of 0.94 for bond stretches, 0.96 for bond angles and 0.92 for torsions.[†]

6.2.2 Gas-Phase Electron Diffraction

GED data: The new refinement for $H_2GaB_3H_8$ reported here is based on the original data set,[3] recorded on the Edinburgh apparatus. It should be noted that the $H_2GaB_3H_8$ vapour was found to react with the emulsion of the photographic plates, resulting in higher than normal noise levels in the GED data sets. Standard programs were used for the data reduction with the scattering factors of Ross *et al.*[12] The weighting points used in setting up the off-diagonal weight matrix, the *s* range, scale factors, correlation parameters and electron wavelengths are given in Table 6.1.

[†] Scale factors used as for B_4H_{10}.[1]

Table 6.1 GED Data Analysis Parameters for $H_2GaB_3H_8$

Camera distance (mm)	Weighting functions (nm^{-1})					Correlation parameter	Scale factor, k^a	Electron wavelength[b] (pm)
	Δs	s_{min}	sw_1	sw_2	s_{max}			
201.08	4	52	72	176	208	0.3799	0.584(30)	5.670
259.48	2	20	40	140	160	0.1114	0.760(29)	5.671

[a] Figures in parentheses are the estimated standard deviations.

[b] Determined by reference to the scattering patterns of benzene vapour.

GED model: The molecular framework and atom numbering scheme of $H_2GaB_3H_8$ are shown in Figure 6.1. As the SARACEN method removes the need to make any structural assumptions, the new model written for this re-refinement includes six more geometric parameters than the original.[3] The six extra parameters allow for the deviation of the bridging hydrogen atoms from the heavy atom planes Ga(2)-B(1)-B(3) and B(1)-B(4)-B(3), tilting of the terminal BH_2 and GaH_2 units in or out of the heavy atom cage and, finally, differences between the terminal distances rB(4)-H(4)$_{endo}$ and rB(4)-H(4)$_{exo}$ [and rGa(2)-H(2)$_{endo}$ and rGa(2)-H(2)$_{exo}$]. These three structural features were found to be significant in the recent re-refinement of the parent compound B_4H_{10}.[1] Moreover, in an effort to reduce correlation effects several of the original parameters describing similar bond distances have been re-defined as weighted averages and differences, rather than defined separately.

A total of twenty geometric parameters are therefore used to define the structure in C_s symmetry in this new refinement (as documented in Table 6.6 on page 184). The gallium and boron cage atoms require four parameters to define their positions, *viz.* a weighted average and difference of the two B-B distances (p_1 and p_2), rB-Ga (p_3) and the butterfly angle (p_{18}), defined as the angle between the planes B(1)-B(4)-B(3) and B(1)-Ga(2)-B(3). The other nine distance parameters, five bond angle parameters and two torsion angles locate the positions of the ten hydrogen atoms in the structure. Parameter p_5 is defined as rGa(2)-H(1,2), p_6 as the weighted average of the B-H distances and p_7 as the average B-H bridge distance minus the average B-H terminal distance. Parameter p_8 is the difference between the outer B(4)-H(1,4) bridging distance and the average of the two inner bridging distances [rB(1)-H(1,2) and rB(1)-H(1,4)], p_9 is rB(1)-H(1,4) minus rB(1)-H(1,2), p_{10} is the difference between the terminal distances rB(1)-H(1) and the average B-H$_{endo/exo}$ distance, and p_{11} is rB-H(4)$_{endo}$ minus rB-H(4)$_{exo}$. Parameters p_{12} and p_{13} are defined as the average and difference of the two terminal Ga-H distances. The five bond angle parameters required are <B(3)-B(1)-H(1) (p_{13}), <H(2)$_{endo}$-Ga(2)-H(2)$_{exo}$ (p_{14}), <H(4)$_{endo}$-B(4)-H(4)$_{exo}$ (p_{15}), and the GaH_2 and BH_2 wing tilt angles (p_{16} and p_{17}) defined as the angles between the bisectors of the H(2)$_{endo}$-Ga(2)-H(2)$_{exo}$ and H(4)$_{endo}$-B(4)-H(4)$_{exo}$ wing

angles and the planes B(1)-B(3)-Ga(2) and B(4)-B(3)-B(1) respectively, positive values indicating tilts into the cage structure (see Figure 6.2). The remaining two torsional angles are defined as "H(1,2) dip" (p_{19}) describing the elevation of the bridging atom H(1,2) above the B(1)-Ga(2)-B(3) plane [*i.e.* the angle between the planes B(1)-Ga(2)-B(3) and B(1)-Ga(2)-H(1,2)] and "H(1,4) dip" (p_{20}) describing similarly the elevation of the H(1,4) bridging atom above the B(1)-B(4)-B(3) plane.
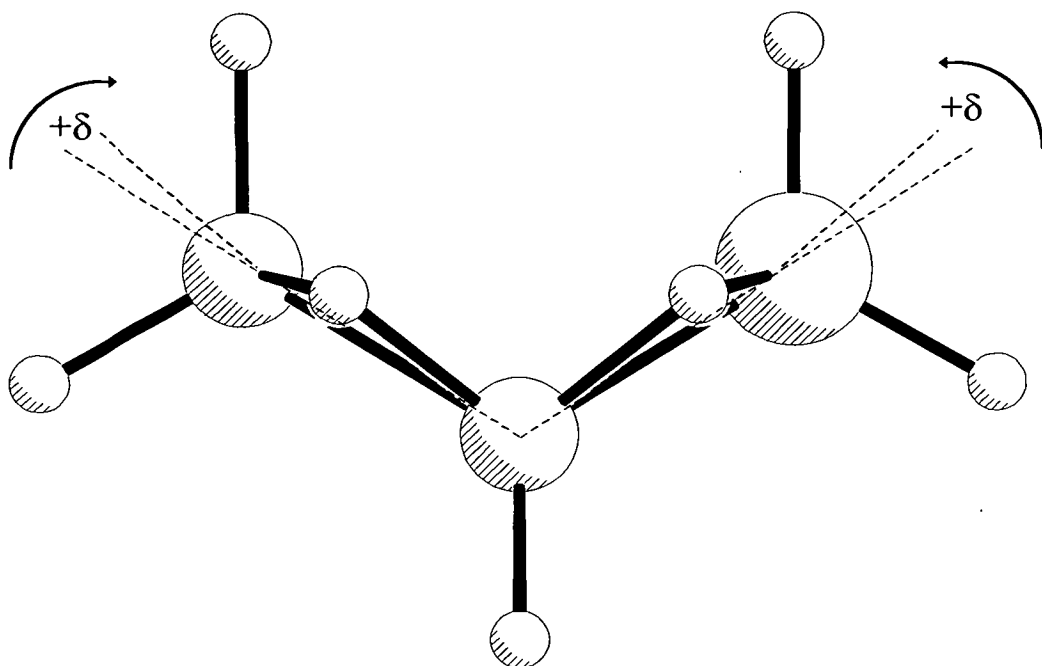

Figure 6.2 Diagram illustrating the tilt of the GaH_2 and BH_2 units

(p_{16} and p_{17} in the GED model)

6.3 Results and Discussion

6.3.1 *Ab Initio* Calculations

Some geometry optimisations for B_4H_{10} have been reported previously, performed at the 3-21G*/SCF, 6-31G*/SCF, 6-31G*/MP2 and 6-31G**/MP2 levels.[15] This range was recently extended[3] to include two larger basis sets (6-31+G*, to assess the effects of diffuse functions on the B atoms, and a TZP basis set composed of Dunning's TZ basis set[16] augmented with one set of d-polarisation functions on B and one set of p-

polarisation functions on H) and two higher levels of theory [MP3 and CCSD(T)]. To allow a direct comparison with calculations performed for $H_2AlB_3H_8$ (see below), this range has now been extended further to include the 6-311G** basis set at the SCF and MP2 levels, and the 6-31G* basis set at MP4 and QCISD levels of electron correlation treatment. Some calculations for $H_2GaB_3H_8$ have also been reported, at 3-21G*/SCF[17], DZ/SCF[18] and single-point calculations at the 3-21G*/MP4 level.[17] This range of calculations is now extended to include the effects of further improvements in basis set to 6-311G** and election correlation at the MP2 level.

The results obtained from the new set of calculations carried out for tetraborane(10) are given in Table 6.2. Several of the changes in geometry observed with improvements in calculation level (some of which have been discussed previously, see Section 5.3.1) are also found in the other compounds of the series (see Tables 6.4-6), with most notable similarities between B_4H_{10} and $H_2AlB_3H_8$, and are reported below. In general, it was observed that the most significant changes in geometry occurred with the introduction of electron correlation at the MP2 level, with smaller changes arising from improvements in basis set.

Cage Structure: The cage distance rB(1)-B(3) for all four compounds was found to be equally sensitive to improvements in basis set quality on going from 6-31G* to 6-311G**, lengthening by *ca.* 0.3 pm at SCF and *ca.* 1 pm at the MP2 level (see Tables 6.3-6). The distance rB(1)-B(4) was also found to behave similarly in all compounds except $H_2GaB_3H_8$, increasing by less than 1 pm at SCF and by about 1.5 pm at the MP2 level of theory for improvements in basis set treatment. In $H_2GaB_3H_8$ the distance shortens by 3.5 pm at the SCF level and remains largely unchanged at the MP2 level of theory. The introduction of electron correlation at the MP2 level showed marked similarities for all four compounds, with rB(1)-B(3) shortening by about 2 pm with the 6-31G* basis set (1.5 pm 6-311G** basis set) and rB(1)-B(4) shortening by 3-7 pm with the 6-31G* basis set (3-5 pm for the 6-311G** basis set). Higher levels of theory (MP3, MP4 and QCISD) employed in calculations for B_4H_{10} and $H_2AlB_3H_8$ have no further significant effect on rB(1)-B(3), and slightly lengthen

rB(1)-B(4). It is worth noting that in calculations performed for all four compounds rB(1)-B(4) is observed to change more than rB(1)-B(3) for both basis set and level of theory improvements.

Of particular interest is the very marked variation in the bond distance B-M (M=Al, Ga or In) with basis set and level of theory improvements. Changing the basis set from 6-31G* to 6-311G** results in rB-M lengthening [except rB-Al and rB-In which shorten by 0.5 pm and 1.6 pm at the SCF level, respectively (Tables 6.4 and 6.6)]. The effect is particularly dramatic for $H_2GaB_3H_8$ (Table 6.5), for which rB-Ga was found to lengthen by 4.6 pm at the MP2 level (7.9 pm SCF) for this basis set improvement. This considerable change can be partly attributed to the poor quality of the Ga 6-31G* basis set, where for such a large atom there is an insufficient number of basis functions describing the core region of the atom. Electron correlation to the MP2 level was found to shorten rB-M in all three molecules: about 3 pm using both the 6-31G* and 6-311G** basis sets for $H_2AlB_3H_8$, 3 pm with the 6-31G* basis set (6 pm with 6-311G**) for $H_2GaB_3H_8$ and by an average of 8.5 pm for $H_2InB_3H_8$ (Table 6.6) with both basis sets.

Bridge Region: The bridging B-H distances were in general found to be less sensitive to change than the B-B/M cage distances for all four compounds. Variations were generally observed to be about 1 pm on improving the basis set from 6-31G* to 6-311G** at both the SCF and MP2 levels of theory, with the exception of rB(4)-H(1,4) in $H_2GaB_3H_8$ which lengthened 4.8 pm at the SCF and 2.8 pm at the MP2 levels of theory. Similarly, introducing electron correlation to the MP2 level resulted in changes averaging about 1 pm, with the exception of rB(4)-H(1,4) in $H_2InB_3H_8$ which shortened by about 2.5 pm using both basis sets.

The M-H bridging distances (where M=B, Al and In) were largely unaffected by improvements in basis set and level of theory, with changes averaging about 1 pm. The exception was rGa(2)-H(1,2) which was found to be heavily dependent on improvements in basis set due to the poor quality of 6-31G*, shortening by 4.1 pm at

the SCF and 5.6 pm at the MP2 level of theory for improving the basis set to 6-311G**.

Terminal Region: For all four compounds the B-H terminal bond distances were found to be largely insensitive to basis set quality and level of theory (see Tables 6.3-6). For the terminal M-H distances improvements in basis set quality at the SCF result in only minor changes (generally less than 0.2 pm); at the MP2 level rAl(2)-H(2)$_{endo/exo}$ shortens by 1.3 pm, rGa(2)-H(2)$_{endo/exo}$ shortens by almost 3 pm and rIn(2)-H(2)$_{endo/exo}$ by almost 2 pm. Electron correlation predicts all M(2)-H(2)$_{endo/exo}$ distances to vary by less than 1 pm, with the exceptions of rGa(2)-H(2)$_{endo/exo}$ and rIn(2)-H(2)$_{endo/exo}$ which shorten by 2 pm with the 6-311G** basis set.

Table 6.2 *Ab Initio* molecular geometries and energies for B_4H_{10} (r_e/pm, $</°$)

Parameter [a]	Basis set/Level of Theory							
	6-31G* /SCF[b]	6-311G** /SCF	6-31G* /MP2[b]	6-31+G* /MP2[b]	6-31G* /MP3	6-31G* /MP4	6-31G* /QCISD	6-311G** /MP2
(a) Bond Distances								
r[B(1)-B(3)]	174.1	174.4	171.8	171.9	172.1	172.0	172.1	173.0
r[B(1)-B(4)]	189.3	189.8	184.0	184.0	184.7	185.0	185.1	185.6
r[B(1)-H(1,4)]	124.7	125.3	125.3	125.3	125.4	125.5	125.5	125.6
r[B(4)-H(1,4)]	142.3	142.9	141.2	141.2	141.3	141.4	141.5	141.9
r[B(1)-H(1)]	118.1	118.0	118.6	118.6	118.7	118.9	119.0	118.2
r[B(4)-H(4)$_{endo}$]	118.8	118.8	119.7	119.8	119.7	119.9	120.0	119.5
r[B(4)-H(4)$_{exo}$]	118.4	118.4	119.2	119.3	119.3	119.4	119.5	118.9
(b) Bond Angles								
B(1)B(2)B(3)	54.8	54.7	55.7	55.7	55.5	55.4	55.4	55.6
B(3)B(1)H(1)	115.6	115.4	115.0	114.9	115.2	115.2	115.2	114.7
H(4)$_{endo}$ B(4)H(4)$_{exo}$	120.2	120.2	118.7	118.6	118.7	118.8	118.8	119.7
BH$_2$ tilt	-2.6	-2.8	-2.2	-2.2	-2.3	-2.3	-2.3	-1.8
(c) Torsional Angles								
Butterfly angle	116.9	117.2	117.4	117.3	117.3	117.2	117.1	116.5
H(1,4) dip	7.9	7.8	8.8	8.7	8.5	8.3	8.2	8.4
Energy/Hartrees	-104.45702	-104.485521	-104.843578	-104.84777	-104.843521	-104.897149	-104.897146	-104.954428

[a] For definition of parameters, see the text. [b] From ref. 1.

Table 6.3 *Ab Initio* molecular geometries and energies for $H_2AlB_3H_8$ (r_e/pm, $</°$)

Parameter [a]	Basis Set/Level of Theory								
	3-21G* /SCF	6-31G* /SCF	6-311G** /SCF	6-31G* /MP2	6-31+G* /MP2	6-31G* /MP3	6-31G* /MP4	6-31G* /QCISD	6-311G** /MP2
(a) Bond Distances									
r[B(1)-B(3)]	178.1	179.2	179.4	177.1	177.2	177.4	177.3	177.3	178.1
r[B(1)-B(4)]	189.6	189.2	189.8	183.5	183.5	184.4	184.6	184.7	185.0
r[B(1)-Al(2)]	231.4	230.8	230.3	227.1	227.3	227.1	227.3	227.5	228.0
r[B(1)-H(1,4)]	125.0	124.9	125.4	125.3	125.4	125.5	125.6	125.6	125.6
r[B(4)-H(1,4)]	142.3	141.6	142.2	140.9	140.9	140.9	141.0	141.0	141.5
r[B(1)-H(1,2)]	124.5	124.8	125.2	124.3	124.3	124.5	124.8	124.9	124.3
r[Al(2)-H(1,2)]	179.9	180.7	180.6	181.8	181.7	181.7	181.7	181.6	181.3
r[B(1)-H(1)]	118.2	118.5	118.4	118.9	119.0	119.1	119.2	119.3	118.6
r[B(4)-H(4)$_{endo}$]	118.4	118.8	118.8	119.6	119.7	119.7	119.9	119.9	119.4
r[B(4)-H(4)$_{exo}$]	118.3	118.6	118.6	119.4	119.5	119.5	119.6	119.7	119.2
r[Al(2)-H(2)$_{endo}$]	157.4	157.1	156.9	157.9	157.8	158.2	158.4	158.6	156.6
r[Al(2)-H(2)$_{exo}$]	157.3	157.0	156.7	157.8	157.7	158.1	158.3	158.4	156.5
Energy/Hartrees	-319.981598	-321.705502	-321.748494	-322.055495	-322.060381	-322.102248	-322.111606	-322.114270	-322.184229

[a] For definition of parameters, see the text.

Table 6.3 cont. *Ab Initio* molecular geometries and energies for $H_2AlB_3H_8$ (r_e/pm, $</°$)

Parameter[a]	Basis Set/Level of Theory								
	3-21G*/ SCF	6-31G* /SCF	6-311G** /SCF	6-31G* /MP2	6-31+G* /MP2	6-31G* /MP3	6-31G* /MP4	6-31G* /QCISD	6-311G** /MP2
(b) Bond Angles									
B(1)B(4)B(3)	56.0	56.5	56.4	57.7	57.7	57.5	57.4	57.4	57.6
B(1)Al(2)B(3)	45.3	45.7	45.8	45.9	45.9	46.0	45.9	45.9	46.0
B(3)B(1)H(1)	113.5	113.3	113.2	112.2	112.2	112.5	112.6	112.6	112.1
H(4)$_{endo}$ B(4)H(4)$_{exo}$	120.8	119.8	119.9	118.2	118.2	118.2	228.2	118.3	119.0
H(2)$_{endo}$ Al(2)H(2)$_{exo}$	128.4	128.0	127.2	128.0	127.9	127.9	127.9	128.0	128.2
AlH$_2$ tilt	-2.6	-3.1	-3.2	-2.6	-2.5	-2.7	-2.6	-2.6	-2.6
BH$_2$ tilt	0.2	0.3	0.6	0.6	0.8	0.5	0.5	0.6	1.6
(c) Torsional Angles									
Butterfly angle	116.2	117.1	116.8	117.6	117.6	117.6	117.5	117.4	116.0
H(1,4) dip	1.0	0.5	1.0	1.0	1.2	0.9	1.0	1.0	2.4
H(1,2) dip	10.0	10.1	10.0	11.4	11.3	11.2	11.0	10.9	10.6
Energy/Hartrees	-319.981598	-321.705502	-321.748494	-322.055495	-322.060381	-322.102248	-322.111606	-322.114270	-322.184229

[a] For definition of parameters, see the text.

Table 6.4 *Ab Initio* molecular geometries and energies for $H_2GaB_3H_8$ (r_e/pm, $</°$)

Parameter [a]	Basis Set/Level of Theory				
	3-21G* /SCF	6-31G* /SCF	6-311G** /SCF	6-31G* /MP2[b]	6-311G** /MP2[b]
(a) Bond Distances					
r[B(1)-B(3)]	178.8	179.6	180.0	177.7	178.4
r[B(1)-B(4)]	187.8	191.8	188.3	184.7	184.6
r[B(1)-Ga(2)]	236.0	227.6	235.5	224.5	229.1
r[B(1)-H(1,4)]	124.7	125.6	125.1	125.7	125.6
r[B(4)-H(1,4)]	142.8	138.5	143.3	139.0	141.8
r[B(1)-H(1,2)]	124.4	124.3	125.7	124.2	125.0
r[Ga(2)-H(1,2)]	186.2	188.2	184.1	188.4	182.8
r[B(1)-H(1)]	118.2	118.5	118.4	118.9	118.6
r[B(4)-H(4)$_{endo}$]	118.4	118.8	118.9	119.6	119.5
r[B(4)-H(4)$_{exo}$]	118.4	118.7	118.6	119.4	119.2
r[Ga(2)-H(2)$_{endo}$]	156.3	155.5	155.5	156.3	153.5
r[Ga(2)-H(2)$_{exo}$]	156.1	155.5	155.4	156.2	153.3
Energy/Hartrees	-1993.185615	-2001.015642	-2003.018018	-2001.383078	-2003.624498

[a] For definition of parameters, see the text. [b] For the method of electron correlation used for Ga, see the text.

Table 6.4 cont. *Ab Initio* molecular geometries and energies for $H_2GaB_3H_8$ (r_e/pm, $</°$)

Parameter[a]	Basis Set/Level of Theory				
	3-21G* /SCF	6-31G* /SCF	6-311G** /SCF	6-31G* /MP2[b]	6-311G** /MP2[b]
(b) Bond Angles					
B(1)B(4)B(3)	56.8	55.8	57.1	57.5	57.8
B(1)Ga(2)B(3)	44.5	46.5	45.0	46.6	45.8
B(3)B(1)H(1)	112.3	112.1	112.5	111.1	111.8
H(4)$_{endo}$B(4)H(4)$_{exo}$	120.7	119.6	119.7	117.9	119.0
H(2)$_{endo}$Ga(2)H(2)$_{exo}$	130.2	129.5	130.4	129.5	131.4
GaH$_2$ tilt	-4.1	-2.9	-3.1	-2.4	-2.5
BH$_2$ tilt	2.7	2.7	-0.1	2.6	0.8
(c) Torsional Angles					
Butterfly angle	118.0	115.6	117.4	116.2	116.7
H(1,4) dip	3.0	3.3	0.1	3.3	0.3
H(1,2) dip	13.2	10.2	10.0	11.5	10.5
Energy/Hartrees	-1993.185615	-2001.015642	-2003.018018	-2001.383078	-2003.624498

[a] For definition of parameters, see the text
[b] For the method of electron correlation used for Ga, see the text

179

Table 6.5 *Ab Initio* molecular geometries and energies for $H_2InB_3H_8$ (r_e/pm, $</°$)

Parameter [a]	Basis Set/Level of Theory				
	3-21G* /SCF	6-31G* /SCF[b]	6-311G** /SCF[b]	6-31G* /MP2[b,c]	6-311G** /MP2[b,c]
(a) Bond Distances					
r[B(1)-B(3)]	179.3	181.4	181.6	178.8	179.6
r[B(1)-B(4)]	188.2	185.9	186.7	182.5	183.9
r[B(1)-In(2)]	259.5	261.9	260.3	252.5	253.1
r[B(1)-H(1,4)]	125.4	124.3	125.0	125.3	125.7
r[B(4)-H(1,4)]	142.0	144.3	144.5	141.6	142.1
r[B(1)-H(1,2)]	124.7	125.5	125.8	124.8	124.8
r[In(2)-H(1,2)]	205.1	203.8	203.5	204.6	203.2
r[B(1)-H(1)]	118.4	118.6	118.6	119.1	118.8
r[B(4)-H(4)$_{endo}$]	118.6	119.0	119.0	119.8	119.6
r[B(4)-H(4)$_{exo}$]	118.5	118.7	118.7	119.6	119.3
r[In(2)-H(2)$_{endo}$]	175.2	174.8	174.6	174.3	172.5
r[In(2)-H(2)$_{exo}$]	175.1	174.8	174.5	174.2	172.4
Energy/Hartrees	-5794.406385	-5819.936690	-5819.967864	-5820.378876	-5820.433682

[a] For definition of parameters, see the text.

[b] For In basis set, see the text. [c] For the method of electron correlation used for In, see the text.

Table 6.5 cont. *Ab Initio* molecular geometries and energies for $H_2InB_3H_8$ (r_e/pm, $</°$)

Parameter[a]	Basis Set/Level of Theory				
	3-21G* /SCF	6-31G* /SCF[b]	6-311G** /SCF[b]	6-31G* /MP2[b,c]	6-311G** /MP2[b,c]
(b) Bond Angles					
B(1)B(4)B(3)	56.9	58.4	58.2	58.7	58.5
B(1)In(2)B(3)	40.4	40.5	40.8	41.5	41.6
B(3)B(1)H(1)	112.6	111.7	111.6	111.1	111.2
H(4)$_{endo}$B(4)H(4)$_{exo}$	120.2	119.3	119.3	117.8	118.7
H(2)$_{endo}$In(2)H(2)$_{exo}$	133.4	133.2	132.8	133.6	134.1
InH$_2$ tilt	-3.1	-3.4	-3.5	-3.0	-2.8
BH$_2$ tilt	2.0	0.8	0.9	1.7	1.8
(c) Torsional Angles					
Butterfly angle	116.9	118.4	118.5	119.4	117.9
H(1,4) dip	3.5	1.6	1.9	13.9	3.0
H(1,2) dip	11.8	11.7	11.9	2.2	12.9
Energy/Hartrees	-5794.406385	-5819.936690	-5819.967864	-5820.378876	-5820.433682

[a] For definition of parameters, see the text.

[b] For In basis set, see the text. [c] For the method of electron correlation used for In, see the text.

6.3.2 GED study of $H_2GaB_3H_8$

As already mentioned, the new structure presented here is a re-refinement of the original GED data.[3] Many assumptions had to be made in the first attempt[3] as it was found that the refinement was much hampered by the marked correlation between several parameters, with *e.g.* B-B and Ga-H_b distances lying close together on the radial-distribution curve (see Figure 6.3). Moreover, the problems encountered were exacerbated by the degree to which the molecular scattering is dominated by the heavier atoms, making it particularly difficult to locate precisely the positions of the hydrogen atoms. As such in the original refinement the following assumptions had to be made: (i) some of the parameters defining the structure of the B_3H_8 group were fixed at corresponding values determined in the original B_4H_{10} study;[17] (ii) the differences between the three different B-H_b distances were set at zero; (iii) the bridging hydrogen atoms were taken to lie in the heavy-atom planes Ga(2)-B(1)-B(3) and B(1)-B(4)-B(3); (iv) The angle H(2)$_{endo}$-Ga(2)-H(2)$_{exo}$ was fixed at 115°; and (v) as no force field was available, vibrational amplitudes were assigned values based on studies of similar compounds carried out at that time, e.g. B_4H_{10}[17], $Me_2GaB_3H_8$[18] and $[H_2GaCl]_2$.[19] In total, six geometric parameters and five amplitudes of vibration were able to refine in this first structural refinement. Several of the features obtained in this refinement, however, were contrary to findings obtained for similar structures by other methods. In particular, the Ga-H_t distance was found to be one of the shortest measured for a gallium hydride, although from vibrational spectroscopy the distance was expected to be comparable with other compounds.[3] Also, the subsequent *ab initio* calculations[17,18] showed rGa-H_b to be significantly longer than measured, the three B-H_b distances quite distinct and <H(2)$_{endo}$-Ga(2)-H(2)$_{exo}$ significantly wider than 115°.

Results obtained in the new refinement of the structure of $H_2GaB_3H_8$ are given in Table 6.2. Of the twenty geometric parameters, only three refined well without the inclusion of restraints, *viz.* av. r(B-B) (p_1), rB-Ga (p_3) and the butterfly torsional angle (p_{18}). Parameters p_5 (av. rB-H) and p_{11} (av. rGa-H), which correspond to distances

located on the first peak on the radial-distribution curve, refined to values somewhat shorter than expected, compared with results obtained for the parent B_4H_{10} compound[1] and the structure calculated *ab initio* (see Table 6.5). The average B-H distance refined to 122.4(6) pm, about 3 pm shorter than expected, and the average Ga-H terminal distance refined to 147.2(12) pm, 6 pm less than calculated *ab initio* (Table 6.5). In light of these significant differences it was decided that both parameters should be restrained in accordance with the SARACEN method, with restraints constructed as shown in Table 6.7(a).[‡] The refined parameters are then the best fit to all available information, both experimental and theoretical, and represent the most probable structure, avoiding subjective preference for one particular type of data.

The remaining fifteen geometric parameters, which describe the location of the hydrogen atoms, required restraints in order to complete the structural refinement.[‡,§] This was expected since the heavy gallium atom, and to a lesser extent boron, dominates the molecular scattering. It is clearly demonstrated on the radial distribution curve (Figure 6.3) that the distance B(1)-Ga(2), at 231.0 pm, is by far the most prominent feature. Other structural information is somewhat suppressed and locating the hydrogen atoms is particularly difficult as a result.

[‡] Each geometric restraint has a value and an uncertainty, derived from the graded series of *ab initio* calculations. Absolute values are taken from the highest level calculation and uncertainties are estimated from values given by lower level calculations, or based on a working knowledge of the reliability of the calculations for electronically similar molecules.

[§] As a result of the large number of basis functions required to describe $H_2GaB_3H_8$ it was not possible to perform calculations to a high enough level to display satisfactory convergence (Table 6.5). However, based on the large array of calculations performed on the parent compound B_4H_{10} (Table 6.3), it is known that the heavy cage atoms are much better described at the MP2 level of electron correlation than at the SCF level. For this reason the uncertainty of 1 pm chosen for the cage parameter ΔrB-B(p_2) is based on the variation observed in the B-B cage distances of B_4H_{10} for calculations performed at MP2 level and above. The derivation of the remaining geometric restraints is based on results obtained from the $H_2GaB_3H_8$ series of calculations, and is documented in Table 6.7(a).

Table 6.6 Geometrical parameters for the SARACEN study of $H_2GaB_3H_8$ (r/pm, $</°$)

Parameter [a,b]	Results[c] (r_α, $<_\alpha$)
Independent	
Bond distances	
p_1 av. rB-B	182.0(12)
p_2 Δ rB-B	6.0(10)
p_3 r[B(1)-Ga(2)]	231.0(2)
p_4 r[Ga(2)-H(1,2)]	181(4)
p_5 av. r(B-H)	124.5(5)
p_6 av. r(B-H)$_b$–av. r(B-H)$_t$	12.8(14)
p_7 Δ [r(B-H)$_b$] (outer-inner)	18.9(22)
p_8 Δ [r(B-H)$_b$] (inner)	0.8(10)
p_9 r[B(1)-H(1)]-av. r[B(4)-H$_t$]	-0.7(3)
p_{10} Δ r(B-H)$_t$ (*endo–exo*)	0.3(1)
p_{11} av. r(Ga-H)$_t$	149.3(14)
p_{12} Δ r(Ga-H)$_t$ (*endo–exo*)	0.2(1)
Angles	
p_{13} <B(3)B(1)H(1)	111.6(10)
p_{14} <H(2)$_{endo}$Ga(2)H(2)$_{exo}$	131.0(19)
p_{15} <H(4)$_{endo}$B(4)H(4)$_{exo}$	119.2(10)
p_{16} GaH$_2$ tilt	-2.5(6)
p_{17} BH$_2$ tilt	0.7(7)
Torsions	
p_{18} Butterfly angle	117.1(7)
p_{19} H(1,2) dip	10.7(10)
p_{20} H(1,4) dip	0.3(2)
Dependent	
<B(1)-B(4)-B(3)	57.8(3)
<B(1)-Ga(2)-B(3)	45.3(4)
r[B(1)-B(3)]	177.9(13)
r[B(1)-B(4)]	184.0(13)
r[B(1)-H(1,4)]	123.7(11)
r[B(4)-H(1,4)]	142.2(18)
r[B(1)-H(1,2)]	123.0(11)
r[B(1)-H(1)]	116.6(8)
r[B(4)-H(4)$_{endo}$]	117.1(8)
r[B(4)-H(4)$_{exo}$]	116.8(8)
r[Ga(2)-H(2)$_{endo}$]	149.4(14)
r[Ga(2)-H(2)$_{exo}$]	149.2(14)

[a] For definition of parameters, see the text. Note, b=bridging, t=terminal.
[b] For atom numbering, see Figure 6.1.
[c] For details of refinement see the text and Table 6.7.

Table 6.7(a) Derivation of the geometric restraints for the SARACEN study of $H_2GaB_3H_8$ (r/pm, $</°$)

	Parameter[a]	6-31G*/SCF	6-311G**/SCF	6-31G*/MP2[b]	6-311G**/MP2[b]	Value used
p_2	$\Delta\,r$(B-B)	12.2	8.3	7.0	6.2	6.2(10)
p_4	r[Ga(2)-H(1,2)]	188.2	184.1	188.4	182.8	183(6)
p_5	av. r(B-H)	125.1	126.2	125.5	126.1	126.1(6)
p_6	av. r(B-H)$_b$–av. r(B-H)$_t$	10.8	12.7	10.4	11.7	11.7(13)
p_7	av. r(B-H)$_b$	130.4	131.4	131.6	130.8	130.8(8)
p_8	av. r(B-H)$_b$ (outer–inner)	13.6	17.9	14.0	16.5	16.5(25)
p_9	$\Delta\,r$(B-H)$_b$	1.3	-0.6	1.5	0.6	0.6(10)
p_{10}	r[B(1)-H(1)]-av. r[B(4)-H$_t$]	-0.1	-0.4	-0.6	-0.7	-0.7(3)
p_{11}	$\Delta\,r$(Ga-H)$_t$ (*endo–exo*)	0.0	0.1	0.1	0.2	0.2(1)
p_{12}	$\Delta\,r$(B-H)$_t$ (*endo–exo*)	0.1	0.3	0.2	0.3	0.3(1)
p_{13}	<B(3)B(1)H(1)	112.1	112.5	111.1	111.8	111.8(10)
p_{14}	<H(2)$_{endo}$ Ga(2)H(2)$_{exo}$	129.5	130.4	129.5	131.4	131.4(20)
p_{15}	<H(4)$_{endo}$ B(4)H(4)$_{exo}$	119.6	119.7	117.9	119.0	119.0(10)
p_{16}	GaH$_2$ tilt	-2.9	-3.1	-2.4	-2.5	-2.5(6)
p_{17}	BH$_2$ tilt	2.7	0.1	2.7	0.8	0.8(7)
p_{19}	H(1,4) dip	3.3	0.1	3.3	0.3	0.3(2)
p_{20}	H(1,2) dip	10.2	10.0	11.5	10.5	10.5(10)

[a] For definition of parameters, see the text.

[b] For method of electron correlation used for Ga, see the text.

In addition to geometric restraints, the SARACEN method allows restraints to be applied to ratios of amplitudes of vibration corresponding to electronically similar pairs of atoms separated by similar distances or, if necessary, directly to amplitudes that would otherwise be unable to refine independently. Values for amplitude restraints are calculated directly from the scaled force field, with uncertainty ranges of 5% considered appropriate for amplitude ratios or 10% for absolute values. For $H_2GaB_3H_8$ only two out of the fifty-five amplitudes of vibration could be refined freely, viz. B(1)-Ga(2) (u_{12}) and B(4)...Ga(2) (u_{15}). By the inclusion of the five amplitude restraints given in Table 6.7(b), a further seven amplitudes were successfully refined. Direct amplitude restraints for u_1[B(1)-B(3)] and u_{11}[B(1)...B(4)] were found to be necessary as the normal practise of restraining ratios resulted in unrealistically short vibrational amplitude values being returned in the least-squares refinement, due to high correlation effects. With the amplitude restraints in place, all amplitudes corresponding to atom pairs contributing 10% or more of the intensity of the most intense feature on the radial-distribution curve were refined. The fixed amplitudes of vibration, all for atom pairs involving hydrogen and of low intensity on the radial-distribution curve, will have little effect on values or standard deviations of those which were refined.

Table 6.7(b) Derivation of vibration amplitude restraints for the SARACEN study of $H_2GaB_3H_8$

Amplitude Restraint	Value[a]	Uncertainty[b]
u_1[B(1)-B(3)]	6.7	0.7
u_8[Ga(2)-H(1,2)]	13.8	1.38
u_{11}[B(1)...B(4)]	8.4	0.8
u_9[Ga(2)-H(2)$_{endo}$]/u_{10}[Ga(2)-H(2)$_{exo}$]	0.999	0.050
u_{14}[Ga(2)-H(1,4)]/u_{13}[Ga(2)-H(1)]	1.024	0.051

[a] Taken from scaled 6-31G*/SCF force field.

[b] Uncertainties are 5% of amplitude ratio, or 10% for direct amplitude restraints.

Cage Structure: For the three heavy-atom cage distances, rB(1)-B(3), rB(1)...B(4) and rB(1)...Ga(2), the final refined values were 177.9(13) pm, 184.0(13) pm and 231.0(2) pm respectively, as compared to their *ab initio* values (6-311G**/MP2) of 178.4 pm, 184.6 pm and 229.1 pm. The small standard deviation measured for the B(1)...Ga(2) distance reflects the fact that gallium and boron are the two dominant electron scatters in the molecule. Note this distance, at 231.0(2) pm, differs from the calculated value by ten standard deviations. This reflects the non-convergence of the *ab initio* data, where the parameter value was significantly affected by both basis set and electron correlation effects (see Table 6.5). Clearly, in this instance, the experimental value is better defined than the calculated. Finally, the butterfly angle (p_{18}) refined to 117.1(7)°, compared to its *ab initio* value of 116.7°.

Bridge Region: The four bridging distances, rB(1)-H(1,4), rB(4)-H(1,4), rB(1)-H(1,2) and rGa(2)-H(1,2), refined to 123.7(11) pm, 142.2(18) pm, 123.0(11) pm and 181(4) pm respectively. These agree to within one or two standard deviation with their 6-311G**/MP2 calculated *ab initio* values. The distance rGa(2)-H(1,2), is poorly defined by the GED data as a result of its close proximity to the bonding B-B distances; values for p_4 were found to drift between 180 and 199 pm with no appreciable change in the R_G factor or in the other refining geometrical parameters. Moreover, the *ab initio* calculations showed a significant variation in this bond length with improvements in basis set and level of theory [see Tables 6.5 and 6.7(a)]. This large variation was reflected in the uncertainty associated with the flexible restraint, a value of 183(6) pm being adopted. This restraint, although extremely flexible, made it possible to locate the rGa(2)-H(1,2) distance on the radial-distribution curve with greater confidence than using GED data alone. Overall, however, its definition remains relatively poor.

Terminal Region: The five terminal B-H and Ga-H distances refined to values slightly shorter than values predicted *ab initio*, with the three B-H distances rB(1)-H(1), rB(4)-H(4)$_{endo}$, rB(4)-H(4)$_{exo}$ agreeing with the *ab initio* predictions to within three standard deviations. The most notable difference between theory and experiment lies with the two Ga-H$_t$ distances, which were found experimentally to be about 4 pm shorter [149.4(14) pm and 149.2(14) pm], compared to theory (153.5 pm and 153.3 pm). These new values are, however, some 5 pm longer than those found in the original refinement,[3] and bring results into much closer agreement with those obtained experimentally for other gallium hydrides.[3] The five angles required to describe the terminal B/Ga-H region, <B(3)B(1)H(1), <H(4)$_{endo}$B(4)H(4)$_{exo}$, <H(2)$_{endo}$Ga(2)H(2)$_{exo}$, BH$_2$ tilt and GaH$_2$ tilt, all refined to within one standard deviation of the *ab initio* values. This is expected with the SARACEN method, as the experimental data provide almost no information about these parameters.

The final R_G factor for the refinement was 0.114, the high value reflecting the noise in the data associated with the fogging of the photographic plates by the H$_2$GaB$_3$H$_8$ vapour. With all twenty geometric parameters and nine vibrational amplitudes refining, this new structure represents the best that can be obtained currently from the available data, both experimental and theoretical; all standard deviations are realistic estimates of the errors, free from any systematic errors inherent in the limitations of the model. A selection of bond distances and vibrational amplitude values for the final structure is given in Table 6.8, the Cartesian coordinates in Table 6.9 and the least-squares correlation matrix in Table 6.10. The final radial-distribution curve and the final combined molecular scattering curve are shown in Figures 6.3 and 6.4, respectively.

Table 6.9 Selected bond distances (r_a/pm) and amplitudes of vibration (u/pm) obtained from the SARACEN study of $H_2GaB_3H_8$

	i	Atom Pair	Distance	Amplitude[a]
Bonding distances	1	B(1)-B(3)	180.0(13)	6.7(3)
	2	B(1)-H(1)	118.2(8)	8.2 fixed
	3	B(1)-H(1,4)	125.2(11)	9.2 fixed
	4	B(1)-H(1,2)	124.3(11)	9.1 fixed
	5	B(4)-H(1,4)	143.3(18)	11.8 fixed
	6	B(4)-H(4)$_{endo}$	119.1(8)	8.3 fixed
	7	B(4)-H(4)$_{exo}$	119.0(8)	8.3 fixed
	8	Ga(2)-H(1,2)	181(4)	14.7(12)
	9	Ga(2)-H(2)$_{endo}$	150.7(14)	14.0(19)
	10	Ga(2)-H(2)$_{exo}$	150.5(14)	14.0(19)
Non-bonding distances	11	B(1)...B(4)	184.1(13)	8.4(4)
	12	B(1)...Ga(2)	231.0(2)	6.3(5)
	13	Ga(2)...H(1)	314.1(9)	15(2)
	14	Ga(2)...H(1,4)	314.3(11)	15(2)
	15	B(4)...Ga(2)	320.2(7)	7.0(10)

[a] Amplitudes which could not be refined are fixed at values derived from the 6-31G*/SCF scaled force field.

Table 6.10 Final coordinates (pm) from the SARACEN study of $H_2GaB_3H_8$ (r_α structure)

		X	Y	Z
Cage	B(1)	0	-89.0	0
	Ga(2)	181.8	0	111.3
	B(3)	0	89.0	0
	B(4)	-137.3	0	84.1
Bridge	H(1,2)	82.3	-146.1	71.3
	H(2,3)	82.3	146.1	71.3
	H(3,4)	-97.8	134.6	60.5
	H(4,1)	-97.8	-134.6	60.5
Terminal	H(1)	0	-131.9	-108.4
	H(3)	0	131.9	-108.4
	H(2)$_{endo}$	170.1	0	260.2
	H(2)$_{exo}$	301.6	0	22.4
	H(4)$_{endo}$	-133.7	0	201.1
	H(4)$_{exo}$	-241.0	0	30.2

Table 6.11 Least-squares correlation matrix (x100) for the SARCEN study of $H_2GaB_3H_8$[a]

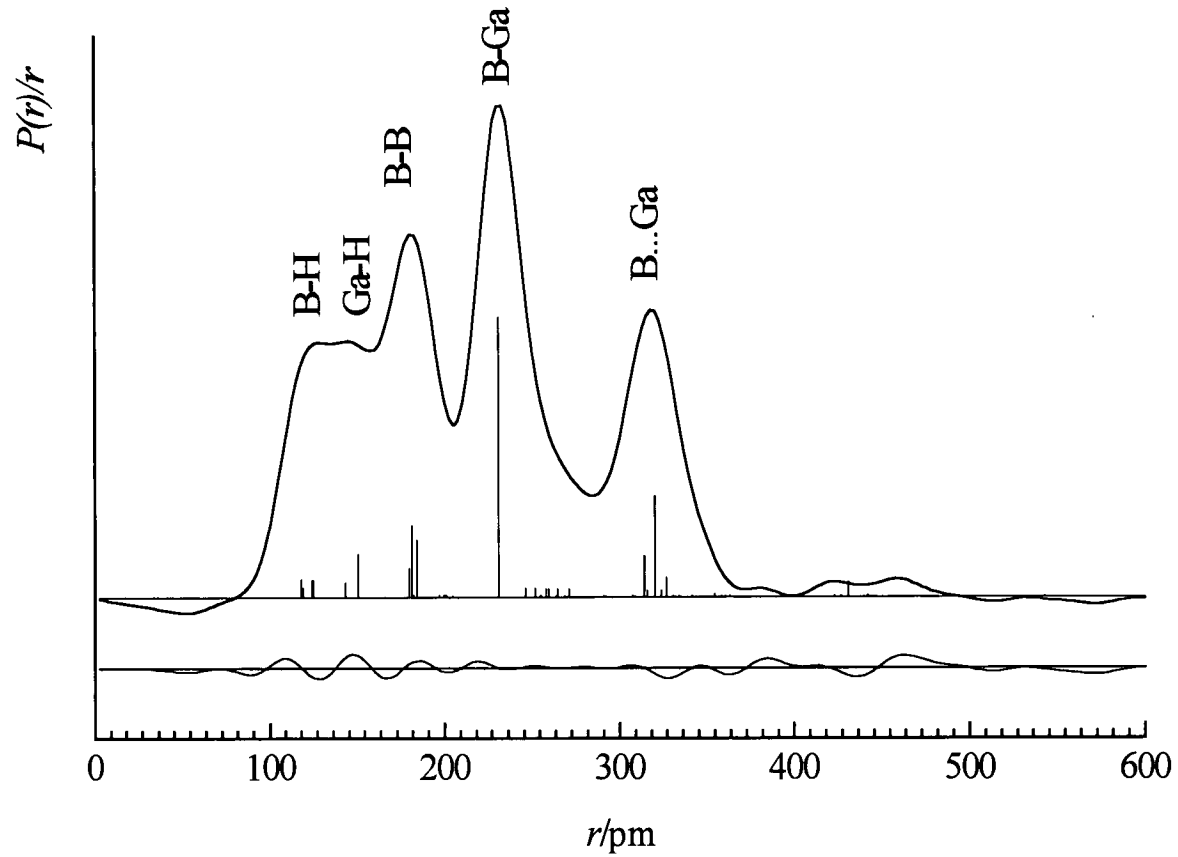|	p_2	p_4	u_9	u_{10}	u_{13}	u_{14}	u_{15}	k_1	k_2
p_1		-88	54	54					
p_4			-70	-70					
p_{18}	-53				-56	-56		-51	
u_9				93					
u_{12}					65	65		84	72
u_{13}						95	-63	72	59
u_{14}							-63	72	59
k_1									74

[a] Only off-diagonal elements with absolute values >50% are shown.

190

Figure 6.3 Observed and final difference radial-distribution curves for $H_2GaB_3H_8$.

Before Fourier inversion the data were multiplied by $s.\exp(-0.00002s^2)/(Z_{Ga}-f_{Ga})(Z_B-f_B)$.

191
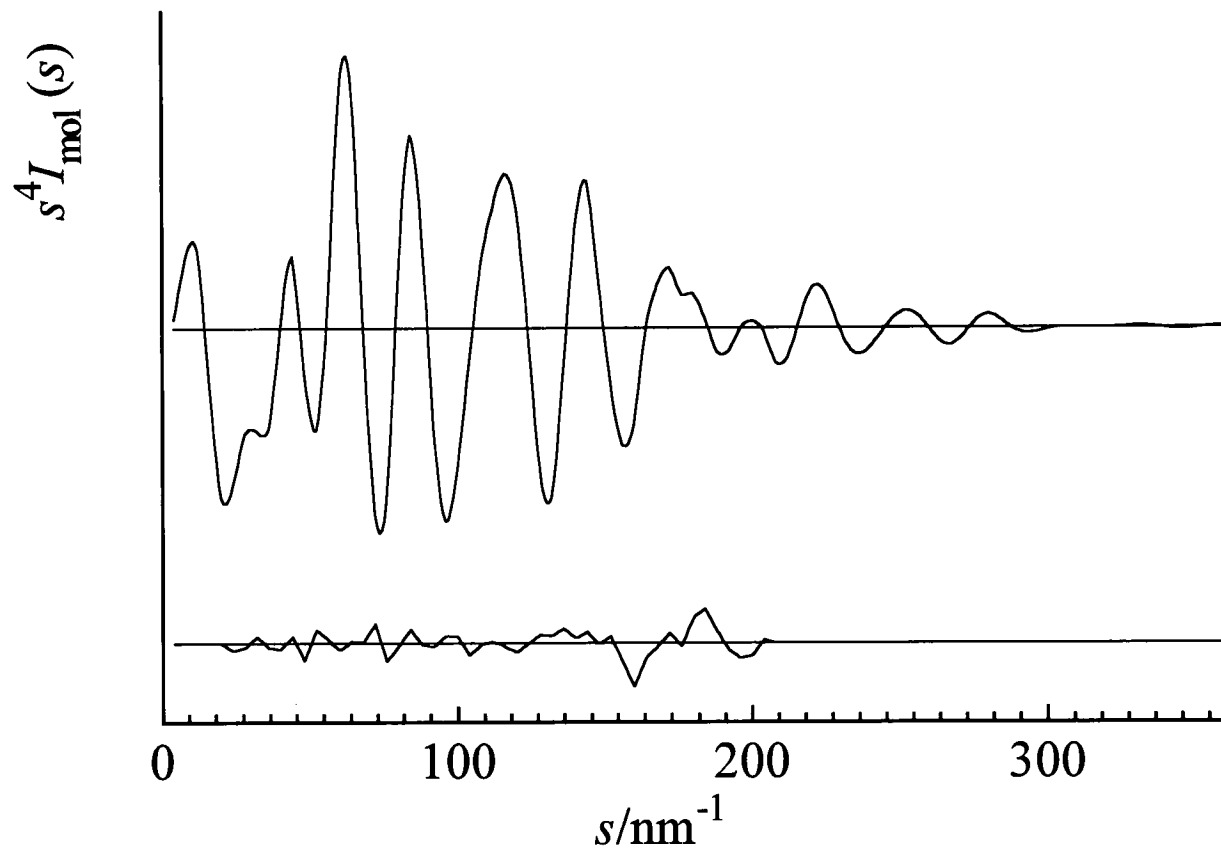
Figure 6.4 Observed and final difference combined molecular scattering curves for $H_2GaB_3H_8$.

6.4 Structural Trends Predicted by *Ab Initio*: The Effects of Changing M

The main structural changes calculated *ab initio* at the 6-311G**/MP2 level for the hydrido series of tetraborane(10) derivatives are presented in Table 6.12. These can be summarised as follows.

1. *Changes in M-B/H distances.* The increasing values of rB(1)-M(2) and rM(2)-H(1,2) on moving from B to In can be attributed mainly to the increase in atomic radius of the atom M (also given in Table 6.12). Significant changes in these parameters occur on replacing boron with aluminium and gallium with indium, but no significant changes are observed on substituting aluminium with gallium.

2. *Angles correlated with atom M.* The widening of angle H(2)$_{endo}$M(2)H(2)$_{exo}$ was largely correlated with the increasing covalent radius of atom M, although a larger than expected change was observed on substituting aluminium for gallium. The bridging angle <B(1)-H(1,2)-M(2) was found to widen significantly upon replacing boron by aluminium, narrow only slightly on replacing aluminium with gallium and finally widen further on substituting gallium with indium.

3. *Changes in B_3H_8 fragment.* The distance B(1)-B(3) was found to be marginally affected by the identity of atom M, lengthening significantly on replacing boron with aluminium and slightly on replacing gallium with indium, but with only a very small change observed on replacing aluminium by gallium, as expected. Similarly, a small narrowing of the B(3)-B(1)-H(1) angle was observed on moving from boron to indium, but this effect can probably be attributed to a correlation effect with rB(1)-B(3). The distance B(1)-B(4) also shortened slightly across the series. The H(1,2) and H(1,4) dip angles reveal that the position of the bridging hydrogen atoms above the BBB/M plane is significantly affected by the identity of atom M. From Table 6.12 it can be seen that the B-H-M bridging hydrogen atoms are elevated more above the B(1)-M(2)-B(3) plane [H(1,2) dip] than the B-H-B hydrogen atoms are above the B(1)-B(4)-B(3) plane [H(1,4) dip]. The value of 0.3° for the H(1,4) dip angle in $H_2GaB_3H_8$ may appear anomalous when compared

with the rest of the series but a study of the values returned for this geometric parameter from the range of *ab initio* calculations performed (see Table 6.5), indicates that this parameter is not well defined, varying in value from 0.1° to 3.7° depending largely on the quality of basis set used. The true value of this parameter may well lie in closer agreement with results obtained for the other compounds of the series. The step-wise increase observed in the H(1,2) dip angle throughout the derivative series is in accordance with the variations in covalent radius of M observed in moving from boron to indium. The final change observed in the B_3H_8 fragment relates to the butterfly angle, which widened slightly only upon substitution with indium.

4. *Distances and angles unchanged by atom M.* The remaining distances and angles in the B_3H_8 fragment [*i.e.* rB(1)-H(1,4), rB(4)-H(1,4), rB(1)-H(1,2) and <H(4)$_{endo}$-B(4)-H(4)$_{exo}$] were effectively unchanged by the varying atomic radius of atom M.

Table 6.12 Structural trends observed in the $H_2MB_3H_8$ series by *ab initio* (6-311G**/MP2) calculations (r/pm, </°)

		B	Al	Ga	In
	covalent radius[a]	88	125	125	140
Cage	rB(1)-B(3)	173.1	178.1	178.4	179.6
	rB(1)-B(4)	185.6	185.0	184.6	183.9
	rB(1)-M(2)	185.6	228.0	229.1	253.1
	butterfly angle	116.6	116.0	116.7	117.9
Bridge	rB(1)-H(1,2)	125.6	124.3	125.0	124.8
	rM(2)-H(1,2)	142.0	181.3	182.8	203.2
	<B(1)-H(1,2)-M(2)	87.6	94.7	94.4	97.1
	H(1,4) dip	8.4	2.4	0.3	3.0
	H(1,2) dip	8.4	10.6	10.5	12.9
Terminal	<H(2)$_{endo}$-M(2)-H(2)$_{exo}$	119.6	128.2	131.4	134.1
	<B(3)-B(1)-H(1)	114.7	112.1	111.8	111.2

[a] Ref. 20

6.5 References

1. P.T. Brain, C.A. Morrison, S. Parsons and D.W.H. Rankin, *J. Chem. Soc., Dalton Trans.,* 1996, 4589.

2. A.J. Blake, P.T. Brain, H. McNab, J. Miller, C.A. Morrison, S. Parsons, D.W.H. Rankin, H.E. Robertson, and B.A. Smart, *J. Phys. Chem.,* 1996, **100**, 12280.

3. C.R. Pulham, A.J. Downs, D.W.H. Rankin and H.E. Robertson, *J. Chem. Soc., Dalton Trans.,* 1992, 1509.

4. Gaussian 94, Revision C.2, M.J. Frisch, G.W. Trucks, H.B. Schlegel, P.M.W. Gill, B.G. Johnson, M.A. Robb, J.R. Cheeseman, T. Keith, G.A. Petersson, J.A. Montgomery, K. Raghavachari, M.A. Al-Laham, V.G. Zakrzewski, J.V. Ortiz, J.B. Foresman, J. Cioslowski, B.B. Stefanov, A. Nanayakkara, M. Challacombe, C.Y. Peng, P.Y. Ayala, W. Chen, M.W. Wong, J.L. Andres, E.S. Replogle, R. Gomperts, R.L. Martin, D.J. Fox, J.S. Binkley, D.J. Defrees, J. Baker, J.P. Stewart, M. Head-Gordon, C. Gonzalez, and J.A. Pople. Gaussian, Inc., Pittsburgh PA. 1995.

5. W.J. Hehre, R. Ditchfield and J.A. Pople, *J. Chem. Phys.,* 1973, **56**, 2257.

6. P.C. Hariharan and J.A. Pople, *Theor. Chim. Acta,* 1973, **28**, 213.

7. M.S. Gordon, *Chem. Phys. Lett.,* 1980, **76**, 163.

8. A.D. McLean and G.S. Chandler, *J. Chem. Phys.,* 1980, **72**, 5639.

9. R. Krishnan, J.S. Binkley, R. Seeger and J.A. Pople, *J. Chem. Phys.,* 1980, **72**, 650.

10. S. Huzinaga and M. Klobukowski, *J. Mol. Struct.,* 1988, **167**, 1.

11. ASYM40 version 3.0, update of program ASYM20. L. Hedberg and I.M. Mills, *J. Mol. Spectrosc.,* 1993, **160**, 117.

12. A.W. Ross, M. Fink and R. Hilderbrandt, *International Tables for Crystallography.* Editor A.J.C. Wilson, Kluwer Academic Publishers: Dordrecht, The Netherlands, Boston, MA, and London, 1992, Vol. C, p 245.

13. M. Bühl and P.v.R. Schleyer, *J. Am. Chem. Soc.,* 1992, **114**, 477.

14. T.H. Dunning, P.J. Hay, *Modern Theoretical Chemistry* 1996, Plenum, New York, Chapter 1, pp. 1-28.

15. M.L. McKee, *Chem. Phys. Lett.*, 1991, **183**, 510.

16. B.J. Duke and H.F. Schaefer III, *J. Chem. Soc., Chem. Commun.*, 1991, 123.

17. C.J. Dain, A.J. Downs, G.S. Laurenson and D.W.H. Rankin, *J. Mol. Struct.*, 1981, **71**, 217.

18. C.J. Dain, A.J. Downs and D.W.H. Rankin, *J. Chem. Soc., Dalton Trans.*, 1981, 2465.

19. M.J. Goode, A.J. Downs, C.R. Pulham, D.W.H. Rankin and H.E. Robertson, *J. Chem. Soc., Chem. Commun.*, 1988, 768.

20. D.D. Ebbing, *General Chemistry,* ed. M.S. Wrighton, Houghton Mifflin, 1987, Chapter 7.

Chapter 7

The Molecular Structures of $(CH_3)_2MB_3H_8$, where M=B, Al, Ga or In

7.1 Introduction

The final stage of the piece of work carried out on tetraborane(10), B_4H_{10}, involved investigating the changes in structure that occured when one wing BH_2 unit is substituted with the fragment $M(CH_3)_2$, where M represents the Group 13 elements boron, aluminium, gallium and indium (see Figure 7.1).

Each molecule in the series was investigated extensively by *ab initio* calculations. A close analysis of the calculations performed then allowed structural trends within the series to be identified, which in turn could then be compared to the hydride structures reported in Chapter 6. In the case of $(CH_3)_2AlB_3H_8$ and $(CH_3)_2GaB_3H_8$ structures were also investigated by gas-phase electron diffraction using the SARACEN method.[1,2] For these types of compounds the amount of structural information which can be obtained by electron diffraction alone is somewhat limited. The distances B-B, M-C and $M-H_b$ are of similar length and therefore strongly correlated, and with the heavy atoms dominating the molecular scattering locating the precise positions of the hydrogen atoms is a particularly difficult exercise. Consequently, in the original refinements reported for these compounds,[3] several parameters had to be fixed at assumed values and other assumptions had to be made to simplify the structural analysis. In addition, no reliable force fields were available for these systems to assess the effects of vibration. Thus, the preliminary structures reported for these compounds are of a very basic nature.[3] With the availability of *ab initio* harmonic force fields and the development of the SARACEN method much improved structures can now by obtained.

The results of the graded series of *ab initio* calculations carried out on the four compounds are presented in Section 7.3.1, and the new gas-phase structures $(CH_3)_2AlB_3H_8$ and $(CH_3)_2GaB_3H_8$ obtained from the analysis of GED data by the SARACEN method are given in Section 7.3.2. The structural trends found in the family of molecules by *ab initio* calculations are discussed in Section 7.4. Finally, the calculated structure of $(CH_3)_2InB_3H_8$ is compared to the experimental structure found in the solid phase[4] in Section 7.5.
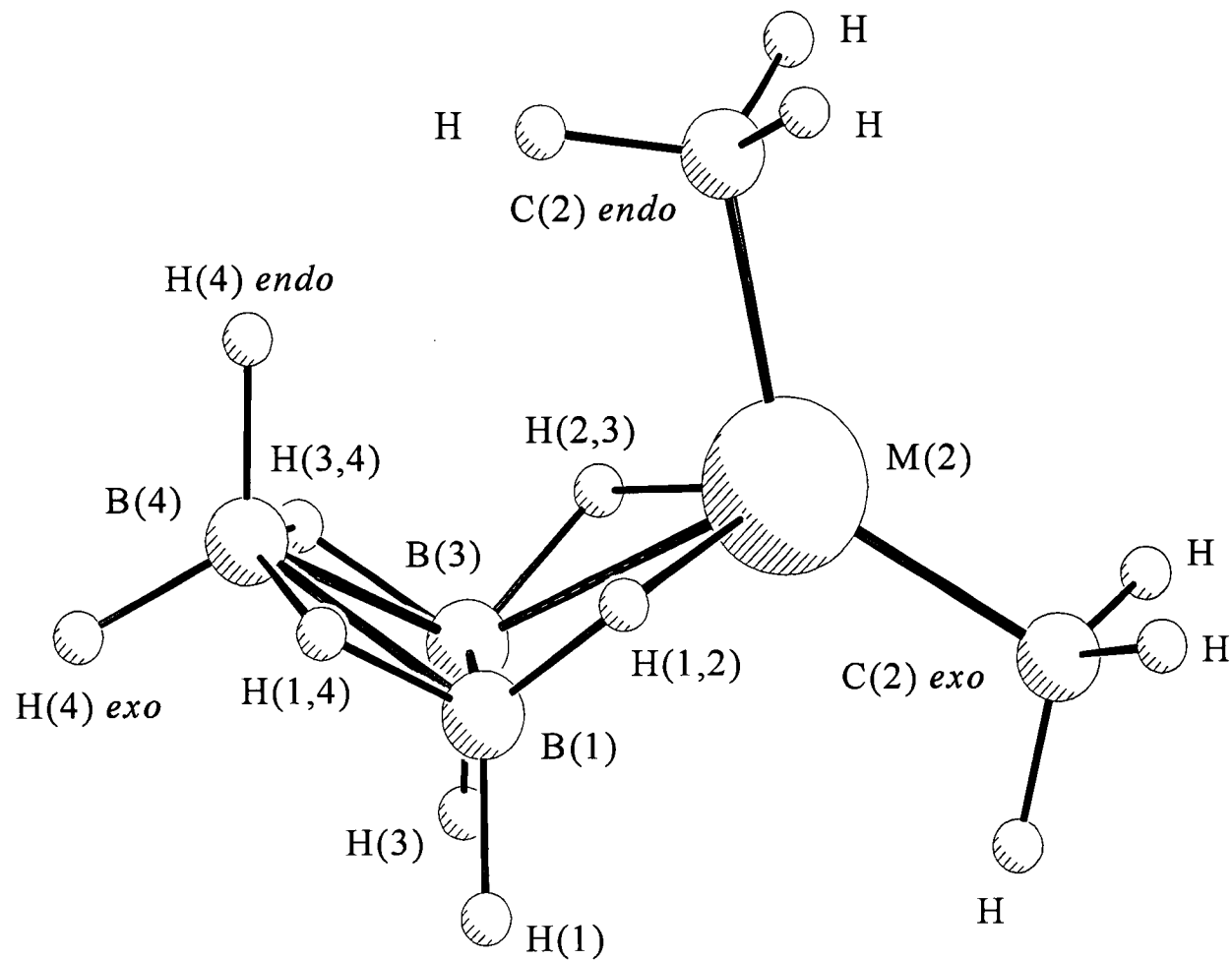
Figure 7.1 The Molecular Structure of $(CH_3)_2MB_3H_8$, where M=B, Al, Ga and In.

7.2 Experimental

7.2.1 *Ab Initio* Calculations

Theoretical Methods: All calculations were carried out on a DEC Alpha APX 1000 workstation, with the exception of the 6-31G*/MP2 and 6-311G**/MP2 $(CH_3)_2InB_3H_8$ calculations, which were carried out on the Rutherford Laboratory DEC Alpha 8400 5/300 workstation. The Gaussian suite of programs was used throughout.[5]

Geometry Optimisations: Details of the graded series of calculations performed for the dimethyl series of compounds are the same as for the hydride series, reported in the preceding chapter. Note that, as no standard basis set for indium is available beyond the 3-21G* level, the basis set of Huzinaga[6] with an additonal diffuse d-function (exponent 0.10), contracted to (21s, 17p, 11+1d)/[15s, 12p, 7+1d], was used throughout higher-level calculations. It is also worth repeating the special treatment used to describe the 3d and 4d electrons of gallium and indium, respectively. The default setting in the Gaussian program placed these orbitals in the core region. A close examination of the calculated orbital energies, however, clearly showed these orbitals to lie closer in energy to the outer valence orbitals, rather than the inner core orbitals. Calculations were therefore performed with these orbitals defined as valence. Calculations beyond the MP2 level of theory were not attempted as higher level calculations were expected to give rise to only small changes in geometry, based on the evidence obtained from the larger series of calculations performed on the hydride analogues.

Frequency Calculations: Frequency calculations were performed at the 6-31G*/SCF level for $(CH_3)_2B_4H_8$, $(CH_3)_2AlB_3H_8$ and $(CH_3)_2GaB_3H_8$, confirming C_s symmetry as a local minimum in each case. Performing the 6-31G*/SCF frequency calculation in C_s symmetry for $(CH_3)_2InB_3H_8$ gave rise to one imaginary frequency (at -5 cm^{-1}), indicating that the C_s geometry is not a local minimum on the potential energy surface

at this level. However, lowering the symmetry to C_1 resulted in the location of a local minimum less than 0.01 kJ mol^{-1} below the C_s geometry at the 6-31G*/SCF level, with the two methyl groups rotated by only 7°. It is not clear whether improvements in the theoretical treatment would lead to a C_s or a C_1 minimum for this compound; however it is clear that the potential-energy surface is very flat and that any distortion from C_s symmetry is small. For $(CH_3)_2AlB_3H_8$ and $(CH_3)_2GaB_3H_8$ the force fields described by Cartesian force constants at the 6-31G*/SCF level were transformed into ones described by a set of symmetry co-ordinates using the program ASYM40.[7] Since no fully assigned vibrational spectra were available for these compounds, the force fields were scaled using scaling factors of 0.94, 0.96 and 0.92 for bond stretches, angle bends and torsions respectively.[†]

7.2.2 Gas-Phase Electron Diffraction

GED data: The new refinements for $(CH_3)_2AlB_3H_8$ and $(CH_3)_2GaB_3H_8$ reported here are based on the original data sets,[3] recorded on the Edinburgh apparatus. As with $H_2GaB_3H_8$, reported in the previous chapter, these compounds were found to react with the photographic emulsion of the GED plates, giving rise to data with higher than usual noise levels. Standard programs were used for the data reduction with the scattering factors of Ross *et al.*[8] The weighting points used in setting up the off-diagonal weight matrix, the s range, scale factors, correlation parameters and electron wavelengths are given in Table 7.1.

GED model: As both $(CH_3)_2AlB_3H_8$ and $(CH_3)_2GaB_3H_8$ possess C_s symmetry, the same set of geometric parameters was used to describe the two structures. The model used was essentially based on that for $H_2GaB_3H_8$ with an additional two parameters [r(C-H) and <HCM] to locate the positions of the hydrogen atoms in the two methyl groups attached to B(4), which were assumed to possess local C_{3v} symmetry (see Figure 7.1). Thus, twenty-two geometric parameters are required to define the structures fully in C_s symmetry (as given in Table 7.6 on page 216). It should be noted

---

[†] Scaling constants as used in the force fields for B_4H_{10} and for $H_2GaB_3H_8$ in the preceding two chapters.

that the new model system encorporates an additional five geometric parameters, compared to the model used in the original refinement.[3] These parameters allow a further five structural features to be investigated, namely the deviations of the bridging hydrogen atoms from the heavy-atom planes M(2)-B(1)-B(3) and B(1)-B(3)-B(4), the differences between the terminal B-H$_{endo/exo}$ and M-C$_{endo/exo}$ distances, and finally the tilting of the terminal BH_2 unit in or out of the heavy-atom cage. Analogous parameters have been introduced in the re-refinements of B_4H_{10} and $H_2GaB_3H_8$ reported in the preceding two chapters.

The heavy cage atoms required four parameters to locate their positions: the weighted average and difference of the two B-B distances ($p_{1,2}$), rB(1)-M(2) (where M=Al or Ga) (p_3) and the butterfly angle (p_{20}) describing the torsional angle between the planes B(1)-B(4)-B(3) and B(1)-M(2)-B(3). The remaining parameters locate the eight hydrogen atoms in the boron cage and the two methyl groups. Parameter p_4 is defined as rM(2)-H(1,2), p_5 as the weighted sum of all B-H distances in the molecule and p_6 as the average B-H bridging distance minus the average B-H terminal distance. Parameter p_7 is the difference between the outer bridging distance B(4)-H(1,4) and the average of the two inner bridging distances B(1)-H(1,2) and B(1)-H(1,4); p_8 is rB(1)-H(1,4) minus rB(1)-H(1,2); p_9 is the difference between rB(1)-H(1) and the average B-H$_{endo/exo}$ distance, and p_{10} rB-H$_{endo}$ minus rB-H$_{exo}$. Parameters p_{11} and p_{12} are defined as the average of and difference between the two M-C distances, respectively, and p_{13} is the distance C-H. The six bond angle parameters required are <B(3)-B(1)-H(1) (p_{14}), <C(2)$_{endo}$-M(2)-C(2)$_{exo}$ (p_{15}), <H(4)$_{endo}$-B(4)-H(4)$_{exo}$ (p_{16}), the MC_2 and BH_2 tilt parameters (p_{17} and p_{18}), defined as the angles between the bisectors of the C(2)$_{endo}$-M(2)-C(2)$_{exo}$ and H(4)$_{endo}$-B(4)-H(4)$_{exo}$ wing angles and the planes B(1)-M(2)-B(3) and B(1)-B(4)-B(3), respectively, with positive values indicating tilting into the heavy atom cage and finally, the angle <H-C-M (p_{19}). The final two parameters are the torsional angles 'H(1,2) dip' and 'H(1,4) dip' (p_{21} and p_{22}), which define the elevation of the H(1,2) and H(1,4) bridging atoms above the B(1)-M(2)-B(3) and B(1)-B(4)-B(3) planes, respectively [$i.e.$ the angles between the two sets of

planes B(1)-M(2)-B(3) and B(1)-M(2)-H(1,2), and B(1)-B(4)-B(3) and B(4)-B(1)-H(1,4)].

Table 7.1 GED Data Analysis Parameters for $(CH_3)_2AlB_3H_8$ and $(CH_3)_2GaB_3H_8$

Compound	Camera distance (mm)	Weighting functions (nm^{-1})					Correlation parameter	Scale factor, k^a	Electron wavelength^b (pm)
		Δs	s_{min}	sw_1	sw_2	s_{max}			
$(CH_3)_2AlB_3H_8$	128.16	4	72	92	280	328	0.1908	0.676(23)	5.8720
	285.06	2	24	42	130	160	0.2430	0.882(17)	5.1189
$(CH_3)_2GaB_3H_8$	128.45	4	68	100	230	288	0.0999	0.871(47)	5.1336
	285.06	2	24	44	130	166	0.2442	0.850(38)	5.0969

^{a} Figures in parentheses are the estimated standard deviations

^{b} Determined by reference to the scattering patterns of benzene vapour

7.3 Results and Discussion

7.3.1 *Ab Initio* Calculations

The results of the range of calculations performed on $(CH_3)_2MB_3H_8$ (M=B, Al, Ga and In) are given in Tables 7.2-5. A number of trends in geometry were observed within the series accompanying improvements in basis set and level of theory, with the most significant changes generally arising as a result of the introduction of electron correlation to the MP2 level.

Cage Structure: The sensitivity of the cage distances to improvements in basis set and level of theory showed many parallels to the cage distances in the $H_2MB_3H_8$ series of derivatives, reported in the previous chapter. In particular, rB(1)-B(3) in both sets of derivatives lengthened by *ca.* 0.3 pm at SCF (*ca.* 1 pm at MP2) on improving the basis set from 6-31G* to 6-311G**. The rB(1)-B(4) distance was found to be more sensitive to change than rB(1)-B(3) for all compounds in the two series; it increased by about 1 pm (or 1.5 pm) at the SCF (or MP2) level for the boron, aluminium and indium analogues (see Tables 7.2, 3 and 5) and shortened by just over 3 pm at SCF (remaining largely unaffected at the MP2 level) for the two gallium compounds (see

Tables 7.4 and 6.4). This difference in behaviour for the gallium compound can largely be attributed to the poor quality of the 6-31G* basis set, where for such a large atom there is an insufficient number of basis functions describing the core region.

The introduction of electron correlation had similar effects for all four compounds in both series, with rB(1)-B(3) shortening by about 2 pm with both the 6-31G* and 6-311G** basis sets. In contrast, rB(1)-B(4) was found to be less affected by electron correlation in the $(CH_3)_2MB_3H_8$ series than the $H_2MB_3H_8$ series. It shortened by 1-2 pm in $(CH_3)_2B_4H_8$ for both basis sets (compared to 4-5 pm in B_4H_{10}), 4-5 pm in $(CH_3)_2AlB_3H_8$ (cf. 5-6 pm in $H_2AlB_3H_8$), ca. 3 pm in $(CH_3)_2GaB_3H_8$ (cf. 4-7 pm in $H_2GaB_3H_8$), and 2-3 pm in $(CH_3)_2InB_3H_8$ (3 pm in $H_2InB_3H_8$) for both basis sets.

The final cage distance rB-M was found to vary in a similar fashion for the two series of derivatives on improving the basis set from 6-31G* to 6-311G**, resulting in the distance lengthening at the SCF and MP2 levels. The exceptions were rB-Al and rB-In which shorten by 0.7 pm (see Table 7.3) and 2.4 pm (see Table 7.5), respectively at the SCF level. The effect was found to be more pronounced in the two gallium derivatives (Tables 7.4 and 6.4), with the distance lengthening by ca. 4.5 pm at the MP2 level for both compounds (7.9 pm in $H_2GaB_3H_8$ and 1.4 pm in $(CH_3)_2GaB_3H_8$ at the SCF level). Electron correlation at the MP2 level resulted in the rB-M distance shortening in both series of derivatives. The effect was more pronounced in the $(CH_3)_2MB_3H_8$ series, with rB-M shortening by ca. 11 pm in $(CH_3)_2B_4H_8$ for both basis sets (Table 7.2) (cf. 4-5 pm in B_4H_{10}); 3-5 pm in $(CH_3)_2AlB_3H_8$ (Table 7.3) (cf. 2-4 pm in $H_2AlB_3H_8$); 7.5-10.5 pm in $(CH_3)_2GaB_3H_8$ (Table 7.4) (cf. 3-6.5 pm in $H_2GaB_3H_8$) and 9-11 pm in $(CH_3)_2InB_3H_8$ (Table 7.5) (7-9 pm in $H_2InB_3H_8$).

Bridge region: Of the three B-H bridging distances, rB(4)-H(1,4) was observed to be the most sensitive to changes in theoretical method. Many changes in the bridging distances were found to parallel those of the $H_2MB_3H_8$ series. In particular, improving the basis set from 6-31G* to 6-311G** resulted in all three B-H distances in the

boron, aluminium and indium compounds in both series lengthening by about 0.5 pm at both the SCF and MP2 levels (Tables 7.2, 3 and 5). The analogous distances in the two gallium compounds also behaved similarly, with rB(1)-H(1,2) increasing by about 1 pm, rB(1)-H(1,4) shortening by about 0.3 pm and rB(4)-H(1,4) lengthening by about 3 pm at both the SCF and MP2 levels (Tables 7.4 and 6.4). This difference in behaviour for the gallium compound can again be largely attributed to the poor quality of the 6-31G* basis set.

The introduction of electron correlation at the MP2 level showed several similarities in the two sets of derivatives with, for example, the inner bridging distances rB(1)-H(1,4) lengthening and rB(1)-H(1,2) shortening on average by 1 pm for all compounds. The most significant difference between the two sets of derivatives relate to the two boron compounds using both basis sets (Tables 7.2 and 6.2); the outer bridging distance rB(4)-H(1,4) shortens by almost 5 pm in $(CH_3)_2B_4H_8$ compared to just 1 pm in B_4H_{10}. In contrast rB(4)-H(1,4) shortens by 1-2 pm in the aluminium and gallium compounds in both series of derivatives and by $ca.$ 3 pm in the two indium compounds on improving the level of theory from SCF to MP2 using both basis sets.

The M-H bridging distance in the two derivative sets were also found to behave in a similar fashion, with rAl(2)-H(1,2) shortening by about 0.5 pm, rGa(2)-H(1,2) shortening by an average 5 pm and rIn(2)-H(1,2) shortening by about 1 pm for improvements in basis set at both levels of theory. Electron correlation results in rM(2)-H(1,2) (M=Al, Ga and In) changing by less than 1 pm using both basis sets.

Terminal region: The B-H terminal distances in all eight compounds were found to be largely insensitive to change, with all distances varying on average less than 0.5 pm with improvements in basis set and less than 1 pm for improvements in the level of theory. Similarly the M-C distances were found to vary by no more than 0.6 pm for basis set improvement and less than 1 pm (M=B or Al) or 2 pm (M=Ga or In) with electron correlation.

Table 7.2 *Ab Initio* molecular geometries and absolute energies for $(CH_3)_2B_4H_8$ (r_e/pm, $</°$)

Parameter[a]	Basis set/Level of theory				
	3-21G*/SCF	6-31G*/SCF	6-311G**/SCF	6-31G*/MP2	6-311G**/MP2
(a) Bond distances					
r[B(1)-B(3)]	174.8	174.9	175.2	172.2	173.5
r[B(1)-B(4)]	185.3	185.5	186.2	183.8	185.3
r[B(1)-B(2)]	203.8	199.9	200.3	188.3	189.9
r[B(1)-H(1,4)]	123.8	124.1	124.7	125.6	125.8
r[B(4)-H(1,4)]	148.7	146.1	146.4	141.2	141.8
r[B(1)-H(1,2)]	124.7	124.5	124.9	123.8	124.1
r[B(2)-H(1,2)]	143.2	143.0	144.2	145.0	145.4
r[B(1)-H(1)]	117.9	118.3	118.2	118.8	118.4
r[B(4)-H(4)$_{endo}$]	118.3	118.7	118.7	119.6	119.4
r[B(4)-H(4)$_{exo}$]	118.2	118.5	118.5	119.2	119.0
r[B(2)-C(2)$_{endo}$]	159.7	160.2	159.9	160.3	160.3
r[B(2)-C(2)$_{exo}$]	159.0	159.6	159.2	159.3	159.3
Energy/Hartrees	-181.512658	-182.544558	-182.595062	-183.195615	-183.369088

[a] For definition of parameters, see the text

Table 7.2 cont. *Ab Initio* molecular geometries and absolute energies for $(CH_3)_2B_4H_8$ (r_e/pm, </°)

Parameter[a]	Basis set/Level of theory				
	3-21G*/SCF	6-31G*/SCF	6-311G**/SCF	6-31G*/MP2	6-311G**/MP2
(b) Bond Angles					
B(1)B(4)B(3)	56.3	56.2	56.1	55.9	55.8
B(1)B(2)B(3)	50.8	51.9	51.9	54.4	54.4
B(3)B(1)H(1)	114.6	115.1	114.9	114.6	114.3
H(4)$_{endo}$B(4)H(4)$_{exo}$	120.3	119.4	119.5	117.8	118.7
C(2)$_{endo}$B(2)C(2)$_{exo}$	122.0	120.3	120.5	118.2	119.0
BH$_2$ tilt	-3.1	-3.7	-3.9	-4.6	-4.4
BC$_2$ tilt	-5.7	-5.7	-5.6	-5.0	-4.9
BCH	111.4	111.5	111.4	111.5	111.2
(c) Torsional Angles					
Butterfly angle	118.7	120.6	120.8	121.4	120.8
H(1,4) dip	6.8	8.3	8.4	10.7	10.6
H(1,2) dip	9.9	10.7	10.7	11.3	11.0
Energy/Hartrees	-181.512658	-182.544558	-182.595062	-183.195615	-183.369088

[a] For definition of parameters, see the text

Table 7.3 *Ab Initio* molecular geometries and absolute energies for $(CH_3)_2AlB_3H_8$ (r_e/pm, $</°$)

Parameter[a]	Basis set/Level of theory				
	3-21G*/SCF	6-31G*/SCF	6-311G**/SCF	6-31G*/MP2	6-311G**/MP2
(a) Bond distances					
r[B(1)-B(3)]	178.4	179.3	179.6	177.1	178.2
r[B(1)-B(4)]	188.8	188.0	188.6	183.1	184.5
r[B(1)-Al(2)]	234.8	234.5	233.8	229.9	230.4
r[B(1)-H(1,4)]	125.1	124.8	125.3	125.4	125.6
r[B(4)-H(1,4)]	142.9	142.4	143.0	141.2	141.9
r[B(1)-H(1,2)]	124.0	124.4	124.8	123.8	124.0
r[Al(2)-H(1,2)]	181.3	182.1	181.9	183.2	182.5
r[B(1)-H(1)]	118.3	118.6	118.5	119.0	118.8
r[B(4)-H(4)_{endo}]	118.5	118.8	118.8	119.7	119.4
r[B(4)-H(4)_{exo}]	118.4	118.6	118.6	119.5	119.2
r[Al(2)-C(2)_{endo}]	196.5	196.5	196.0	195.9	195.3
r[Al(2)-C(2)_{exo}]	196.3	196.3	195.7	195.6	195.1
Energy/Hartrees	-379.660675	-399.798830	-399.864063	-400.414073	-400.606445

[a] For definition of parameters, see the text

Table 7.3 cont. *Ab Initio* molecular geometries and absolute energies for $(CH_3)_2AlB_3H_8$ $(r_e/\text{pm}, </°)$

Parameter[a]	Basis set/Level of theory				
	3-21G*/SCF	6-31G*/SCF	6-311G**/SCF	6-31G*/MP2	6-311G**/MP2
(b) Bond Angles					
B(1)B(4)B(3)	56.4	56.9	56.9	57.9	57.8
B(1)Al(2)B(3)	44.6	45.0	45.2	45.3	45.5
B(3)B(1)H(1)	113.3	113.2	113.1	112.3	112.1
H(4)$_{endo}$B(4)H(4)$_{exo}$	120.3	119.3	119.5	117.7	118.6
C(2)$_{endo}$Al(2)C(2)$_{exo}$	120.8	127.5	126.9	128.3	128.6
BH$_2$ tilt	-0.5	0.4	-0.3	0.0	0.8
AlC$_2$ tilt	-4.3	-4.7	-4.8	-4.6	-4.6
AlCH	111.4	111.8	111.6	111.6	111.5
(c) Torsional Angles					
Butterfly angle	118.5	119.6	119.6	120.5	119.2
H(1,4) dip	0.1	0.5	0.1	0.2	1.5
H(1,2) dip	11.6	13.2	12.3	14.0	13.4
Energy/Hartrees	-379.660675	-399.798830	-399.864063	-400.414073	-400.606445

[a] For definition of parameters, see the text

Table 7.4 *Ab Initio* molecular geometries and absolute energies for $(CH_3)_2GaB_3H_8$ (r_e/pm, $</°$)

Parameter[a]	Basis set/Level of theory				
	3-21G*/SCF	6-31G*/SCF	6-311G**/SCF	6-31G*/MP2[b]	6-311G**/MP2[b]
(a) Bond distances					
r[B(1)-B(3)]	178.4	179.3	179.6	177.1	178.2
r[B(1)-B(4)]	188.8	188.0	188.6	183.1	184.5
r[B(1)-Ga(2)]	234.8	234.5	233.8	229.9	230.4
r[B(1)-H(1,4)]	125.1	124.8	125.3	125.4	125.6
r[B(4)-H(1,4)]	142.9	142.4	143.0	141.2	141.9
r[B(1)-H(1,2)]	124.0	124.4	124.8	123.8	124.0
r[Ga(2)-H(1,2)]	181.3	182.1	181.9	183.2	182.5
r[B(1)-H(1)]	118.3	118.6	118.5	119.0	118.8
r[B(4)-H(4)$_{endo}$]	118.5	118.8	118.8	119.7	119.4
r[B(4)-H(4)$_{exo}$]	118.4	118.6	118.6	119.5	119.2
r[Ga(2)-C(2)$_{endo}$]	196.5	196.5	196.0	195.9	195.3
r[Ga(2)-C(2)$_{exo}$]	196.3	196.3	195.7	195.6	195.1
Energy/Hartrees	-379.660675	-399.798830	-399.864063	-400.414073	-400.606445

[a] For definition of parameters, see the text.

[b] For method of electron correlation used for Ga, see the text.

Table 7.4 cont. *Ab Initio* molecular geometries and absolute energies for $(CH_3)_2GaB_3H_8$ (r_e/pm, $</°$)

Parameter[a]	Basis set/Level of theory				
	3-21G*/SCF	6-31G*/SCF	6-311G**/SCF	6-31G*/MP2[b]	6-311G**/MP2[b]
(b) Bond Angles					
B(1)B(4)B(3)	56.4	56.9	56.9	57.9	57.8
B(1)Ga(2)B(3)	44.6	45.0	45.2	45.3	45.5
B(3)B(1)H(1)	113.3	113.2	113.1	112.3	112.1
H(4)$_{endo}$B(4)H(4)$_{exo}$	120.3	119.3	119.5	117.7	118.6
C(2)$_{endo}$Ga(2)C(2)$_{exo}$	120.8	127.5	126.9	128.3	128.6
BH$_2$ tilt	-0.5	0.4	-0.3	0.0	0.8
AlC$_2$ tilt	-4.3	-4.7	-4.8	-4.6	-4.6
AlCH	111.4	111.8	111.6	111.6	111.5
(c) Torsional Angles					
Butterfly angle	118.5	119.6	119.6	120.5	119.2
H(1,2) dip	11.6	13.2	12.3	14.0	13.4
H(1,4) dip	0.1	0.5	0.1	0.2	1.5
Energy/Hartrees	-379.660675	-399.798830	-399.864063	-400.414073	-400.606445

[a] For definition of parameters, see the text.

[b] For method of of electron correlation used for Ga, see the text.

Table 7.5 *Ab Initio* molecular geometries and absolute energies for $(CH_3)_2InB_3H_8$ $(r_e/pm, </°)$

Parameter[a]	Basis Set/Level of Theory				
	3-21G*/SCF	6-31G*/SCF[b]	6-311G**/SCF[b]	6-31G*/MP2[b,c]	6-311G**/MP2[b,c]
(a) Bond lengths					
$r[B(1)-B(3)]$	179.7	182.0	182.1	178.9	179.7
$r[B(1)-B(4)]$	187.0	184.7	185.7	182.0	183.5
$r[B(1)-In(2)]$	265.8	267.3	264.9	256.5	256.3
$r[B(1)-H(1,4)]$	125.2	124.2	124.8	125.3	125.7
$r[B(4)-H(1,4)]$	143.2	145.5	145.4	141.9	142.4
$r[B(1)-H(1,2)]$	124.2	125.1	125.4	124.4	124.4
$r[In(2)-H(1,2)]$	207.3	206.1	205.6	207.1	205.2
$r[B(1)-H(1)]$	118.6	118.8	118.7	119.3	119.0
$r[B(4)-H(4)_{endo}]$	118.6	119.1	119.1	119.9	119.6
$r[B(4)-H(4)_{exo}]$	118.6	118.8	118.8	119.6	119.4
$r[In(2)-C(2)_{endo}]$	217.5	219.1	219.2	217.3	217.2
$r[In(2)-C(2)_{exo}]$	217.5	218.9	219.0	217.0	216.9
Energy/Hartrees	-5872.082843	-5898.0187495	-5898.069181	-5898.748746	-5898.926062

[a] For definition of parameters, see the text.

[b] For In basis set, see the text.

[c] For the method of electron correlation used for In, see the text.

Table 7.5 cont. *Ab Initio* molecular geometries and absolute energies for $(CH_3)_2InB_3H_8$ (r_e/pm, $</°$)

Parameter[a]	Basis set/Level of theory				
	3-21G*/SCF	6-31G*/SCF[b]	6-311G**/SCF[b]	6-31G*/MP2[b,c]	6-311G**/MP2[b,c]
(b) Bond angles					
B(1)B(4)B(3)	57.4	59.0	58.7	58.9	58.7
B(1)In(2)B(3)	39.5	39.8	40.2	40.8	41.1
B(3)B(1)H(1)	112.5	111.4	111.4	111.0	111.1
H(4)$_{endo}$B(4)H(4)$_{exo}$	119.8	118.9	119.0	117.4	118.3
C(2)$_{endo}$In(2)C(2)$_{exo}$	137.0	136.0	135.2	136.9	137.2
BH$_2$ tilt	1.5	0.4	0.7	1.5	1.9
InC$_2$ tilt	-4.3	-4.5	-4.6	-4.4	-4.5
InCH	110.6	110.9	110.7	110.3	110.3
(c) Torsional angles					
Butterfly angle	118.6	120.4	120.5	121.5	120.2
H(1,2) dip	13.0	13.6	13.9	16.3	15.4
H(1,4) dip	3.0	1.4	1.7	2.6	3.3
Energy/Hartrees	-5872.082843	-5898.0187495	-5898.069181	-5898.748746	-5898.926062

[a] For definition of parameters, see the text.

[b] For In basis set, see the text.

[c] For the method of electron correlation used for In, see the text.

7.3.2 Gas Phase Electron Diffraction (GED)

In the original refinements of $(CH_3)_2AlB_3H_8$ and $(CH_3)_2GaB_3H_8$ several structural assumptions had to be made since the amount of information that can be derived from the GED data is somewhat limited.[3] In particular, the B-B, M-C and M-H_b distances, being of similar length, are all subject to strong correlation, and locating the hydrogen atoms is a particularly difficult task as the heavy atoms dominate the molecular scattering. In the first refinements the following assumptions had to be made: (a) several parameters were fixed at values derived from the original B_4H_{10} study[9], *i.e.* the two B-B distances, <B(3)-B(1)-H(1), <H(4)$_{endo}$-B(4)-H(4)$_{exo}$, the difference between the outer B(4)-H(1,4) and inner B(4)-H(1,4) bridging distances, and finally the difference between rB(1)-H(1) and the average B(4)-H(4)$_{endo/exo}$ distance; (b) the difference between the two inner B-H_b distances were set at zero; (c) the bridging hydrogen atoms were taken to lie in the heavy-atom planes M(2)-B(1)-B(3) and B(1)-B(4)-B(3); (d) finally, as no force field was available, vibrational amplitudes were fixed at values in line with those determined for related molecules B_4H_{10}[9] and $M(BH_4)(CH_3)_2$ (M=Al or Ga).[10]

In the original work[3] nine or ten of the seventeen geometric parameters used to describe the structures were successfully refined, along with three or four vibrational amplitudes. Final R_G values recorded were 0.159 and 0.139 for $(CH_3)_2AlB_3H_8$ and $(CH_3)_2GaB_3H_8$, respectively. The structures obtained were largely in accord with structures for other similar compounds. However, with almost half of the geometric parameters fixed at assumed values, several severe structural assumptions made and a very crude approximation adopted concerning vibrational effects, the quality of the original refinements is necessarily limited. As the SARACEN method allows the refinement of all geometric parameters and removes the need to make any structural assumptions in the GED model, a more flexible model can now be used, leading to much more reliable and realistic structures. In addition, the determination of reliable harmonic force fields by *ab initio* calculations removes the assumptions made in the original work concerning the effects of vibration on the molecular structures.

$(CH_3)_2AlB_3H_8$

The results obtained in the new refinement of the structure of $(CH_3)_2AlB_3H_8$ are given in Table 7.6. The radial-distribution curve [shown in Figure 7.2(a)] is composed mainly of four peaks, with distances $rB(1)-Al(2)$, $rAl(2)-C(2)_{endo/exo}$, $rB(1)-B(2)$ and $rB(1)-B(3)$ forming the most dominant features. The parameters p_1 (the average B-B distance), p_3 [$rB(1)-Al(2)$], p_5 (the average B-H distance), p_{11} (the average Al-C$_{endo/exo}$ distance) could all be refined freely, together with p_{13} ($rC-H$) and p_{19} ($<AlCH$) which, with multiplicities of six, would be expected to be well defined by the GED data. In addition the angles $<C(2)_{endo}-M(2)-C(2)_{exo}$ (p_{15}), MC$_2$ tilt (p_{17}) and the butterfly angle (p_{20}) were also able to refine to realistic values with reliable esds. The remaining thirteen geometric parameters could only be refined successfully with the aid of flexible restraints (documented in Table 7.7) in accordance with the SARACEN method.[‡,§]

[‡] Each geometric restraint has a value and an uncertainty, derived from the graded series of *ab initio* calculations. Absolute values are taken from the highest level calculation and uncertainties are estimated from values given by lower level calculations, or based on a working knowledge of the reliability of the calculations for electronically similar molecules.

[§] As a result of the large number of basis functions required to describe $(CH_3)_2AlB_3H_8$ and $(CH_3)_2GaB_3H_8$ it was not possible to perform calculations to a high enough level to display satisfactory convergence (see Tables 7.3 and 4). However, based on the large array of calculations performed on the parent compound B_4H_{10} (see previous chapter), it is known that the heavy cage atoms are much better described at the MP2 level of electron correlation that at the SCF level. For this reason the uncertainty of 1 pm chosen for the cage parameter Δr(B-B) (p_2) for both refinements is based on the variation observed in the B-B cage distances of B_4H_{10} for calculations performed at the MP2 level and above. The derivation of the remaining geometric restraints is based on results obtained from the $(CH_3)_2AlB_3H_8$ and $(CH_3)_2GaB_3H_8$ series of calculations, and is documented in Tables 7.7 and 7.12).

Table 7.6 Geometric parameters for the SARACEN studies of $(CH_3)_2AlB_3H_8$ and $(CH_3)GaB_3H_8$

Parameter[a,b]		Results[c]	
Independent		$Me_2AlB_3H_8$	$Me_2GaB_3H_8$
Bond distances			
p_1	av. $[r(B\text{-}B)]$	182.3(9)	182.5(22)
p_2	$\Delta\, r(B\text{-}B)$	6.1(13)	5.3(13)
p_3	$r[B(1)\text{-}M]$	231.6(7)	234.2(8)
p_4	$r[M(2)\text{-}H(1,2)]$	182.5(13)	186(6)
p_5	av. $r(B\text{-}H)$	126.5(7)	123.4(14)
p_6	av. $r(B\text{-}H)_b$ - $r(B\text{-}H)_t$	11.6(12)	11.6(18)
p_7	$\Delta\, [r(B\text{-}H)_b]$ (outer–inner)	17.2(6)	17(3)
p_8	$\Delta\, [r(B\text{-}H)_b]$ (inner)	1.6(13)	1.3(13)
p_9	$r[B(1)\text{-}H(1)]$–av. $r[B(4)\text{-}H_t]$	-0.5(4)	-0.6(1)
p_{10}	$\Delta\, r(B\text{-}H)_t$ (*endo–exo*)	0.2(1)	0.3(3)
p_{11}	av. $r[M\text{-}C]$	193.9(5)	193.2(4)
p_{12}	$\Delta\, r(M\text{-}C)$ (*endo-exo*)	0.2(1)	0.3(3)
p_{13}	$r(C\text{-}H)$	107.2(4)	111.0(10)
Angles			
p_{14}	$<B(3)B(1)H(1)$	112.3(12)	111.6(13)
p_{15}	$<C(2)_{endo}M(2)C(2)_{exo}$	132.0(23)	132.3(15)
p_{16}	$<H(4)_{endo}B(4)H(4)_{exo}$	118.5(13)	118.5(13)
p_{17}	MC_2 tilt	-7.1(4)	-4.7(23)
p_{18}	BH_2 tilt	0.7(13)	0.5(21)
p_{19}	$<HCM$	111.0(15)	108.6(10)
Torsions			
p_{20}	butterfly angle	123.8(20)	119.8(13)
p_{21}	$H(1,2)$ dip	13.4(13)	14.3(16)
p_{22}	$H(1,4)$ dip	1.5(16)	-0.2(21)
Dependent			
	$<B(1)B(4)B(3)$	57.8(4)	58.1(5)
	$<B(1)M(2)B(3)$	45.3(3)	44.9(7)
	$r[B(1)\text{-}B(3)]$	178.2(12)	178.9(23)
	$r[B(1)...B(4)]$	184.4(10)	184.3(23)
	$r[B(1)\text{-}H(1,4)]$	126.2(11)	122.9(18)
	$r[B(4)\text{-}H(1,4)]$	142.6(11)	140(3)
	$r[B(1)\text{-}H(1,2)]$	124.6(11)	121.6(18)
	$r[B(1)\text{-}H(1)]$	119.4(10)	116.3(17)
	$r[B(4)\text{-}H(4)_{endo}]$	119.8(10)	116.8(17)
	$r[B(4)\text{-}H(4)_{exo}]$	119.6(10)	116.5(17)
	$r[M(2)\text{-}C(2)_{endo}]$	194.0(5)	193.4(4)
	$r[M(2)\text{-}C(2)_{exo}]$	193.8(5)	193.1(4)

[a] For definition of parameters, see the text. [b] For atom numbering, see Figure 7.1.
[c] Values in parentheses are the estimated standard deviations. For details of the refinements, see the text.

Table 7.7 Derivation of the geometric restraints used in the GED refinement of $(CH_3)_2AlB_3H_8$ (r/pm, $</°$)

	Parameter[a]	3-21G*/SCF	6-31G*/SCF	6-311G**/SCF	6-31G*/MP2	6-311G**/MP2	Value used
	Bond distances						
p_2	$\Delta\, r$(B-B)	10.4	8.7	9.0	6.0	6.3	6.3(10)
p_4	r[Al(2)-H(1,2)]	181.3	182.1	181.9	183.2	182.5	182.5(10)
$p6$	av. B-H_b - av. B-H_t	12.3	11.9	12.4	10.7	11.4	11.4(10)
p_7	$\Delta\, [r$(B-H)$_b$] (outer–inner)	18.4	17.8	18.0	16.6	17.1	17.1(5)
p_8	$\Delta\, [r$(B-H)$_b$] (inner)	1.1	1.4	0.5	1.6	1.6	1.6(1)
p_9	r[B(1)-H(1)]–av. r[B(4)-H_t]	-0.2	-0.1	-0.2	-0.6	-0.5	-0.5(1)
p_{10}	$\Delta\, r$(B-H)$_t$ (*endo–exo*)	0.1	0.2	0.2	0.2	0.2	0.2(1)
p_{12}	$\Delta\, r$(Al-C) (*endo-exo*)	0.2	0.2	0.3	0.3	0.2	0.2(1)
	Bond angles						
p_{14}	<B(3)B(1)H(1)	113.3	113.2	113.1	112.3	112.1	112.1(10)
p_{16}	<H(4)$_{endo}$B(4)H(4)$_{exo}$	120.3	119.3	119.5	117.7	118.6	118.6(10)
p_{18}	BH_2 tilt	-0.6	0.4	-0.3	0.0	0.8	0.8(10)
	Torsions						
p_{21}	H(1,2) dip	11.6	13.2	12.3	14.0	13.4	13.4(10)
p_{22}	H(1,4) dip	0.1	0.5	0.1	0.2	1.5	1.5(13)

[a] For definition of the parameters, see the text

Four amplitudes of vibration, corresponding to distances u_{13}[B(1)...Al(2)], u_{17}[B(1)...C(2)$_{endo}$], u_{18}[B(1)...C(2)$_{exo}$] and u_{21}[B(4)...Al(2)] could be refined. With the inclusion of thirteen vibrational amplitude restraints (given in Table 7.8) a further seventeen vibrational amplitudes were refined (see Table 7.9). Thus all amplitudes associated with distances contributing greater than 10% weighting of the most intense feature in the radial-distribution curve were refined. Values for the amplitude restraints were calculated directly from the scaled 6-31G*/SCF force field, with uncertainty ranges of 5% adopted for amplitude ratios or 10% for absolute values. Direct amplitude restraints were found to be necessary in the case of u_2[B(1)-H(1)], u_3[B(1)-H(1,4)] and u_4[B(1)-H(1,2)] as the normal practise of restraining ratios resulted in unrealistic vibrational amplitude values being returned in the least-squares refinement due to high correlation effects.

Table 7.8 Derivation of vibration amplitude restraints for the SARACEN study of $(CH_3)_2AlB_3H_8$

Amplitude Restraint	Value	Uncertainty
u_1[B(1)-B(3)]/u_{12}[B(1)...B(4)]	0.83	0.04
u_2[B(1)-H(1)]	8.2	0.82
u_3[B(1)-H(1,4)]	9.1	0.91
u_4[B(1)-H(1,2)]	9.1	0.91
u_5[B(4)-H(1,4)]	12.9	1.29
u_8[Al(2)-C(2)$_{endo}$]/u_9[Al(2)-C(2)$_{exo}$]	1.0	0.05
u_{10}[Al(2)-H(1,2)]	12.6	1.26
u_{14}[Al...H(methyl)$_{endo}$]/u_{15}[Al...H(methyl)$_{exo}$]	1.0	0.05
u_{16}[C(2)$_{endo}$-C(2)$_{exo}$]	11.0	1.1
u_{19}[Al(2)-H(1,4)]/u_{20}[Al(2)-H(1)]	0.96	0.05
u_{22}[B(4)...C(2)$_{endo}$]	12.9	1.29
u_{23}[B(4)...C(2)$_{exo}$]	21.8	2.2

Cage Structure: The three cage distances rB(1)-B(3), rB(1)...B(4) and rB(1)...Al(2) refined to final values of 178.2(12) pm, 184.4(10) pm and 231.6(7) pm respectively, compared to their 6-311G**/MP2 *ab initio* values of 178.2 pm, 184.5 pm and 230.4 pm. The small standard deviation measured for the B(1)...Al(2) distance reflects the fact that aluminium and boron are the principal scatterers of electrons. The butterfly angle (p_{20}) refined to 123.8(20)°, compared to its *ab initio* value of 119.2°.

Bridge Region: The four bridging distances rB(1)-H(1,4), rB(4)-H(1,4), rB(1)-H(1,2) and rAl(2)-H(1,2) refined to 126.2(11)pm, 142.6(11) pm, 124.6(11) pm and 182.5(13) pm respectively, in agreement with their 6-311G**/MP2 *ab initio* values to within one standard deviation.

Terminal Region: The three terminal B-H distances, rB(1)-H(1), rB(4)-H(4)$_{endo}$ and rB(4)-H(4)$_{exo}$, refined to values 119.4(10) pm, 119.8(10) pm and 119.6(10) pm respectively, in agreement with their respective 6-311G**/MP2 *ab initio* values to within one standard deviation. The final two terminal distances, rAl-C$_{endo}$ and rAl-C$_{exo}$, at 194.0(5) pm and 193.8(5) pm, are slightly shorter than their predicted *ab initio* values of 195.3 pm and 195.1 pm. Of the six angles required to define the locations of the terminal atoms four parameters (p_{14}, p_{16}, p_{18}, and p_{19}) all refined to values within one standard deviation of their *ab initio* values. Angle <C(2)$_{endo}$-Al(2)-C(2)$_{exo}$ (p_{15}) refined to 132.0(23)°, within two esds of its *ab initio* value of 128.6°, and the AlC$_2$ tilt angle (p_{17}) refined to -7.1(4)°, compared to its *ab initio* value of -4.6°. The negative value indicates a tilt out of the heavy atom cage.

Table 7.9 Selected bond distances (r_a/pm) and amplitudes of vibration (u/pm) obtained from the SARACEN study of $(CH_3)_2AlB_3H_8$

	i	Atom Pair	Distance	Amplitude[a]
Bonding distances	1	B(1)-B(3)	178.7(12)	7.2(13)
	2	B(1)-H(1)	121.8(10)	7.8(10)
	3	B(1)-H(1,4)	128.2(11)	9.2(11)
	4	B(1)-H(1,2)	126.1(12)	9.0(11)
	5	B(4)-H(1,4)	143.9(11)	13.0(16)
	6	B(4)-H(4)$_{endo}$	122.1(10)	8.3 fixed
	7	B(4)-H(4)$_{exo}$	122.3(10)	8.3 fixed
	8	Al(2)-C(2)$_{endo}$	194.8(5)	6.4(5)
	9	Al(2)-C(2)$_{exo}$	194.5(5)	6.4(5)
	10	Al(2)-H(1,2)	183.0(13)	12.7(16)
	11	C-H(methyl)	108.7(4)	8.0(8)
Non-bonding distances	12	B(1)...B(4)	185.2(10)	8.7(16)
	13	B(1)...Al(2)	231.6(7)	9.9(5)
	14	Al...H(methyl)$_{endo}$	253(7)	22(4)
	15	Al...H(methyl)$_{exo}$	253(7)	22(4)
	16	C(2)$_{endo}$...C(2)$_{exo}$	355(3)	10.9(14)
	17	B(1)...C(2)$_{endo}$	366.5(22)	9.3(21)
	18	B(1)...C(2)$_{exo}$	340(3)	9(4)
	19	Al(2)...H(1,4)	325(3)	6(6)
	20	Al(2)...H(1)	314.6(13)	7(6)
	21	B(4)...Al(2)	331(3)	19(9)
	22	B(4)...C(2)$_{endo}$	405(3)	13.8(14)
	23	B(4)...C(2)$_{exo}$	480.6(17)	20.5(24)

[a] Amplitudes which could not be refined are fixed at values derived from the 6-31G*/SCF scaled force field.

The R_G factor recorded for this final refinement was 0.081. With all twenty-two geometric parameters and all significant vibrational amplitudes refining the structure is the best that can be obtained using all available data, both experimental and theoretical, and all standard deviations should be reliable estimates, free from systematic errors resulting from limitations of the model. Cartesian co-ordinates from the final refinement are given in Table 7.10 and the covariance matrix in Table 7.11. The final radial-distribution curves and combined molecular scattering curves are shown in Figures 7.2(a) and 7.2(b) respectively.

Table 7.10 Cartesian Coordinates (pm) obtained for $(CH_3)_2AlB_3H_8$ from the final SARACEN refinement

		X	Y	Z
Cage	B(1)	0.0000	-89.12	0.0000
	Al(2)	188.51	0.0000	100.72
	B(3)	0.0000	89.12	0.0000
	B(4)	-142.34	0.0000	76.05
Bridge	H(1,2)	84.59	-146.98	70.84
	H(2,3)	84.59	146.98	70.84
	H(3,4)	-102.30	135.59	57.51
	H(1,4)	-102.30	-135.59	57.51
Terminal	H(1)	0.0000	-134.50	-110.50
	H(2)	0.0000	134.50	-110.50
	$C(2)_{endo}$	198.84	0.0000	294.47
	$H(methyl)_{endo}$	100.99	0.0000	338.21
	$H(methyl)_{endo}$	250.83	-86.63	330.22
	$H(methyl)_{endo}$	250.83	86.63	330.22
	$C(2)_{exo}$	325.54	0.0000	-36.35
	$H(methyl)_{exo}$	282.00	0.0000	-134.28
	$H(methyl)_{exo}$	388.11	-86.63	-28.19
	$H(methyl)_{exo}$	388.11	86.63	-28.19
	$H(4)_{endo}$	-146.35	0.0000	195.79
	$H(4)_{exo}$	-243.52	0.0000	15.55

Table 7.11 Least-squares correlation matrix (x100) for the SARACEN refinement of $(CH_3)_2AlB_3H_8$[a]

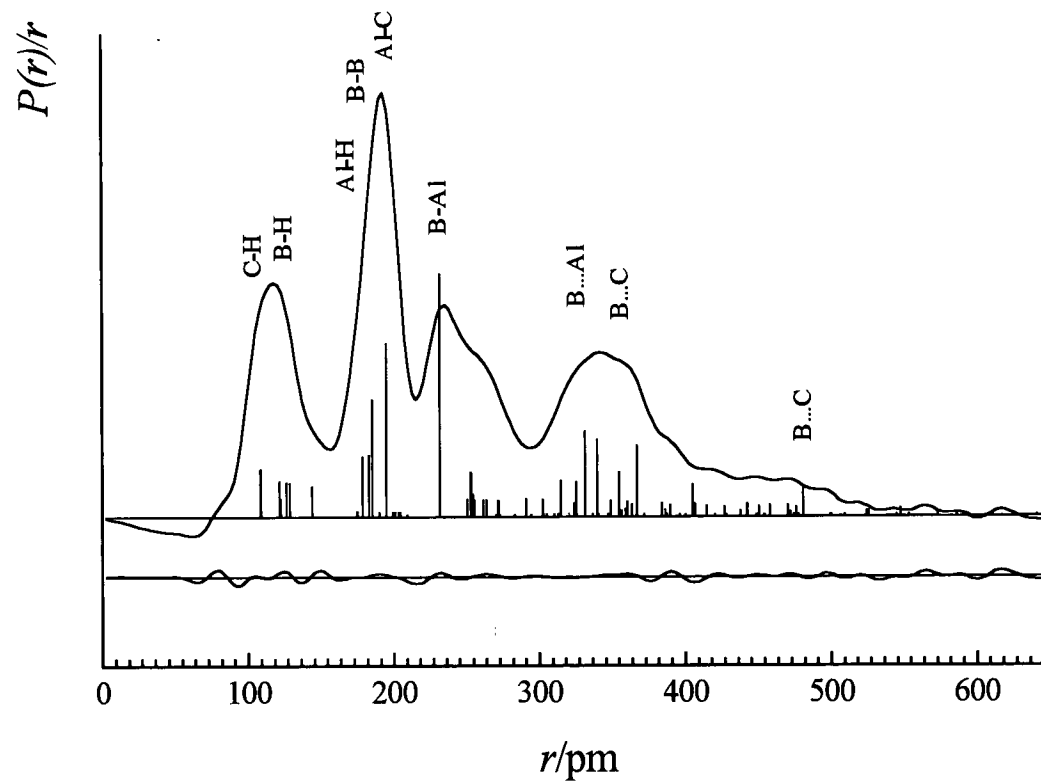|	p_{11}	p_{17}	p_{19}	u_1	u_8	u_9	u_{11}	u_{12}	u_{17}	u_{18}	u_{19}	u_{20}	u_{21}	k_2
p_1	62			53	60	61		57						
p_5							-53							
p_{11}				-81				-85						
p_{20}		80							76	-63	-74	-74	63	
p_{15}			-57						70	-72	-73	-73	73	
p_{19}									-57				-55	
u_1					60	61		93						
u_8						62		60						
u_9								61						
u_{11}														
u_{17}										-52	-67	-67	68	
u_{18}											90	90	-88	
u_{19}												100	-88	
u_{20}													-87	
k_1														54

[a] Only off-diagonal elements with absolute values >50% are shown

Figure 7.2(a) Observed and final difference radial distribution curves for $(CH_3)_2AlB_3H_8$.

Before Fourier inversion the data were multiplied by $s.\exp(-0.00002s^2)/(Z_{Al}-f_{Al})(Z_C-f_C)$.
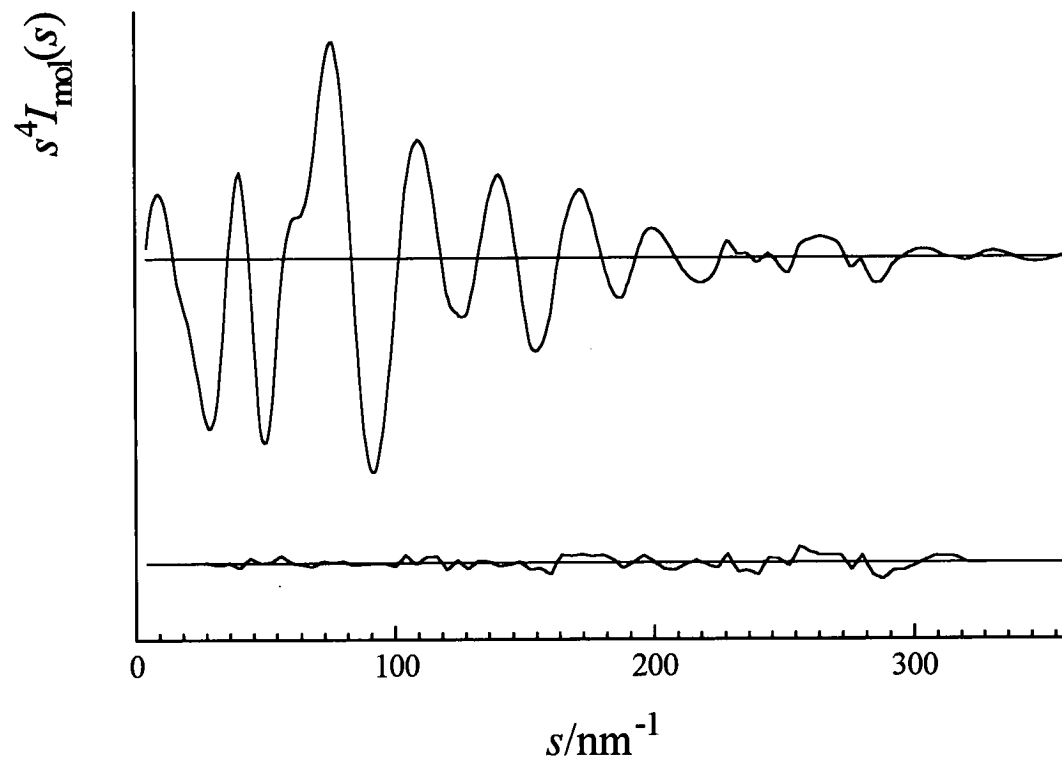
Figure 7.2(b) Observed and final difference combined molecular scattering curves for $(CH_3)_2AlB_3H_8$

$(CH_3)_2GaB_3H_8$

The results obtained for the new refinement of the structure of $(CH_3)_2GaB_3H_8$ are also given in Table 7.2. The radial-distribution curve [given in Figure 7.3(a)] shows many similarities to the radial-distribution curve of $(CH_3)_2AlB_3H_8$ [see Figure 7.2(a)] resulting from similarities in molecular structure. The main difference between the two curves relates to the relative contributions from distances associated with gallium compared with aluminium. With an atomic number more than two times larger than aluminium, distances involving gallium are much more dominant and contributions from other atom-pairs give rise to less structural information. Consequently, only seven of the twenty-two geometric parameters in $(CH_3)_2GaB_3H_8$ could be refined freely [*viz.* p_1 av.r(B-B), p_3 rB(1)-Ga(2), p_5 av.rB-H, p_{11} av. rGa-C$_{endo/exo}$, p_{17} GaC$_2$ tilt and p_{19} <HCGa], compared with nine for $(CH_3)_2AlB_3H_8$. The derivation of the fifteen geometric restraints required to allow all geometric parameters to refine is given in Table 7.12. Values adopted for the restraints were derived in the same way as for the aluminium analogue, with p_2 [Δr(B-B)] based on a larger array of calculations performed on the parent compound B_4H_{10}.

Table 7.12 Derivation of the geometric restraints used in the SARACEN refinement of $(CH_3)_2GaB_3H_8$ (r/pm, $</°$)

	Parameter[a]	3-21G*/ SCF	6-31G*/ SCF	6-311G**/ SCF	6-31G*/ MP2[b]	6-311G**/ MP2[b]	Value used
	Bond distances						
p_2	$\Delta\,r$(B-B)	7.4	10.6	7.0	6.1	5.5	5.5(10)
p_4	r[Ga(2)-H(1,2)]	188.7	190.2	186.2	190.7	185.0	185.0(50)
p_6	av. r(B-H)$_b$ - av. r(B-H)$_t$	12.4	10.8	12.8	10.2	11.6	11.6(14)
p_7	Δ [r(B-H)$_b$] (outer–inner)	19.6	14.8	19.2	14.7	17.2	17.2(20)
p_8	Δ [r(B-H)$_b$] (inner)	0.8	1.6	-0.2	2.0	1.2	1.2(10)
p_9	r[B(1)-H(1)]–av. r[B(4)-H$_t$]	0.0	-0.1	-0.2	-0.5	-0.6	-0.6(1)
p_{10}	$\Delta\,r$(B-H)$_t$ (endo–exo)	0.1	0.0	0.2	0.1	0.3	0.3(2)
p_{12}	$\Delta\,r$(Ga-C) (endo-exo)	0.3	0.0	0.2	0.1	0.3	0.3(2)
p_{13}	r(C-H)	108.6	108.6	108.6	109.4	109.4	109.4(15)
	Bond angles						
p_{14}	<B(3)B(1)H(1)	112.1		112.2	110.9	111.6	111.6(10)
p_{15}	<C(2)$_{endo}$Ga(2)C(2)$_{exo}$	132.4	129.9	131.2	131.2	132.4	132.4(12)
p_{16}	<H(4)$_{endo}$B(4)H(4)$_{exo}$	120.0	119.1	119.2	117.3	118.4	118.4(10)
p_{18}	BH$_2$ tilt	1.6	2.2	-0.6	2.2	0.6	0.6(16)
	Torsions						
p_{21}	H(1,2) dip	15.1	12.8	12.0	14.0	13.2	13.2(12)
p_{22}	H(1,4) dip	1.8	2.0	0.7	2.8	0.2	0.2(16)

[a] For definition of the parameters, see the text.

[b] For details of electron correlation treatment used for Ga, see the text.

In addition, three amplitudes of vibration, u_{13}[B(1)...Ga], u_{15}[B(1)...C(2)$_{endo}$], and u_{16}[B(1)...C(2)$_{exo}$], could be refined freely. A further nine were successfully refined with the inclusion of eight amplitude restraints (given in Table 7.13), resulting in the refinement of all amplitudes associated with distances contributing greater than 10% weighting of the most intense feature in the radial-distribution curve.

Cage Structure: The three cage distances rB(1)-B(3), rB(1)...B(4) and rB(1)...Ga(2) refined to 178.9(23) pm, 184.3(23) pm and 234.2(8) pm respectively, compared to their 6-311G**/MP2 *ab initio* values of 178.6 pm, 184.1 pm and 232.6 pm. The small standard deviation for rB(1)...Ga(2) reflects the dominant electron scattering properties of the gallium and boron atoms. The butterfly angle (p_{20}) refined to 119.8(13)°, compared to its *ab initio* value of 119.6°.

Bridge Region: The four bridging distances, rB(1)-H(1,4), rB(4)-H(1,4), rB(1)-H(1,2) and rGa(2)-H(1,2) refined to 122.9(18) pm, 140(3) pm, 121.6(18) pm and 186(6) pm, respectively, in agreement with their 6-311G**/MP2 *ab initio* values to within one or two standard deviations. The distance rGa(2)-H(1,2), with a standard deviation of 6 pm, was found to be poorly defined by the GED data as a result of its close proximity to the B-B distances. In the derivation of the restraint for this parameter [185(5) pm] it was necessary to stipulate a large uncertainty to allow for the significant variation that occurs in this bond length with improvements in basis set and level of theory (see Table 7.12). Although this restraint is very flexible, it enabled the Ga(2)-H(1,2) distance to be determined with much greater confidence than using the GED data alone.

Terminal Region: The terminal B-H distances, rB(1)-H(1), rB(4)-H(4)$_{endo}$ and rB(4)-H(4)$_{exo}$, refined to 116.3(17) pm, 116.8(17) pm and 116.5(17) pm, in agreement with their respective 6-311G**/MP2 *ab initio* values to within two standard deviations. rGa-C$_{endo}$ and rGa-C$_{exo}$ [like rAl-C$_{endo}$ and rAl-C$_{exo}$ in (CH$_3$)$_2$AlB$_3$H$_8$] refined to values slightly shorter than their predicted *ab initio* values [193.4(4)pm and 193.1(4) pm by GED, 195.6 pm and 195.3 pm *ab initio*]. Four of the six angles required to define the

locations of the terminal atoms, p_{14-16} and p_{18}, refined to values within one standard deviation of their 6-311G**/MP2 *ab initio* values. Parameters p_{17}, MC$_2$ tilt, and p_{19}, <HCGa, refined freely to values -4.7(23)° and 108.6(10)°, compared to their *ab initio* values of -4.8° and 110.6°.

The R_G factor recorded for this refinement was 0.111, with the slightly high value being attributable to the high noise levels in the data resulting from fogging of the photographic plates by the $(CH_3)_2GaB_3H_8$ vapour. With all twenty-two geometric parameters and all significant vibrational amplitudes refining the structures are the best that can be obtained using all available data, both experimental and theoretical, and all standard deviations should be reliable estimates, free from systematic errors resulting from limitations of the model. The covarience matrix obtained in the final refinement is given in Table 7.14, the final set of distances and vibrational amplitudes in Table 7.15 and the Cartesian co-ordinates in Table 7.16. The final radial-distribution curves and combined molecular scattering curves are shown in Figures 7.3(a) and 7.3(b) respectively.

Table 7.14 Least-squares correlation matrix (x100) for the SARACEN study of $(CH_3)_2GaB_3H_8{}^a$

	p_4	p_{13}	u_8	u_9	u_{14}	u_{15}	u_{16}	u_{17}	k_1	k_2
p_1	-55		68	68						
p_3					70	70				
p_5		-55							60	65
p_{17}							80	79		
u_8				83						
u_{13}					73	73				
u_{14}						97				
u_{16}								100		
k_1										76

^{a} Only off-diagonal elements with absolute values >50% are shown

Table 7.15 Selected bond distances (r_a/pm) and amplitudes of vibration (u/pm) obtained from the SARACEN refinement of $(CH_3)_2GaB_3H_8$

	i	Atom Pair	Distance	Amplitude[a]
Bonding distances	1	B(1)-B(3)	179.4(23)	6.7(9)
	2	B(1)-H(1)	118.5(17)	8.3 fixed
	3	B(1)-H(1,4)	124.5(18)	9.0 fixed
	4	B(1)-H(1,2)	123.7(19)	9.2 fixed
	5	B(4)-H(1,4)	140(3)	13.9 fixed
	6	B(4)-H(4)$_{endo}$	119.4(17)	8.3 fixed
	7	B(4)-H(4)$_{exo}$	118.7(17)	8.3 fixed
	8	Ga(2)-C(2)$_{endo}$	194.1(4)	5.9(7)
	9	Ga(2)-C(2)$_{exo}$	193.9(4)	5.8(7)
	10	Ga(2)-H(1,2)	186(6)	15.3(19)
	11	C-H(methyl)	112.4(9)	7.6 fixed
Non-bonding distances	12	B(1)...B(4)	185(23)	8.5(11)
	13	B(1)...Ga(2)	234.4(8)	7.5(9)
	14	Ga...H(methyl)$_{endo}$	253(7)	11(3)
	15	Ga...H(methyl)$_{exo}$	253(7)	11(3)
	16	B(1)...C(2)$_{endo}$	364(5)	11(5)
	17	B(1)...C(2)$_{exo}$	346(5)	12(6)
	18	Ga(2)...H(1,4)	321(3)	13.6(19)
	19	Ga(2)...H(1)	316.1(18)	14.6(20)
	20	B(4)...Ga(2)	328.0(15)	9.3(20)

[a] Amplitudes which could not be refined are fixed at values derived from the 6-31G*/SCF scaled force field.

Table 7.16 Cartesian Coordinates (pm) obtained for $(CH_3)_2GaB_3H_8$ from the final SARACEN refinement

|		X	Y	Z
Cage	B(1)	0.0000	-89.47	0.0000
	Ga(2)	187.30	0.0000	108.55
	B(3)	0.0000	89.47	0.0000
	B(4)	-139.38	0.0000	80.78
Bridge	H(1,2)	78.43	-147.00	73.05
	H(2,3)	78.43	147.00	73.05
	H(3,4)	-100.01	131.9	57.52
	H(1,4)	-100.01	-131.9	57.52
Terminal	H(1)	0.0000	-132.21	-108.20
	H(2)	0.0000	132.21	-108.20
	C(2)$_{endo}$	182.03	0.0000	301.83
	H(methyl)$_{endo}$	75.91	0.0000	334.36
	H(methyl)$_{endo}$	233.64	-91.10	338.66
	H(methyl)$_{endo}$	233.64	91.10	338.66
	C(2)$_{exo}$	333.64	0.0000	-17.36
	H(methyl)$_{exo}$	291.88	0.0000	-120.19
	H(methyl)$_{exo}$	394.79	-91.10	-0.58
	H(methyl)$_{exo}$	394.79	91.10	-0.58
	H(4)$_{endo}$	-139.61	0.0000	197.57
	H(4)$_{exo}$	-241.6	0.0000	25.02
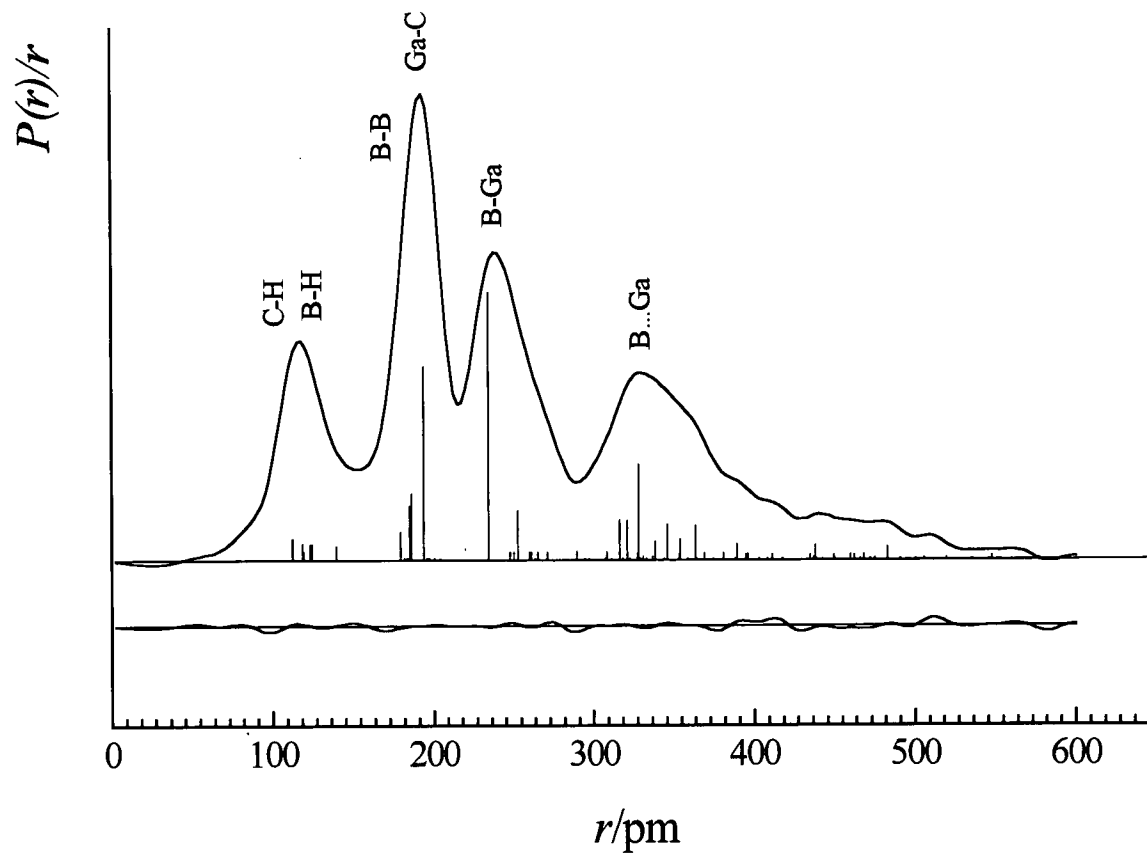
Figure 7.3(a) Observed and final difference radial distribution curves for $(CH_3)_2GaB_3H_8$.
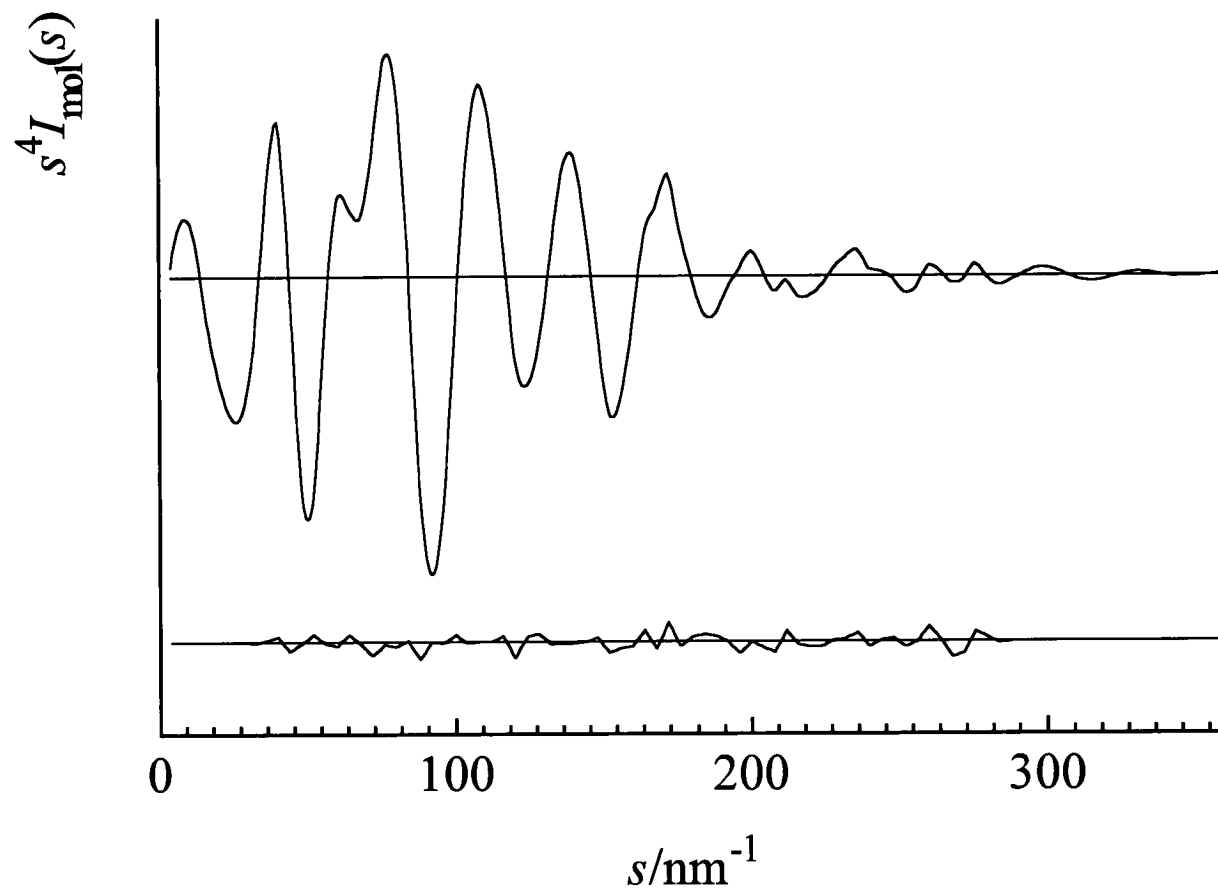Before Fourier inversion the data were multiplied by $s.\exp(-0.00002s^2)/(Z_{Ga}-f_{Ga})(Z_C-f_C)$.

Figure 7.3(b) Observed and final difference combined molecular scattering curves for $(CH_3)_2GaB_3H_8$

6.4 Structural Trends Predicted by *Ab Initio*: The Effects of Changing M

The main structural changes predicted by the 6-311G**/MP2 *ab initio* calculations for the series of dimethyl tetraborane(10) derivatives $(CH_3)_2MB_3H_8$ (M=B, Al, Ga and In) are given in Table 7.17. Many of the trends observed with this series were also found in the hydride series reported earlier, and can be summarised as follows.

1. **Changes in M-B/H distances.** As with the hydride derivative series reported in the previous chapter, the increasing values of rB(1)-M(2), rM(2)-H(1,2), on moving from B to In can be attributed largely with the increase in atomic radius of the atom 'M' (see Table 7.17). Thus, significant changes in these bond distances occur on replacing boron with aluminium and gallium with indium, but small changes are also observed on substituting aluminium with gallium. In general the two distances are 1-4 pm longer in the dimethyl series than in the hydride.

2. **Angles correlated with atom M.** The angle <C(2)$_{endo}$-M(2)-C(2)$_{exo}$ was found to widen largely in agreement with the increasing size of atom M; however, as with the angle <H(4)$_{endo}$-B(4)-H(4)$_{exo}$ in the hydride series, the change observed on substituting aluminium with gallium was somewhat larger than expected. The bridging angle <B(1)-H(1,2)-M(2) varied in accordance with the increasing covalent radius of atom M; significant changes observed on substituting B with Al and Ga with In. This angle was found to be *ca.* 1° wider in the dimethyl series than in the hydride.

3. **Changes in the B_3H_8 fragment.** As with the hydride series the distance B(1)-B(3) was found to be marginally affected by the identity of atom M, with a significant lengthening observed when B is replaced with Al, and a further slight lengthening when In replaces Ga. The distance was found to be less than 1 pm longer in the dimethyl series. The angle B(3)-B(1)-H(1) was observed to narrow slightly on moving from B to In, possibly due to a correlation effect with rB(1)-B(3). As observed with the hydrides, rB(1)-B(4) shortened slightly across the dimethyl series. The same general trend was observed in both sets of derivatives for the positions of the bridging hydrogen atoms above the BBB/M plane [the H(1,2) and

H(1,4) dip angles], with the bridging atoms elevated more above the B(1)-M(2)-B(3) plane [H(1,2) dip] than the B(1)-B(4)-B(3) plane [H(1,4) dip]. The variation in the H(1,2) dip angle was found to be largely consistent in the two derivative series, although more pronounced in the dimethyl series, with H(1,2) raised *ca.* 13° above the B(1)-M(2)-B(3) plane in the aluminium and gallium compounds (*cf. ca.* 10.5° in $H_2AlB_3H_8$ and $H_2GaB_3H_8$), rising to 15° in $(CH_3)_2InB_3H_8$ (*cf.* 14° in $H_2InB_3H_8$). Once again, the *ab initio* value obtained for the H(1,4) dip angle in $(CH_3)_2GaB_3H_8$, at just 0.2°, appears to be anomalous compared with the rest of the series. However, a close examination of the complete range of *ab initio* calculations carried out (see Table 7.4) indicates that this parameter shows a significant variation from 0.2° to 2.8° which can in the most part be attributed to improvements in basis set quality. An uncertainty of about 3° in the 6-311G**/MP2 value of 0.2° would allow this parameter to be more consistent with the results obtained for the other compounds in this series.

4. **Distances and angles unchanged by atom M.** The distances B(1)-H(1,4), B(4)-H(1,4) and B(1)-H(1,2) and angles $<H(4)_{endo}$-B(4)-H(4)$_{exo}$ and the butterfly angle were largely unaffected by the identity of atom M. The butterfly angle, dimethyl *vs.* hydride , was found to be wider by *ca.* 4° when M=B, 3° when M=Al and Ga and 1° when M=In.

Table 7.17 Structural trends observed in the $(CH_3)_2MB_3H_8$ series by *ab initio* (6-311G**/MP2)[a] calculations (r_e/pm, $</°$)

	Parameter[b]	B	Al	Ga	In
	covalent radius[c]	88	125	125	140
Cage	rB(1)-B(3)	173.5	178.2	178.6	179.9
	rB(1)-B(4)	185.3	184.5	184.1	183.5
	rB(1)-M(2)	189.9	230.4	232.6	256.3
	butterfly angle	120.8	119.2	119.6	120.2
Bridge	rB(1)-H(1,2)	124.1	124.0	124.4	124.4
	rM(2)-H(1,2)	145.4	182.5	185.0	205.2
	<B(1)-H(1,2)-M(2)	89.2	95.6	95.5	99.1
	H(1,4) dip	10.6	1.5	0.2	3.3
	H(1,2) dip	11.0	13.4	13.2	15.4
Terminal	<C(2)$_{endo}$M(2)C(2)$_{exo}$	119.0	128.6	132.4	137.2

[a] For In basis set, see the text
[b] For definition of parameters, see the text
[c] From ref. 11.

7.5 $(CH_3)_2InB_3H_8$: comparison of *ab initio* and X-ray diffraction molecular structures

The final aspect of this work involved drawing a comparison between the molecular structure of $(CH_3)_2InB_3H_8$ obtained by *ab initio* calculations and the structure obtained from X-ray diffraction (see Table 7.18).[4] *Ab initio* calculations determine the molecular structure of one discrete molecule and so, in the absence of GED or any other gas-phase experimental structural data, represents the closest we can obtain to the gas-phase structure of this molecule at the present time. Therefore, a direct comparison of the geometric parameters obtained by the two techniques will allow differences in the gas and solid-phase structures to be identified.

A word of caution should be noted, however, in performing this type of comparison. Differences in molecular structure are to be expected as a consequence of the fundamental differences in the two techniques. First, the definition of bond length is different for the two methods; *ab initio* methods calculate the difference between the positions of atomic nuclei whilst X-ray diffraction measures the difference between centres of electron density. Secondly, the *ab initio* geometry is a static, vibration-free equlibrium structure; the crystal structure, measured at 150 K, is subject to vibrational and librational averaging effects. For these reasons only fairly gross structural differences between the two methods have been considered significant.

The main structural differences, X-ray *vs. ab initio*, were found to centre around the indium atom, with (i) rB(1)-In(2) approximately 20 pm longer, (ii) the internal cage angle <H(1,2)-In(2)-H(2,3) approximately 15° narrower and (iii) <C(2)$_{endo}$-In(2)-C(2)$_{exo}$ approximately 20° wider in the solid phase, compared to the discrete structure calculated *ab initio*. The explanation for these structural differences is evident upon closer examination of the crystal structure: two neighbouring molecules interact with the indium centre through hydrogen H(1) atoms, effectively increasing the co-ordination number of the indium centre from four to six. As a result of this change in coordination <H(1,2)-In(2)-H(2,3) will narrow, rB(1)-In(2) will lengthen to maintain the rB(1)-B(3) distance and <C(2)$_{endo}$-In(2)-C(2)$_{exo}$ will widen to force the two methyl groups apart to accommodate the two new co-ordinating species.

The changes also reflect the increasing ionic character of compounds and the increasing metallic character of Group 13 elements on desending the group. Thus indium will have a high coordination number (typically six), and a greater ionic character will be apparent in the solid. Therefore the molecule $(CH_3)_2InB_3H_8$ can be thought of as approaching $[(CH_3)_2In]^+[B_3H_8]^-$, in which $[(CH_3)_2In]^+$ would be linear, and thus <CH$_3$-In-CH$_3$ would be wider in the solid phase structure compared to that in the gas.

Table 7.18 Comparison of some geometrical parameters for $(CH_3)_2InB_3H_8$ (r/pm, $</°$)

	Parameter	*Ab Initio*	X-ray Diffraction (averaged values)[a]
Cage	rB(1)-B(3)	179.7	178.4(8)
	rB(1)-B(4)	183.5	180.5(10)
	rB(1)-In(2)	256.3	274.4(11)
	Butterfly angle	120.2	124.(2)
Bridge	rB(1)-H(1,4)	125.7	115(4)
	rB(4)-H(1,4)	142.4	140(7)
	rB(1)-H(1,2)	124.4	112(5)
	rIn(2)-H(1,2)	205.2	224(11)
	H(1,2) dip	15.4	14(3)
	H(1,4) dip	3.3	3(1)
	<H(1,2)-In(2)-H(1,4)	95.5	81(2)
Terminal	rIn-C$_{endo}$	217.2	210.6(1)
	rIn-C$_{exo}$	216.9	210.5(1)
	<C(2)$_{endo}$-In(2)-C(2)$_{exo}$	137.2	158.0(1)

[a] Two molecules, of C_1 symmetry were located in the asymmetric unit. Parameters are averaged, and the errors quoted to one sigma.

References

1.   A.J. Blake, P.T. Brain, H. McNab, J. Miller, C.A. Morrison, S. Parsons, D.W.H. Rankin, H.E. Robertson, and B.A. Smart, *J. Phys. Chem.*, 1996, **100**, 12280.

2.   P.T. Brain, C.A. Morrison, S. Parsons and D.W.H. Rankin, *J. Chem. Soc., Dalton Trans.*, 1996, 4589.

3.   C.J. Dain, A.J. Downs and D.W.H. Rankin, *J. Chem. Soc., Dalton Trans.*, 1981, 2465.

4.   S. Aldridge, A.J. Downs and S. Parsons, *J. Chem. Soc., Chem. Com.*, 1996, **17**, 2055.

5.   Gaussian 94, Revision C.2, M.J. Frisch, G.W. Trucks, H.B. Schlegel, P.M.W. Gill, B.G. Johnson, M.A. Robb, J.R. Cheeseman, T. Keith, G.A. Petersson, J.A. Montgomery, K. Raghavachari, M.A. Al-Laham, V.G. Zakrzewski, J.V. Ortiz, J.B. Foresman, J. Cioslowski, B.B. Stefanov, A. Nanayakkara, M. Challacombe, C.Y. Peng, P.Y. Ayala, W. Chen, M.W. Wong, J.L. Andres,

E.S. Replogle, R. Gomperts, R.L. Martin, D.J. Fox, J.S. Binkley, D.J. Defrees, J. Baker, J.P. Stewart, M. Head-Gordon, C. Gonzalez, and J.A. Pople. Gaussian, Inc., Pittsburgh PA. 1995.

6.   S. Huzinaga and M. Klobukowski, *J. Mol. Struct.*, 1988, **167**, 1.

7.   ASYM40 version 3.0, update of program ASYM20. L. Hedberg and I.M. Mills, *J. Mol. Spectrosc.*, 1993, **160**, 117.

8.   A.W. Ross, M. Fink and R. Hilderbrandt, *International Tables for Crystallography.* Editor A.J.C. Wilson, Kluwer Academic Publishers: Dordrecht, The Netherlands, Boston, MA, and London, 1992, Vol. C., p 245.

9.   C.J. Dain, A.J. Downs, G.S. Laurenson and D.W.H. Rankin, *J. Mol. Struct.*, 1981, **71**, 217.

10.   M.T. Barlow, A.J. Downs, P.D.P.Thomas, and D.W.H. Rankin, *J. Chem. Soc.,Dalton Trans.*, 1979, 1793.

11.   D.D. Ebbing, *General Chemistry*, ed. M.S. Wrighton, Houghton Mifflin, 1987, Chapter 7.

Chapter 8

Further Work

8.1 Background

The Edinburgh Structural Chemistry Group can now solve GED data from increasingly large and more complex molecular structures. The reason for this growth in ability is primarily due to the recent up-grading of the GED data analysis and refinement program. The new program (called ED96)[1] can handle model systems with up to 100 refinable geometric parameters and over 1000 different atom pair distances, compared to only 20 geometric parameters and 100 distances in the older version of the program (ED92). In addition, the development of the SARACEN[2,3] method outlined in this thesis will, in principle, give rise to more reliable and realistic solutions to GED data sets. Hence larger systems can now be tackled with greater confidence.

One such example is the compound $P\{CH[Si(CH_3)_3]_2\}$ illustrated in Figure 8.1. The crystal structure for this compound is already known. In the solid phase molecules aggregate into dimers, with each molecule possessing C_2 symmetry. Interest in the gas-phase structure arises since if this structure were known it would be possible to determine the degree of molecular distortion in the solid phase.

The compound is a radical and comprises some 57 atoms (of which 19 are 'heavy') thereby presenting a considerable challenge for *ab initio* calculations. From the electron diffraction perspective the structure requires some 31 geometric parameters in order to be described in C_2 symmetry, and contains 1653 intermolecular distances. Determining a structure by either method is therefore a non-trivial exercise. Work on this compound is on-going.
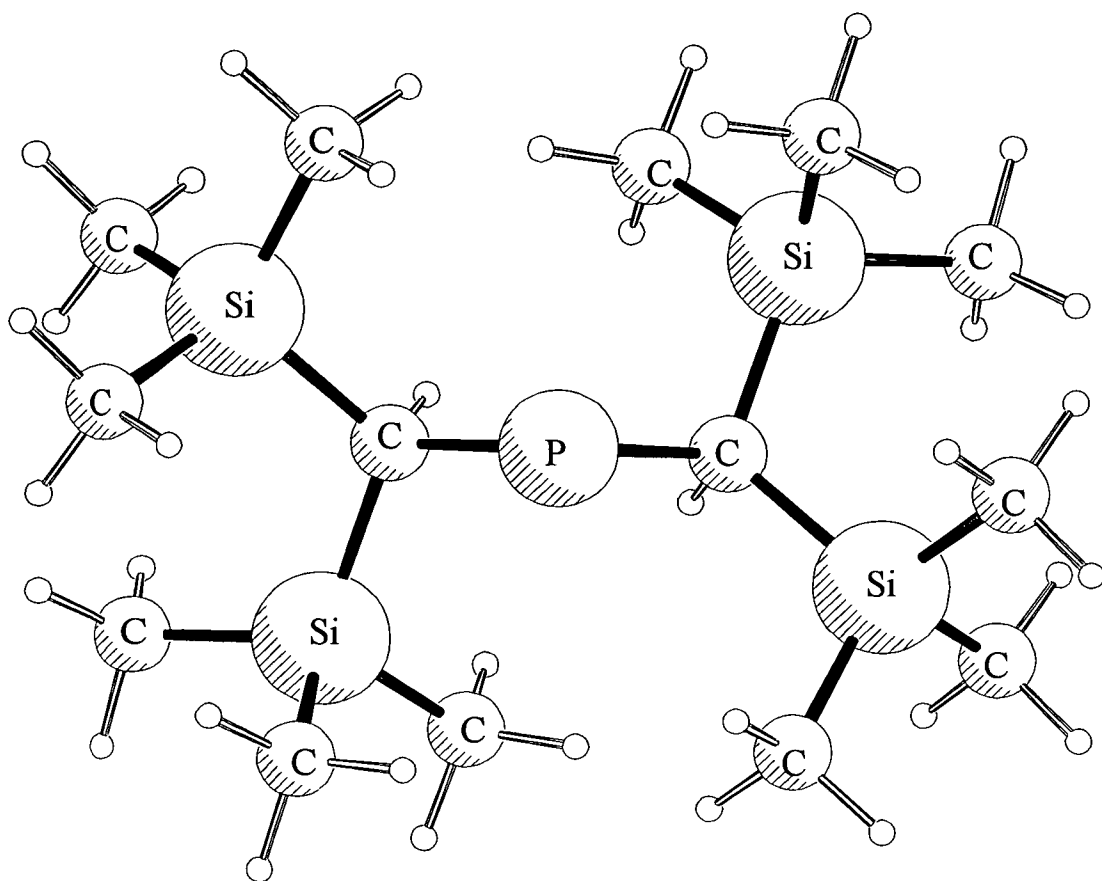
Figure 8.1 The Molecular Structure of $P\{CH[Si(CH_3)_3]_2\}_2$

8.2 References

1. The up-grading of ED92 to ED96 was performed by Dr. N. Mitzel, University of Edinburgh.

2. A.J. Blake, P.T. Brain, H. McNab, J. Miller, C.A. Morrison, S. Parsons, D.W.H. Rankin, H.E. Robertson, and B.A. Smart, *J. Phys. Chem.,* 1996, 100, 12280.

3. P.T. Brain, C.A. Morrison, S. Parsons, D.W.H. Rankin *J. Chem. Soc., Dalton Trans.,* 1996, 4589.

Appendix I

Publications

1. *'Perfluorocyclopropene: Experimental and Theoretical Studies of Its Structure in Gaseous, Solution and Crystalline Phases'*
    B.T. Abdo, I.L. Alberts, C.J. Attfield, R.E. Banks, A.J. Blake, P.T. Brain, A. P. Cox, C.R. Pulham, D.W.H. Rankin, H.E. Robertson, V. Murtagh, A. Heppeler and C. A. Morrison, *J. Am. Chem. Soc.*, 1996, **118**, 209.

2. *'Structure Analysis Restrained by Ab Initio Calculations: The Molecular Structure of 2,5-Dichloropyrimidine in Gaseous and Crystalline Phases'*
    A.J. Blake, P.T. Brain, H. McNab, J. Miller, C.A. Morrison, S. Parsons, D.W.H. Rankin, H.E. Robertson, and B.A. Smart, *J. Phys. Chem.*, 1996, **100**, 12280.

3. *'Tetraborane(10), B_4H_{10}: structures in gaseous and crystalline phases'*
    P.T. Brain, C.A. Morrison, S. Parsons, D.W.H. Rankin *J. Chem. Soc., Dalton Trans.*, 1996, 4589.

4. *'Gaseous and Crystalline Phase Molecular Structures of 4,6 Dichloropyrimidine, 2,6-Dichloropyrazine and 3,6-Dichloropyridazine'*
    C. A. Morrison, B. A. Smart, S. Parsons, E. M. Brown, D.W.H. Rankin, H. E. Robertson and J.Miller *J. Chem. Soc., Perkin Trans. 2*, 1997, 857.

5. *'The Molecular Structure of 1,3,5-Triazine in Gas, Solution and Crystal Phases and by Ab Initio calculations'*
    C. A. Morrison, B.A. Smart, D.W.H. Rankin, H.E. Robertson, M. Pfeffer, W. Bodenmüller, R. Ruber, B. Macht, A. Ruoff and V. Typke. *Manuscript accepted by J. Phys. Chem. for publication.*

6. *'The molecular structures of tetraborane(10) derivatives: ab initio calculations for $H_2MB_3H_8$ (M=B, Al, Ga or In) and gas-phase electron diffraction study of $H_2GaB_3H_8$'*

C.A. Morrison, B.A. Smart, P.T. Brain and D.W.H. Rankin. *Manuscript submitted to J. Chem. Soc., Dalton Trans. for publication.*

7.   '*The molecular structures of tetraborane(10) derivatives: ab initio calculations for (CH₃)₂MB₃H₈ (M=B, Al, Ga or In) and gas-phase electron diffraction studies of (CH₃)₂AlB₃H₈ and (CH₃)₂GaB₃H₈*'
C.A. Morrison, B.A. Smart, P.T. Brain and D.W.H. Rankin. *Manuscript submitted to J. Chem. Soc., Dalton Trans. for publication.*

8.   '*The Molecular Structure of Thiazole, determined by the Combined Analysis of Gas-Phase Electron Diffraction and Microwave Data.*'
S. F. Bone, B. A. Smart, H. Gierens, C. A. Morrison, P. T. Brain, D.W.H. Rankin. *Manuscript in preparation.*

Appendix II

Conferences and Courses attended

- Introduction to Unix   December 1994

- Enhance your Unix skills   December 1994

- Socrates-ERASMUS Action 2 Programme

  X-ray Crystallography Placement

  University of Bergen, Norway, April-June 1996

  Awarded Scottish International Education Trust Grant

  Oral presentation at Universities of Bergen and Trondheim

- Postgraduate Lecture Courses:

  Dr. Donald McKeen

  'Infrared Spectroscopy: Practice and Theory'

  Dr. David Reid

  'Applications of NMR to Inorganic and Organometallic Systems'

- University of Edinburgh Inorganic Section meetings 1995-1997

- Conferences:

  Royal Society of Chemistry, Scottish Dalton Symposium

  University of Paisley, March 1995

  6th European Symposium on Gas-Phase Electron Diffraction

  Firbush, Scotland, 19th-23rd June 1995

  Poster Presentation: *Total Structure Analysis: A New Approach*

  Sixteenth Austin Symposium on Molecular Structure

  The University of Texas at Austin, Texas, USA, March 1996

  Oral Presentation: *Total Structure Analysis - The Marriage of Gas-Phase Electron Diffraction and Ab Initio Calculations*

Poster Presentation: C.A. Morrison, B.A. Smart, P.T. Brain and D.W.H. Rankin: *Total Structure Analysis - Some Results*

University of Strathclyde Inorganic Chemistry (USIC) Conference
University of St. Andrews, September 1996
Oral Presentation: *A Structural Study of some Derivatives of Tetraborane(10)*

Royal Society of Chemistry, Dalton Division Symposium,
University of Edinburgh, December 1996

7th European Symposium on Molecular Structure,
Prague, Czech Republic, June 1997
Poster Presentations: C.A. Morrison, B.A. Smart, P.T. Brain, D.W.H. Rankin: *A Structural Study of some Derivatives of Tetraborane(10);*
S. Bone, B.A. Smart, H. Gierens, C.A. Morrison, P.T. Brain, D.W.H.Rankin: *Joint Analysis of Thiazole*

University of Strathclyde Inorganic (USIC) Conference
University of Edinburgh, September 1997
Member of Organising Committee